Impact of protein-protein interactions and phosphorylation on RNA decapping for nonsense mediated mRNA decay (NMD)

Agathe Gilbert

▶ **To cite this version:**

Agathe Gilbert. Impact of protein-protein interactions and phosphorylation on RNA decapping for nonsense mediated mRNA decay (NMD). Biochemistry [q-bio.BM]. Sorbonne Université, 2022. English. NNT : 2022SORUS386 . tel-04265647

HAL Id: tel-04265647

https://theses.hal.science/tel-04265647

Submitted on 31 Oct 2023

HAL is a multi-disciplinary open access archive for the deposit and dissemination of scientific research documents, whether they are published or not. The documents may come from teaching and research institutions in France or abroad, or from public or private research centers.

L'archive ouverte pluridisciplinaire **HAL**, est destinée au dépôt et à la diffusion de documents scientifiques de niveau recherche, publiés ou non, émanant des établissements d'enseignement et de recherche français ou étrangers, des laboratoires publics ou privés.

Sorbonne Université

ED515 - Complexité du vivant

Génétique des Interactions Macromoléculaires, Institut Pasteur

Impact of protein-protein interactions and phosphorylation on RNA decapping for nonsense mediated mRNA decay (NMD)

Par Agathe Gilbert

Thèse de doctorat de Biochimie et Biologie structurale

Dirigée par Cosmin Saveanu

Présentée et soutenue publiquement le 29 septembre 2022

Devant un jury composé de :

Saveanu, Cosmin, Directeur de Recherche, Directeur de thèse

Chakrabarti, Sutapa, Group Leader, Rapporteure

Iwasaki, Shintaro, Chief Scientist, Rapporteur

Weil, Dominique, Directrice de Recherche, Examinatrice

Bénard, Lionel, Directeur de Recherche, Président du Jury

Fiorini, Francesca, Chargée de Recherche, Examinatrice

Heyd, Florian, Professor, Examinateur

Except where otherwise noted, this work is licensed under
http://creativecommons.org/licenses/by-nc-nd/3.0/

A ma mère,

Acknowledgments

I would like to express my deepest gratitude to Shintaro Iwasaki and Sutapa Chakrabarti for giving me the honor to review my thesis manuscript. I also would like to thank Dominique Weil, Francesca Fiorini and Lionel Bénard for agreeing to take part in my thesis jury. Thank you as well to Florian Heyd for stepping in last minute and agreeing to review my work. Then my thanks go to Bertrand Séraphin and Sébastien Durand for their pieces of advice and their kindness during my thesis comities.

I would like to thank Alain Jacquier and everyone in my lab for welcoming me into their team. More particularly, I would like to thank my thesis director Cosmin Saveanu for eventually entrusting me with this project and for teaching me what tenacity is. Ultimately, this thesis was accomplished in the best deadline possible.

Je voudrais aussi remercier bien fort Laurence Decourty pour son aide constante et sa bienveillance pendant ces trois années de thèse. Merci à Abdelkader Namane pour son expertise en spectrométrie de masse et son sens de l'humour au quotidien. Maïté et Lucia, je tenais à vous remercier pour toute votre bonne humeur et pour votre gentillesse. Non seulement votre aide et votre présence au laboratoire m'ont été précieuses mais nos moments en pause-café m'étaient toujours agréables. Je souhaitais aussi remercier chaleureusement Frank Feuerbach pour tous ses conseils durant mon master et ma thèse avant son départ. Merci pour ton aide qui arrivait toujours à point nommé et d'une simplicité bienveillante. Enfin, j'aimerais remercier Emmanuelle Permal pour son aide, son soutien et sa pédagogie. Les analyses avec toi deviennent soudain simples et efficaces, tout ça dans la bonne humeur.

Je suis profondément reconnaissante envers mon tuteur de l'Institut Pasteur, Quentin Giai Gianetto, pour son soutien, ses précieux conseils et son aide sans faille pour finir cette thèse. Merci surtout d'avoir cru en moi jusqu'au bout.

Ces années de thèse ont aussi été difficiles du fait du contexte si particulier qu'a apporté la crise sanitaire. En ce qui concerne le travail, je suis reconnaissante envers l'Institut Pasteur et mon équipe de nous avoir toujours privilégiés et de nous avoir permis de continuer nos travaux de thèse dans de bonnes conditions. Cependant, toutes les activités autour ont été plus ou moins arrêtées impactant considérablement notre bien-être et la balance vie professionnelle /

vie personnelle. C'est pourquoi, je ne pourrais jamais assez remercier les personnes qui m'ont accompagnée dans cette aventure et ce surtout en dehors de l'univers travail.

Léna ma work bestie. Merci beaucoup pour tout. Sans toi à mes côtés pour ces trois ans, je n'aurais pas réussi à aller au bout. Merci pour ton soutien, pour tes explications, pour ta patience et pour ton amitié. Je suis vraiment contente d'avoir partagé cette aventure avec toi.

Margot, Daria, Vi, je suis désolée de ne pas rester pour une quatrième année. Finalement, the 4 PhD of the 4th floor ne termineront pas en même temps. Mais merci pour ces trois ans. Merci pour les brunchs, pour les sorties et pour les moments de décompression.

Je voudrais aussi remercier chaleureusement mes camarades d'open-space : David, Cécile, Madison, Colin, Stéphane, Corinne et Salhia. L'ambiance était studieuse mais il y avait aussi de franches rigolades et des gens généreux vers qui je pouvais me tourner.

Je suis aussi très reconnaissante d'avoir pu lors de cette aventure faire un bout de chemin avec Estelle. Merci pour tous tes conseils et ta joie de vivre. Merci d'être restée à mes côtés même en changeant de travail. Que ce soit à la danse, lors des brunchs, escape game ou autre, ta présence était essentielle pour moi.

Cette aventure m'a aussi permis de rencontrer – ou retrouver – des gens fabuleux et bienveillants : Samia, Baptiste, Simon, Olivia, Lucie, Thomas, Laureline, Mélanie. Merci à tous.

Je voudrais aussi remercier Anne-Hélène, Laetitia et le groupe de danse qui ne m'ont jamais lâchée même pendant les confinements. Les cours Zoom m'ont été indispensables. Merci pour votre dynamisme et votre joie de vivre.

Et le meilleur pour la fin, je remercie de manière générale ma famille pour leur soutien inconditionnel. Adrien, merci de m'avoir proposé de relire ma thèse et d'avoir bien voulu m'écouter parler de ma thèse en long en large et en travers. Hugo, merci pour les petits-déjeuners où on refaisait le monde. Mais surtout, je voudrais remercier mes parents qui ont dû composer avec mes angoisses et mes mauvaises humeurs pendant trois ans. Certains diront que vous avez l'habitude avec déjà deux thésards dans la fratrie. Merci aussi de m'avoir accueillie pendant les confinements moi et mon chat. Ma santé mentale vous remercie bien fort.

Table of Contents

Acknowledgments *2*

Table of Contents *4*

Introduction *6*

I. mRNA's life cycle **6**

1. Production of mRNA 6
2. Main degradation pathways in eukaryotes 8
3. Co-translational surveillance mechanisms 13

II. Nonsense-mediated mRNA decay (NMD) **15**

1. Core NMD Factors 16
2. Other NMD factors in yeast 20
3. The particular case of the Smg proteins 24
4. Different mechanisms in higher eukaryotes 35
5. Targets and possible roles of NMD in disease 38

III. Caseine Kinase Hrr25 ..... **40**

1. Identification 40
2. Functions and targets 41

IV. Scope of this work **46**

Material and Method *48*

Efficient yeast nonsense-mediated mRNA decay (NMD) involves the protein kinase Hrr25 *66*

Hrr25 kinase activity is needed for NMD **66**

One of Hrr25's target is Upf1 CTD **90**

Similarities between phosphor-Upf1 in yeast and in human cells. **93**

Hrr25 and its interactions with other NMD factors **96**

Ebs1 96
Dcp2 97

Recruitment of Hrr25 into NMD complexes **98**

Discussion and Perspectives *101*

Bibliography *108*

Strains *145*

Plasmids *147*

Oligonucleotides *148*

Oligonucleotides used for construction of yeast strain and plasmids **148**

Oligonucleotides used for qPCR experiments **150**

Oligonucleotides used for the triple mutant strain **151**

List of Abbreviations *152*

List of Figures..... *156*
List of Tables..... *161*

Introduction

I. mRNA's life cycle

1. Production of mRNA

DNA (or DeoxyriboNucleic Acid) is a double stranded macromolecule that holds genetic information in all cells. The first step to access to this information is transcription, allowing production of RNA (RiboNucleic Acid). Multiple types of RNA exist such as rRNA - ribosomal - or tRNA - transfer. However, only one contains the information to produce proteins: mRNA or messenger RNA. It can be divided into 3 parts: 5'-Untranslated Region (UTR), coding sequence or Open Reading Frame (ORF) and 3'-UTR. In eukaryotes, this sequence is protected at the 5'-end by a cap structure – m^7Gppp – and at the 3'-end by a poly-A tail. Translation of mRNA by the ribosomal machinery produces functional proteins. Maintaining and regulating protein levels are essential for life and transcriptional, post-transcriptional and post-translational mechanisms are involved.

Capping and polyadenylation

mRNA are products of DNA transcription by the RNA polymerase II. Co-transcriptionally, the pre-mRNA will undergo multiple modifications in order to prevent its immediate degradation.

First, there will be protection of its 5'-end thanks to the addition of a cap structure: **capping.** This step occurs early in transcription, after 30 to 50 nucleotides (nt) (Hocine et al., 2010). It consists of the addition of a guanosyl-triphosphate as the result of the action of a triphosphatase and a guanylyl transferase. In *S. cerevisiae,* the two enzymes in action are Cet1 and Ceg1. Then, methylation of this guanosyl group is necessary to form the final structure m^7-GpppN. The methyltransferase involved in *S. cerevisiae* is Abd1. The capping mechanism has been the subject of an in-depth review (Ramanathan et al., 2016). This structure is then recognised by a heterodimer of two proteins Cbc1 and Cbc2 (CBP80 and CBP20 in humans) that form the cap binding complex. This complex participates to the mRNA export from the nucleus through the nuclear pore complex (Hocine et al., 2010).

At the end of transcription, a signal – AAUAAA - is recognized by a complex cleaving and thus freeing the pre-mRNA (Shatkin and Manley, 2000). This signal also allows addition of a **poly-A tail** in 3'. Its length depends on the organisms. In *S. cerevisiae*, it revolves around 70 A, but it can go up to 250 A in other eukaryotes. This tail will be protected from 3' exoribonucleases attacks by poly-A binding proteins (PABP). Several enzymes have been identified. In *S. cerevisiae,* Pab1 corresponds to the cytoplasmic 3' exoribonuclease while Nab2 acts in the nucleus (Sachs et al., 1986). For metazoans, five enzymes are located in the cytosol, PABPC1 to PABPC5, while one enzyme takes on this activity in the nucleus, PABPN (Grange et al., 1987). This structure also participates in export to the cytoplasm, translation and degradation.

Splicing

Transcription leads to a pre-mRNA. This nascent transcript sometimes possesses uncoding regions, named introns, unnecessary for later translation and that must be removed to join coding regions, named exons. This maturation step is called **splicing** and will lead to the mature mRNA with its final ORF. This step involves 5 small nuclear ribonucleoproteins (snRNP) complexes and more than 150 associated proteins that together form the spliceosome (Black, 2003; Valadkhan and Jaladat, 2010). Splicing can be associated with the addition, in certain organisms like humans, of a complex upstream the junction of two exons, named the exon junction complex (EJC) (Le Hir et al., 2000a, 2000b).

Transcription and different events

Transcription of DNA allows production of many RNAs, and in particular, mRNA whose translation will produce protein necessary for the cell. It is important to transcribe the exact information kept by DNA. Thus, quality of mRNAs is checked at multiple levels so that no aberrant transcripts undergo translation. Here, aberrant means that the protein produced will differ from the original functional protein. Those types of transcripts can come from insertion or deletion of nucleotide leading to frameshift. They can also come from a default in splicing leading to intron retention. Those mistakes might induce a Premature Termination Codon (PTC) and might create truncated proteins (Hall and Thein, 1994). Truncated proteins can have a negative dominant effect, can aggregate (van Leeuwen et al., 1998) or can lose its functional activity due to a dose effect (Fan et al., 2001).

Advances in technology led to development of RNA sequencing and hence, discovery of new categories of non-translated RNAs. The phenomenon leading to these RNAs was termed

pervasive transcription. These advances showed that eukaryotic promoters are bidirectional (Core et al., 2008; Jin et al., 2017; Neil et al., 2009; Seila et al., 2008; Xu et al., 2009). It also showed that transcription can start upstream or downstream canonical transcription sites (Malabat et al., 2015; Pelechano et al., 2013; Zhang and Dietrich, 2005). Different categories of RNA were described. The first class of transcripts to be discovered, were characterised in a strain with Rrp6 – nuclear exosome co-factor – depleted (Davis and Ares, 2006; Houalla et al., 2006; Wyers et al., 2005). Those RNAs have an abnormal transcription termination and are thus targeted for degradation directly in the nucleus by a surveillance complex recognizing premature stop of transcription. This category of transcripts corresponds to Cryptic Unstable Transcripts (CUT). Some escapes degradation and can be exported to the cytoplasm where they can be degraded by other surveillance pathways. Another class is less sensitive to Rrp6 activity and has a normal termination of transcription making those transcripts detectable in wild-type conditions (David et al., 2006; Neil et al., 2009; Xu et al., 2009). Therefore, this category is named Stable Unannotated transcripts (SUT) and can be more easily exported to the cytoplasm. Finally, depletion of Xrn1, the cytoplasmic 5'-3' exoribonuclease – led to the characterisation of another class of pervasive transcripts: Xrn1-sensitive unstable transcripts (XUT) (van Dijk et al., 2011). As SUT, the termination of those transcripts is normal and thus export to the cytoplasm is possible. However, their turnover is quick and depends on Xrn1 making those transcripts not easily detectable in wild-type conditions. More details on pervasive transcription can be found in Jensen, Jacquier and Libri (2013)(Jensen et al., 2013).

2. Main degradation pathways in eukaryotes

Degradation of mRNAs is a major post-transcriptional regulatory step for gene expression. It occurs by different and redundant mechanisms that can be triggered by various molecular events. In eukaryotes and in particular in yeast, the major catalytic activities associated with mRNA degradation belong to exonucleases, both in the 5' to 3' and in the 3' to 5' direction. The major exonucleolytic enzymes are conserved in all eukaryotes. In the classic model of mRNA degradation, established by experiments performed in yeast, the initial step corresponds to the shortening of the poly-A tail first by the activity of the Pan2/3 deadenylation complex, then by the activity of the Ccr4/Pop2/Not deadenylation complex up to a size of about 12A (Das et al., 2017). The shortened poly-A tail through interactions with the Lsm1-7/Pat1 complex, activates the removal of the cap structure at the 5' end of the RNA through the action of the decapping complex, composed, in yeast, of the catalytic subunit Dcp2 and the tightly

associated co-factors Dcp1 and Edc3. Cleavage of the pyrophosphate bond between the cap and the mRNA leaves a monophosphate at the 5'-end of the RNA. This 5' phosphate end allows degradation by the Xrn1 exonuclease. Alternatively, degradation of the mRNA by the exosome from the 3'-end is also possible in the 3' to 5' decay pathway. The different pathways for mRNA degradation are summarized in **Figure 1**.

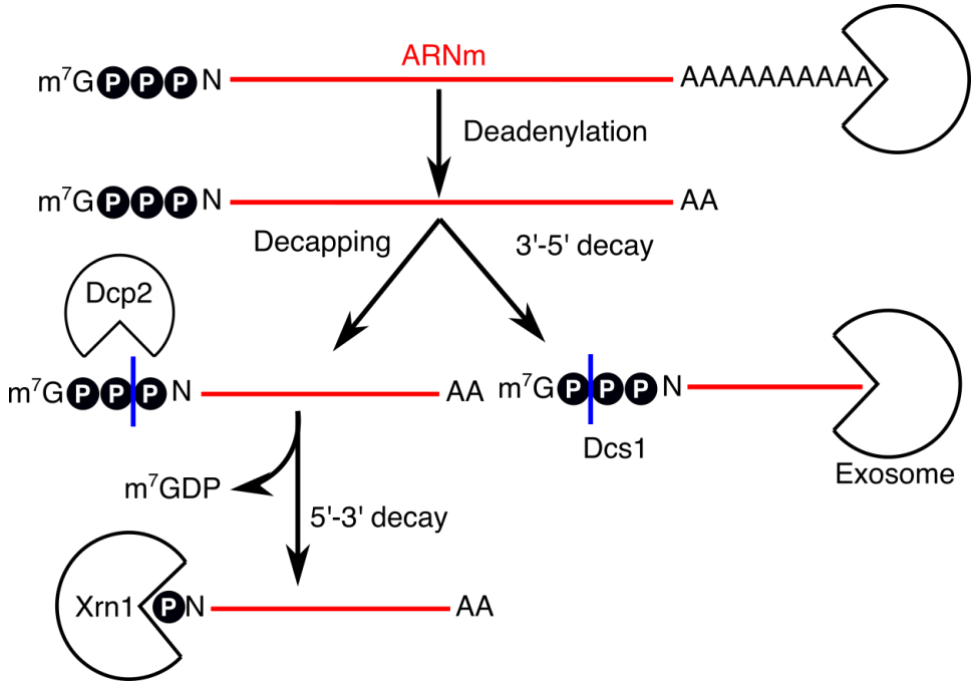

Figure 1: mRNA degradation pathways in eukaryotes (simplified from Kramer and McLennan, 2019).

Deadenylation

As explained previously, deadenylation occurs thanks to the action of two complexes in sequence: first Pan2/3 (Boeck et al., 1996; Brown et al., 1996) then Ccr4/Pop2/Not (Pop2 for S. cerevisiae; CAF1 for mammals) (Tucker et al., 2001).

The first complex to initiate deadenylation is thus composed of Pan2/3. This complex is recruited on the mRNA thanks to the interaction between Pan3 and Pab1 (Siddiqui et al., 2007). Pan3 consists of a regulatory subunit while Pan2 is the catalytic enzyme. It is an exonuclease 3'-5' belonging to the RNAse D family. This step in deadenylation is often quite rapid from 90 nt to 65 nt approximately in yeast (Brown and Sachs, 1998; Yi et al., 2018). This can come from the fact that Pab1 promotes Pan2/Pan3 activity (Boeck et al., 1996). In addition, it has been shown recently that this first complex acts in wild-type (WT) conditions on the part of the polyA tail that does not bind to Pab1 and is thus left unprotected (Yi et al., 2018).

Then comes the second complex into action (Tucker et al., 2002; Yi et al., 2018): Ccr4/Pop2/Not. This complex is composed of two catalytic subunits Ccr4 and Pop2 (CAF1 in mammals) that are in interaction (Basquin et al., 2012; Bianchin et al., 2005; Daugeron et al., 2001; Thore et al., 2003). *In vitro*, those two proteins seem to have redundant activities. However, *in vivo*, they seem to have substrates' specificities, at least in yeast. For example, Ccr4 seems more active on regions rich in Pab1 while Pop2 seems to prefer regions poor in Pab1 (Webster et al., 2018). Thus, the two enzymes could have complementary roles even though, in yeast, Ccr4 depletion impacts more growth of the cells than Pop2's (Tucker et al., 2002) suggesting that, at least in yeast, Ccr4 might have a more important part to play. Nevertheless, complete deadenylation of mRNAs happens only if the two catalytic enzymes are present in the cells. Pulse-chase experiments on inhibition of both proteins shows a cooperation mechanism that seems more important in humans (Tucker et al., 2001). This second complex is recruited on mRNAs thanks to interactions with proteins linked to the 3'-UTR. For example, the Puf family (Pumilio Family) holds such a role in *S. cerevisiae* (Olivas and Parker, 2000). As for the Not proteins, Not2/3/5 promotes decapping thanks to an interaction with Pat1 (Alhusaini and Coller, 2016) and Not1 acts as a hub protein (Bai et al., 1999), allowing binding between Pop2 and other subunits of Not complex.

Once deadenylation arrives to the last 10-12 nt of the polyA tail, a pause is observed before the following step of the degradation of the mRNA (Decker and Parker, 1993).

Decapping

During RNA decay, decapping for eukaryotes is an important step since it allows degradation through 5'-end by exonucleases. Decapping can also occur on RNA fragments following 3' to 5' degradation of RNA. Four different classes of enzyme for decapping are known (reviewed in Kramer and McLennan, 2019):

- Nudix hydrolases, such as RppH and Dcp2, participate to 5' to 3' RNA decay pathway.
- DXO family members are in charge of decapping and degrading mRNAs with incomplete caps at the 5'-end, such as Dxo1p in *S. cerevisiae* (Grudzien-Nogalska and Kiledjian, 2017).
- HIT family members such as Dcs1 (DcpS in Human) are scavenger proteins. They hydrolyse the cap of the mRNA fragment left after 3' to 5' degradation.
- ApaH-like phosphatase is the major decapping enzyme of trypanosomes.

The main decapping enzymes in yeast are Dcs1 that takes part in the 3' to 5' decay pathway and Dcp2 that is the catalytic enzyme in the decapping complex for the 5' to 3' decay pathway. The cleavage site of each enzyme is showed in **Figure 2**.

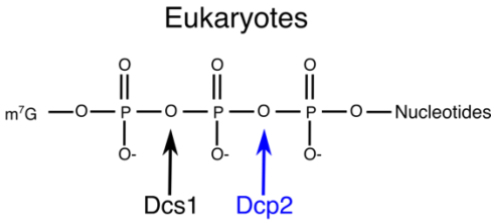

Figure 2: Cleavage sites of different hydrolase enzymes in eukaryotes (simplified from Kramer and McLennan, 2019). The names of the enzymes correspond to *S. cerevisiae* (Dcs1 and Dcp2)

Decapping is generally an irreversible step leading to mRNA degradation. Hence, it affects gene expression by modulating the half-life of mRNA. Dcp2 activity is affected by multiple cofactors. A first cofactor involved is Dcp1, considered initially as holding the decapping activity (LaGrandeur and Parker, 1998). It enhances Dcp2 decapping activity (Deshmukh et al., 2008; She et al., 2006; van Dijk et al., 2002). Another close cofactor to Dcp2 is Edc3 that releases Dcp2 from its auto-inhibitory effect (Harigaya et al., 2010; He and Jacobson, 2015). It was also seen in interaction with Dcp2 in its active form (Charenton et al., 2016). Dcp2 was also seen in interaction with RNA-binding proteins, such as the Lsm1-7-Pat1 complex and the RNA helicase Dhh1 (Coller et al., 2001). Several structural models of the catalytic site of the catalytic domain of Dcp2 from different organisms try to explain the action of the direct interacting factors and the intimate molecular mechanisms involved in decapping (reviewed in Valkov et al., 2017). However, these models show a high degree of divergence, and little is known on how other associated factors can regulate decapping.

Moreover, the C-terminal domain of Dcp2 in yeast is not conserved throughout organisms and is not necessary for decapping. Indeed, it has been shown that only the first 300 amino acids of Dcp2 are sufficient for decapping activity (Dunckley and Parker, 1999). The C-terminal domain is useful for interactions with multiple cofactors such as Pat1, Edc3 or Upf1 (He and Jacobson, 2015). It might allow a layer for selectivity of substrates or might be needed for other functions of Dcp2 such as transcription in yeast (Grousl et al., 2009; Shalem et al., 2011). Another cofactor of Dcp2 found in mammals is Edc4 (Chang et al., 2014). It is not present in organisms that contains this long C-terminal domain of Dcp2, and thus might replace it to fine tune Dcp2 decapping activity.

After deadenylation of the mRNA to the final 10-12 bases, Pab1 is exchanged by the complex Pat1/Lsm1-7 (Chowdhury et al., 2007; Tharun and Parker, 2001). This recruitment might consist in a signal for the activation of decapping. Indeed, Pat1 not only allow recruitment of Xrn1, the 5'-3' exoribonuclease, but also recruits Dcp1/Dcp2 for decapping of the 5'-end (Charenton et al., 2017; Fromont-Racine et al., 2000; Ho et al., 2002; Krogan et al., 2006; Tarassov et al., 2008; Tong et al., 2004). Pat1 also helps decapping by inhibiting translation and enhancing Dcp2 activity (Nissan et al., 2010).

However, decapping can also occur in a deadenylation independent degradation. For example, some transcripts are degraded in a pathway decapping-dependent with the help of the cofactor Edc3 such as Rps28b that needs both Edc3 and its protein Rps28 for degradation (Badis et al., 2004; He et al., 2014). NMD is another deadenylation-independent degradation pathway that relies on decapping that we will see in more detail later on.

While decapping regulation is an open question, the process is a direct target of viral factors in eukaryotic cells. Viruses use different defence mechanisms in order to modify the 5' to 3' decay pathway enzymes to their advantage. For example, ((+)RNA) viruses such as the viruses belonging to the *Flaviviridae* family, subvert host decapping activators Lsm1-7, Pat1 and Dhh1 in order to enhance translation of their RNA genome (Jungfleisch et al., 2016). Another example are the decapping proteins produced by vaccinia virus, protein D9 and D10. These decapping enzymes allow the virus to degrade both host mRNAs in cooperation with host Xrn1 and viral mRNAs that anneal with host transcripts in order to avoid host innate immune response (Kramer and McLennan, 2019).

Degradation in 5'-3'

Cleavage of the cap structure at the 5'-end, as said previously, leaves a monophosphate group. This is the requirement to allow activity of 5'-3' exonuclease (Stevens, 1978). Xrn1 is the major cytoplasmic 5'-3' exonuclease and is involved in the main degradation pathway after decapping (Stevens, 1980). This degradation by Xrn1 is parallel to translation (Hu et al., 2009; Pelechano et al., 2015).

Degradation in 3'-5' (reviewed in Zinder and Lima, 2017)

First discovered in yeast (Mitchell et al., 1997), this pathway corresponds to the action of the exosome on the mRNA. The exosome is a complex composed of 10 proteins. Rrp44 (Dis3) has been identified as the catalytic enzyme possessing endonuclease and 3'-5' exonuclease activity (Bousquet-Antonelli et al., 2000; Dziembowski et al., 2007; Lebreton et

al., 2008; Liu et al., 2006; Schaeffer et al., 2009; Schneider et al., 2009). The complex contains also an Exo9 core composed of the other noncatalytic subunits. It is doughnut-shaped with a hexameric ring of 6 RNase PH-like domain-containing proteins, that means a domain like RNase PH from *E. coli* (Rrp41, Rrp42, Rrp43, Rrp45, Rrp46 and Mtr3). This ring is capped by a ring of 3 proteins named S1/KH (Rrp4, Rrp40 and Csl4). This structure allows formation of a central channel wide enough to accommodate ssRNA (Liu et al., 2006). This channel will allow guiding of the processed RNA to the catalytic site of Dis3 (Bonneau et al., 2009).

This degradation pathway also involves other proteins: the Ski complex. Those proteins were discovered before the exosome in yeast thanks to a genetic screen (Ridley et al., 1984; Toh-E et al., 1978). SKI comes from SuperKIller since mutations of these genes led to increase levels of a killer toxin produced by the M viral dsRNA. The Ski complex for 3'-5' degradation is composed of three proteins, Ski2, Ski3 and Ski8 (Brown et al., 2000). Ski7 acts as a bridge since it interacts both with the Ski complex and the exosome (Araki et al., 2001; van Hoof et al., 2002; Wang et al., 2005). The Ski complex as the Exo9 core forms a channel to guide the RNA towards the exosome (Halbach et al., 2013). Ski2 is a DExH-box helicase allowing unwinding of RNA structures to ease its degradation.

Exosome intervenes for degradation of RNAs once the 3'-end is not or no longer protected and on RNAs possessing specific motifs (Chen et al., 2001). However, its mechanism remains unclear. The exosome degradation is important since it acts on nearly every class of RNA (Chekanova et al., 2007; Gudipati et al., 2012; Pefanis et al., 2014; Schneider et al., 2012).

Indeed, the exosome is also needed for degradation of RNAs in the nucleus. There, it contains 12 components; the core complex associates with Rrp6 and its binding partner C1D (Allmang et al., 1999; Feigenbutz et al., 2013). It is helped by the TRAMP complex, Trf-Air-Mtr 4 polyadenylation complex, that prepares RNA substrates for degradation by this 12-components complex (LaCava et al., 2005; Wyers et al., 2005). The TRAMP complex is also involved in degradation of CUTs and processing of rRNAs (LaCava et al., 2005; Wyers et al., 2005).

3. Co-translational surveillance mechanisms

Quality control of mRNA will ensure production of functional proteins. This control is necessary considering that RNA polymerase makes a hundred times more errors than DNA polymerase during replication. Indeed, during transcription, up to four errors per million bases can be made (Gout et al., 2017) while during replication, the mutation rate is below 10^{-7}

mutations per nucleotides site per generation and in some organisms can even be 1000 times less (Lynch et al., 2016).

During translation, different mechanisms can check the quality of the mature mRNA: Non-Stop Decay (NSD), No-Go Decay (NGD) and Nonsense-mediated mRNA Decay (NMD). NMD will be presented in more detail in the following chapter (see Nonsense-mediated mRNA decay (NMD)). Those degradation pathways are conserved throughout eucaryotes and specific to them.

NGD and NSD have a very similar mechanism. What mostly differs between those degradation pathways are the transcripts they target for degradation. These mechanisms are well explained in the reviews Powers et al, 2000 and Karamyshev and Karamysheva, 2018 (Karamyshev and Karamysheva, 2018; Powers et al., 2020). Briefly, while NGD degrades transcripts with strong secondary structures, rare codon repeats or leading to nascent peptides with specific features (Kuroha et al., 2010; Tsuboi et al., 2012), NSD targets transcripts that do not contain a stop codon. This feature can come from a polyadenylation within the ORF or cleavage of the ORF leading to no STOP codon nor polyA-tail (Graille and Séraphin, 2012; Ozsolak et al., 2010). Those features will lead in both cases to stalling of elongating ribosomes. From then on two proteins are involved: Dom34 (or Pelota) and Hbs1 (Doma and Parker, 2006; Pisareva et al., 2011; Saito et al., 2013; Tsuboi et al., 2012). These proteins are structural homologues of eRF1 and eRF3a (Atkinson et al., 2008). As such, they interact with the A-site of the stalled ribosome and recruit Rli1 (ABCE1 in mammals) to promote dissociation of translation elongation complex and ribosome recycling (Becker et al., 2011; Saito et al., 2013; Shoemaker et al., 2010; Tsuboi et al., 2012).

This event also leads to endonucleolytic cleavage of the mRNA and thus its degradation. In budding yeast, the Cue2 protein binds to disomes during stalling of ribosomes and is involved in NGD and NSD (D'Orazio et al., 2019). As for C. elegans, the endonuclease involves in those degradation pathways is Nonu-1 (Glover et al., 2020), and in human, N4BP2 plays this part (Nicholson-Shaw et al., 2022).

NSD has another mechanism possible. Indeed, in yeast Ski7 an eRF3 homologue can intervene as well (Frischmeyer et al., 2002; van Hoof et al., 2002). Ski7 is also a homologue of Hbs1 and binds to the stalled ribosome followed by recruitment of the exosome and its cofactors (reviewed in Klauer and van Hoof, 2012).

II. Nonsense-mediated mRNA decay (NMD)

NMD is a universally conserved degradation pathway in eukaryotes (reviewed in Kurosaki et al., 2019). First described as a degradation pathway specific for mRNAs containing a Premature Termination Codon (PTC), hence its name, NMD is also capable of targeting mRNAs in order to modulate gene expression (He and Jacobson, 2015). Indeed, in mammals, 10% of its transcriptome is affected by NMD (Mendell et al., 2004). Thus, RNAs that are destabilized through this pathway are natural products of RNA polymerase II transcription or RNA produced through splicing errors, or, less frequently, the result of DNA base changes that introduce PTC. The typical NMD substrate is an RNA that contains a short coding sequence followed by a long 3'-UTR. Cellular mRNAs coding for functional proteins can be NMD targets and their rapid degradation may be a pre-requisite for important cellular processes, such as embryo development (e.g., GADD45A (Nelson et al., 2016)).

Degradation of NMD substrates depends on the core factors Upf1, Upf2 and Upf3 (illustrated in **Figure 3**)(Cui et al., 1995; Leeds et al., 1992, 1991; Perlick et al., 1996; Pulak and Anderson, 1993). First discovered in yeast through a genetic screen (Culbertson et al., 1980), those proteins were seen as universally conserved throughout eukaryotes (Behm-Ansmant et al., 2007b; Chen et al., 2008; Culbertson and Leeds, 2003; Kadlec et al., 2006). Later, six other essential factors for NMD were discovered in a screen in *C. elegans* (Hodgkin et al., 1989). Specific mutations led to genital malformation and thus, were named Suppressors with Morphogenic effect on Genitalia (smg). The corresponding genes are hence SMG1 to SMG7 (Cali et al., 1999; Hodgkin et al., 1989; Pulak and Anderson, 1993). Smg2, Smg3 and Smg4 are respectively the homologues of Upf1, Upf2 and Upf3 (Aronoff et al., 2001; Page et al., 1999). Apart from the upf proteins, the smg proteins have no homologues in yeast. Nevertheless, all other organisms and mammals possess orthologues of the smg proteins (Applequist et al., 1997; Chiu et al., 2003; Denning et al., 2001; Lykke-Andersen et al., 2000; Mendell et al., 2000; Perlick et al., 1996; Yamashita et al., 2001). The components of NMD mechanism are summarized in the **Table 1**. The enzymes eventually responsible for degradation of NMD substrates are the 5'-3' exonuclease Xrn1 (He and Jacobson, 2015) and also the cytoplasmic exosome for the 3'-5' end (Mitchell and Tollervey, 2003; Takahashi et al., 2003).

One of the best models explaining how NMD substrates are recognized as aberrant is called "False 3'-UTR" (Amrani et al., 2004). It is based on the stimulatory role that the protein Pab1, which binds the poly-A tail of mRNAs has on translation, and potentially translation

termination. When the poly-A tail is far from the termination codon, translation termination becomes impaired and creates the conditions for recruitment of NMD factors. This model was experimentally tested in mammalian cells as well. Other models exist and will be later explained in this chapter. How exactly the main NMD factors, Upf1, Upf2 and Upf3 are recruited, and how they activate downstream steps, decapping in yeast, and decapping and endonucleolytic cleavage in mammals, is not clear.

S. cerevisiae	*C. elegans*	*H. sapiens*
Upf1 Upf2 Upf3	SMG-2 SMG-3 SMG-4	UPF1 UPF2 UPF3a/b
	SMG-6	SMG6
	SMG-5 SMG-7	SMG5 SMG7
	SMG-1 (Kinase)	SMG1 (Kinase)

Table 1: Core proteins involved in the NMD mechanisms.

1. Core NMD Factors

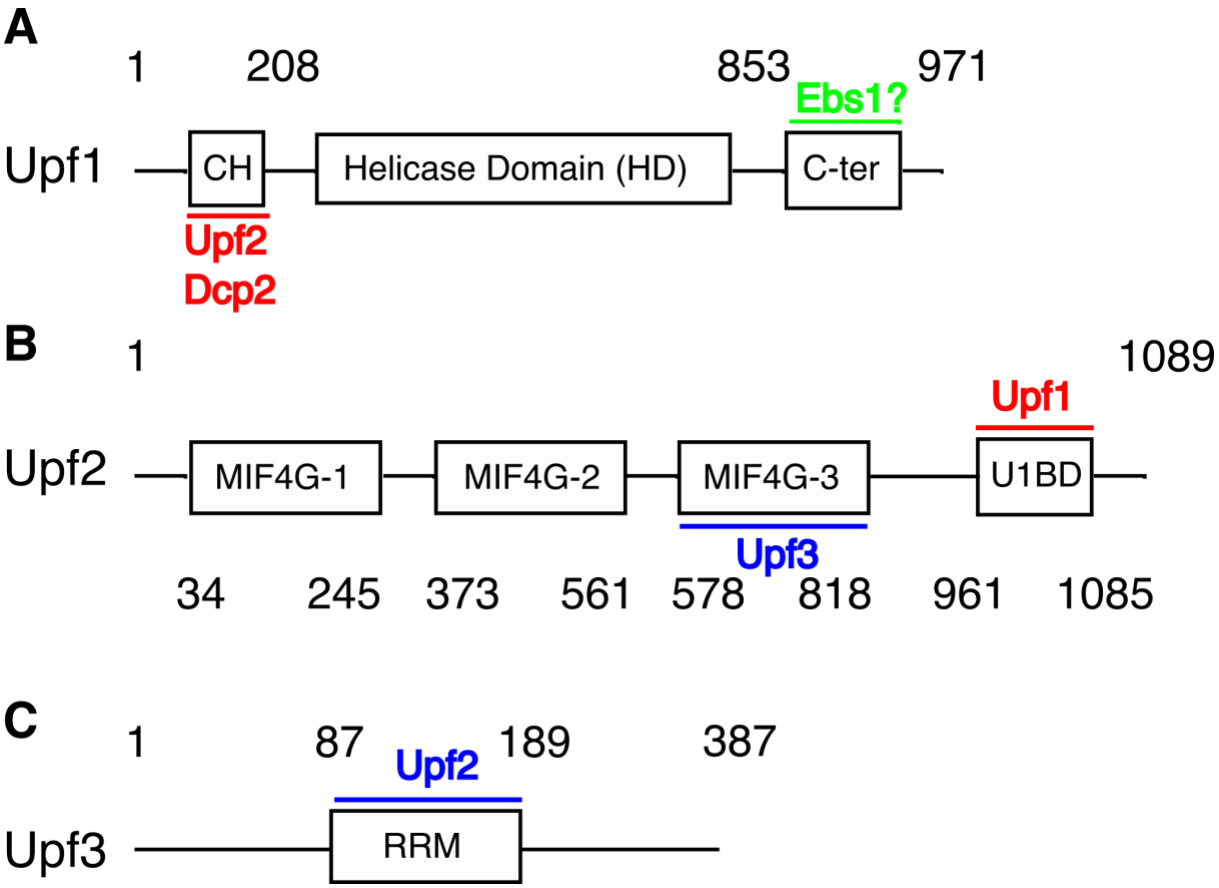

Figure 3: The Upf proteins. Domains and interactions of Upf1 (A), Upf2 (B) and Upf3 (C).

a. Upf1/Nam7

As said previously, the Upf factors are the core proteins involved in NMD mechanism. Indeed, depletion of Upf1 leads to complete inhibition of NMD in all organisms. While this inhibition of NMD does not prevent normal growth in yeast (Cui et al., 1995; Leeds et al., 1991), it is very important in other organisms such as mouse or *D. rerio*, where inhibition of NMD leads to death of the embryo (Medghalchi et al., 2001; Wittkopp et al., 2009). Upf1 is the most conserved of the three Upf proteins: human and yeast protein sequences have 48% of identity whereas human and drosophilae protein sequences have 62% of identity (Culbertson and Leeds, 2003).

Upf1 is composed of two principal regions. In N-terminal, a zinc-finger domain was described which is rich in cysteine and histidine residues, also called CH domain. This region allows interaction with not only Upf2 but also eRF1, eRF3 and Dcp2 (Czaplinski et al., 1998; He et al., 1996; He and Jacobson, 2015, 1995; Ivanov et al., 2008). The C-terminal domain corresponds to the catalytic region with an ATPase/helicase domain also named HD. This

domain corresponds to the superfamily of ARN and ADN SF1 helicase. Two subregions RecA can be determined – RecA1 and Rec2. In this region, an RNA binding site is also found. Upf1 can bind to different RNAs (Hwang et al., 2010). However, specific features are preferred by this protein for interaction with RNA such as a long 3'-UTR or existence of an EJC complex downstream a PTC (Hogg and Goff, 2010; Kurosaki and Maquat, 2013).

Both helicase and ATPase activities of Upf1 are needed for NMD to function (Weng et al., 1996). Indeed, ATPase activity has a role to play to recognize RNA containing a PTC (Lee et al., 2015). It is also essential for recycling of NMD factors on RNA (Franks et al., 2010). Helicase activity allows translocation of Upf1 from 5' to 3' (Fiorini et al., 2012) and has also been described as required for NMD (Sun et al., 1998). Those two activities can be regulated in multiple ways. Inhibition can occur through interaction with factors such as eRF1 and eRF3, at least *in vitro* (Czaplinski et al., 1998). This inhibition also comes from the CH and C-terminal domain (Fiorini et al., 2015, 2013). Interaction of Upf2 changes Upf1 conformation and can thus bring insights on this intrinsic auto-inhibitory effect on the HD (Chakrabarti et al., 2011; Chamieh et al., 2008). The N-terminal and C-terminal domains of Upf1 contains also Serine residues that are phosphorylated by PI3KK (Phosphatidylinositol 3-kinase related kinase) such as SMG1. Moreover, this phosphorylation seems essential for NMD mammals. This regulation of Upf1 activity and interactions through phosphorylation will be discussed in more details later in this chapter.

NMD mechanism remains unclear and requires us to find answers to multiple questions. One of them concerns the recruitment of Upf1 on the site of recognition of a NMD substrate such as PTC. Two hypotheses are favoured. The first one considers that Upf1 bind to all RNAs and are removed progressively thanks to the translation machinery so that Upf1 is only associated with the 3'-UTR at the end. This hypothesis is supported by RNA immunoprecipitation experiments using hUpf1 after inhibition of translation (Zünd et al., 2013). The second hypothesis promotes the idea that Upf1 is directly recruited to the PTC or the 3'-UTR (Shigeoka et al., 2012). Proposed NMD mechanisms at play are later described in part II.4 Different mechanisms in higher eukaryotes.

b. Upf2/Nmd2

Conservation of Upf2 in eukaryotes is less than for Upf1. Indeed, human Upf2 and yeast Upf2 have 21% identity and human Upf2 and drosophilae Upf2 have 34% identity (Culbertson and Leeds, 2003). As seen previously, Upf2 can help regulate Upf1 helicase activity in NMD

thanks to changes in conformation. Another important role of Upf2 in NMD is to link Upf1 and Upf3 (Chamieh et al., 2008; He et al., 1997). Indeed, Upf2 is composed of three MIF4G-like domains (Middle domain of eukaryotic initiation factor 4G) (Clerici et al., 2014). This domain initially allows binding of eIF4G to other initiation factors and to RNA. The third domain in Upf2 is actually the binding site of Upf3. Moreover, in its C-terminal, Upf2 possesses a UBD1 domain allowing interaction with Upf1 CH domain. The first MIF4G domain seems to also have a role in NMD since mutations in this domain prevent NMD (Fourati et al., 2014).

In addition, Upf2 might also regulate Upf1 activity in NMD by acting on its phosphorylation. Indeed, an interaction between Upf2 and Smg1 has been described not only in complex with Upf1 (Melero et al., 2014) but also independently of Upf1 (Kashima et al., 2006; Melero et al., 2014). Comparing those structures with kinases from the same family (mTOR, Yang et al., 2013) and taking into account other results (Ivanov et al., 2008; Kashima et al., 2006), Melero and colleagues suggest that Upf2 is necessary for activation of Smg1 and thus phosphorylation of Upf1.

Similarly to Upf1, Upf2 has been described as a phospho-protein (Chiu et al., 2003). In budding yeast, phosphorylated residues have been characterized in the N-terminal region and they seem to have a role in NMD (Wang et al., 2006) even though no kinase has been described for this phosphorylation yet.

c. Upf3

Upf3 is the least conserved of the three Upf proteins. In mammals, two paralogs exist: Upf3 or Upf3a on the chromosome 13 and Upf3X or Upf3b on chromosome X (Serin et al., 2001). While Upf3b is essential to NMD, the role of Upf3a is more limited (Lykke-Andersen et al., 2000). Upf3b has been described as the main protein involved in NMD (Chan et al., 2007). This is mostly due to the fact that Upf3a and Upf3b compete for binding with Upf2 (Chan et al., 2009). Yet, free Upf3a molecules are unstable. Since Upf3b mRNA is 3-fold higher expressed than Upf3a mRNA, Upf3b is in larger amount than Upf3a preventing binding to Upf1 and hence leading to degradation of Upf3a. Cho and colleagues showed that this corresponds to Upf3b protein levels being 100-fold higher than Upf3a protein levels (N. H. Cho et al., 2022).

The role of Upf3a in NMD have been unclear up until recently. Early studies supported the hypothesis that as Upf3b, Upf3a could trigger NMD (Gehring et al., 2003; Lykke-Andersen et al., 2000). The difference between the two comes from their C-terminal domain: R419 in Upf3b corresponds to A432 in Upf3a. This difference in residue seems to weaken the

interaction between Upf3a and the EJC and thus, induce a weaker effect of Upf3a in NMD (Kunz et al., 2006). However, a study seems to indicate that Upf3b and Upf3a has opposite effect on NMD and that Upf3a is an inhibitor of NMD (Shum et al., 2016). With evolving methods and analysis, role of both paralogs appears to be more determined. Overexpression and knockout of Upf3a and/or Upf3b in HEK293 show that Upf3a and Upf3b have redundant function in NMD (Wallmeroth et al., 2022).

Upf3 contains a RRM (RNA Recognition Motif) like domain. This region does not bind to RNA due to lack of aromatic residue (Kadlec et al., 2004). However, it does allow binding but to Upf2 (Kadlec et al., 2004).

As we will see later in this chapter, two models exist for NMD. One is only present in complex organisms since it depends on the Exon Junction Complex (EJC). In this model, Upf3 is part of this complex and interacts thanks to an EBM (EJC Binding Motif) domain to the subunit Y14 (Gehring et al., 2003; Kim et al., 2001). Upf3 is localized in the nucleus but can travel to the cytoplasm (Lykke-Andersen et al., 2000; Serin et al., 2001). Thus, Upf3 binds to the EJC in the nucleus. Then it travels to the cytoplasm and on RNA containing a PTC, Upf3 allows the junction of the complex containing Upf1 at the PTC and the EJC. However, in other organisms where EJC is not present or not essential to NMD, Upf3's role in NMD is less clear. It seems in budding yeast that Upf3 is still necessary for binding of Upf2 to RNA since depletion of Upf3 leads to loss of Upf2 in the polysomes (Atkin et al., 1997). Furthermore, Upf3 seems to interact with the ribosome and this interaction slows down termination of translation and offers a platform for interaction of Upf1 and Upf2 (Neu-Yilik et al., 2017).

2. Other NMD factors in yeast

Large scale protein complex purification and quantitative mass spectrometry in my host laboratory led to a better description of the complexes involved in yeast NMD, summarized in the Detector/Effector model (Dehecq et al., 2018). This model is based on the formation of two different complexes that revolve around Upf1. The first one is composed of Upf1 coupled with Upf2 and Upf3 and was named "Detector". This first complex would allow detection of NMD substrates. Then the composition of the complex Upf1 changes in order to give the "Effector" complex. It was named that way since the decapping enzymes, Dcp2 and Dcp1, and decapping regulators such as Edc3 are part of this complex. However no functional test was performed on this complex to show whether the decapping enzyme is active.

S. cerevisiae	*C. elegans*	*H. sapiens*
Upf1 Upf2 Upf3	SMG-2 SMG-3 SMG-4	UPF1 UPF2 UPF3a/b
Nmd4	SMG-6	SMG6
Ebs1	SMG-5 SMG-7	SMG5 SMG7
	SMG-1 (Kinase)	SMG1 (Kinase)

Table 2: Core proteins involved in the NMD mechanisms with new possible functional homologues of Smg5, Smg6 and Smg7 in yeast.

In their study, Dehecq and colleagues looked at NMD phenotype of Nmd4 and Ebs1 in different conditions and they saw that under limiting conditions Nmd4 and Ebs1 can be essential to NMD. They used a complementation assay. Indeed, overexpression of the C-terminal domain of Upf1 can complement NMD (Weng et al., 1996). However, deletion of Nmd4 or Ebs1 prevent this complementation.

Hence, this study suggests that Nmd4 and Ebs1 can affect NMD and thus correspond to NMD factors. Their characteristics show that Nmd4 can be the equivalent of Smg6 and Ebs1 the equivalent of Smg5/7. **Table 2** summarize the different yeast NMD factors and their equivalent in other organisms.

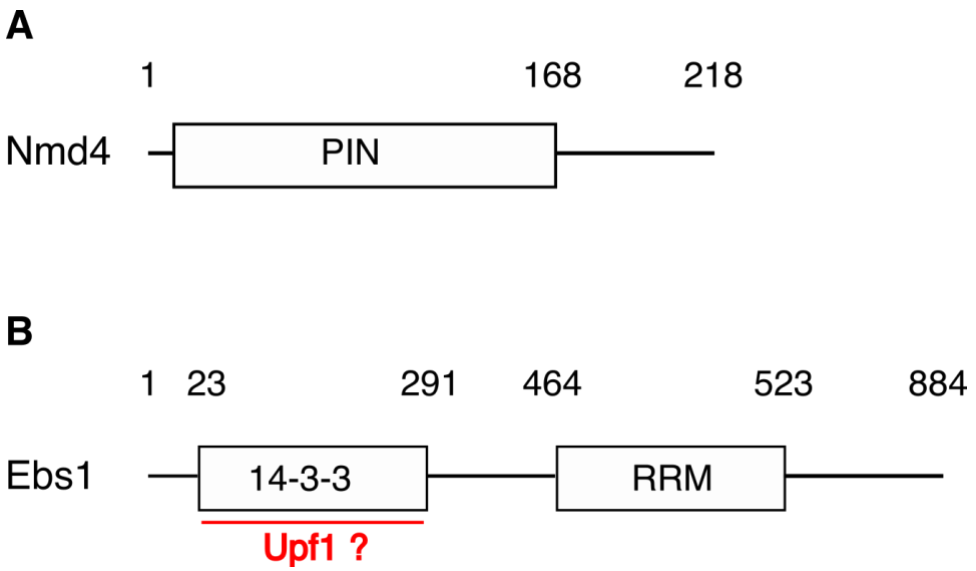

Figure 4: Domains and interactions of Nmd4 (A) and Ebs1 (B).

a. Nmd4

Nmd4 was first identified in a two-hybrid screen for factors that specifically interact with Upf1 (He and Jacobson, 1995). This study then focused on Nmd2/Upf2 and left Nmd4 no further characterized. Later on, deletion of this protein led to a positive genetic interaction with the deletion of Upf1 (Wilmes et al., 2008). Thanks to affinity purification followed by mass spectrometry, Dehecq and colleagues observed Nmd4 in interaction with Upf1 and thanks to treatment with RNase, determined that this interaction is independent of RNA. Using only fragments of Upf1, they narrowed down Nmd4 binding site to Upf1 HD domain. Moreover, this interaction could only be found in the second complex, Effector, and not the one containing the three upf proteins, showing that Nmd4 interaction with Upf1 Is specific to the conformation of Upf1 present in the Upf1-decapping complex (Dehecq et al., 2018). Nmd4 contains an endonuclease-like region corresponding to the PIN domain family (**Figure 4**A)(Clissold and Ponting, 2000) similar to Smg6, but its catalytic activity is not yet known.

b. Ebs1

Sequence similarity analysis allowed identification of Ebs1 as a potential yeast equivalent of human Smg7. Before its implication in NMD, Ebs1 was described as the homologue of Est1 (Zhou et al., 2000). Both proteins have 27% identity, mainly in the RRM (RNA Recognition Motif). Similarly as its homologue, deletion of Ebs1 leads to short telomeres (Zhou et al., 2000). Then, Ebs1 was described as acting on translation (Ford et al., 2006).

During this study, no effect on NMD could be observed nor interaction with Upf1. However, one year later, Luke and colleagues were able to co-purify Ebs1 with Upf1 and showed an impact of Ebs1 on NMD. They also saw that Ebs1 is very similar to Smg5, Smg6 and Smg7, and in particular, in the N-terminal 14-3-3 domain (**Figure 4**B)(Luke et al., 2007). Thanks to affinity purification and mass spectrometry, interaction between Ebs1 and Upf1 could be confirmed (Dehecq et al., 2018) and this binding is independent of the RNA. Further experiments showed that Ebs1 interacts specifically with Upf1 HD-Cter domain.

3. The particular case of the Smg proteins

Received: 29 December 2021 | Accepted: 2 March 2022

DOI: 10.1002/bies.202100296

BioEssays

THINK AGAIN

Insights & Perspectives

Unusual SMG suspects recruit degradation enzymes in nonsense-mediated mRNA decay

Agathe Gilbert | Cosmin Saveanu

Institut Pasteur, Sorbonne Université, CNRS UMR-3525, Paris F-75015, France

Correspondence
Cosmin Saveanu, Institut Pasteur, Sorbonne Université, CNRS UMR-3525, Génétique des Interactions Macromoléculaires, F-75015, Paris, France.
Email: cosmin.saveanu@pasteur.fr

Abstract

Degradation of eukaryotic RNAs that contain premature termination codons (PTC) during nonsense-mediated mRNA decay (NMD) is initiated by RNA decapping or endonucleolytic cleavage driven by conserved factors. Models for NMD mechanisms, including recognition of PTCs or the timing and role of protein phosphorylation for RNA degradation are challenged by new results. For example, the depletion of the SMG5/7 heterodimer, thought to activate RNA degradation by decapping, leads to a phenotype showing a defect of endonucleolytic activity of NMD complexes. This phenotype is not correlated to a decreased binding of the endonuclease SMG6 with the core NMD factor UPF1, suggesting that it is the result of an imbalance between active (e.g., in polysomes) and inactive (e.g., in RNA-protein condensates) states of NMD complexes. Such imbalance between multiple complexes is not restricted to NMD and should be taken into account when establishing causal links between gene function perturbation and observed phenotypes.

KEYWORDS
NMD, premature termination codon, RNA degradation, RNA translation, RNA-protein complexes

INTRODUCTION

Nonsense-mediated mRNA decay (NMD) is a conserved degradation pathway initiated by translation termination at premature termination codons (PTC). PTCs are abundant in the transcriptome of eukaryotic cells and are present also, for example, in viral-related transcripts.[1–3] In addition to limiting viral replication, NMD also cleans up the transcriptome from numerous RNA isoforms synthesized with unusual transcription initiation or termination sites, e.g.,[4] or by alternative or inefficient splicing ([5] for a review). Due to its ancient origin and presence in most eukaryotes, NMD participates to the regulation of gene expression for processes requiring rapid RNA turnover, such as embryo development.[6]

Despite the conservation of NMD factors, the proposed molecular mechanisms of NMD are surprisingly diverse (reviewed by[7,8]). This divergence of mechanisms can be real, but some of it also comes from technical limitations of the experiments used to study NMD in yeast, worm, plant or human cells. RNA sequencing, the use of a variety of new reporter systems and improved genetic manipulation tools are affecting the picture of NMD factors and mechanisms. Some of the new results, discussed here, challenge established NMD models about the order of recruitment of late NMD factors and their role in triggering RNA degradation. They also suggest, for example, that affecting the balance of distinct NMD complexes by depletion of an NMD protein can indirectly affect NMD because factors critical for RNA degradation are present in low, limiting amounts in cells.[9]

Since NMD mechanism affect host pathogen interactions, tumor progression or monogenic disease potential treatments ,e.g., cystic fibrosis mutations,[10] they are of interest for a broad category of scientists. It is thus important to point out new results and how they challenge previously proposed models, explored in depth in a recent review.[7] The available data challenges established views, including the role of NMD factors in translation termination, the redundancy of RNA degradation pathways in NMD and the importance of protein phosphorylation in the dynamics of NMD complexes. Fresh data should lead to an adjustment of the accepted views on NMD mechanisms. This

 © 2022 Wiley Periodicals LLC

should be similar to how past ideas, such as the nuclear localization of NMD or its restriction to the first round of mRNA translation, were invalidated by later studies.[11–14]

We start by presenting the diversity of RNA molecules degraded through NMD and why cytoplasmic noncoding RNAs are excellent NMD substrates. Next, we provide a brief overview of NMD factors conserved in eukaryotes and present a compilation of data on the protein-protein interactions in this pathway. Finally, once the context is set up, we discuss recent results about how RNA degradation is initiated during NMD, specifically the role of the SMG5/7 heterodimer. These results suggest that phenotypes of cells in which NMD factors were depleted can be interpreted in terms of an imbalance between NMD complexes active or inactive for RNA degradation. Similar considerations probably apply to other processes involving populations of RNA and DNA molecules, such as chromatin modification, DNA repair, DNA transcription or RNA splicing and intracellular transport.

TRANSLATION OF NONCODING RNAS INITIATES THEIR DEGRADATION THROUGH NMD

Knowing what makes an RNA unstable through NMD is essential to understand the origin and diversity of this class of transcripts. Two complementary strategies identified NMD substrates, one measured changes in cellular RNA levels and another tested artificial reporter molecules in cells in which NMD was removed. The obtained results were also correlated with data on the physical association of NMD factors to both reporters and cellular transcripts, for example.[15–19] These studies allowed a better description of PTCs, considered as the defining elements of NMD-sensitive RNAs. The idea of a PTC originated from initial studies in which inclusion of a stop codon upstream the normal translation termination signal led to degradation of a reporter mRNA. The PTC denomination can be misleading when there is no obvious coding sequence present in an RNA. This is the case for thousands of noncoding RNAs that are produced in most eukaryotic cells. Noncoding RNAs lack a long open reading frame and, most often, are not conserved among eukaryotes.[20] However, if they reach the cytosol, random short open reading frames present in their sequence are translated,[21] making noncoding RNAs excellent targets for NMD, for example.[4] In yeast, such noncoding RNA sensitive to NMD include several populations of RNAs issued from pervasive transcription. A class of these transcripts was named SUT, for stable unannotated transcripts,[22] but the "stable" refers only to the fact that the SUT levels are generally unaffected when nuclear RNA degradation is defective. The SUT population of transcripts partially overlaps with RNAs observed to accumulate in the absence of the major 5′–3′ exonuclease XRN1.[23] Since XRN1 is responsible for the degradation of RNAs recognized by the NMD machinery, pervasive transcripts escaping the nucleus are an important source of NMD substrates in yeast.[24]

Thus, situations that create PTCs, initially considered to be restricted to rare cases of nonsense point mutations or infrequent splicing defects, are diverse and exist for many different types of transcripts, as depicted in Figure 1A. They all have in common the presence, downstream of the PTC, of a long untranslated RNA region or of an exon-exon junction at more than 50 nucleotides from the stop.[25,26] While the presence of a long 3′ UTR region drives RNA instability through NMD in all eukaryotes, downstream exon-exon junctions and the associated exon junction complex (EJC) enhance NMD only in some organisms, where it might have evolved as a supplementary control mechanism (for a discussion on NMD evolution see [27]). Similar to how a long 3′ UTR does not automatically lead to instability of RNA through NMD in yeast,[28] the presence of an exon junction downstream a stop codon may not be followed by instability of a reporter mRNA in human cells.[29]

In addition to noncoding RNAs, a surprising source of NMD substrates was found when RNA sequencing methods that could differentiate between alternative 5′ ends of transcripts became available. For example, stop codons that function as PTCs are frequently added to transcripts since RNA polymerase II is promiscuous about start site selection. RNA isoforms generated by transcription that begins upstream, and even downstream, the canonical start, can contain short open reading frames (uORFs) that end in PTCs.[4,35] Start codons on such RNAs are followed by randomly positioned stops, usually close to the transcript end. The RNA region situated downstream such translation termination is a potentially long 3′ UTR. The short coding sequence followed by a long 3′ UTR is typical for NMD substrates that are efficiently degraded in eukaryotes. Of note, alternative transcription termination sites, downstream the canonical ones, also produce RNAs with longer 3′ UTRs.

Being an excellent NMD substrate is not necessarily a bad thing. Pro-NMD features can even be selected and are desirable to avoid the production of truncated proteins, toxic through aggregation, for example.[36] A nice example of the imprint of NMD on evolution of genome sequence is the analysis of the frequency by which intron retention occurs in transcripts of the ciliate *Paramecium tetraurelia*. An advantage of this organism is that its introns are very short, between 20 and 35 nucleotides, making intron retention identification by sequencing straightforward. In line with the idea that NMD plays an important error correction function but needs a PTC to be effective, retained introns show an excess of in-frame stop codons.[37] NMD is thus intimately linked with splicing efficiency and imposes constraints on genome sequence evolution.[38]

Intriguingly, when no uORF or no long 3′ UTR are present, cellular RNAs can still be subject to premature termination leading to NMD due to a ribosomal frame shift long before reaching the canonical stop codon (Figure 1A). In this case, the frame shifting ribosome encounters a random stop codon, temporarily transforming a region of the annotated coding sequence in a 3′ UTR, thus creating conditions that are favorable for NMD.[39] The frequency at which such frame shifts followed by NMD occur is, for the moment, unknown.

VIRUSES FIGHT NMD

The SARS-CoV2 subgenomic RNA that serves as messenger for the synthesis of the structural viral protein spike (S) has a 3′ UTR regions

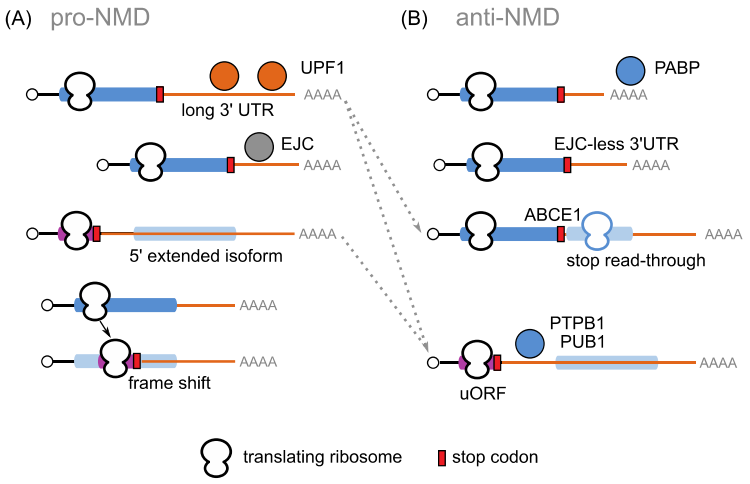

FIGURE 1 Configuration and origin of NMD substrates. (A) Conditions that favor degradation of RNA through NMD include the presence of a long 3′ UTR (due to transcription termination or to the inclusion of an early stop codon via defective splicing), of an exon junction downstream the stop codon, of short upstream ORFs, or ribosome frame shifts. (B) Conditions that allow immunity to NMD in specific cases include the opposite of those favoring NMD, such as a short 3′ UTR or lack of an exon exon junction downstream the stop codon, but also binding of specific factors or stop codon read-through. Arrows indicate relationships between various scenarios, depending on the origin of the NMD signal. Other proteins indicated and involved in NMD are the poly(A) binding protein (PABP), the exon junction complex (EJC),[30] the ABCE1 factor[31,32] affecting translation termination, or RNA binding PTPB1, in mammals [33] and PUB1, in yeast.[34]

with a length of about 5000 nucleotides.[40] Compared with cellular mRNA, with a median length of the 3′ UTRs of about 500 nucleotides, such a long 3′ UTR might induce RNA degradation through NMD. Whether subgenomic RNA instability is a limiting factor for SARS-CoV2 replication is unclear, but inactivation of NMD benefits the related murine hepatitis virus, at least in cell culture.[41] Thus, viral proteins that inhibit NMD mechanisms are likely to benefit viral replication. This hypothesis has received experimental evidence from studies done, for example, on human and animal coronaviruses, hepatitis C virus, West Nile, Dengue, Semliki Forest, Zika or human T-lymphotrophic type 1, viruses (reviewed in [1–3]).

Viral infections are not the only situations in which inhibition of NMD occurs. Anti-NMD features can be present in the architecture of many transcripts, as depicted in Figure 1B. Improved gene expression through immunity to NMD occurs in the absence of introns in the 3′ UTR region, through progressive loss of upstream open reading frames, to avoid uORFs, or by preferential use of early transcription termination sites for shorter 3′ UTR regions. When uORFs are essential parts of translation regulation, as in the case of the GCN4 transcription factor,[42] recruitment of anti-NMD factors ensures stability of the RNA. In the case of GCN4, it is not clear how the RNA binding protein Pub1 protects the RNA from NMD in yeast.[34] A reasonable hypothesis is that PUB1 interferes with translation termination at the potential PTC, leading to increased read-through of the stop codon of the uORF with removal of destabilizing elements from downstream region. Alternatively, Pub1 could also directly affect the binding of the NMD factor UPF1 to the RNA. Since the presence of UPF1 on 3′ UTRs correlates with degradation of the RNA through NMD,[15,16] its removal could inhibit NMD. This type of mechanism has been proposed for the NMD inhibition effects of RNA binding proteins PTBP1[33,43] and hnRNP L[44] in mammals.

Since various RNA features can lead to immunization against NMD, they can also give clues about how a PTC is detected as an RNA destabilization feature. A short 3′ UTR, for example, leads to the proximity of the stop codon to the poly(A) binding protein, Pab1 in yeast,[45] or PABPC1 in mammals.[46] This proximity was proposed to ensure normal translation termination, which would be perturbed if the 3′ UTR is long and led to the "faux 3′UTR" model for the identification of NMD substrates. Here, "faux," "false" in French, refers to the fact that some 3′ UTRs might not fulfill their role in ensuring normal RNA export, stability, and transport and, instead, promote RNA degradation via NMD. This model is appealing because it is simple: a PTC is a stop codon far from the downstream poly(A) tail and for which Pab1, the poly(A) binding protein, cannot assist translation termination, as it would normally do.[45] However, ribosome stalling at the stop codon might not be the only explanation for the role of poly(A) distance to stop in NMD, since ribosome stalling on NMD substrates was not detected in a different experimental system.[47] While it remains unclear whether ribosome stalling at a stop codon marks it as a PTC, translation termination defects, and especially stop codon read-through, decrease NMD degradation of a reporter in cells depleted for the ribosome recycling factor ABCE1.[31,32]

Altogether, both pro- and anti-NMD mechanisms depend on factors that are either dedicated to this process, such as the RNA helicase UPF1, or are essential participants, such as the ribosome.

NMD FACTORS AND COMPLEXES ARE SIMILAR ACROSS SPECIES

Recent screens for NMD factors in mammalian cells[31,48–50] confirmed that previous studies in *S. cerevisiae* and *C. elegans* identified most if not all the most conserved genes dedicated to this pathway in eukaryotes. Additional NMD factors were discovered through genetic screens in *C. elegans*, for example,[51] and at least one of them, the Nbas protein, might be involved in an ER-specific metazoan RNA degradation version of the NMD pathway.[52] What a "dedicated to NMD" factor means is not straightforward because many proteins are required for the process but have a primary role elsewhere. An example of the latter case of a NMD-related factor is the exonuclease XRN1 that degrades any RNA with an available 5′ monophosphate group.[53] XRN1's action occurs late in the NMD pathway and is thus dependent on earlier RNA degradation events that remove the 5′ cap structure or cleave the RNA. Similar to XRN1, translation termination factors eRF1 and eRF3 are important for triggering NMD, but are difficult to be considered primarily as NMD factors due to their major role in ribosome function. Finally, EJC components are also NMD-associated factors even if their primary role is related to premRNA splicing.

To help with the nomenclature of NMD factors, in practice two abbreviations indicate if a gene is involved in NMD: UPF and SMG. UPF is short for "up frameshift" and indicates that mutations in yeast UPF factors could increase the expression levels for a HIS4 gene having a +1 frame shift mutation leading to the presence of an out of frame PTC.[54,55] SMG genes were identified in *C. elegans* based on the ability of mutants to correct a defect in myosin class II heavy chain, UNC-54, production. This defect is the consequence of the loss of normal transcription termination for the r293 allelle of *unc-54*, leading to the probable use of a downstream termination signal and creating an unusually long 3′ UTR region. Since suppressor mutations also led to defects in the formation of male worm bursa and hermaphrodite vulva, the "suppressor with morphogenetic effect on genitalia," SMG, abbreviation was proposed.[56] There are three *UPF* genes, *UPF1*, *UPF2*, and *UPF3* and several *SMG* genes: *SMG1*, with cofactors *SMG8* and *SMG9*, *SMG6*, *SMG5 and SMG7*.

A unique nomenclature of NMD factors might have rendered life of scientists easier, but the numbers of *SMG* and *UPF* genes were not matched, with SMG2 being the equivalent of UPF1, SMG3, the equivalent of UPF2 and SMG4, the equivalent of UPF3. A reason for maintaining these two types of names for *NMD* genes is also the observation that UFP1, UPF2, and UPF3 are universally conserved from yeast to humans, while *SMG* genes, 1, 5, 6, and 7, were only found initially in multicellular organisms. As illustrated in Figure 2A, the probable conservation of these different NMD factors spans all eukaryotes, with factors missing in some organisms or having minimal roles in others. While the equivalent of the protein kinase SMG1 in yeast remains elusive, unrelated protein kinases, including the casein kinase two complex (CKA1, CKA2, CKB1, CKB2) and HRR25, are associated with NMD complexes[57] and mutant UPF1 can accumulate as a phosphoprotein[58] in this organism. Analysis of the interaction domains of UPF1 with other NMD factors suggests that the equivalent of SMG6 in yeast is NMD4, even if it is likely that the yeast protein has lost the endonucleolytic activity that characterizes SMG6 in other species.[59–61] SMG5 and SMG7, whose interaction to form a heterodimer is important for their role in human NMD[62] have probably a single equivalent in yeast, the EBS1 protein.[57,63] In *Arabidopsis thaliana* there is no equivalent of SMG5, and SMG1 has been recently lost[64] but the NMD pathway is present and active in this model organism.[65]

Since core NMD factors are present in most eukaryotes, NMD mechanisms are likely to be conserved. These mechanisms depend on molecular interactions that are under active investigation. We compiled a set of interactions among NMD factors based only on recent results using only affinity and proximity labeling approaches followed by mass-spectrometry analysis (Figure 2B).

The interactions among human NMD factors depicted in Figure 2B are not entirely compatible with the current NMD models. For example, translation termination factors and their interaction with SMG1 and UPF1, proposed to be part of the SURF complex,[72] were not detected. It is possible that the mass-spectrometry based approaches are not yet sensitive enough or were not performed under conditions that allow the accumulation of specific NMD complexes. It is also possible that transient interactions of NMD factors with the translation termination machinery are specific to mutant forms of UPF1[73] or depend on the action on translation termination of other NMD factors, such as UPF3B.[74]

Among the interactions that were not recovered by large-scale approaches are those between SMG1, a protein kinase crucial for mammalian NMD, and UPF2 and UPF3B, even if a complex containing all these factors and UPF1 was proposed to exist. Identification of NMD mechanisms is a challenging task since some NMD factors, such as UPF2 and UPF3, have low abundance. Potential interactions might be too weak to resist purification conditions and involve a heterogeneous population of RNA molecules. Finally, catalytically active NMD complexes involved in decapping or endonucleolytic cleavage might not be easily distinguished from complexes of identical composition but having no enzymatic effect on RNA molecules.

THE CURIOUS CASE OF UPF1 PHOSPHORYLATION CYCLE

UPF1 phosphorylation, particularly in the C-terminal domain of the protein, is an important event in NMD and SMG1, the protein kinase responsible for this reversible modification, is required for NMD in many organisms. Even in *D. melanogaster*, where SMG1 mutants have a mild effect on NMD,[75] this protein kinase becomes important when the function of another NMD factor, SMG5, is perturbed.[76] SMG5 and SMG7 contain tetratricopeptide repeat (TPR) domains

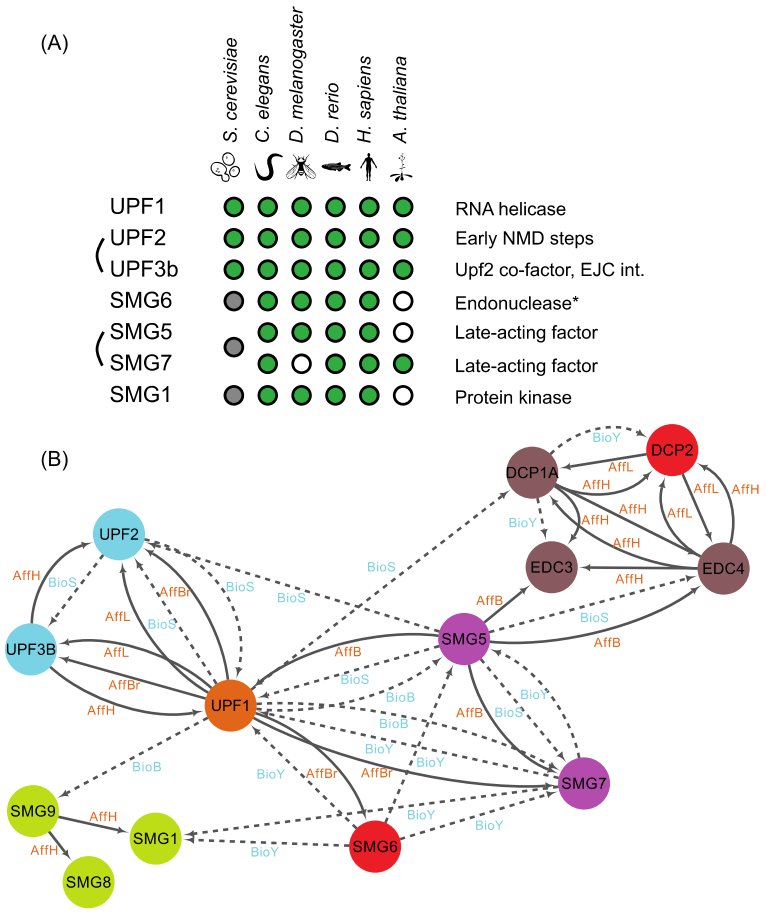

FIGURE 2 Conservation and interactions of core NMD factors. (A) Presence of equivalents for the core NMD factors in various species is indicated with green dots. Gray dots indicate partial similarity and white dots indicate the absence of a clear equivalent. SMG8 and SMG9, not shown, are SMG1 partners that follow the same conservation pattern.[66] For SMG6, an asterisk indicates that in some organisms the enzymatic activity of the protein is probably absent. (B) Interactions of human NMD factors detected through approaches based on affinity purification (solid lines, labeled "Aff") or proximity labeling (dashed lines, labeled "Bio"). The codes of the affinity-based interactions correspond to initials of first author in the corresponding publications: "AffB" Boehm,[9] "AffBr" Brannan,[67] "AffH" Hein,[68] "AffL" Li [69] and for the biotin labeling interactions correspond to: "BioB" Boehm,[9] "BioS" Schweingruber,[70] "BioY" Youn.[71] The arrows orientation indicate which proteins were used as "bait". SMG6 and DCP2, RNA cleavage enzymes, are depicted in red

that allow specific binding to phospho-UPF1.[77,78] Purification of SMG5 and SMG7 shows preference to the phosphorylated form of UPF1.[79] While the relative amounts of phosphorylated Upf1 under steady-state conditions are relatively low, they increase when the function of SMG5, SMG6, and SMG7 is perturbed in *C. elegans*[80] or human cells.[81] SMG5 and SMG7 form a heterodimer and were proposed to act as recruiters of the protein phosphatase PP2A.[82] These observations integrate into a sequence of events occurring at a PTC, in which activation of SMG1, potentially in a UPF1/2/3 complex, creates the conditions for UPF1 phosphorylation and binding of SMG/SMG7 and of the endonuclease SMG6.

What if UPF1 phosphorylation is just a mark of transient, but crucial, association of UPF1 with SMG1 during NMD ? This alternative interpretation fits with the fact that the interaction of the SMG6 endonuclease with UPF1 is only partially dependent on UPF1 phosphorylation.[78,83] It can also explain surprising recent results about SMG7. Mutants in the TPR domains of SMG7 (K66E/R163E), which remove the ability of the protein to bind phospho-UPF1,[77] also

perturb its association with nonphosphorylated UPF1. However, and unexpectedly, these mutations do not cancel the ability of SMG7 to function in NMD, when overexpressed.[9] By comparison, the formation of the SMG5/7 heterodimer turned out to be crucial for NMD, as studied in a cell line in which endogenous SMG7 was knocked out. Contrary to previous observations, proposing that a role of SMG5 and SMG7 is to recruit the protein phosphatase complex PP2A,[82] SMG5 was not found to be specifically associated with components of this phosphatase. Moreover, a specific association of SMG5, SMG7 or any other NMD factor with a protein phosphatase was not revealed by mass-spectrometry approaches (Figure 2B, references in the figure legend).

In light of the current results, the proposed molecular events at the PTC, including the formation of a SURF complex (SMG1, UPF1, eRF), might need to be re-evaluated. SURF includes, in addition to the core NMD factor UPF1, SMG1 and translation termination factors eRF1 and eRF3. SURF was proposed to form at PTCs and transition to a decay inducing complex (DECID), in which UPF1 interacts with UPF2 and UPF3 for the next step in NMD.[72] As discussed above, other scenarios are possible. Phosphorylation of UPF1, for example, might be not a cause, but a consequence of other molecular events involved in NMD, specifically the association of SMG1 to NMD complexes. This association might require the kinase activity of SMG1 for autophosphorylation,[84] to allow further remodeling of the NMD complex. Persistent association between UPF1 and SMG1, in the absence of the later SMG5-7 factors, would lead to UPF1 hyperphosphorylation, an idea that has been already suggested.[85] Similarly, the absence of UPF2, for example, which leads to decreased phosphorylation of UPF1, would be a sign that SMG1-UPF1 association was diminished, placing SMG1 association to UPF1 downstream the interaction of UPF1 with UFP2, and probably UPF3B. Finally, UPF1 dephosphorylation, proposed to be mediated by the recruitment of the serine/threonine phosphatase 2A,[79,82] might occur only on specific conformations of the NMD complexes, when the phosphorylated residues are accessible. Thus, the hyperphosphorylation of UPF1 after depletion of SMG5 and SMG7 could be interpreted as an increased insulation from highly active and relatively nonspecific cellular phosphatases.[86] The phosphorylation cycle of UPF1 in NMD needs further evaluation, to distinguish correlations from mechanistic cause and effect.

SMG5 AND SMG7, RNA DECAPPING AND ENDONUCLEOLYTIC ACTIVATORS ?

RNA degradation in NMD is initiated by either endonucleolytic cleavage through the activation of SMG6 catalytic activity in proximity of a PTC or by stimulation of RNA decapping by the DCP2 complex. UPF1 coordinates these events as it interacts with both the endonuclease SMG6 and with the decapping complex (Figure 2B). But is the recruitment of SMG6 and decapping factors in proximity of an RNA through UPF1 enough to trigger RNA degradation ? Tethering experiments, in which SMG6 was bound to a reporter RNA, showed that its RNA destabilization activity requires UPF1 and SMG1, but not UPF2, SMG5 or SMG7, when individually knocked-down. Strangely, the interaction of SMG6 with UPF1 occurs in the helicase domain of UPF1 and is independent on the phosphorylation of the protein,[83] which occurs on both N and C-terminal regions of UPF1. How the SMG1 protein kinase assists the activation of the endonucleolytic activity of SMG6 if its interactions do not seem to depend on UPF1 phosphorylation,[78,85] remains unclear.

Contrary to the lack of effect of individual SMG5 and SMG7 depletion on SMG6 activity, concomitant inactivation of these SMG genes leads to a loss of a SMG6-dependent RNA fragment from an NMD reporter.[9] This observation led to the proposal that SMG6 abundance might be limiting for the NMD process and can be viewed in the context of the equilibrium established among various forms of NMD complexes (Figures 3A, B). The persistence of SMG6 in UPF1 complexes in the absence of SMG5 and SMG7 indicates that biochemical analysis of NMD complexes and their dynamics in mutant cells is only partially informative of molecular mechanisms.[9]

Removal of both SMG5 and SMG7 decreases NMD to a large extent and leads, in addition to SMG6 inactivation, to the apparent accumulation of full-length NMD reporter RNA, at least for a studied transcript.[9] This observation is consistent with previous proposals for a mechanism of action of the SMG5 and SMG7 in RNA decay to occur through activation of RNA decapping. Decapping activation seems to be a universal feature of NMD mechanisms and predominates in yeast[87] and plant NMD.[88] However, how exactly the decapping is activated during NMD in all organisms remains unclear. Is it dependent on an acceleration of deadenylation[62] or could it be promoted by a direct interaction with UFP1[89] or some of its cofactors ?

The idea that in mammalian cells SMG5/7 would be responsible for accelerated deadenylation, which in turns activates decapping, comes from the study of the C-terminal region of SMG7 and on its ability to induce degradation of RNA in tethering experiments. This effect was independent on other NMD factors and was correlated with an interaction of the SMG7 domain with a component of the CCR4-NOT deadenylation complex, the deadenylase POP2.[62] The absence of the C-terminal domain of SMG7 does not abolish its ability to assist tethered SMG5 in destabilizing an RNA, as long as UPF1 is present.[90] Correlated with this result, removal of the C-terminal domain of SMG7 does not affect the ability of SMG7 to complement the NMD phenotype generated by the absence of the protein in SMG7 knock-out cells.[9] Moreover, deadenylases are not among the proteins associated with NMD complexes (Figure 2B), making it unlikely that accelerated deadenylation plays a major role in NMD.

If deadenylation acceleration is not responsible for the action of SMG5 and SMG7 in NMD, these proteins could participate to recruitment of the decapping complex. Decapping activation was proposed to occur through the interaction between SMG5 and PNRC2, a decapping cofactor. While PNRC2 was required in a tethered UPF1 RNA degradation assay, the observed interaction between PNRC2 and SMG5[91,92] was not robustly detected in more recent work.[90] Further studies will be required to understand whether PNRC2 is an essential component linking UPF1 with activation of decapping during NMD. Of note, in addition to the N and C-terminal regions of UPF1, the CH domain

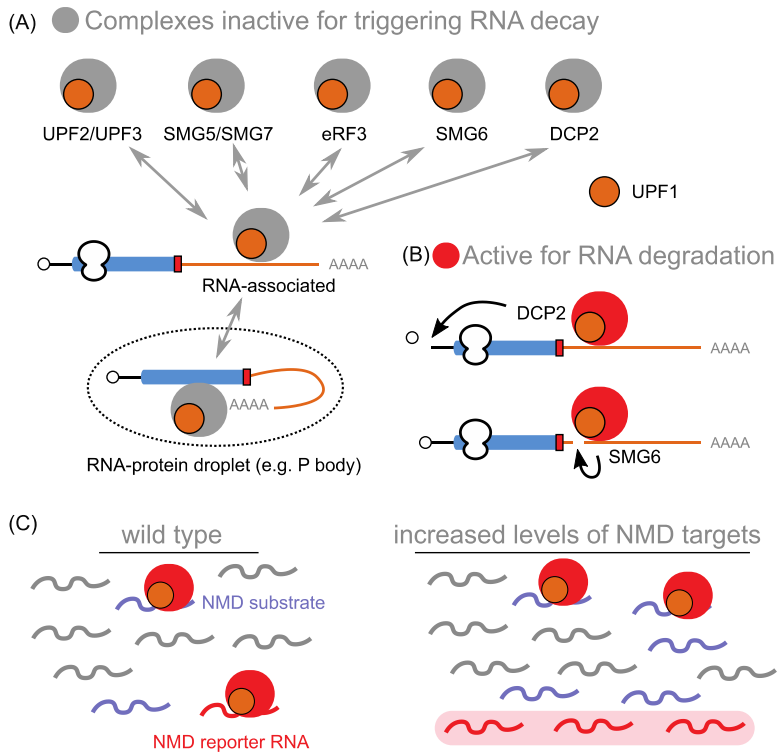

FIGURE 3 Challenges in the study of NMD mechanisms. Global evaluation of NMD complexes composition can be ineffective to distinguish active from inactive complexes in RNA degradation. Schematic representation of NMD complexes containing the core factor UPF1 in inactive (gray, A), or active for RNA degradation (red, B) configurations. Changes in the balance between the various forms might not be reflected by changes in the average composition of NMD complexes. (C) Low abundance NMD factors can become limiting for NMD by indirect mechanisms. A hypothetical scenario in which large amounts of RNAs that are NMD substrates are produced in a cell, bind available NMD factors, leading indirectly to accumulation of an NMD reporter molecule

was identified as important for the interaction with DCP2 in human cells.[62] This is surprisingly similar to the requirement for the CH domain of UPF1 for its interaction with the decapping machinery in yeast.[57] Thus, UFP1 could directly recruit the decapping machinery in mammalian NMD through a conformational change that depends on the late acting NMD factors SMG5 and SMG7. This hypothesis implies that recruitment of SMG6 and decapping activation are dependent on the association of the heterodimer SMG5/7 with UPF1[9] and is consistent with RNA level changes observed following NMD factors depletion, in which both decapping and endonucleolysis are involved.[93,94]

A coordination of decapping and endonucleolytic cleavage of NMD substrates shows surprising similarities with RNA degradation in bacteria. For example, in *E. coli*, endonucleolysis via RNAse E is partially dependent on the presence of a mono-phosphate group at the 5′ end of the RNA.[95] One of the enzymes responsible for the removal of phosphates from 5′ triphosphate and biphosphate RNA is rppH,[96] which is also active *in vitro* in removing the cap structure of eukaryotic RNA.[97] Even if the molecular players are different in bacteria and eukaryotes, removal of 5′ end protection of RNA and endonucleolytic cleavage are probably coordinated.

Since SMG5/7 can affect the function of SMG6 without an apparent loss of interaction of the protein with NMD complexes,[9] an alternative for the role of this heterodimer in NMD was proposed. Based on the observation that SMG6 is the lowest abundance NMD protein in human cells, its levels are probably a limiting factor and trapping the protein in dead-end complexes should decrease global NMD activity (Figure 3C). This scenario suggests that depletion of NMD factors can shift the balance between, for example, those with an active endonucleolytic activity and those, with a similar composition, that are not associated with RNA or are trapped in RNA-protein condensates (Figure 3A). The presence of proteins and RNA in liquid separated droplets can affect the catalytic activity of the decapping enzyme, DCP2.[98] Moreover, some of the best known phase separated granules, the yeast P bodies, contain high concentrations of NMD factors, such as UPF1.[99]

However, it is not clear to what extent affinity purification methods have access to complexes located in liquid droplets since these structures have been mostly explored through microscopy and fluorescence activated cell sorting.[100]

Changing the levels of RNAs that are substrates for NMD can affect NMD complexes and availability of SMG6 for RNA degradation. This is probably why depletion of the XRN1 exonuclease, which leads to accumulation of RNA degradation intermediated affects the observed composition of NMD complexes, with an increase in the association of SMG6 with UPF1.[85]

Distinguishing direct from indirect effects in NMD is crucial for understanding its molecular mechanisms. NMD has global effects on hundreds or thousands of RNA molecules. Low abundance, limiting NMD factors, could be effectively diluted if the amount of NMD substrates in a cell increases. This is not a hypothetical scenario, as similar situations have been already described. For example, flooding cells with high levels of a "decoy" RNA that contains motifs bound by the Nrd1:Nab3 complex, decreases its ability to assist transcription termination in yeast.[101] This relatively simple mechanism can explain why defects in nuclear RNA degradation, leading to accumulation of noncoding RNA in the nucleus and a decrease of Nrd1:Nab3 availability, are followed by transcription termination defects.[102] Interestingly, even relatively abundant proteins, such as the poly(A) binding protein (e.g., PABPC1) can be limiting under specific situations. The difference in the amount of protein produced from a short tail reporter mRNA (29 As) and a long tail reporter (139 As) in frog oocytes can be erased by overexpressing PABPC1. Thus, long poly(A) tail RNAs are able to restrict the availability of PABPC1 for shorter tail RNAs, thus limiting translation of these transcripts.[103]

We expect a decrease in NMD efficiency, as observed using a reporter molecule, if large amounts of NMD substrates are generated in a cell. This could occur, for example, in cells with splicing defects and could explain why EJC component depletion can, probably indirectly, affect the stability of an NMD reporter that has no exon-exon junction downstream its stop codon.[48] Thus, NMD phenotypes can be observed through indirect effects that provoke an imbalance in the population of NMD complexes.

Altogether, variations of in the amounts of proteins associated with NMD complexes need careful examination and, if possible, dissection based on RNA association or presence in aggregates (Figure 3). This is a technical and conceptual challenge for future studies of NMD and RNA degradation mechanisms.

ACKNOWLEDGMENTS

This work was funded, in whole or in part, by the Institut Pasteur, CNRS and ANR (grant ANR-18-CE11-0003-04). For the purpose of open access, the author has applied a CC-BY public copyright license to any Author Manuscript version arising from this submission. We thank our colleagues of the Genetics of Macromolecular Interactions laboratory for fruitful discussions.

CONFLICT OF INTEREST

The authors declared no conflict of interest.

DATA AVAILABILITY STATEMENT

Data sharing not applicable to this article as no datasets were generated during the current study.

ORCID

Cosmin Saveanu https://orcid.org/0000-0002-1677-7936

REFERENCES

1. Popp, M. W.-L., Cho, H., & Maquat, L. E. (2020). Viral subversion of nonsense-mediated mRNA decay. *RNA*, *26*, 1509–1518.
2. May, J. P., & Simon, A. E. (2021). Targeting of viral RNAs by Upf1-mediated RNA decay pathways. *Current Opinion in Virology*, *47*, 1–8.
3. Balistreri, G., Bognanni, C., & Mühlemann, O. (2017). Virus escape and manipulation of cellular nonsense-mediated mRNA decay. *Viruses*, *9*, 24.
4. Malabat, C., Feuerbach, F., Ma, L., Saveanu, C., & Jacquier, A. (2015). Quality control of transcription start site selection by Nonsense-Mediated-mRNA Decay. *Elife*, *4*, e06722.
5. Supek, F., Lehner, B., & Lindeboom, R. G. H. (2021). To NMD or not to NMD: Nonsense-mediated mRNA decay in cancer and other genetic diseases. *Trends in Genetics*, *37*, 657–668.
6. Nelson, J. O., Moore, K. A., Chapin, A., Hollien, J., & Metzstein, M. M. (2016). Degradation of Gadd45 mRNA by nonsense-mediated decay is essential for viability. *Elife*, *5*, e12876.
7. Lavysh, D., & Neu-Yilik, G. (2020). UPF1-mediated RNA decay – danse macabre in a cloud. *Biomolecules*, *10*, 999.
8. Kishor, A., Fritz, S. E., & Hogg, J. R. (2019). Nonsense-mediated mRNA decay: The challenge of telling right from wrong in a complex transcriptome. *WIREs RNA*, *10*, e1548.
9. Boehm, V., Kueckelmann, S., Gerbracht, J. V., Kallabis, S., Britto-Borges, T., Altmüller, J., Krüger, M., Dieterich, C., & Gehring, N. H. (2021). SMG5-SMG7 authorize nonsense-mediated mRNA decay by enabling SMG6 endonucleolytic activity. *Nature Communication*, *12*, 3965.
10. Oren, Y. S., Pranke, I. M., Kerem, B., & Sermet-Gaudelus, I. (2017). The suppression of premature termination codons and the repair of splicing mutations in CFTR. *Current Opinion in Pharmacology*, *34*, 125–131.
11. Durand, S., & Lykke-Andersen, J. (2013). Nonsense-mediated mRNA decay occurs during eIF4F-dependent translation in human cells. *Nature Structural & Molecular Biology*, *20*, 702–709.
12. Rufener, S. C., & Mühlemann, O. (2013). eIF4E-bound mRNPs are substrates for nonsense-mediated mRNA decay in mammalian cells. *Nature Structural & Molecular Biology*, *20*, 710–717.
13. Hoek, T. A., Khuperkar, D., Lindeboom, R. G. H., Sonneveld, S., Verhagen, B. M. P., Boersma, S., Boersma, S., Vermeulen, M., Tanenbaum, M. E., & Tanenbaum, M. E. (2019). Single-molecule imaging uncovers rules governing nonsense-mediated mRNA decay. *Molecular Cell*, *75*, 324–339.e11.e11.
14. Maderazo, A. B., Belk, J. P., He, F., & Jacobson, A. (2003). Nonsense-containing mRNAs that accumulate in the absence of a functional nonsense-mediated mRNA decay pathway are destabilized rapidly upon its restitution. *Molecular and Cellular Biology*, *23*, 842–851.
15. Johansson, M. J. O., He, F., Spatrick, P., Li, C., & Jacobson, A. (2007). Association of yeast Upf1p with direct substrates of the NMD pathway. *Proceedings of the National Academy of Sciences of the United States of America*, *104*, 20872–20877.
16. Hogg, J. R., & Goff, S. P. (2010). Upf1 senses 3'UTR length to potentiate mRNA decay. *Cell*, *143*, 379–389.
17. Hurt, J. A., Robertson, A. D., & Burge, C. B. (2013). Global analyses of UPF1 binding and function reveal expanded scope of nonsense-mediated mRNA decay. *Genome Research*, *23*, 1636–1650.
18. Zünd, D., Gruber, A. R., Zavolan, M., & Mühlemann, O. (2013). Translation-dependent displacement of UPF1 from coding sequences

causes its enrichment in 3′ UTRs. *Nature Structural & Molecular Biology*, *20*, 936–943.
19. Kurosaki, T., Li, W., Hoque, M., Popp, M. W.-L., Ermolenko, D. N., Tian, B., & Maquat, L. E. (2014). A post-translational regulatory switch on UPF1 controls targeted mRNA degradation. *Genes & Development*, *28*, 1900–1916.
20. Palazzo, A. F., & Koonin, E. V. (2020). Functional long non-coding RNAs evolve from junk transcripts. *Cell*, *183*, 1151–1161.
21. Wilson, B. A., & Masel, J. (2011). Putatively noncoding transcripts show extensive association with ribosomes. *Genome Biology and Evolution*, *3*, 1245–1252.
22. Xu, Z., Wei, W., Gagneur, J., Perocchi, F., Clauder-Münster, S., Camblong, J., Guffanti, E., Stutz, F., Huber, W., & Steinmetz, L. M. (2009). Bidirectional promoters generate pervasive transcription in yeast. *Nature*, *457*, 1033–1037.
23. van Dijk, E. L., Chen, C. L., d'Aubenton-Carafa, Y., Gourvennec, S., Kwapisz, M., Roche, V., Bertrand, C., Silvain, M., Legoix-Né, P., Loeillet, S., Nicolas, A., Thermes, C., & Morillon, A. (2011). XUTs are a class of Xrn1-sensitive antisense regulatory non-coding RNA in yeast. *Nature*, *475*, 114–117.
24. Marquardt, S., Hazelbaker, D. Z., & Buratowski, S. (2011). Distinct RNA degradation pathways and 3′ extensions of yeast non-coding RNA species. *Transcription*, *2*, 145–154.
25. Thermann, R., Neu-Yilik, G., Deters, A., Frede, U., Wehr, K., Hagemeier, C., Hentze, M. W., & Kulozik, A. E. (1998). Binary specification of nonsense codons by splicing and cytoplasmic translation. *Embo Journal*, *17*, 3484–3494.
26. Cheng, J., Fogel-Petrovic, M., & Maquat, L. E. (1990). Translation to near the distal end of the penultimate exon is required for normal levels of spliced triosephosphate isomerase mRNA. *Molecular and Cellular Biology*, *10*, 5215–25.
27. Hamid, F. M., & Makeyev, E. V. (2016). Exaptive origins of regulated mRNA decay in eukaryotes. *Bioessays*, *38*, 830–838.
28. Decourty, L., Doyen, A., Malabat, C., Frachon, E., Rispal, D., Séraphin, B., Feuerbach, F., Jacquier, A., & Saveanu, C. (2014). Long open reading frame transcripts escape nonsense-mediated mRNA decay in yeast. *Cell Reports*, *6*, 593–598.
29. Singh, G., Rebbapragada, I., & Lykke-Andersen, J. (2008). A competition between stimulators and antagonists of Upf complex recruitment governs human nonsense-mediated mRNA decay. *PLoS Biology*, *6*, e111.
30. Le Hir, H., Gatfield, D., Izaurralde, E., & Moore, M. J. (2001). The exon-exon junction complex provides a binding platform for factors involved in mRNA export and nonsense-mediated mRNA decay. *Embo Journal*, *20*, 4987–4997.
31. Zhu, X., Zhang, H., & Mendell, J. T. (2020). Ribosome recycling by ABCE1 links lysosomal function and iron homeostasis to 3′ UTR-directed regulation and nonsense-mediated decay. *Cell Reports*, *32*, 107895.
32. Annibaldis, G., Domanski, M., Dreos, R., Contu, L., Carl, S., Kläy, N., & Mühlemann, O. (2020). Readthrough of stop codons under limiting ABCE1 concentration involves frameshifting and inhibits nonsense-mediated mRNA decay. *Nucleic Acids Research*, *48*, 10259–10279.
33. Ge, Z., Quek, B. L., Beemon, K. L., & Hogg, J. R. (2016). Polypyrimidine tract binding protein 1 protects mRNAs from recognition by the nonsense-mediated mRNA decay pathway. *Elife*, *5*, e11155.
34. Ruiz-Echevarría, M. J., & Peltz, S. W. (2000). The RNA binding protein Pub1 modulates the stability of transcripts containing upstream open reading frames. *Cell*, *101*, 741–751.
35. Arribere, J. A., & Gilbert, W. V. (2013). Roles for transcript leaders in translation and mRNA decay revealed by transcript leader sequencing. *Genome Research*, *23*, 977–987.
36. Monsellier, E., & Chiti, F. (2007). Prevention of amyloid-like aggregation as a driving force of protein evolution. *Embo Reports*, *8*, 737–742.
37. Jaillon, O., Bouhouche, K., Gout, J.-F., Aury, J.-M., Noel, B., Saudemont, B., Nowacki, M., Serrano, V., Porcel, B. M., Ségurens, B., Mouël, A. L., Lepère, G., Schächter, V., Bétermier, M., Cohen, J., Wincker, P., Sperling, L., Duret, L., & Meyer, E. (2008). Translational control of intron splicing in eukaryotes. *Nature*, *451*, 359–362.
38. Saudemont, B., Popa, A., Parmley, J. L., Rocher, V., Blugeon, C., Necsulea, A., Meyer, E., & Duret, L. (2017). The fitness cost of mis-splicing is the main determinant of alternative splicing patterns. *Genome Biology*, *18*, 208.
39. Celik, A., He, F., & Jacobson, A. (2017). NMD monitors translational fidelity 24/7. *Current Genetics*, *63*, 1007–1010.
40. Kim, D., Lee, J.-Y., Yang, J.-S., Kim, J. W., Kim, V. N., & Chang, H. (2020). The architecture of SARS-CoV-2 transcriptome. *Cell*, *181*, 914–921.e10.
41. Wada, M., Lokugamage, K. G., Nakagawa, K., Narayanan, K., & Makino, S. (2018). Interplay between coronavirus, a cytoplasmic RNA virus, and nonsense-mediated mRNA decay pathway. *Proceedings of the National Academy of Sciences of the United States of America*, *115*, E10157.
42. Hinnebusch, A. G. (2011). Molecular mechanism of scanning and start codon selection in eukaryotes. Microbiol. *Microbiology and Molecular Biology Reviews*, *75*, 434–467.
43. Fritz, S. E., Ranganathan, S., Wang, C. D., & Hogg, J. R. (2020). The RNA-binding protein PTBP1 promotes ATPase-dependent dissociation of the RNA helicase UPF1 to protect transcripts from nonsense-mediated mRNA decay. *Journal of Biological Chemistry*, *295*, 11613–11625.
44. Kishor, A., Ge, Z., & Hogg, J. R. (2019). hnRNP L-dependent protection of normal mRNAs from NMD subverts quality control in B cell lymphoma. *The EMBO Journal*, *38*, e99128.
45. Amrani, N., Ganesan, R., Kervestin, S., Mangus, D. A., Ghosh, S., & Jacobson, A. (2004). A faux 3′-UTR promotes aberrant termination and triggers nonsense-mediated mRNA decay. *Nature*, *432*, 112–118.
46. Behm-Ansmant, I., Gatfield, D., Rehwinkel, J., Hilgers, V., & Izaurralde, E. (2007). A conserved role for cytoplasmic poly(A)-binding protein 1 (PABPC1) in nonsense-mediated mRNA decay. *Embo Journal*, *26*, 1591–1601.
47. Karousis, E. D., Gurzeler, L.-A., Annibaldis, G., Dreos, R., & Mühlemann, O. (2020). Human NMD ensues independently of stable ribosome stalling. *Nature Communications*, *11*, 4134.
48. Zinshteyn, B., Sinha, N. K., Enam, S. U., Koleske, B., & Green, R. (2021). Translational repression of NMD targets by GIGYF2 and EIF4E2. *PLoS Genetics*, *17*, e1009813.
49. Baird, T. D., Cheng, K. C.-C., Chen, Y.-C., Buehler, E., Martin, S. E., Inglese, J., & Hogg, J. R. (2018). ICE1 promotes the link between splicing and nonsense-mediated mRNA decay. *Elife*, *7*, e33178.
50. Alexandrov, A., Shu, M.-D., & Steitz, J. A. (2017). Fluorescence amplification method for forward genetic discovery of factors in human mRNA degradation. *Molecular Cell*, *65*, 191–201.
51. Longman, D., Plasterk, R. H. A., Johnstone, I. L., & Cáceres, J. F. (2007). Mechanistic insights and identification of two novel factors in the C. elegans NMD pathway. *Genes & Development*, *21*, 1075–1085.
52. Longman, D., Jackson-Jones, K. A., Maslon, M. M., Murphy, L. C., Young, R. S., Stoddart, J. J., Hug, N., Taylor, M. S., Papadopoulos, D. K., & Cáceres, J. F. (2020). Identification of a localized nonsense-mediated decay pathway at the endoplasmic reticulum. *Genes & Development*, *34*, 1075–1088.
53. Stevens, A. (1978). An exoribonuclease from Saccharomyces cerevisiae: Effect of modifications of 5′ end groups on the hydrolysis of substrates to 5′ mononucleotides. *Biochemical and Biophysical Research Communications*, *81*, 656–661.
54. Leeds, P., Peltz, S. W., Jacobson, A., & Culbertson, M. R. (1991). The product of the yeast UPF1 gene is required for rapid turnover of mRNAs containing a premature translational termination codon. *Genes & Development*, *5*, 2303–2314.

55. Leeds, P., Wood, J. M., Lee, B. S., & Culbertson, M. R. (1992). Gene products that promote mRNA turnover in Saccharomyces cerevisiae. *Molecular and Cellular Biology*, *12*, 2165–77.
56. Hodgkin, J., Papp, A., Pulak, R., Ambros, V., & Anderson, P. (1989). A new kind of informational suppression in the nematode Caenorhabditis elegans. *Genetics*, *123*, 301–313.
57. Dehecq, M., Decourty, L., Namane, A., Proux, C., Kanaan, J., Le Hir, H., Jacquier, A., & Saveanu, C. (2018). Nonsense-mediated mRNA decay involves two distinct Upf1-bound complexes. *Embo Journal*, *37*, e99278.
58. de Pinto, B., Lippolis, R., Castaldo, R., & Altamura, N. (2004). Overexpression of Upf1p compensates for mitochondrial splicing deficiency independently of its role in mRNA surveillance. *Molecular Microbiology*, *51*, 1129–1142.
59. Huntzinger, E., Kashima, I., Fauser, M., Saulière, J., & Izaurralde, E. (2008). SMG6 is the catalytic endonuclease that cleaves mRNAs containing nonsense codons in metazoan. *RNA*, *14*, 2609–2617.
60. Eberle, A. B., Lykke-Andersen, S., Mühlemann, O., & Jensen, T. H. (2009). SMG6 promotes endonucleolytic cleavage of nonsense mRNA in human cells. *Nature Structural & Molecular Biology*, *16*, 49–55.
61. Gatfield, D., & Izaurralde, E. (2004). Nonsense-mediated messenger RNA decay is initiated by endonucleolytic cleavage in Drosophila. *Nature*, *429*, 575–578.
62. Loh, B., Jonas, S., & Izaurralde, E. (2013). The SMG5–SMG7 heterodimer directly recruits the CCR4–NOT deadenylase complex to mRNAs containing nonsense codons via interaction with POP2. *Genes & Development*, *27*, 2125–2138.
63. Luke, B., Azzalin, C. M., Hug, N., Deplazes, A., Peter, M., & Lingner, J. (2007). Saccharomyces cerevisiae Ebs1p is a putative ortholog of human Smg7 and promotes nonsense-mediated mRNA decay. *Nucleic Acids Research*, *35*, 7688–7697.
64. Lloyd, J. P. B. (2018). The evolution and diversity of the nonsense-mediated mRNA decay pathway. *F1000Res*, *7*, 1299.
65. Kurihara, Y., Matsui, A., Hanada, K., Kawashima, M., Ishida, J., Morosawa, T. Tanaka, M., Kaminuma, E., Mochizuki, Y., Matsushima, A., Toyoda, T., Shinozaki, K., & Seki, M. (2009). Genome-wide suppression of aberrant mRNA-like noncoding RNAs by NMD in Arabidopsis. *PNAS*, *106*, 2453–2458.
66. Causier, B., Li, Z., De Smet, R., Lloyd, J. P. B., Van de Peer, Y., & Davies, B. (2017). Conservation of nonsense-mediated mRNA decay complex components throughout eukaryotic evolution. *Science Reports*, *7*, 16692.
67. Brannan, K. W., Jin, W., Huelga, S. C., Banks, C. A. S., Gilmore, J. M., Florens, L., Washburn, M. P., Van Nostrand, E. L., Pratt, G. A., Schwinn, M. K., Daniels, D. L., & Yeo, G. W. (2016). SONAR discovers RNA-binding proteins from analysis of large-scale protein-protein interactomes. *Molecular Cell*, *64*, 282–293.
68. Hein, M. Y., Hubner, N. C., Poser, I., Cox, J., Nagaraj, N., Toyoda, Y., Gak, I. A., Weisswange, I., Mansfeld, J., Buchholz, F., Hyman, A. A., & Mann, M. (2015). A human interactome in three quantitative dimensions organized by stoichiometries and abundances. *Cell*, *163*, 712–723.
69. Li, S., Wang, L., Fu, B., Berman, M. A., Diallo, A., & Dorf, M. E. (2014). TRIM65 regulates microRNA activity by ubiquitination of TNRC6. *Proceedings of the National Academy of Sciences of the United States of America*, *111*, 6970–6975.
70. Schweingruber, C., Soffientini, P., Ruepp, M.-D., Bachi, A., & Mühlemann, O. (2016). Identification of interactions in the NMD complex using proximity-dependent biotinylation (BioID). *PLoS One*, *11*, e0150239.
71. Youn, J.-Y., Dunham, W. H., Hong, S. J., Knight, J. D. R., Bashkurov, M., Chen, G. I., Bagci, H., Rathod, B., MacLeod, G., Eng, S. W. M., Angers, S., Morris, Q., Fabian, M., Côté, J.-F., & Gingras, A.-C. (2018). High-density proximity mapping reveals the subcellular organization of mRNA-associated granules and bodies. *Molecular Cell*, *69*, 517–532.e11.
72. Kashima, I., Yamashita, A., Izumi, N., Kataoka, N., Morishita, R., Hoshino, S., Dreyfuss, G., & Ohno, S. (2006). Binding of a novel SMG-1–Upf1–eRF1–eRF3 complex (SURF) to the exon junction complex triggers Upf1 phosphorylation and nonsense-mediated mRNA decay. *Genes & Development*, *20*, 355–367.
73. Serdar, L. D., Whiteside, D. L., & Baker, K. E. (2016). ATP hydrolysis by UPF1 is required for efficient translation termination at premature stop codons. *Nature Communication*, *7*, 14021.
74. Neu-Yilik, G., Raimondeau, E., Eliseev, B., Yeramala, L., Amthor, B., Deniaud, A., Deniaud, A., Huard, K., Kerschgens, K., Hentze, M. W., Schaffitzel, C., & Kulozik, A. E. (2017). Dual function of UPF3B in early and late translation termination. *Embo Journal*, *36*, 2968–2986.
75. Chen, Z., Smith, K. R., Batterham, P., & Robin, C. (2005). Smg1 nonsense mutations do not abolish nonsense-mediated mRNA decay in Drosophila melanogaster. *Genetics*, *171*, 403–406.
76. Nelson, J. O., Förster, D., Frizzell, K. A., Luschnig, S., & Metzstein, M. M. (2018). Multiple nonsense-mediated mRNA processes require SMG5 in drosophila. *Genetics*, *209*, 1073–1084.
77. Jonas, S., Weichenrieder, O., & Izaurralde, E. (2013). An unusual arrangement of two 14-3-3-like domains in the SMG5–SMG7 heterodimer is required for efficient nonsense-mediated mRNA decay. *Genes & Development*, *27*, 211–225.
78. Chakrabarti, S., Bonneau, F., Schüssler, S., Eppinger, E., & Conti, E. (2014). Phospho-dependent and phospho-independent interactions of the helicase UPF1 with the NMD factors SMG5-SMG7 and SMG6. *Nucleic Acids Research*, *42*, 9447–9460.
79. Ohnishi, T., Yamashita, A., Kashima, I., Schell, T., Anders, K. R., Grimson, A., Hachiya, T., Hentze, M. W., Anderson, P., & Ohno, S. (2003). Phosphorylation of hUPF1 induces formation of mRNA surveillance complexes containing hSMG-5 and hSMG-7. *Molecular Cell*, *12*, 1187–1200.
80. Page, M. F., Carr, B., Anders, K. R., Grimson, A., & Anderson, P. (1999). SMG-2 is a phosphorylated protein required for mRNA surveillance in Caenorhabditis elegans and related to Upf1p of yeast. *Molecular and Cellular Biology*, *19*, 5943–5951.
81. Okada-Katsuhata, Y., Yamashita, A., Kutsuzawa, K., Izumi, N., Hirahara, F., & Ohno, S. (2012). N- and C-terminal Upf1 phosphorylations create binding platforms for SMG-6 and SMG-5:SMG-7 during NMD. *Nucleic Acids Research*, *40*, 1251–1266.
82. Anders, K. R., Grimson, A., & Anderson, P. (2003). SMG-5, required for C.elegans nonsense-mediated mRNA decay, associates with SMG-2 and protein phosphatase 2A. *Embo Journal*, *22*, 641–650.
83. Nicholson, P., Josi, C., Kurosawa, H., Yamashita, A., & Mühlemann, O. (2014). A novel phosphorylation-independent interaction between SMG6 and UPF1 is essential for human NMD. *Nucleic Acids Research*, *42*, 9217–9235.
84. Denning, G., Jamieson, L., Maquat, L. E., Thompson, E. A., & Fields, A. P. (2001). Cloning of a novel phosphatidylinositol kinase-related kinase: Characterization of the human SMG-1 RNA surveillance protein. *Journal of Biological Chemistry*, *276*, 22709–22714.
85. Durand, S., Franks, T. M., & Lykke-Andersen, J. (2016). Hyperphosphorylation amplifies UPF1 activity to resolve stalls in nonsense-mediated mRNA decay. *Nature Communication*, *7*, 12434.
86. Rowland, M. A., Harrison, B., & Deeds, E. J. (2015). Phosphatase specificity and pathway insulation in signaling networks. *Biophysical Journal*, *108*, 986–996.
87. Muhlrad, D., & Parker, R. (1994). Premature translational termination triggers mRNA decapping. *Nature*, *370*, 578–581.
88. Nagarajan, V. K., Kukulich, P. M., von Hagel, B., & Green, P. J. (2019). RNA degradomes reveal substrates and importance for dark and nitrogen stress responses of Arabidopsis XRN4. *Nucleic Acids Research*, *47*, 9216–30.

89. Lykke-Andersen, J. (2002). Identification of a human decapping complex associated with hUpf proteins in nonsense-mediated decay. *Molecular and Cellular Biology*, *22*, 8114–8121.
90. Nicholson, P., Gkratsou, A., Josi, C., Colombo, M., & Mühlemann, O. (2018). Dissecting the functions of SMG5, SMG7, and PNRC2 in nonsense-mediated mRNA decay of human cells. *RNA*, *24*, 557–573.
91. Cho, H., Kim, K. M., & Kim, Y. K. (2009). Human proline-rich nuclear receptor coregulatory protein 2 mediates an interaction between mRNA surveillance machinery and decapping complex. *Molecular Cell*, *33*, 75–86.
92. Cho, H., Han, S., Choe, J., Park, S. G., Choi, S. S., & Kim, Y. K. (2013). SMG5–PNRC2 is functionally dominant compared with SMG5–SMG7 in mammalian nonsense-mediated mRNA decay. *Nucleic Acids Research*, *41*, 1319–1328.
93. Colombo, M., Karousis, E. D., Bourquin, J., Bruggmann, R., & Mühlemann, O. (2017). Transcriptome-wide identification of NMD-targeted human mRNAs reveals extensive redundancy between SMG6- and SMG7-mediated degradation pathways. *RNA*, *23*, 189–201.
94. Lykke-Andersen, S., Chen, Y., Ardal, B. R., Lilje, B., Waage, J., Sandelin, A., & Jensen, T. H. (2014). Human nonsense-mediated RNA decay initiates widely by endonucleolysis and targets snoRNA host genes. *Genes & Development*, *28*, 2498–2517.
95. Celesnik, H., Deana, A., & Belasco, J. G. (2007). Initiation of RNA decay in Escherichia coli by 5′ pyrophosphate removal. *Molecular Cell*, *27*, 79–90.
96. Deana, A., Celesnik, H., & Belasco, J. G. (2008). The bacterial enzyme RppH triggers messenger RNA degradation by 5′ pyrophosphate removal. *Nature*, *451*, 355–358.
97. Song, M.-G., Bail, S., & Kiledjian, M. (2013). Multiple Nudix family proteins possess mRNA decapping activity. *RNA*, *19*, 390–399.
98. Tibble, R. W., Depaix, A., Kowalska, J., Jemielity, J., & Gross, J. D. (2021). Biomolecular condensates amplify mRNA decapping by biasing enzyme conformation. *Nature Chemical Biology*, *17*, 615–623.
99. Xing, W., Muhlrad, D., Parker, R., & Rosen, M. K. (2020). A quantitative inventory of yeast P body proteins reveals principles of composition and specificity. *Elife*, *9*, e56525.
100. Hubstenberger, A., Courel, M., Bénard, M., Souquere, S., Ernoult-Lange, M., Chouaib, R., Yi, Z., Morlot, J., Munier, A., Fradet, M., Daunesse, M., Bertrand, E., Pierron, G., Mozziconacci, J., Kress, M., & Weil, D. (2017). P-body purification reveals the condensation of repressed mRNA regulons. *Molecular Cell*, *68*, 144–157.e5.
101. Villa, T., Barucco, M., Martin-Niclos, M.-J., Jacquier, A., & Libri, D. (2020). Degradation of non-coding RNAs promotes recycling of termination factors at sites of transcription. *Cell Reports*, *32*, 107942.
102. Castelnuovo, M., Rahman, S., Guffanti, E., Infantino, V., Stutz, F., & Zenklusen, D. (2013). Bimodal expression of PHO84 is modulated by early termination of antisense transcription. *Nature Structural & Molecular Biology*, *20*, 851–858.
103. Xiang, K., & Bartel, D. P. (2021). The molecular basis of coupling between poly(A)-tail length and translational efficiency. *eLife*, *10*, e66493.

How to cite this article: Gilbert, A., & Saveanu, C. (2022). Unusual SMG suspects recruit degradation enzymes in nonsense-mediated mRNA decay Pieces in the puzzle of the role of SMG5/SMG7 heterodimer in activating RNA degradation enzymes during NMD. *BioEssays*, e2100296. https://doi.org/10.1002/bies.202100296

4. Different mechanisms in higher eukaryotes

NMD, as stated previously, is a degradation pathway that depends on translation. Indeed, inhibition of translation either by RNA secondary structures (Belgrader et al., 1993) or chemical compounds (Carter et al., 1995) leads to stabilisation of mRNAs sensitive to NMD. First, this pathway was described as targeting mRNA containing PTC (Losson and Lacroute, 1979) coming from mutations, intron retention (He et al., 1993; Sayani et al., 2008) or frameshifting (Belew et al., 2011). However, thanks to development of sequencing technologies, NMD possesses a more diverse role and degrades transcripts coming from the lack of precision of initiation of transcription. Thus, the possible substrates are RNA containing small ORF upstream the actual start of initiation (uORF, such as DAL7) (Gaba et al., 2005; Guan et al., 2006; Oliveira and McCarthy, 1995; Ruiz-Echevarría and Peltz, 2000; Welch and Jacobson, 1999) or downstream corresponding to internal Transcription Start Site (Malabat et al., 2015). Another source of NMD substrates is pervasive transcription (XUT, SUT). Malabat and colleagues showed that in budding yeast 47% of the genes can generate such RNAs and in fact, NMD can affect 5 to 10% of the transcriptome.

Multiple models explaining NMD mechanism have been developed throughout the organisms, yeast to mammals. All have in common an event that discriminate a premature termination of translation from a normal translation termination.

a. EJC-dependent NMD: SURF/DECID

This model was described more particularly in mammals and came first from the observation that only PTCs located upstream the last exon-exon junction were targeted by NMD (Cheng et al., 1990; Daar and Maquat, 1988) suggesting that events during splicing might help later in the recognition of a PTC. Then, with experiments on both mRNA of the triosephosphate isomerase and of the human β-globin, Zhang and colleagues determined that the minimal distance between the PTC and the last intron to trigger degradation is of 50 nucleotides (Zhang et al., 1998a, 1998b). Analysis of genes from fungi, plants, insects and other organisms allowed the definition of the 50-55 nt rule stating that a stop codon is considered premature if situated 50 to 55 nt upstream an exon-exon junction (Nagy and Maquat, 1998). This rule explains thus that PTCs located in the last exon do not undergo NMD (Hall and Thein, 1994). This distance of 50 nt could be explained by the important steric hindrance of the ribosome and going closer to the splicing site will remove the corresponding Exon Junction Complex (EJC).

EJC binds to mRNA 20 to 24 nt upstream an exon-exon junction during splicing (Le Hir et al., 2000a, 2000b). It is composed of many proteins, but its core is composed of eIF4A3, MLN51, Y14 and Magoh (Andersen et al., 2006; Ballut et al., 2005; Tange et al., 2005). eIF4A3 is a DEAD box helicase that binds to the mRNA allowing binding of other factors of the EJC (Chan et al., 2004; Shibuya et al., 2004). While MLN51 (Barentz in Drosophilae) interacts with N-terminal domain of eIF4A3 to stimulate its activity and enhance its binding to mRNA (Ballut et al., 2005), Y14 and Magoh forms a heterodimer that binds to C-terminal domain of eIF4A3 to, on the contrary, inhibit its activity (Ballut et al., 2005; Kataoka et al., 2000, 2001; Le Hir et al., 2001a). This complex forms thus a platform allowing binding of other proteins to the mRNA and thus permitting multiples cellular processes such as export, localisation, translation or degradation of mRNA (Le Hir et al., 2001b; Tange et al., 2005).

Depletion of EJC factors thanks to siRNA induced inhibition of NMD (Ferraiuolo et al., 2004; Gehring et al., 2003; Shibuya et al., 2004). Furthermore, mutations preventing formation of heterodimer Y14/Magoh led also to inhibition of NMD (Fribourg et al., 2003). Those experiments showed that EJC have a role to play in mammals NMD. In the end, as explained previously, Upf3a and Upf3b interacts with Y14 (Gehring et al., 2003; Kim et al., 2001).

Kashima and colleagues observed the formation of a complex composed of hUpf1, Smg1, eRF1 and eRF3 (eRF corresponds to eukaryotic Release Factor) named SURF. This complex is independent of EJC and forms before binding of Upf1 to the EJC (Kashima et al., 2006). This complex allows phosphorylation of Upf1 and then with binding to EJC, a second complex appears: DECID (Decay inducing complex). Binding of phosphorylated Upf1 to the EJC can happen thanks to Upf2 and/or Upf3 (Ivanov et al., 2008; Kashima et al., 2006). Phosphorylation of Upf1 enhances binding to Smg5/Smg7 heterodimer (Durand et al., 2016). Smg6 is also recruited to Upf1 to initiate degradation through endonucleolytic cleavage (Boehm et al., 2014; Lykke-Andersen et al., 2014).

b. EJC-independent NMD

Even though the EJC-dependent model has been more studied, EJC is not conserved throughout organisms and is not essential for recognition of PTC in *C. elegans*, in *D. melanogaster* and in *S. pombe* (Gatfield et al., 2003; Longman et al., 2007; Wen and Brogna, 2010). In *S. cerevisiae*, the EJC proteins are not present and less than 5% of genes contain an intron (Culbertson and Leeds, 2003). In mammals, important physiological targets of NMD do

not depend on EJC for their degradation by NMD such as the transcript GADD45A (Chapin et al., 2014; Lykke-Andersen et al., 2014).

DSE (Downstream Sequence Element) model

Such as in EJC-dependent degradation pathway, a second signal might be needed to initiate degradation through NMD. In this model, the second signal is a sequence named DSE downstream the PTC where proteins for degradation could bind (Hagan et al., 1995; Hennigan and Jacobson, 1996; Peltz et al., 1993; Zhang et al., 1995). The main protein recognising this sequence is Hrp1 that then interacts with Upf1 and proceed with degradation of mRNA (González et al., 2000). However, this interaction DSE-Hrp1 was only seen on one reporter, PGK1 (González et al., 2000), suggesting that a minority of NMD substrates are concerned by this model.

"Faux" 3'UTR model

In multiple organisms, *S. cerevisiae* (Amrani et al., 2004; Muhlrad and Parker, 1999), *D. melanogaster* (Behm-Ansmant et al., 2007a) and *C. elegans* (Longman et al., 2007), transcripts with a long distance between the PTC and the polyA-tail are degraded through NMD pathway. NMD could thus be dependent on the length of the 3'-UTR. Indeed, this long 3'-UTR could prevent the interaction between eRF3 and Pab1 that normally leads to normal termination and instead induce eRF3 GTP hydrolysis (Amrani et al., 2006; Hoshino et al., 1999; Kononenko et al., 2010). This would be the signal for intervention of NMD factors (Czaplinski et al., 1998; Ivanov et al., 2008; Singh et al., 2008; Wang et al., 2001). Hence, the "Faux" 3'-UTR (Amrani et al., 2004) suggests that the PTC induces an abnormal translation termination context preventing the ribosome from interacting with its usual partner such as Pab1. This abolished or slowed down translation termination is the signal for recruitment of NMD factors and thus degradation of the mRNA (Amrani et al., 2006, 2004). This model evolved with the hypothesis that the mRNA is a closed loop with the interaction of Pab1 with eIF4G. If this site of circularisation is close to the stop codon the translation termination is efficient and occurs normally (Fatscher et al., 2014; Joncourt et al., 2014). However, in the context of a PTC, the stop codon is further from this site and translation termination is slowed down allowing recruitment of the NMD factors.

In budding yeast, to this dependence of the 3'-UTR length is added a dependency of the ORF length (Decourty et al., 2014). This study showed that the stability of an RNA is inversely correlated to the length of the ORF and that a long ORF stabilises NMD substrates.

Detector/Effector mechanism

Recently, a study in yeast (Dehecq et al., 2018) has been able to highlight the formation of two complexes revolving around Upf1 thanks to affinity purification and mass spectrometry. The two complexes are exclusive and are composed as followed: Upf1/2/3 and Upf1/Nmd4/Ebs1/decapping complex (**Figure 5**). Not only did these experiments start to unravel the possible molecular mechanism for EJC-independent pathway, but they also suggest that NMD mechanisms might be more conserved than previously thought.

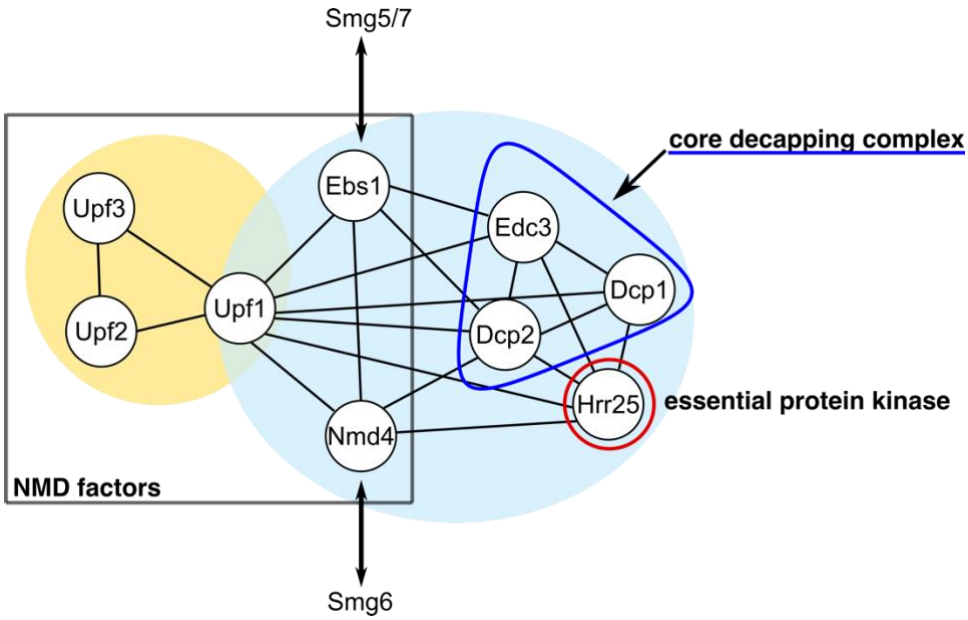

Figure 5: Yeast NMD complexes revolving around Upf1 (Dehecq et al., 2018) and their possible equivalent in mammals.

5. Targets and possible roles of NMD in disease

As mentioned previously, not only does NMD degrade RNA containing PTC, but it affects the regulation of 3 to 10% of the transcriptome in mammals (Mendell et al., 2004; Schweingruber et al., 2013; Tani et al., 2012; Wittmann et al., 2006). This degradation pathway is thus very important in multiple cellular pathways. During maturation of lymphocytes B and T, genes coding for T-cell receptors (TCR) and immunoglobulins must go through multiple rearrangements of their segments (Jung et al., 2006). Sometimes, those rearrangements are not functional. NMD thus intervenes and is essential for maintaining functional TCR and immunoglobulin production (Li and Wilkinson, 1998).

Good regulation of NMD is hence necessary to maintain cellular pathways. As an example, NMD helps regulate Ptbp1 and Ptbp2 (Polypyrimidine-Tract-Binding Proteins 1 and

2) which are splicing regulators (Keppetipola et al., 2012). Indeed, Ptbp1 can regulate itself and its homologue through NMD by changing its alternative splicing (Spellman et al., 2005; Wollerton et al., 2004). This balance between the two proteins is important for neuronal differentiation and thus NMD here is a regulator of this differentiation (Boutz et al., 2007; Makeyev et al., 2007). In the Fragile X syndrome, one of the most common causes of intellectual disability, loss of the fragile X protein (FRMP) FRM1 induces misregulation of NMD and thus delays brain development (Kurosaki et al., 2021).

Moreover, 30% of monogenic diseases are induced by a PTC coming from a mutation, from frameshifting or intron retention (Frischmeyer and Dietz, 1999; Holbrook et al., 2004; Miller and Pearce, 2014). In particular, around 20% of those diseases come from a non-sense mutation (Mort et al., 2008). There are two cases when a PTC appears. Either it escapes NMD and leads to formation of a truncated protein or it is degraded by NMD, and no protein is produced from this allele. In some cases of β-thalassemia, PTC is on the last exon and thus escapes NMD. This non-sense mutation leads to production of a truncated β-globin and association of this version with α-globin forms an unfunctional hemoglobin (Hall and Thein, 1994). In the other case, degradation of the mutated mRNA provokes consequently no production of protein and can thus inactivate expression of the gene. Some forms of cystic fibrosis or Duchenne muscular dystrophy are induced by such mutations leading to silencing of a particular gene (Crawford et al., 2000; Sheppard et al., 1994).

Non-sense mutation can also lead to inactivation of tumor suppressor genes such as TP53, RB1 or PTEN and can favorize development of cancer (Supek et al., 2021). Indeed, mutation of TP53, gene encoding for p53, occurs in 50% of human cancers (Joerger and Fersht, 2007) and around 8% of mutations in this gene are non-sense mutations (Petitjean et al., 2007). Another factor for cancer development is the mutation in NMD proteins (reviewed in Popp and Maquat, 2018) and in particular in Upf1. Indeed, somatic Upf1 mutations could be found in pancreatic adenosquamous carcinoma tumors (Liu et al., 2014) and in lung inflammatory myofibroblastic tumors (Lu et al., 2016).

Hence, understanding the different mechanisms by which NMD can target its substrate and how degradation occurs on a molecular level is relevant to later apprehend how unfunctional NMD can happen and how to correct its dysfunction.

III. Caseine Kinase Hrr25

Affinity purification and mass spectrometry in budding yeast led to the observation of two complexes revolving around Upf1 (Dehecq et al., 2018). During those experiments, two kinases were found in association with the different NMD factors: Hrr25 and CK2. Hrr25 was seen in association with the Upf1-decapping complex (Dehecq et al., 2018). Can yeast NMD also be regulated by a kinase and phosphorylation of NMD factors? (**Table 3**)

S. cerevisiae	*C. elegans*	*H. sapiens*
Upf1 Upf2 Upf3	SMG-2 SMG-3 SMG-4	UPF1 UPF2 UPF3a/b
Nmd4	SMG-6	SMG6
Ebs1	SMG-5 SMG-7	SMG5 SMG7
Possible kinases involved: Hrr25 CK2	SMG-1 (Kinase)	SMG1 (Kinase)

Table 3: Core proteins involved in the NMD mechanisms with new possible functional homologues of Smg5, Smg6, Smg7 and Smg1 in yeast.

1. Identification

Hrr25 belongs to the family of caseine kinase 1 (CK1) (reviewed in Fulcher and Sapkota, 2020). This family was the first kinase family to be discovered (Kumar and Tao, 1975). In human, this family is composed of CK1α, CK1α-like, CK1∂, CK1ε, CK1γ1, CK1γ2, CK1γ3. In *S. cerevisiae*, only four proteins were associated to this family: Yck1, Yck2, Yck3 and Hrr25 (Babu et al., 2004; Hoekstra et al., 1991; Robinson et al., 1993). Hrr25 is closer to CK1∂ and CK1ε and expression of CK1ε can complement a strain depleted in Hrr25 even though it remains sick (Laurent et al., 2019; repeated in the laboratory). Through experiments done *in vitro*, proteins from this family were first thought to be constitutively active (Gross and Anderson, 1998; Knippschild et al., 2005). However, it was later discovered that these enzymes can be activated through direct interaction with cellular proteins (Cruciat et al., 2013). These kinases phosphorylate Serine and Threonine (Ser/Thr) residues on targeted proteins by using

exclusively ATP as a source of phosphate (Flotow et al., 1990; Tuazon and Traugh, 1991). However, Hrr25 has been reported to phosphorylates Tyrosine (Tyr) residues as well (Hoekstra et al., 1994).

In humans, enzymes of the CK1 family are very important for many cellular pathways such as Wnt signalling pathway (Amit et al., 2002; Bryja et al., 2007; Cruciat, 2014; Del Valle-Pérez et al., 2011; Gao et al., 2002; Liu et al., 2002), p53 signalling (Dumaz et al., 1999; Elyada et al., 2011; Huart et al., 2009; Järås et al., 2014; Knippschild et al., 1997; Milne et al., 1992; Winter et al., 2004; Wu et al., 2012), Hippo signalling (Liu et al., 2010; Xu et al., 2014; Zhao et al., 2010), Hedgehog signalling (Chen et al., 2011; Varjosalo and Taipale, 2008), cell division (Behrend et al., 2000; Brockman et al., 1992; Stöter et al., 2005; Wang et al., 2013) and cell death (Brockschmidt et al., 2008; Hanna-Addams et al., 2020; Izeradjene et al., 2004; Lee et al., 2019; Li et al., 2020). CK1∂ and CK1ε have an important part to play in the circadian rhythm (Akashi et al., 2002; Eide et al., 2002; Etchegaray et al., 2009; King and Takahashi, 2000; Meng et al., 2008; Reppert and Weaver, 2002; Takano et al., 2004; Vielhaber et al., 2000). The consensus sequence of phosphorylation for this family are summarized in the following table (**Table 4**).

Sequence	Explanation	Reference
pS/pT-X-X-S*/T*	In –3 position, there is a priming phosphorylation event. X corresponds to any amino acid and S*/T* represents the CK1-phosphorylation residue.	Flotow et al., 1990; Meggio et al., 1992, 1991
D/E-X-X-S*/T*	Acidic amino acid in –3 position and a cluster of acidic residues upstream the phosphorylation site can substitute the priming phosphorylation site.	Agostinis et al., 1989; Flotow and Roach, 1991; Graves et al., 1993; Marin et al., 1994; Pulgar et al., 1999
S-L-S	This sequence needs also a cluster of acidic residues downstream the phosphorylation site. It corresponds to a non-canonical motif.	Knippschild et al., 2005; Marin et al., 2003
K/R-X-K/R-X-X-S/T		Kawakami et al., 2008

Table 4: Sequence of CK1 phosphorylation sites (reviewed in Fulcher and Sapkota, 2020).

2. Functions and targets

The name of Hrr25 comes from "HO and radiation repair". It was first discovered in 1991 (Hoekstra et al., 1991) in a genetic screen to detect genes involved in DNA damage repair after oxidative stress. Since then, Hrr25 has proven to be a multi-functions protein (see **Figure 6**)

with not only a role in DNA damage repair (Ho et al., 1997; Hoekstra et al., 1991) but also in vesicle traffic (Lord et al., 2011), selective autophagy (Nakatogawa, 2015; Pfaffenwimmer et al., 2014; Zientara-Rytter et al., 2018) and meiosis with phosphorylation of Mam1 (Ye et al., 2016) but also of Rec8 (Argüello-Miranda et al., 2017; Katis et al., 2010). More importantly for us, Hrr25 is involved in translation - with the maturation of the 40S subunit and modification of tRNA anticodon - and possibly in transcription termination. Yet, NMD acts on transcripts and is dependent on translation. For better understanding of this study, those three functions of Hrr25 are developed in this chapter.

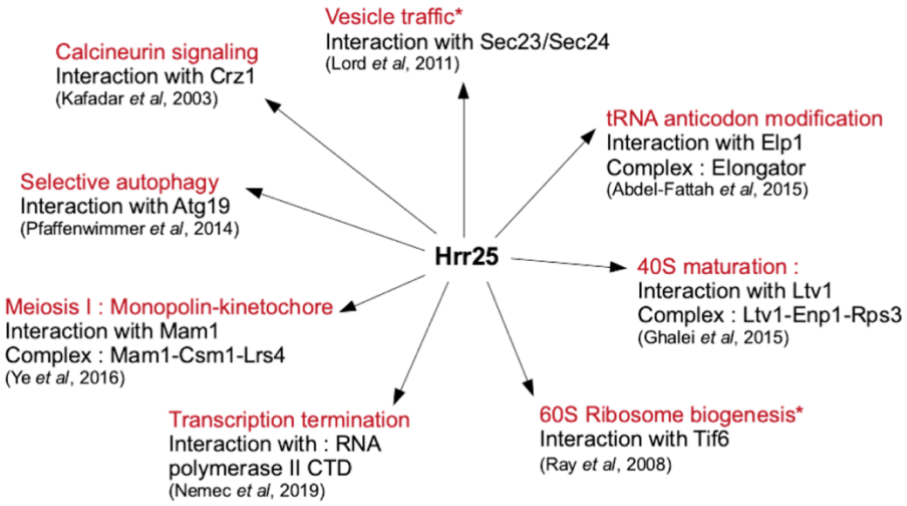

Figure 6: Hrr25 is a multi-functions protein (adapted from BioGRID[1])

a. Pre-40S maturation

Affinity purification using Enp1 in both 90S and 40S fractions coupled then with mass spectrometry allowed to identify proteins specific of the precursors of the 40S ribosomal subunit (Schäfer et al., 2003). In this analysis, Hrr25 was identified only in the 40S fraction (Schäfer et al., 2003). Structural analysis of purified complexes showed that the difference between pre-40S and mature 40S is the formation of a beak (Schäfer et al., 2006). Presence of both Hrr25 and Rio2 suggested that phosphorylation might help regulate maturation of this subunit. Indeed, gel-shift revealed that Enp1, Rps3 and Ltv1 can be phosphorylated by Hrr25 and that a cycle of phosphorylation/dephosphorylation allows changes of protein composition

[1] Available on: https://thebiogrid.org/35980/summary/saccharomyces-cerevisiae/hrr25.html (last viewed the 06/15/2022).

in the pre-40S and later formation of the beak (Schäfer et al., 2006). Finally, the target of Hrr25 has been identified as Ltv1 (Ghalei et al., 2015; Mitterer et al., 2016) thanks to radioactivity and use of the ATP-analogue sensitive mutant hrr25 I82G. Potential phosphorylation sites have been identified: S336, S339, S342, S344, S345 and S346 (Mitterer et al., 2016). Point mutations of these sites prevents normal growth of the cells and double deletion of Hrr25 and Ltv1 rescue growth defect from *hrr25*Δ suggesting that function of Hrr25 in maturation of 40S subunit is the essential function of Hrr25 in yeast. Mechanistic insights of 40S maturation went further and can be described as followed (Mitterer et al., 2019): Ltv1 release needs two signals done in parallel. On one side, interaction of Rps20 with Rio2 leads to hydrolysis of ATP by Rio2. On the other side, interaction of Rps20 with Rps3 leads to recruitment of Hrr25 by Ltv1 and this action disrupts the binding with Enp1 inducing phosphorylation of Ltv1. Once those two actions are done, Ltv1, Hrr25 and Rio2 are released from the pre-40S and maturation can move forward (Mitterer et al., 2019).

b. tRNA anticodon modification

The Elongator complex (reviewed in Glatt et al., 2012b) has long been associated with multiple cellular functions such as histone acetylation (Winkler et al., 2002; Wittschieben et al., 1999), acetylation of α-tubulin and the protein Bruchpilot (Creppe et al., 2009; Miśkiewicz et al., 2011; Solinger et al., 2010) and in yeast, transcriptional silencing, replication-coupled nucleosome assembly (Li et al., 2009) and polarized secretion (Rahl et al., 2005). However, now the main function attributed to this complex is a conserved role in the modification of the wobble uridine in tRNA anticodon for 11 eukaryotic tRNAs (Chen et al., 2009; Huang et al., 2005; Lin et al., 2013; Mehlgarten et al., 2010). This modification consists in addition of 5-methoxycarbonylmethyl (mcm^5), 5-carbamoylmethyl (ncm^5) and 5-methoxycarbonymethyl-2-thio (mcm^5s^2) group to the wobble base position. The Elongator complex is composed of two sub-complexes and each protein is contained in two copies (Glatt et al., 2012a) and is highly conserved throughout eukaryotes (Glatt and Müller, 2013): Elp1/2/3 (Otero et al., 1999) and Elp4/5/6 (Winkler et al., 2001). Elp3 is composed of a lysine acetyl transferase (KAT) domain and a S-adenosylmethionine binding (SAM) domain and its structure shows that those two domains create a tRNA binding pocket and thus form the active site (Glatt et al., 2016).

In addition to the Elp proteins, other factors have been involved in the modification of tRNA. As mutations in the Elp proteins, mutations in those genes led to resistance to a killer toxin secreted by *K. lactis*. Therefore, those genes were named Killer Toxin Insensitive Kti11,

Kti12 and Kti13 (Fichtner and Schaffrath, 2002; Frohloff et al., 2001; Jablonowski et al., 2001b). Kti11 and Kti12 were actually found in interaction with subunits of the Elongator (Fichtner et al., 2003, 2002). Mutations in another gene led to zymocin resistance, Kti14, also known as Hrr25, and found in interaction with Elongator complex (Ho et al., 2002; Huang et al., 2008; Mehlgarten et al., 2009; Mehlgarten and Schaffrath, 2003). Elp1 is a phosphoprotein and its dephosphorylation depends on Sit4 (Jablonowski et al., 2004, 2001a). First, Hrr25 interaction to Elongator through Kti12 (Mehlgarten et al., 2009) was thought to affect Elp1 phosphorylation indirectly through regulation of Sit4 (Mehlgarten et al., 2009). However, Hrr25 seems to phosphorylate Elp1 on sites S1198 and S1202 and this action seems to impact the interaction of Elongator with Kti12 and Hrr25 (Abdel-Fattah et al., 2015).

c. Transcription termination

A universally conserved sequence YSPTSPS throughout the eukaryotes composes the C-terminal repeat domain (CTD) of the largest subunit of the RNA polymerase II (Pol II). This consensus sequence is repeated twenty-six times in yeast and fifty-two times in mammals (Corden et al., 1985). The residues on this sequence are phosphorylated and sequential modification of those amino acids is essential for good timing in recruiting the different factors for transcription initiation, elongation and termination (Corden, 2013; Eick and Geyer, 2013; Zhang et al., 2012). Indeed, unphosphorylated CTD seems to be the only one able to assemble to pre-initiation complexes at the promoter while elongating polymerase II is in a hyperphosphorylated state (Dahmus, 1996, 1995). Four kinases have been involved with phosphorylation of the major sites pSer7, pSer5 and pSer2. Srd10 and Kin28/CDK7 are associated with the process of initiation (Hengartner et al., 1998; Liao et al., 1995) and thus promote transcription (Liu et al., 2004). More particularly, Kin28 can phosphorylate Ser5 and Ser7 for transcription initiation (Akhtar et al., 2009; Feaver et al., 1994) and those marks recruit the capping enzyme complex (Bharati et al., 2016; Cho et al., 1997; Rodriguez et al., 2000; Schroeder et al., 2000). Phosphorylation of Ser5 is also important for downstream process since this modification recruits kinase Bur1/CDK9 (Qiu et al., 2009), which in turn phosphorylates Ser2 (Murray et al., 2001). Once the CTD is hyperphosphorylated, it can then recruit and be phosphorylated at Ser2 by Ctk1/CDK12/13 (Jones et al., 2004). These two last kinases and pSer2 are associated with productive elongation (Cho et al., 2001; Keogh et al., 2003; Lee and Greenleaf, 1997; Murray et al., 2001; Prelich, 2002). In addition, pSer2 is also involved in histone modification, co-transcriptional splicing, and transcription termination since pSer2

helps recruit Pcf11, involved in 3'-end formation (Corden, 2013; Eick and Geyer, 2013; Licatalosi et al., 2002; Phatnani and Greenleaf, 2006; Zhang et al., 2012). To strengthen this regulation by phosphorylation, two phosphatases in yeast have been involved in transcription: Fcp1 and Ssu72 (Chambers and Dahmus, 1994; Chambers and Kane, 1996; Kobor et al., 1999; Krishnamurthy et al., 2004).

Hrr25 has been linked to transcription elongation for two reasons. First, in the context of DNA damage due to methyl methanesulfonate (MMS) or treatment with hydroxyurea (HU), Hrr25 has been involved in mediating the transcriptional response because of its interaction with Swi6 that is also a target of Hrr25 phosphorylation (Ho et al., 1997; Hoekstra et al., 1991). Still in this context, deletion of hrr25 in cells leads to defects in the transcriptional induction of RNR (Ribonucleotide Reductase) gene expression (Ho et al., 1997). Same phenotype in DNA damage response is observed in *ctk1*Δ cells, a kinase of the CTD Pol II (Ostapenko and Solomon, 2003). Then as described previously in this chapter, mutations in Hrr25 (or KTI14) leads to zymocin resistance. This phenotype is also linked to the CTD Pol II and its phosphorylation. Indeed, truncation of the CTD or absence of the four CTD kinases cited previously leads to zymocin hypersensitivity, whereas overexpression of Fcp1 confers zymocin resistance (Jablonowski et al., 2001b; Jablonowski and Schaffrath, 2002; Kitamoto et al., 2002). It was then no surprise to see that Hrr25 interacts with the phosphoCTD Pol II (Phatnani et al., 2004). This binding is direct and requires the CTD to be already phosphorylated (Phatnani et al., 2004).

Another residue can be phosphorylated in the CTD: Thr4. However, its role is less defined. This mark has been involved with 3'end processing of histone mRNA in chicken cells (Hsin et al., 2011), pre-mRNA splicing (Harlen et al., 2016), termination of snoRNA transcripts (Nemec et al., 2017) and progression through M phase (Hintermair et al., 2016). Even though, this modification seems to also have a global role in supporting transcription elongation of protein-coding genes (Hintermair et al., 2012), it seems to target more subset of genes to allow a finer tune of regulation in transcription. In chicken cells and in human cells, the kinase allowing Thr4 phosphorylation has been identified: CDK9 (Hsin et al., 2011) and PLK3 (Hintermair et al., 2012) respectively. In yeast cells, the most active kinase for pThr4 corresponds to Hrr25 (Nemec et al., 2019). Indeed, irreversible inhibition of Hrr25 led to reduced pThr4 levels, a delay in engagement in termination machinery, and snoRNA readthrough suggesting a defect in termination of snoRNA transcripts (Nemec et al., 2019).

IV. Scope of this work

NMD has first been discovered and described in yeast. Yet this organism is no longer considered as the model for the NMD degradation pathway. Indeed, even though it contains the universally conserved Upf proteins, the Smg proteins essential for mammals NMD have no clear equivalent. What's more, the most studied mechanism in mammals for NMD, involves the EJC complex that does not exist in *S. cerevisiae.* This mechanism relies on two proteins complexes (SURF/DECID) and on phosphorylation for recruitment of enzymes responsible for degradation of aberrant RNAs. However, this pathway cannot explain degradation of all NMD substrates in mammals and EJC is not essential for NMD in other organisms such as *C. elegans* and *D. melanogaster*. Recently, a study in *S. cerevisiae* reshuffled the cards on possible conservation mechanisms in eucaryotes (Dehecq et al., 2018). Indeed, thanks to affinity purification coupled to mass spectrometry, the authors showed that Upf1 is the centre of two exclusive proteins complexes named Detector/Effector involving potential functional homologues of Smg7 and Smg6, Ebs1 and Nmd4 respectively. In this study, kinases were also observed in those affinity purification. As explained previously, one of them, Hrr25, has been seen in the Effector complex and thus, seemed particularly interesting.

This thesis aims to continue the work done in this study (Dehecq et al., 2018) but looking more particularly at this casein kinase. Our objectives were to see if Hrr25 has a role to play in yeast NMD and if so, which one. To do so, we used a mutant hrr25 I82G that allows binding to ATP-analogue and thus will be specifically and quickly inhibited. This allows to see the impact of Hrr25 kinase activity inhibition on phenotype of NMD. However, since Hrr25 is involved in many functions and more particularly transcription and translation, it was important to differentiate potential effect on NMD and effects in those cellular mechanisms. The choice of NMD reporter was a challenge to meet all requirements. The choice of experiments was also an issue since phosphorylation is a transient state and as seen in human cells, multiple point mutations are often needed to see effect on the cell (Durand et al., 2016). As we will see later in more details (see Results), we were able to observe that Hrr25 has indeed an impact on yeast NMD and that this function seemed independent of DNA transcription and mRNA translation. One possible target of Hrr25 in NMD context was the C-terminal domain of Upf1 in similar way of Smg1 phosphorylation of Upf1 in mammals (developed in Discussion). This led us to think that NMD might have a mechanism better conserved as previously thought. However, other results showed that timing of regulation in those organisms might differ, and this might

be more complex. Studying yeast NMD can thus give a new perspective on mammals NMD and help understand better the mechanism at play here.

Material and Method

Yeast strains

Saccharomyces cerevisiae strains were derived from BY4741 (mat a) and BY4742 (mat α) strains. The full list of strains used in this study is provided in **Table 9**.

C-terminal TAP-tagged strains came from the collection of systematically built strains (Ghaemmaghami et al., 2003). Deletion strains were part of the systematic yeast gene deletion collection (Giaever et al., 2002) distributed by EuroScarf [2]. Some were built by transformation of BY4741 strain with a cassette containing a selection marker cassette flanked by long recombination arms located upstream and downstream the open reading frame of the gene. Deletions were tested by PCR amplification of the modified locus.

Media and growth conditions

Yeast cells were grown in YPD (Yeast extract Peptone Dextrose)(20g.L^{-1} glucose, 10g.L^{-1} yeast extract, 20g.L^{-1} bacto-peptone, 20g.L^{-1} bactoagar for plates only) and in synthetic media without uracil to select transformants and maintain URA3 plasmids. All yeast strains were freshly thawed from frozen stocks and grown at 30°C.

Bacterial strains were grown in LB media, supplemented with antibiotics – mostly Ampicillin (Ampi) in this study -, when necessary, at 37°C.

Construction of new yeast strains

Principle

The GAL1 promoter region was introduced upstream HRR25 in the yeast genome so that Hrr25 is produced only in presence of galactose, with a strong repression of RNA synthesis when cells are grown in a glucose-containing medium. High efficiency transformation of cells with large amounts of a PCR product that contains regions of identity with the targeted genomic locus allows homologous recombination and insertion of the region of interest together with a selection cassette in the yeast genome. This method of genome modification uses the high rates of double-strand break and homologous recombination that occurs naturally on yeast chromosomes (Aylon and Kupiec, 2004).

We used as template to synthesize the fragment to integrate, the vector pFA6-GAL-HA-KanMX6 (Longtine et al., 1998). This vector contains the cassette KanMX6 which confers

[2] EuroScarf website. Available on: http://www.euroscarf.de (last visited on 26/06/2022).

resistance to geneticin (G418), allowing the selection of the clones that stably incorporated the cassette. Primers for the PCR reaction are composed of two parts: one that anneals with the plasmid template to amplify the cassette (3' tail) and the other one that is homologous with the region of insertion for the cassette (5' tail). Therefore, each end of the PCR product contains a 50 nucleotide-length region that is identical to the region upstream and downstream the annotated ATG of the HRR25 gene respectively. The PCR product inserted upstream the position corresponding to the start codon in the HRR25 mRNA will replace both the original gene promoter and the region corresponding to the 5'-UTR of the mRNA (**Figure 7**).

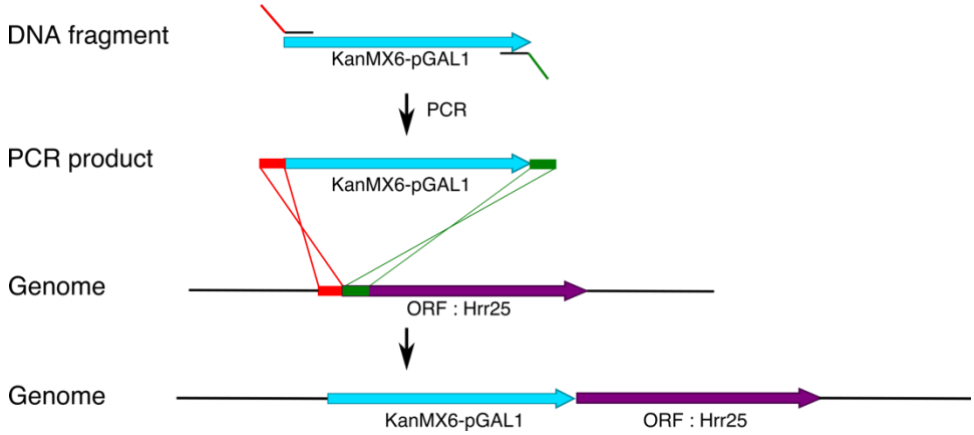

Figure 7: Strategy for the insertion of the GAL1 promoter with a selection marker upstream genomic HRR25 in yeast using homologous recombination.

Clones that are resistant to G418 were further tested to verify that the resistance cassette was inserted at the desired locus by performing a PCR reaction on genomic DNA (protocol below). One of the PCR primers is specific to the cassette introduced and the second one is specific to genomic HRR25, so that amplification of a DNA fragment of known size can only occur if the promoter was inserted upstream HRR25. Since HRR25 is an essential gene, a second validation step for the obtained clones was to test cell growth in a glucose-containing medium.

<u>High efficiency yeast transformation</u>

This protocol was adapted from the protocol established by Schiestl and Gietz, 1989 (Schiestl and Gietz, 1989). For each transformation, dilute an overnight culture to an absorbance of 0.1 at 600 nm in 20 mL of medium YPD. Collect the cells from exponential phase culture (absorbance between 0.4-0.6) by centrifugation. Wash the cells with sterile water and with 0.1M LiCl and 1X TE (TrisHCl 10mM, EDTA 1mM, pH 7.5). Then, resuspend the cells in 50 µL of 0.1M LiCl and 1X TE per transformation. Leave the cells at 30°C for 15 to 30 min. For each

transformation, add 50 µg of DNA carrier previously denatured, around 0.5 µg of plasmid or equivalent for PCR product, 50 µL of cells and 350 µL of PEG4000 LiCl/TE. Mix well. Leave the cells at 30°C for 30 min.

If using a plasmid, leave the cells at 42°C for 20 min. Wash with water and then resuspend the cells in water. Spread the cells on selective medium.

If using a PCR product, an additional step is required since genomic integration of the PCR product is necessary. Thus, add 50 µL of DMSO. Mix well. Leave the cells at 42°C for 20 min. Wash with water and then resuspend the cells in YPD. Leave the cells at 30°C for at least one hour. Collect the cells by centrifugation and resuspend them in water. Then spread the cells on selective medium. Addition of the DMSO increases the frequency of homologous recombination for genomic integration and is not required for the transformation of a replicative plasmid.

DNA extraction from yeast cells

A pellet of cells is resuspended in the extraction buffer (2% Triton X100, 1% SDS, 100 mM NaCl, 10 mM TrisHCl pH 8, 1 mM EDTA). Then, one volume of acid-washed glass beads and one volume of phenol-chloroform pH 8 are added to the suspension. Mixing and lysis are done by vortexing at high speed for 7 minutes. One volume of TE 1X is added and separation of phases is done by centrifugation at maximum speed on a benchtop centrifuge (around 16000 g) for 5 minutes at room temperature. The aqueous phase, corresponding to the upper phase, is collected in a new tube and 1 mL of 100% EtOH is added. Centrifugation for 15 min leads to the formation of a white pellet. The pellet is washed with 70% ethanol. After centrifugation, DNA is resuspended in 1X TE containing 10 ng/mL RNase A.

Construction of plasmids for HRR25 expression

Gibson assembly and cloning strategy

The main objective of building the pGAL1-HRR25 yeast strain was to test complementation with plasmids with different variants of HRR25 and allow, for example, the study of the cells phenotype after specific inhibition of the catalytic activity of Hrr25. Endogenous HRR25 is expressed only in media containing galactose and its expression can be switched off in the presence of glucose.

The vector used to construct these plasmids was pCM189 (Garí et al., 1997). It contains a tetO7 site, codes for a doxycyclin-sensitive transcription activator, and replicates both in yeast, as it contains a chromosomal centromeric region, and in *E. coli* cells. The tetO7 region consists of a repetition of 7 "tet" operator sequences bound by a chimeric transcription activator only in the

absence of doxycycline (DOX). In our case, it is a tetOFF system. If Doxycycline is introduced in the culture medium, transcription initiated at the tetO7 sequence is inactivated and the HRR25 mRNA is no longer produced (Bellí et al., 1998; Garí et al., 1997). We used a variant of Gibson assembly to generate the plasmids. The HRR25 coding sequence was amplified from genomic DNA using specific primers that have homologous regions to the plasmid in their tails. For mutant HRR25, 2 PCR amplifications were performed, which allowed the insertion of desired mutation at specific positions in the HRR25 sequence. The pCM189 vector was linearized using restriction enzymes *BamH*I and *Not*I. The PCR products contained at their 5'-end a region similar to the insertion region in the destination vector together with a *BamH*I site, to allow the possibility of further constructions. The 3'-end of the inserts also contained a region coding for a HA tag in fusion with the Hrr25 section, that will allow detection and quantitation of the produced protein by immunoblot. A mix of linearized plasmid and PCR product was incubated with the T5 exonuclease, leading to partial degradation of one of the strands to allow annealing between the PCR product and pCM189. Phusion DNA polymerase allows to fill the missing nucleotides and ligation occurs once the plasmid is transformed in *E. coli*. The principle of Gibson assembly is illustrated in **Figure 8**.

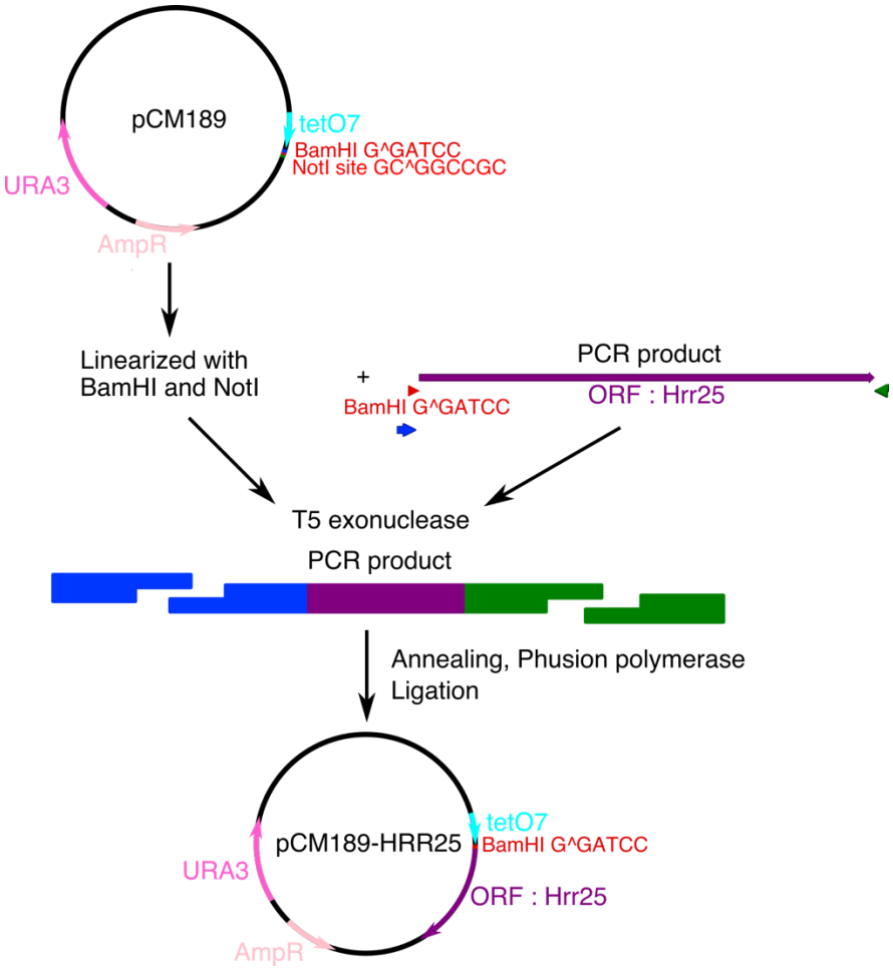

Figure 8: Construction of a pCM189-Hrr25 plasmid using Gibson assembly.

Bacterial plasmid DNA from selected clones is extracted and plasmid construction is checked by enzymatic digestion (*Nco*I in our case, since 2 restriction sites exist in the empty vector while 3 sites are found in the plasmid containing the insert) and sequencing. Once the insert is sequenced, and the vector is validated, it is transformed in wild type (WT) and pGAL1-HRR25 yeast strains.

Technical details for Gibson assembly

To linearize the vector with restriction enzymes 2 µg of the pCM189 plasmid was incubated with *BamH*I (20000 U/ mL) and *Not*I (10000U/ mL) for 1 hour at 37°C, then DNA was extracted with phenol-chloroform and precipitated with a mix of EtOH/NH_4AC. To amplify HRR25 coding sequence, a PCR reaction was performed on genomic DNA extracted from BY4741, a frequently used reference yeast strain. For Hrr25 wild-type only one PCR was needed whereas the introduction of mutations needed two different fragments. The following primers were used:

- Hrr25: AG8:AG9
- *hrr25*-I82G: AG8:AG10 and AG9:AG11
- *hrr25*-K38A: AG8:AG12 and AG9:AG13

The sequences of all oligonucleotides are referenced in the **Table 11**, **Table 12** and **Table 13**. PCR products were loaded on a 1% agarose gel and purified using the Qiaquick gel extraction kit from QIAgen. PCR products were combined with the linearized vector using the Hot Fusion protocol, a variant of Gibson assembly that employs direct transformation of the annealed DNA in bacteria instead of an *in vitro* ligation step, thus making it cheaper and faster (Fu et al., 2014). The product of this reaction was transformed in NEB 10-beta *E. coli* competent cells.

Growth test in a 96-well format

The tested strains are grown to saturation in GAL-URA+DOX to allow normal growth. After centrifugation to collect cells, they are washed with water and diluted to obtain a culture at an absorbance of 0.2. In a transparent 96 wells microplate, introduce 100 µL of the medium to be tested and 5 µL of diluted culture per well so that initial 1 cm absorbance is around 0.01.
Using a Tecan SUNRISE instrument, kinetic measurements are done by reading absorbance at 620 nm (optical filter). The parameters that were found to allow good cell proliferation are: shake mode - Inside, shake intensity - High, shake duration - 570 s, settle 30s, 96 cycles, 10 min between each point and temperature between 29 and 31°C. To test the effect of various concentrations of nucleotide analogues (3MB-PP1), the tested strains are grown overnight in medium lacking uracil. Absence of galactose inhibit production of endogenous Hrr25, and absence of Doxycycline allows expression of Hrr25 from the plasmid. After centrifugation, the cells are resuspended in medium lacking uracil to an absorbance of 0.2. The first concentration of the tested media is medium lacking uracil to keep selectivity with 5 µM 3MB-PP1 then 6 dilutions by 2 of the inhibitor are performed in series. Since 3MB-PP1 is diluted in DMSO, the same amount of DMSO is introduced in medium lacking uracil and the same dilutions are performed. In a transparent 96 wells microplate, introduce 100 µL of medium to be tested and 5 µL of diluted culture per well so that absorbance is around 0.01.
Using the Tecan infinite M200 plate reader, absorbance is measured every 2-3 hours and cells are left to grow overnight. An endpoint measure is taken after 30 hours of growth at 30°C.

Serial dilutions for growth test on plates

Serial dilutions of a cell culture are deposited on a culture plate and incubated for various periods of time at one or several temperatures. Before performing the test, Petri dishes with the

required medium must be prepared. An overnight saturated culture is diluted to an approximate absorbance (600 nm) of 0.2-0.4. Five serial dilutions by 10 are done. From those dilutions, 4 µL are layered on top of the medium. The serial dilutions ensure the presence of individual colonies that can help in estimating growth and homogeneity of the population of yeast cells.

Point genomic mutations:

The method used come from Erdeniz, Mortensen and Rothstein, 1997 (Erdeniz et al., 1997). In order to introduce the three desired point mutations in Upf1, S869A, S884A and S887A, the PCRs were performed using the following oligonucleotides: AG67/AG68, CS1199/CS1200, CS1201/CS1202. The sequences of all oligonucleotides are referenced in the **Table 11**, **Table 12** and **Table 13**. The templated used are the following: 1715, plasmid containing the Upf1 sequence with the mutations S884A and S887A, and 1328, containing the URA K. lactis sequence. The different plasmids are referenced in **Table 10**. The desired PCR products were transformed in LMA5463 (Upf1-HA) and BY4741 using the high efficiency yeast transformation protocol. DNA of transformants was verified by PCR with primers CS1218 and CS1213 and sequenced with primer CS1218. Valid transformants were then spread on 5FOA to induce removal of URA sequence. The DNA of clones present on 5FOA plates were verified by PCR with primers CS1218/CS1217, sequenced with primers CS1217/CS1218 and the produced protein was observed through WB.

RT-qPCR

From an overnight culture, dilute cells in 50 mL of selective medium per condition to test to have a 600 nm absorbance of 0.15. Wait so that the cells are at exponential growth phase – 0.4 to 0.6 600 nm absorbance. Then aliquot the culture per 50 mL, introduce the drug of interest – 3MB-PP1 5µM final or Cycloheximide (CHX) 50 µg/mL final - or the control (DMSO) and collect cells at the end of the incubation time – 30 min. Wash pellet with water. Resuspend the cells in 400 µL TES RNA Buffer (10 mM TrisHCl pH 7.4, 10 mM EDTA, 0.5% SDS). Add 400 µL phenol-chloroform. Heat at 65°C during 30 min mixing from time to time (1400 rpm 30s mix 30s rest). Put on ice 5 min, collect lysate, corresponding to the upper phase, at 4°C. Repeat at room temperature the phenol-chloroform extraction 3 times in total. Then 1 time with only chloroform. The final upper phase, add 1 mL EtOH/NH_4OAc (85/15). Mix well. Leave at -20°C at least 30 minutes. Collect the precipitate by centrifugation 4°C at least 15 minutes maximum speed. Wash twice with 70% EtOH. Resuspend RNA in 100µL H_2O.

The obtained RNA is treated with DNase to get rid of any remaining trace of DNA. Per reaction, use 10 µg of RNA, 1µL Turbo DNase, 5µL Buffer 10X and complete with H_2O up to 50µL.

The reaction is incubated at 37°C for 30 min. Complete with H_2O up to 200 µL. Then add 1 volume of phenol/chloroform. Vortex well. Centrifuge 5 min maximum speed at room temperature. Transfer the upper phase to a new tube and add 2µL Linear acrylamide (20µg) with EtOH/NH_4OAc (3.5X the sample volume). Vortex well. Leave at -20°C at least 30 minutes. Collect the precipitate by centrifugation 4°C at least 15 minutes maximum speed. Wash twice with 70% EtOH. Resuspend RNA in 10 µL H_2O.

Reverse transcription:

This experiment is performed in 500 µL tubes for PCR machines. It is composed of two steps with two different mixes:

- Mix 1: 1µg RNA, 0.3µL Mix oligonucleotide 100µM, 2µL FSB 5X QSP H_2O to 10 µL;
- Mix 2 (introduced in step 3 from the PCR program): 2 µL FSB 5X, 2 µL DTT 0.1M, 1 µL dNTP 10 mM, 0.5µL SuperScript III QSP H_2O to 10 µL.

The PCR program is the following (**Table 5**):

Temperature (°C)	80	65	42 (Mix 2)	42	70	10
Time (min)	5	10	10	20	10	Infinite

Table 5: PCR program used for the Reverse transcription using SuperSript III enzyme.

qPCR using SYBR Green

The cDNA samples obtained with reverse transcription are diluted 4 times in series with 1/8 as dilution factor. For a well and corresponding to one target, the mix used is: 3 µL cDNA, 10 µL 2X BioRad, 1.25µL 20µM Primer fw, 1.25 µL 20µM Primer rv, QSP H_2O to 20 µL.

The qPCR program used is the following (**Table 6**):

Temperature (°C)	95	95 60	95 65 95
Time	2 min	30s 45s x40	5s 5s 5C

Table 6: qPCR program used.

Affinity purification

Principle:

In my host laboratory, several strains expressing proteins of interest for NMD, such as Upf1 and Dcp1, in fusion with the TAP tag (Rigaut et al., 1999) are available. This tag contains 3 domains:

- Protein A region, composed of two repeats of the *S. aureus* protein A fragments that binds Fc of the IgGs.
- TEV cleavage site. This domain can be cleaved by a specific endoprotease - TEV (Tobacco Etch Virus protease) - to elute the proteins.
- Calmodulin Binding Peptide (CBP): affinity domain. This domain binds calmodulin in the presence of Ca^{2+} and thus allows a second purification after cleavage by the TEV enzyme.

To purify the tagged proteins and the associated factors, cells are lysed using a French press or vortexing with glass beads. The obtained lysate is then mixed with magnetic beads on which IgG are fixed. Protein A at the end of the TAP-tag is recognized by the constant domain of the IgG fixed on the beads custom-made by chemical coupling of IgG to activated paramagnetic beads.

Hence, during washing of the beads only proteins tagged, and their associated proteins will be retained. Other proteins will be in the supernatant and will thus be washed away. The principle of affinity purification with TAP-tag is illustrated in **Figure 9**.

Functional tests can then be performed directly on the beads. Otherwise, elution of the proteins bound on the beads can be performed either by cleaving with the TEV protease, by using high salt concentration, or a denaturing agent such as SDS (Sodium Dodecyl Sulfate). Once eluted, presence of the proteins of interest can be checked by Western Blot (WB) using PAP (Peroxidase Anti-Peroxidase) complex for TAP-tag or anti-HA antibodies (if a second control protein tagged with the HA tag was present in the tested cells).

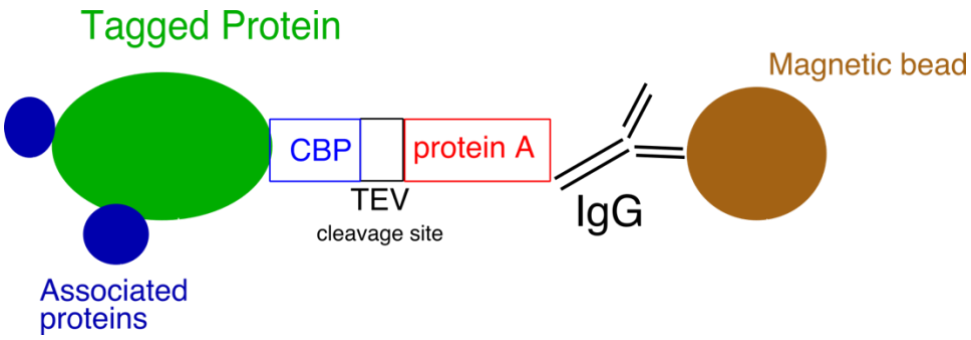

Figure 9: Affinity purification using TAP and IgG magnetic beads.

Purification:

A typical purification starts with 2 litres of yeast culture in YPD medium at mid-log growth phase, at 600 nm absorbance around 2. Collect cells by centrifugation for 10 minutes at 3000 rpm (4°C). Recover the pellets by vortexing with cold water and recentrifuge the cells. The cells can be stored frozen at -80°C.

Thaw rapidly the cells, add an equal volume of Lysis Buffer (100mM KoAc, 20mM HEPES pH 7.4 and for 50 mL solution 2 tablets of Roche complete protease inhibitor) and homogenize. Two different methods:

- Magnalyser: transfer in cryotubes with 500 µL acid washed beads. 2 times 90s 4000 rpm. Then centrifuge 15 min 4°C maximum speed.
- FastPrep: transfer to a new 50-mL Falcon tube with 1 Volume of acid washed beads. Program yeast/S. Cerevisiae twice. Then centrifuge 20 min 4°C maximum speed.

Decant the supernatant to 15- or 50-mL Falcon tubes.

Equilibrate 15µL suspension of IgG magnetic beads (Dynabeads M270 Epoxy)/purification in binding buffer (100 mM KoAc, 20 mM HEPES pH 7.4 and 0.5% Triton-X100).

Keep a fraction of the extract as "input". Add 15µL of IgG Dynabeads suspension equilibrated into binding buffer (can be resuspended in 100 µL for easier pipetting). Mix and incubate at 4°C for at least 30 minutes on a rotating wheel. The IgG Dynabeads are collected by transferring the tube to a rack exerting a magnetic field. It pulls the beads to the tube walls, allowing the complete removal of the supernatant. Add 1mL of washing buffer on the beads, transfer the beads to a 1.5 mL Eppendorf tube. Transfer the Eppendorf tube containing the beads to the rack exerting a magnetic field. Discard the supernatant carefully with 1 mL tip. Repeat this washing step four times using 1 mL of washing buffer (or binding buffer) - total five washes. Each time, resuspend the beads by gently inverting the tube several times. Proceed with elution.

Elution:

Add 100µL Tris-EDTA pH 7.5, SDS 2%. Incubation 10 min at 65°C. Then collect supernatant thanks to magnetic rack.

Mass spectrometry: purify extract through methanol/chloroform protocol (Wessel and Flügge, 1984).

Add 4 volumes of Methanol. Vortex well. Add 1 volume of Chloroform. Vortex well. Add 3 volumes of H_2O. Vortex for at least 1 min. Centrifuge 15 to 30 min at 4°C 13000 rpm. Remove the upper phase – be careful to not touch the interphase. Add 3 volumes of Methanol. Vortex

well. Transfer the solution to Eppendorf Lowbind 1.5 mL. Leave 10 min on ice or overnight at -20°C. Centrifuge 10 to 20 min at 4°C maximum speed. Eliminate supernatant carefully. Air dry 5 min at room temperature. Keep the sample at -20°C dry.
WB: to 20µL purification, add 6 µL SB4X and for 3µL input, add 15 µL SB4X

Kinetics test

Experiment:
Plasmid 1490 bears an NMD substrate sequence whose expression is under the control of a tetOFF system.
Strains used with plasmid 1490:

- BY4741
- LMA5096: hrr25 I82G

From an overnight culture at 30°C, dilute the cells in 30mL of selective medium per kinetic point for each condition to have a 600 nm absorbance of 0.2. Incubate at 25°C 180 rpm so that the cells are at exponential phase – 0.4 to 0.6 600 nm absorbance. Collect a certain volume of cells in order to have approximately the same number of cells per condition. Centrifuge 5 min at 3500 rpm room temperature. Eliminate supernatant and resuspend the cells in 60 mL selective medium. Dispatch 30 mL per strain in two different Erlenmeyer and incubate them with either DMSO or 5 µM 3MB-PP1 for 15 minutes at 180 rpm. Then dispatch 5 mL per condition in a 24 wells plate and add 100 µL Doxycycline 500 µg/mL (10µg/mL final) for the first time point – 30 minutes – and continue to do so for each time point until end of incubation. 3 minutes before incubation, centrifuge the plate 3 minutes at maximum speed room temperature. Eliminate the supernatant and dip the bottom of the plate in dry ice and EtOH (approximate temperature -60°C). Store at -80°C.
Resuspend the cells in 400 µL TES RNA Buffer (10 mM TrisHCl pH 7.4, 10 mM EDTA, 0.5% SDS). Transfer to an Eppendorf tube containing already 400 µL phenol-chloroform. Heat at 65°C during 30 min mixing from time to time (1400 rpm 30s mix 30s rest). Put on ice 5 min, collect lysate, corresponding to the upper phase, at 4°C. Repeat at room temperature the phenol-chloroform extraction 3 times in total. Then 1 time with only chloroform. The final upper phase, add 1 mL EtOH/NH_4OAc (85/15). Mix well. Leave at -20°C at least 30 minutes. Collect the precipitate by centrifugation 4°C at least 15 minutes maximum speed. Wash twice with 70% EtOH. Resuspend RNA in 100µL H_2O.
The obtained RNA is treated with DNase to get rid of any remaining trace of DNA. Per reaction, use 10 µg of RNA, 1µL Turbo DNase, 5µL Buffer 10X and complete with H_2O up to 50µL.

The reaction is incubated at 37°C for 30 min. Complete with H_2O up to 200 µL. Then add 1 volume of phenol/chloroform. Vortex well. Centrifuge 5 min maximum speed at room temperature. Transfer the upper phase to a new tube and add 2µL Linear acrylamide (20µg) with EtOH/NH_4OAc (3.5X the sample volume). Vortex well. Leave at -20°C at least 30 minutes. Collect the precipitate by centrifugation 4°C at least 15 minutes maximum speed. Wash twice with 70% EtOH. Resuspend RNA in 10 µL H_2O.
Follow protocol of RT-qPCR as stated previously with the following target:

- Transcript 1490: AG45/46
- PGK1: CS1020/1021
- ALA1: CS1038/1039

The sequences of all oligonucleotide are referenced in the **Table 11**, **Table 12** and **Table 13**.

Western Blot

The first for a Western is to perform a protein gel. According to the resolution wanted, we used two types of gel:

- Nupage 4% to 12%, 1X MOPS 100 to 150 Volts
- Gel 6% polyacrylamide (**Table 7**): 1X Electrophoresis Buffer (25 mM Tris, 200 mM Glycine and 0,1% SDS) up to 180V

Gel 6% (Vf = 10 mL)		Gel stacking (Vf = 5 mL)	
Acrylamide/bis (Proteogel)	2 mL	Acrylamide/bis (Proteogel)	0.75 mL
Buffer 4X pH 8.8	2.5 mL	Buffer 4X pH 6.8	1.25 mL
Teemed	10 µL	Teemed	5 µL
APS 10X	100 µL	APS 10X	50 µL
H_2O	5.4 mL	H_2O	2.95 mL

Table 7: Composition of the gel 6% (on the left) and of the stacking gel (on the right).

Then the gel was transferred on a nitrocellulose membrane using the semi-dry BioRad system (Transfer blot Turbo). The program used is List, BioRad, 1 minigel, High MW then RUN. For the blocking step, the membrane is immersed for at least 30 min in a 5% milk in PBST solution. The dilution and time used for the different antibodies are the following (**Table 8**):

Antibody	Dilution	Time
PAP	1/ 2,000	30 minutes
Anti-HA	1/ 1,000	Between 30 minutes and 2 hours
G6PDH	1/ 50,000	1 hour
NOG1	1/ 1,000	1 hour
Anti-Rabbit	1/ 10,000	30 minutes

Table 8: Dilution and incubation time used in this study according to the antibody used.

AID (Auxin-inducible degradation) system

This system is based on the two different proteins, TIR1 from *O. sativa* and IAA17 (Li et al., 2019). Indeed, the domain miniAID from the protein IAA17 is recognised by the drug Auxin. Auxin first binds to TIR1 and can thus target the protein containing this miniAID domain for ubiquitination and then degradation by the proteasome. To create auxin-inducible degron strains, the indicated genes were C-terminally tagged with a polyG-3Flag-miniAID-kanMX6 cassette amplified by PCR using plasmid 1451 as a matrix (see **Table 10**).

Sucrose gradients and polysomes profiling

Strains used:

- Upf1-HA
- Upf1-HA, *ebs1*Δ
- Upf1-HA, hrr25 I82G

Solutions:

- *1000X CHX:* 250mg in 5 mL EtOH for a final concentration of 50mg/mL
- *Lysis Buffer:* 20mM HEPES pH 7.4, 100 mM KOAc, 10 mM $MgCl_2$, 50 µg/mL CHX and for 50 mL final volume, add 1 table of protease inhibitors.
- *Lysis Buffer 2:* 10 mL Lysis Buffer with 1 tablet of Pierce phosphatase inhibitor.

Protocol:

From a 200 mL of cells culture in exponential phase, that is an absorbance between 0.4 and 0.6, add 200µL from 1000X CHX. Mix well the culture then transfer the culture in cold bucket centrifuge. Centrifuge 10 min at 4000 x g at 4°C. Resuspend the cells in 10 mL Lysis Buffer and transfer to a 15 mL tube. Centrifuge 5 min at maximum speed at 4°C. Resuspend the cells in 400 µL Lysis Buffer 2 and transfer the cells in a cryotube with 500 µL acid washed beads. Magnalyser: 3 times 1 min at 3000. Centrifuge 5 min at 16000 x g at 4°C. Transfer the

supernatant in an Eppendorf tube and centrifuge once again. Transfer the supernatant to a new tube.

Measure the Optical Density (OD) from a 1/500 dilution at 260 nm with a quartz tub. Then aliquot the sample. Either store the sample at -80°C or proceed with the protocol. For each sample, 10 uOD of total extract is carefully introduce on the surface of tube containing the 10-50% sucrose gradient with Lysis Buffer HEPES/KOAc. Each gradient must be equilibrated two by two with their pot and cap. Ultracentrifugation: 39 000 rpm, 2 hours and 45 minutes at 4°C with acceleration and deceleration at maximum level.

Collection of fractions using Fluorinert, an immiscible organic fluid with high density. Time between each fraction: 30 seconds. Output used: 11.5. Number of fractions obtained: around 24.

Extraction of proteins:

100 µL of each fraction are pooled down two by two. Add 40 µL TCA 40% and 3.3 µL Na deoxycholate (carrier). Vortex for 10 seconds then leave on ice for 5 min. Centrifuge 20 min at maximum speed at 4°C. Eliminate carefully the supernatant. Clean with EtOH 95% cold. Centrifuge once again 20 sec. Air dry for 10 min. Resuspend in 30 µL SB2X. Store at -20°C.

Mass spectrometry

Protein samples were treated with Endoprotease Lys-C (Wako) and Trypsin (Trypsin Gold Mass Spec Grade; Promega). Peptide samples were desalted using OMIX C18 pipette tips (Agilent Technologies). The peptides mixtures were analysed by nano-LC-MS/MS using an Ultimate 3000 system (Thermo Fisher Scientific) coupled to an LTQ-Orbitrap Velos mass spectrometer or LTQ-Orbitrap XL (Thermo Fisher Scientific). Peptides were desalted on-line using a trap column (C18 Pepmap100, 5µm, 300µmÅ~5mm (Thermo Scientific)) and then separated using 120min RP gradient (5–45% acetonitrile/0.1% formic acid) on an Acclaim PepMap100 analytical column (C18, 3µm, 100., 75µm id x 150mm, (Thermo Scientific)) with a flow rate of 0.340µL.min−1. The mass spectrometer was operated in standard data dependent acquisition mode controlled by Xcalibur 2.2. The instrument was operated with a cycle of one MS (in the Orbitrap) acquired at a resolution of 60,000 at m/z 400, with the top 20 most abundant multiply-charged (2+ and higher) ions subjected to CID fragmentation in the linear ion trap. An FTMS target value of 1e6 and an ion trap MSn target value of 10000 were used. Dynamic exclusion was enabled with a repeat duration of 30s with an exclusion list of 500 and exclusion duration of 60s. Lock mass of 445.12002 was enabled for all experiments.

Analysis used the following software: MaxQuant and Perseus.

This protocole has been adapted from the general protocol described in Namane and Saveanu, 2022 (Namane and Saveanu, 2022).

RNA sequencing

Cell culture conditions:

Strains used:

- BY4741
- LMA5096: hrr25 I82G
- LMA5334: Nam7-degron

From an overnight culture, dilute cells in 50 mL of YPD per condition to test to have a 600 nm absorbance of 0.15. Wait so that the cells are at exponential phase – 0.4 to 0.6 600 nm absorbance. Then aliquot the culture per 50 mL. For the first two strains the cultures are treated with either 3MB-PP1 5µM final or the control DMSO. As for the last strain, the cultures are treated with either IAA 0.1mM final or with the control EtOH. Collect cells at the end of the incubation time – 30 min.

Total RNA extraction:

Resuspend the cells in 400 µL TES RNA Buffer (10 mM TrisHCl pH 7.4, 10 mM EDTA, 0.5% SDS). Add 400 µL phenol-chloroform. Heat at 65°C during 30 min mixing from time to time (1400 rpm 30s mix 30s rest). Put on ice 5 min, collect lysate, corresponding to the upper phase, at 4°C. Repeat at room temperature the phenol-chloroform extraction 3 times in total. Then 1 time with only chloroform. The final upper phase, add 1 mL EtOH/NH_4OAc (85/15). Mix well. Leave at -20°C at least 30 minutes. Collect the precipitate by centrifugation 4°C at least 15 minutes maximum speed. Wash twice with 70% EtOH. Resuspend RNA in 100µL H_2O.

Removal of rRNA:

This step was performed using the kit RiboMinus™ with the protocol recommended by the supplier. I used 10 µg of my total RNA sample and completed it at 20µL. The protocol consists of a hybridisation step using the RiboMinus™ probe, at 37°C for 5min and then on ice for at least 30s. Then removal of the rRNA could be performed with the RiboMinus™ magnetic beads previously prepared. Incubation of the sample with those beads at 37°C for 15min. Magnetic stand allows to collect the supernatant free of rRNAs. Then precipitation of RNAs was performed still using the recommendations of the supplier. RNA samples were precipitated with 20µg glycogen, 1/10th sample volume of 3M sodium acetate and 2.5X sample volumes of 100% EtOH placed at -20°C for at least 30min. The pellet was collected by centrifugating at 4°C at

least 15 min at maximum speed. The pellet was washed twice with EtOH 70%. RNAs were resuspended in 10 µL H_2O.

Sequencing:

We used the Kit TruSeq Illumina (kit B for the index) with the protocol Low Sample protocol. We followed strictly this protocol except for the first step. The latter is a purification of the samples using the poly-A tail. This step is not used here. Thus, the protocol starts directly with the fragmentation step.

The index used were the number 1, 3, 8, 9, 10, 11, 20, 21, 22, 23, 25 and 27. To determine the final amount of each sample to have a final concentration of 2 nm the KAPA Library Quantification kit was used.

Analysis:

Demultiplexing: on the **Institut Pasteur's cluster**.

```
module load bcl2fastq/2.20.0
srun -q fast -p dedicated -c 8 bcl2fastq  \
   -p 8 --barcode-mismatches 0 \
   --intensities-dir ./220110_NB501291_0426_AHY3KGBGXK/Data/Intensities \
    --sample-sheet 20220322_demultiplexagesheet_RNAseq.txt  \
    --runfolder-dir ./220110_NB501291_0426_AHY3KGBGXK \
    --ignore-missing-controls  \
    --no-bgzf-compression  \
    --ignore-missing-bcls  \
    --no-lane-splitting  \
    --output-dir Fastq_Nextseq20220323
```

Sample sheet: 20220322_demultiplexagesheet_RNAseq.txt

```
[Header]
IEMFileVersion,4
Investigator Name,aggilber
Experiment Name,220110_NB501291_0426_AHY3KGBGXK
Date,23/03/2022
Workflow,GenerateFASTQ
Application,FASTQ Only
Assay,RNAseq
Description,
```

Chemistry,Default
[Reads]
75
150
[Settings]
ReverseComplement,1
Adapter,GTGACTGGAGTTCAGACGTGTGCTCTTCCGATCT
[Data]
Sample_ID,Sample_Name,Sample_Plate,Sample_Well,I7_Index_ID,index,Sample_Project,Description
A,BY4741_D2,,,AD001,ATCACG,20220111_AG_RNAseq,
B,BY4741_3MB2,,,AD003,TTAGGC,20220111_AG_RNAseq,
C,5096_D2,,,AD008,ACTTGA,20220111_AG_RNAseq,
D,5096_3MB2,,,AD009,GATCAG,20220111_AG_RNAseq,
E,5334_EtOH2,,,AD010,TAGCTT,20220111_AG_RNAseq,
F,5334_IIA2,,,AD011,GGCTAC,20220111_AG_RNAseq,
G,BY4741_D3,,,AD020,GTGGCC,20220111_AG_RNAseq,
H,BY4741_3MB3,,,AD021,GTTTCG,20220111_AG_RNAseq,
I,5096_D3,,,AD022,CGTACG,20220111_AG_RNAseq,
J,5096_3MB3,,,AD023,GAGTGG,20220111_AG_RNAseq,
K,5334_EtOH3,,,AD025,ACTGAT,20220111_AG_RNAseq,
L,5334_IIA3,,,AD027,ATTCCT,20220111_AG_RNAseq,

Use of the **Galaxy server** for data analysis

Commands:

- **FastQC:ReadQC**: this command takes as input the file .fastq.gz and gives as output a report on the quality of the data.
- Trimming using **AlienTrimer**: this allows removal of the adapter for the sequencing on the reads of the fastq data.
- Mapping using **RNA STAR**: this mapping allows production of the bam file.
- **Bowtie2**: gives the percentage of reads for rRNA to know the contamination of our samples.

- **featureCounts**: this command takes as input the bam file and gives as output the table with counts of reads for each transcript. The format output for SARTools DESeq2 must be put on TRUE, Specify strand information on Stranded (Forward), GFF feature type filter on gene, Allow reads to map to multiple features -O –M
- **Preprocess files for SARTools**: two preprocessing were made for two different analyses
    - One with all the replicates but with a blocking factor: day
    - One with only replicate 2 and 3 but with no blocking factor
- **SARTools DESeq2 (Love et al., 2014)**: Statistical analysis using BH as the method for p-value adjustment. Two were made as two different preprocess:
    - All replicates: factor of interest on group, Reference biological condition on BYD (WT strain with DMSO), Adding a blocking factor with batch as factor.
    - Only replicate 2 and 3: factor of interest on group, Reference biological condition on BYD (WT strain with DMSO), Adding a blocking factor on NULL.
- **Biwig**: to obtain wig and thus allowing visualisation on Integrative Genomics Viewer (IGV).
    - Normalisation: RPKM

Files used:

- adapt.fa: files with the adapters from the truseq kit from illumina.
- Saccharomyces_cerevisiae.R64-1-1.dna.toplevel.fa: genome file from ensembl.
- ScGFF2GTF_final14.gtf: counting file produced by my supervisor Cosmin Saveanu and processed by our colleague Emmanuelle Permal to be used on Galaxy.
- results32723.fa: file containing the sequence of rRNAs from YeastMine from SGD. It has been produced thanks to the tool Queary builder and the parameters chosen so that it contains a brief description of the rRNA and its sequence.

Efficient yeast nonsense-mediated mRNA decay (NMD) involves the protein kinase Hrr25

In this chapter, we will concentrate on testing if Hrr25 has an impact on yeast NMD and try to build a path for studying its function in this degradation pathway. First, we will demonstrate that Hrr25 kinase activity allows efficient NMD in yeast using different reporter systems for NMD either endogenous or plasmid-borne. Looking at those reporters at equilibrium and with kinetics degradation assays will allow us a first glance at the importance of Hrr25 in NMD and RNA-sequencing will give a more global perspective. Then, using tagged proteins and Western Blot, we looked for the target for Hrr25 phosphorylation and found that Upf1 is a phosphorylated protein due to Hrr25 kinase activity. We tried characterising the phosphorylated state of Upf1 according to the different complexes in which it is present. We also looked at the effect of Hrr25 in NMD according to the composition of NMD complexes by depletion of proteins or domains of protein. Finally, through affinity purification and mass spectrometry, we managed to find first leads on how Hrr25 is recruited in this NMD complex.

Hrr25 kinase activity is needed for NMD

1) Hrr25 kinase is required for efficient NMD (preliminary results)
    a. An ATP-analogue strategy for rapid inhibition of Hrr25 kinase activity *in vivo*

Since Hrr25 is essential for the yeast cells with the genetic background that we are using, and participates in several major cellular processes, a simple method to test its importance in NMD is the rapid inactivation of its kinase activity followed by measurement of NMD efficiency *in vivo*, a strategy suggested by my colleague Frank Feuerback. To study this condition, a specific mutant in which Ile 82 is substituted with a Gly (hrr25-I82G) was used. This mutation enlarges the protein pocket that binds to ATP. Due to this widening, this pocket can accommodate an ATP-analogue such as 1NA-PP1 or 3MB-PP1 (see **Figure 10**) (Zhang et al., 2013). Without the drug, Hrr25 (I82G) kinase should work like the wild-type protein. However, introducing the analogue should inhibit kinase activity, an inhibition that should lead to a strong growth inhibition due to function in maturation of 40S subunit (42). This strategy is interesting because cells can be exposed to the drug for a short period, thus allowing detecting direct effects of the protein kinase activity inhibition.

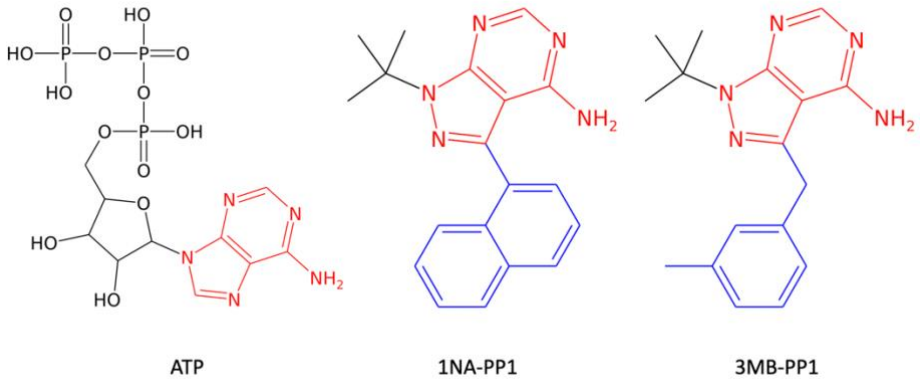

Figure 10: Structure of ATP-analogues, 1NA-PP1 and 3MB-PP1, compared to the structure of ATP (inspired from Zhang et al., 2013). In red is the common structure binding to the ATP pocket. In blue is the different structures constructed for going into the widening induced by the mutation I82G.

To be able to test different Hrr25 variants, a plasmid-based strategy that could maintain and switch on and off even kinase dead variants of Hrr25 in a stable genetic background was used. A GAL1 promoter was inserted, using homologous recombination (see Materials and Methods), upstream Hrr25. Endogenous Hrr25 was thus expressed only if galactose was present in the medium. Then, using Gibson Assembly (see Materials and Methods) plasmids containing different versions of hrr25 were transformed into the pGAL1-HRR25 strain (LMA5209). Several plasmids were designed bearing:

- HRR25 wild type.
- hrr25-I82G: this mutation leads to sensitivity of the kinase activity to ATP-analogue and allows to see what happens to NMD when kinase activity is inefficient.
- hrr25-K38A: kinase deficient.

The principle of this strategy is illustrated by **Figure 11**.

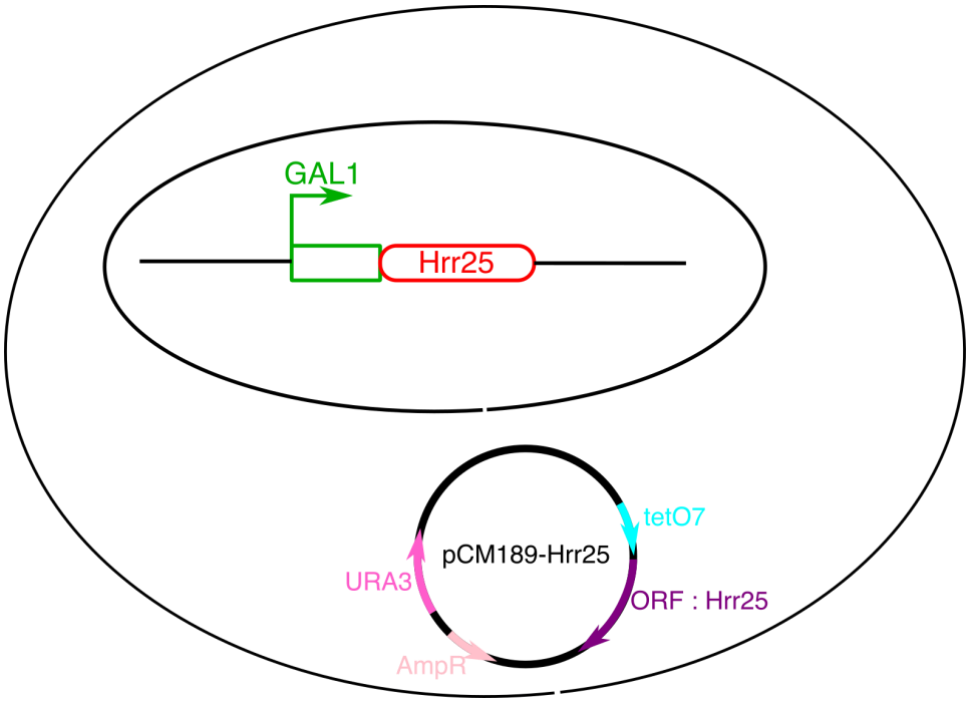

Figure 11: Complementation test principle for the pGAL1-HRR25 strain using plasmids with variants of Hrr25.

The various plasmids were built and sequenced before their transformation in yeast. Plasmid-bearing cells were selected on medium lacking uracil (selective marker) and containing galactose, but not glucose. The observed transformation efficiency was low and several strong growth phenotypes and heterogeneity were observed: heterogeneity in clones for some plasmids and less clones for the strain GAL-HRR25 and not for the control (data not shown). Since these effects could be the result of overexpressing Hrr25, the transformation was repeated and spread on a medium lacking uracil (selective marker), containing galactose and doxycycline. As plasmids contain a tetOFF system, this drug will inhibit expression of HRR25 and its variants from plasmids. Only endogenous HRR25 is expressed in these conditions. Then 3 clones per construction were isolated and streaked on three different media represented in Figure 12. All media were lacking uracil to maintain selection. The first medium is the same as the one the cells were streaked on after transformation. Hence, endogenous HRR25 was expressed but not HRR25 from the plasmid. The second medium also possessed galactose instead of glucose but did not contain any drug. Endogenous HRR25 was expressed and so was HRR25 from plasmid. The last medium contained no galactose and no drug. Hence, endogenous HRR25 could not be expressed in the pGAL1-HRR25 strain. Only HRR25 from plasmid was expressed. This

condition showed if complementation by constructed plasmid was possible. The different conditions are schematised **Figure 12**A.

Observations of clone's growth brought interesting insights. Complementation with constructed plasmids was possible. Compared to wild type, top half of the pictures, no growth defect was observed when endogenous gene was impaired. The only exception, as expected, was the construction with the hrr25-K38A, kinase defective mutant (**Figure 12**D). Overexpression of wild-type Hrr25 was toxic for the cells (**Figure 12**B). However, overexpression of mutant I82G was not toxic for the cells, which was unexpected, since this mutant should act the same as wild type in absence of inhibitor (**Figure 12**C). An explanation to this phenomenon may be a difference in the abundance of protein Hrr25 for wild type and mutant I82G. The observed differences needed more characterisation to be fully understood.

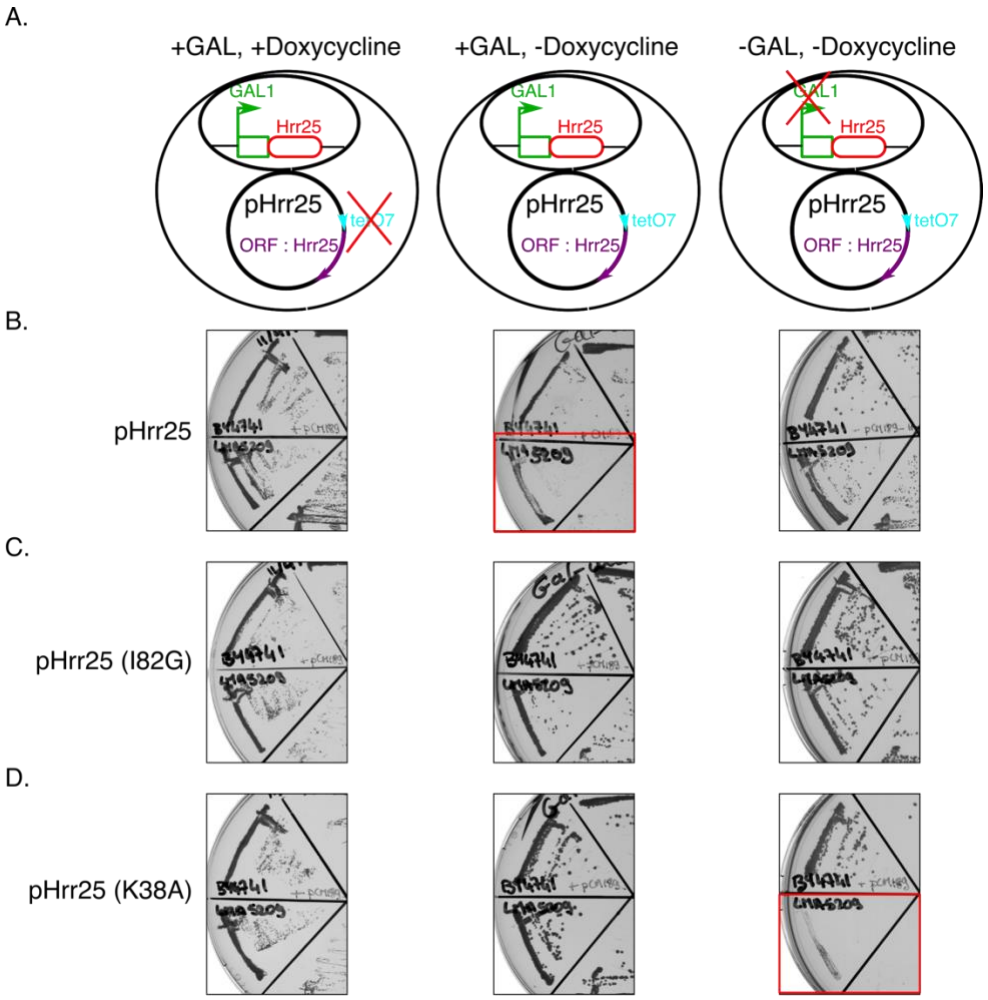

Figure 12: Complementation of the lack of HRR25 with plasmid-borne Hrr25 variants. **A.** Representation of which HRR25 is expressed in each condition (chromosomal, from plasmid, or from both). **B.** Isolation of clones for transformation of plasmid containing HRR25 wild type

in BY4741 on top and pGAL1-HRR25 strain on bottom. Clones were streaked on three different media. **C.** Same as B, but with the plasmid bearing *hrr25*-I82G. **D.** Same as B, with *hrr25*-K38A.

To confirm the observations obtained with growth tests, we used a different system. Growth of 8 constructions was tested in the same media as before and with medium containing doxycycline but no galactose. In the latter, strains containing GAL1 promoter did not express any Hrr25, so no growth is possible contrary to the wild type (**Figure 13**C). In presence of galactose, growth was normal, if HRR25 gene from the plasmid was not expressed (**Figure 13**A). However, the cells showed growth inhibition, when Hrr25 from plasmid was expressed. Like in the case of previous tests, overexpression of wild type was more deleterious than mutant hrr25-I82G (**Figure 13**B). Finally, the last condition allows testing complementation by plasmid: no galactose and no doxycycline in the medium. Plasmid containing HRR25 wild type and plasmid containing hrr25-I82G allowed normal growth but plasmid containing inactive kinase mutant - hrr25-K38A - could not grow (**Figure 13**D), as expected.

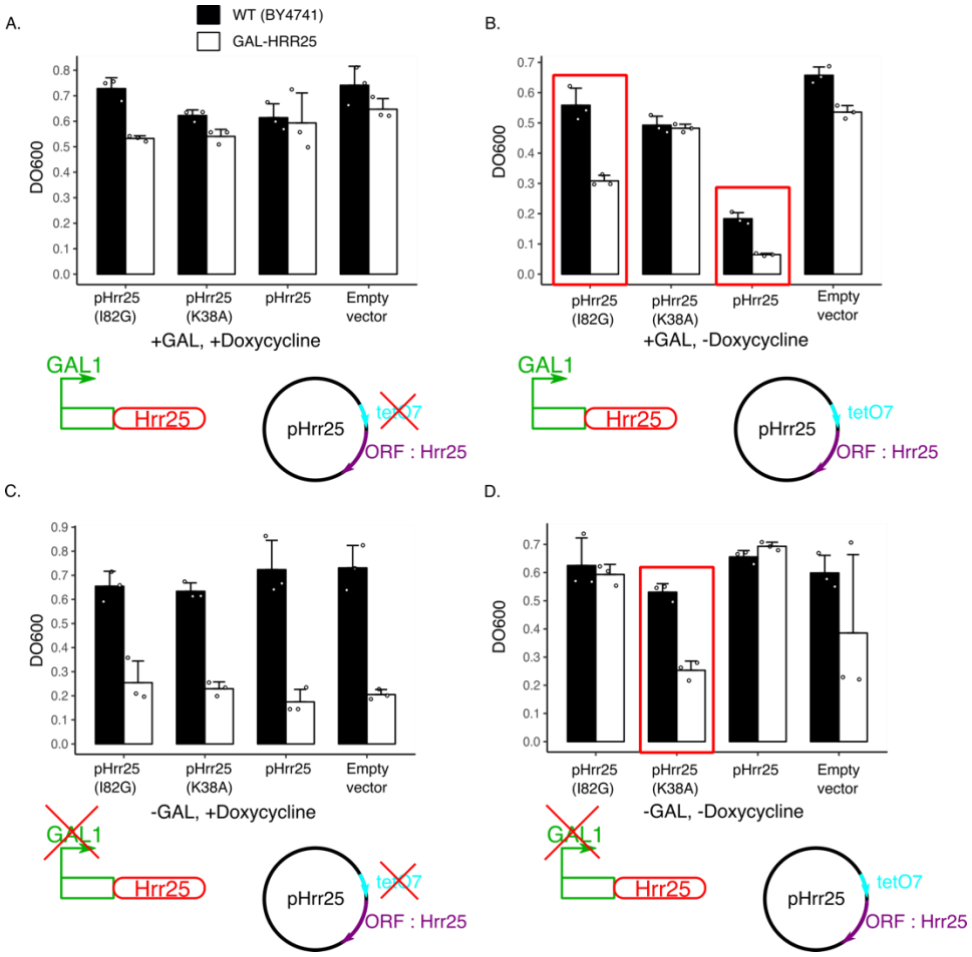

Figure 13: Absorbance at 600 nm after 24 hours of growth in liquid media. **A.** Absorbance at 600 nm for cultures of different constructions in medium containing galactose and doxycycline. Endogenous HRR25 in pGAL1-HRR25 strain is expressed but not HRR25 from plasmid. **B.** Absorbance at 600 nm for cultures of different constructions in medium containing galactose only. Endogenous HRR25 in pGAL1-HRR25 strain is expressed, together with HRR25 from the plasmid. **C.** Absorbance at 600 nm for cultures of different constructions in glucose containing medium containing doxycycline. Endogenous HRR25 in pGAL1-HRR25 strain is not expressed neither is HRR25 from plasmid. **D.** Absorbance at 600 nm for cultures of different constructions in medium containing no galactose and no doxycycline. HRR25 from plasmid strain is expressed but not endogenous HRR25 in pGAL1-HRR25. Error bars represent standard deviation of technical replicate values.

Complementation of pGAL1-HRR25 strain with Hrr25 expressed from a plasmid was validated. The next step was to test the mutant hrr25-I82G inhibition by an ATP-analogue. Many ATP-analogues exist in the literature, such as 1NA-PP1 and 3MB-PP1. The latter is described as the most efficient one for modified casein kinases (Zhang et al., 2013). In our

laboratory, the used ATP-analogue was 1NA-PP1. Hence, 1NA-PP1 and 3MB-PP1 were both used in growth test at 5 µM and 10 µM concentrations. At both concentrations, the effect of 3MB-PP1 was visible (**Figure 14**A) and this experiment confirmed that 3MB-PP1 is more efficient, at least in this case. For further experiments, the inhibitor 3MB-PP1 was therefore used. Then a growth test using two different clones for pGAL1-HRR25 with hrr25-I82G mutant was realized with decreasing concentrations of 3MB-PP1 to define the minimal concentration necessary to see an effect on growth. At 625 nM of the drug, growth was mildly impaired whereas starting at 1.25 µM, cells could not grow anymore (**Figure 14**B).

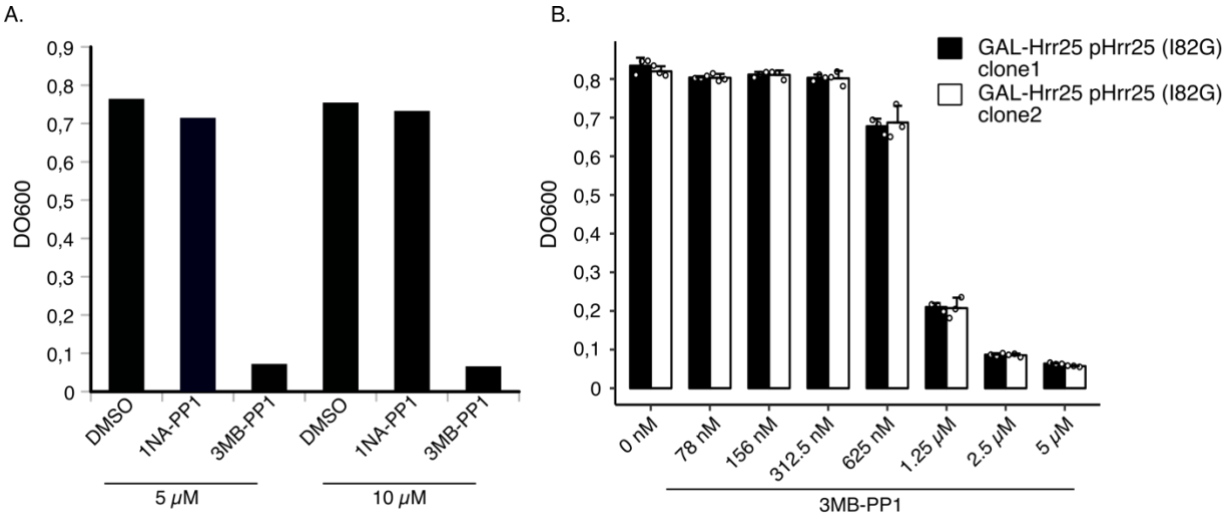

Figure 14: 3MB-PP1 blocks growth of the hrr25-I82G mutant strain. A. Absorbance at 600 nm of the pGAL1-HRR25 strain with plasmid containing hrr25-I82G after 29 hours of growth in medium lacking uracil in presence of ATP-analogue, inhibitor of mutant I82G, or in presence of the same amount of DMSO. B. Absorbance at 600 nm of strain pGAL1-HRR25 with plasmid containing hrr25-I82G after 30 hours of growth in medium lacking uracil in presence of different concentrations of 3MB-PP1. Error bars represent standard deviation of technical replicate values.

To ensure a maximum effect on inhibition of Hrr25 kinase activity, further experiments were thus done with 5 µM final concentration for 3MB-PP1.

b. NMD is affected after rapid inhibition of Hrr25 kinase activity

To study the impact of Hrr25 kinase activity on NMD, the fold-change between the pre-mRNA and the RNA of the protein RPL28 was studied through RT-qPCR. NMD, as seen previously, targets usually a transcript that has a short ORF and a long 3' UTR. This feature can come from the introduction of a premature stop codon hence its name nonsense mediated.

Nevertheless, this feature can also appear with a defect in splicing and thus intron retention. In this intron, a stop codon might be present and if this transcript leaks into the cytoplasm, the NMD pathway will degrade it. This is the case for the pre-mRNA of the ribosomal protein L28. Some are not well spliced and escape degradation in the nucleus, leaking in the cytoplasm. Hence, we can look at NMD directly with the reporter fold change and using as reference the mRNA of the ribosomal protein L28 (schematized in **Figure 15**).

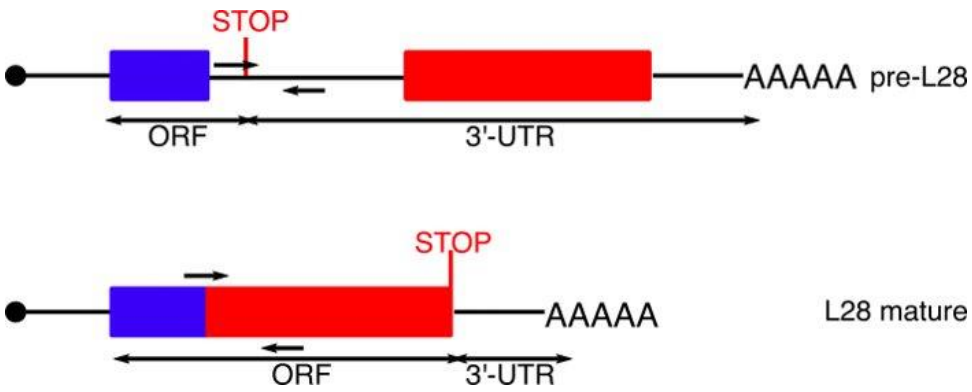

Figure 15: Representation of two targets of qPCR for NMD measurement. For pre-L28, NMD substrate, the two primers used were CS887 and CS888. Both are located in the intron. For L28 mature, the two primers used were CS889 and CS946. CS946 overlaps the two exons so that only mature mRNA is amplified.

As a positive control for NMD phenotype, the strain *upf1*Δ was used. Depletion of Upf1, the core NMD factor, allows stabilization of all NMD substrates. We can see here that the fold-change of the reporter was superior to 10 showing maximum stabilization of this substrate (**Figure 18**A). Introducing the ATP-analogue, 3MB-PP1 for 30 minutes in both the WT strain and the pGAL-strain containing Hrr25 WT led to no significant change in the fold change of our NMD reporter. However, 30 minutes of incubation with 3MB-PP1 in the pGAL-strain containing hrr25 I82G induced a raise in the fold change of the pre-mRNA of RPL28 (**Figure 18**A). This raise is above 5 and corresponds to approximately half the stabilization occurring in the *upf1*Δ. This experiment was also performed with 10 min incubation with 3MB-PP1 and no accumulation of the NMD reporter was observed. Thus, further experiments were performed with 30 min incubation only.

Further questions arose, such as the impact of Hrr25 inhibition on its many functions in cellular processes including translation. However, this system, using a tetOFF operator,

prevented the use of another reporter, the transcript produced from the plasmid 1490, developed in the laboratory by my supervisor Cosmin Saveanu. This plasmid carries a sequence allowing transcription of a NMD substrate. The coding sequence of the transcript carried by the plasmid 1490 is composed of an HA tag and a fragment of ALA1 gene (schematized in **Figure 16**). Its 3'UTR is the coding sequence for Kanamycin resistance. Thus, this configuration gives a short coding sequence and a long 3'UTR making this transcript a target for NMD.

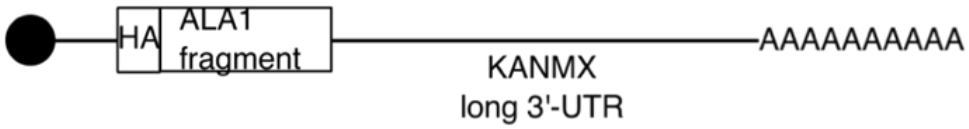

Figure 16: Representation of the transcript produced by the plasmid 1490.

This sequence is interesting for two reasons:

- The transcription of this substrate can be controlled by a tetOFF system thanks to the cassette tetO7. This means that introducing Doxycycline in our culture will inhibit specifically the transcription of our NMD substrate.
- The transcript allows translation of a HA tagged protein with a very short half-life. So, the protein signal can be followed by Western Blot (WB) and protein levels vary rapidly with RNA and translation.

However, plasmids have the same selective marker, and both Hrr25 and the reporter transcriptions are under the same tetOFF operator. Hence, to use this plasmid we used another strain produced by my former colleague Frank Feuerbach. This strain contains the mutation I82G in the endogenous Hrr25. Another advantage of this strain is that regulation of Hrr25 is endogenous. Hence, toxicity due to surexpression of Hrr25, as seen previously, will not be an issue. For further experiment, this mutation was introduced in multiple strains such as Dcp1-TAP and Nmd4-CRAP – a particular version of the TAP tag optimised for CRAC experiment (Bohnsack et al., 2012). To verify if the mutation was well incorporated, serial dilution test using media containing or not the ATP analogue 3MB-PP1 was performed. As seen in **Figure 17**, all strains grew well in the typical medium YPD behaving like the wild-type (WT) strain – BY4741. However, on a medium containing the drug, no more growth was observed for the strains containing the mutation I82G while strains containing the WT Hrr25 grew perfectly well.

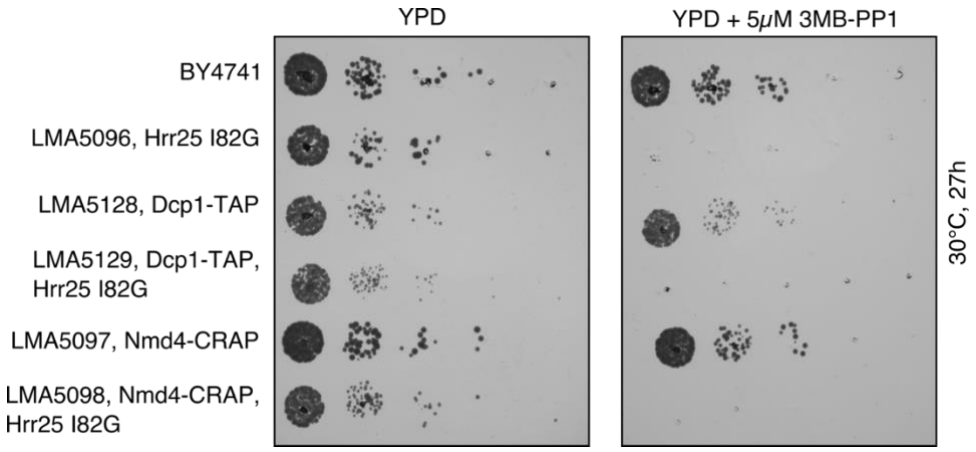

Figure 17: The ATP analogue 3MB-PP1 can specifically inhibit the kinase activity of the mutant hrr25 I82G. Growth test of strains containing hrr25-I82G mutant and controls. Serial dilutions were performed on YPD plates with or without 3MB-PP1. Plates were observed after 27h of incubation at 30°C.

With the new strain, we studied the stabilization of the NMD substrate 1490 by looking at its fold change compared to the mature mRNA of the protein RPL28 levels through RT-qPCR (**Figure 18**B). As positive control, the strain *upf1*Δ was used. Since we want to look at translation afterward, we also used treatment with CHX, a translation inhibitor, on our strain of interest. Indeed, NMD depends on translation. Hence, if translation is inhibited, NMD will be as well and NMD substrates are going to be stabilized. With these new results, we could see that both treatments induce stabilization of the NMD substrate at the same level as the strain *upf1*Δ with was rather surprising since it was only 30 minutes treatment (**Figure 18**B). However, this result was consistent with the previous results.

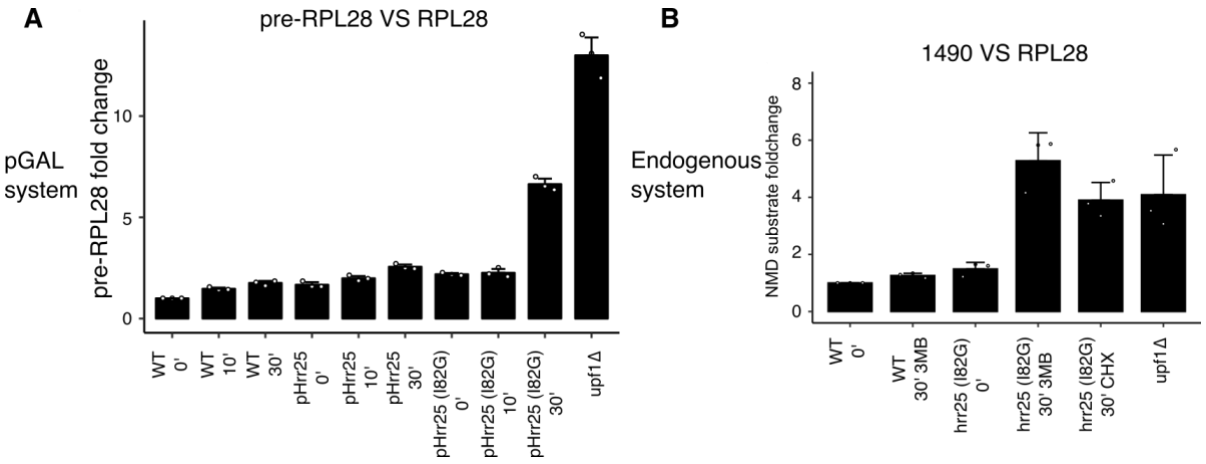

Figure 18: Inhibition of Hrr25 activity leads to stabilisation of an NMD substrate in yeast. **A.** In the pGAL1-HRR25 system, Fold change comparing changes of NMD substrate pre mRNA of L28 in the pGAL1-HRR25 strain with plasmid containing HRR25 WT or hrr25-I82G with changes of NMD substrate in WT strain with or without introduction of inhibitor 3MB-PP1. The strain *upf1*Δ does not have the core NMD factor Upf1 and hence, NMD is inhibited. This is the positive control. **B.** In the system where hrr25 I82G is endogenous, fold change levels comparing changes of NMD substrate transcript 1490 in the strain hrr25-I82G with changes in WT with 30 min treatment of 3MB-PP1 or of CHX. Here the positive controls are treatment with CHX and the *upf1*Δ strain. The housekeeping gene for the reference used here is RPL28.

In order to have a more global view on what happens after inhibition of Hrr25 kinase activity, a global study of the transcriptome after introduction of 3MB-PP1 was done through RNA sequencing with Illumina technology. For this analysis, WT strain and hrr25 I82G strain were treated with 5 µM 3MB-PP1. As a positive control, we did not use the strain *upf1*Δ since we wanted a dynamic system as well. Instead, my colleague Frank Feuerbach constructed a Nam7-degron strain. This system consists in adding an Auxin-inducible Degradation (AID) domain to the protein of interest, Upf1. This domain is recognized by the drug Auxin (IAA) and will induce polyubiquitination of the desired protein, targeting this protein for degradation by the proteasome (schematized in **Figure 19**) (Shetty et al., 2019). Hence, this system allows rapid depletion of the tagged protein. We preferred this system to a complete depletion of Upf1 to be able to see stabilisation of NMD substrates after 30 min of drug induction and thus, be able to compare depletion of Upf1 to inhibition of Hrr25 kinase activity.

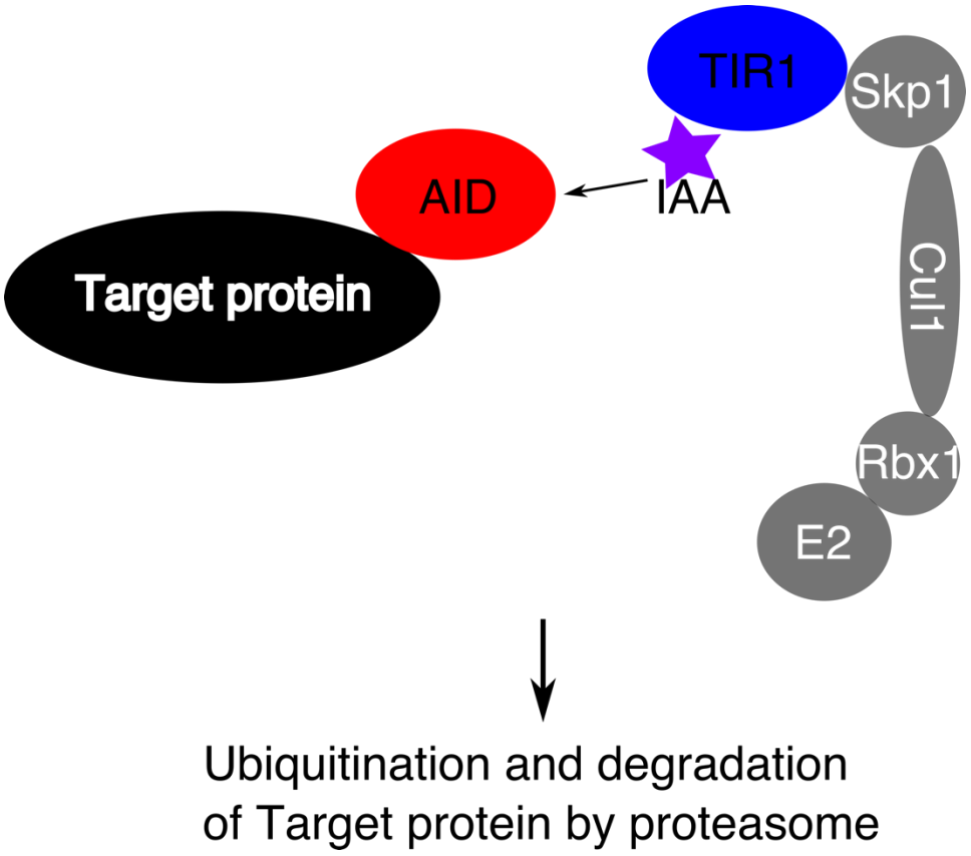

Figure 19: Representation of the AID system (simplified from Shetty et al., 2019).

For analysis, this experiment was done in triplicate. However, the first replicate wasn't done on the same day and gave less depth compared to the other two (only 300 000 reads against a million for the other replicates). To avoid bias, the analysis was thus done only considering replicates 2 and 3. Comparison of the different conditions was performed thanks to SARTools DESeq2. The reference and control for this analysis was the WT strain treated with DMSO only. First two analyses to look at are the comparison between WT strain treated and the control (**Figure 20**F) and the comparison between hrr25 I82G not treated and the control (**Figure 20**B). To observe the comparison, a volcano plot was used with in x-axis the Log2 of the Fold-change given by DESeq2 and in y-axis –Log2 of the adjusted p-value for DESeq2. With both comparisons we can see that minimal changes were observed in the different conditions and most importantly, NMD substrates did not vary with either introduction of the drug 3MB-PP1 or the mutation I82G. As expected, upon depletion of Upf1, NMD substrates were strongly upregulated (**Figure 20**D and E). However, upregulation of NMD substrates was stronger compared to the control and slight upregulation can be seen already with no introduction of Auxin for the degron system. We observed in the laboratory with multiple AID tagged proteins

that degradation can already happen even when Auxin is not introduced. A better system will be suggested later in the discussion. Then finally, when comparing hrr25 I82G treated or not, multiple observations were made:

- Many transcripts were affected by inhibition of Hrr25 kinase activity. Regulation of more than 5000 transcripts were either going down or up over 12,275 total transcripts analysed.
- Most NMD substrates were upregulated in those conditions – in red in the volcano plots.
- A strong downregulation of ribosomal proteins (RPL and RPS) can be seen specifically when Hrr25 kinase activity was inhibited – in blue in the volcano plots. A typical example is mature RNA of RPL28.

To compare the effect of Upf1 depletion and of inhibition of Hrr25 kinase activity on the NMD substrates, I took the name of all the transcripts that DESeq2 designed as upregulated in the comparison hrr25 I82G treated VS control and in the comparison Nam7-degron treated VS control. Using the Venn diagram plot, we observed that 229 transcripts were found in common in those two comparisons (**Figure 20**C).

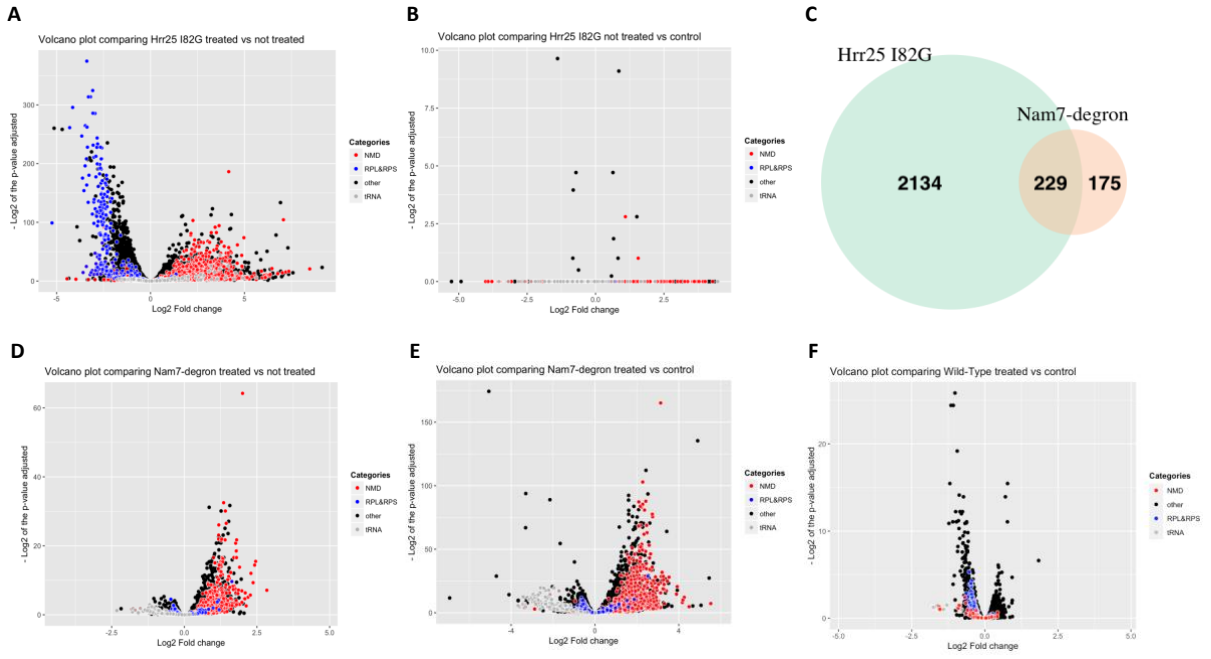

Figure 20: Inhibition of Hrr25 kinase activity highly affects transcriptome and most particularly the NMD substrates. **A.** Volcano plot of the comparison of Hrr25 I82G treated with 3MB-PP1 vs Hrr25 I82G not treated. On the x-axis is the Log2 Fold Change of the comparison and on the y-axis is the –Log2 of the adjusted p-value. Black represents all points. Red represents the NMD substrates. Blue represents the ribosomal protein transcripts. Grey

represents the transcripts for the tRNA. **B.** The same as A but for the comparison of Hrr25 I82G not treated vs the control (BY4741 with DMSO). **C.** Venn diagram comparing the transcripts upregulated in the comparison Hrr25 I82G treated vs the control and the transcripts upregulated in the comparison Nam7-degron treated vs the control. The intersection of both circles represents the transcripts in common in both conditions. **D.** The same as A but for the comparison of Nam7-degron treated with IAA vs Nam7-degron not treated. **E.** The same as A but for the comparison of Nam7-degron treated vs the control. F. The same as A but for the comparison of Wild-Type strain (BY4741) treated with 3MB-PP1 vs the control.

Many transcripts were upregulated following the inhibition of Hrr25 kinase activity. One may ask if transcripts affected both by Upf1 depletion and Hrr25 inhibition might be a coincidence coming for this large number of upregulated transcripts. To explore this option, in the condition of inhibition of Hrr25 kinase activity, we selected only the transcript with a log2 Foldchange superior to one so that Foldchange is strictly superior to 2. In this condition, 157 transcripts remained in common and most of them are typical NMD substrates: XUT and SUT that come from pervasive transcription (Jensen et al., 2013)(**Figure 21**E). To be able to compare those two treatments, we chose to do another visualisation: scatterplot. As previously, we used the data coming from either the comparison between hrr25 I82G treated and the control or the comparison between Nam7-degron treated and the control. Then, we plotted on the x-axis the Log2 Foldchange of the first comparison (hrr25 I82G treated) and in the y-axis the Log2 Foldchange of the second comparison (Upf1-degron treated) (**Figure 21**A). For further clarity the different groups of transcripts were dissociated (**Figure 21**B, C and D). We can see for the ribosomal protein in blue (**Figure 21**B) that the group tended to the upper side of the cloud of points, suggesting that the enrichment was higher in the Upf1-degron treatment than in the inhibition of kinase activity. This can be explained by the downregulation of those transcripts saw in the inhibition of Hrr25 whereas depletion of Nam7/Upf1 did not impact this category of RNAs. Moreover, we can see for the tRNAs in grey (**Figure 21**D) that the group tended to the down right side of the cloud of points suggesting that the enrichment was higher in the hrr25 I82G treatment than in the depletion of Upf1. Since the depletion of Upf1 did not affect this category of transcript, it could suggest that inhibition of Hrr25 kinase activity upregulates tRNAs. This will be confirmed in with visualisation of examples with IGV later on. As for the NMD substrates in red (**Figure 21**C), contrary to the two other categories, no specific orientation could be seen. The same enrichment seems to happen in both conditions suggesting that this category of transcript is common to both treatments.

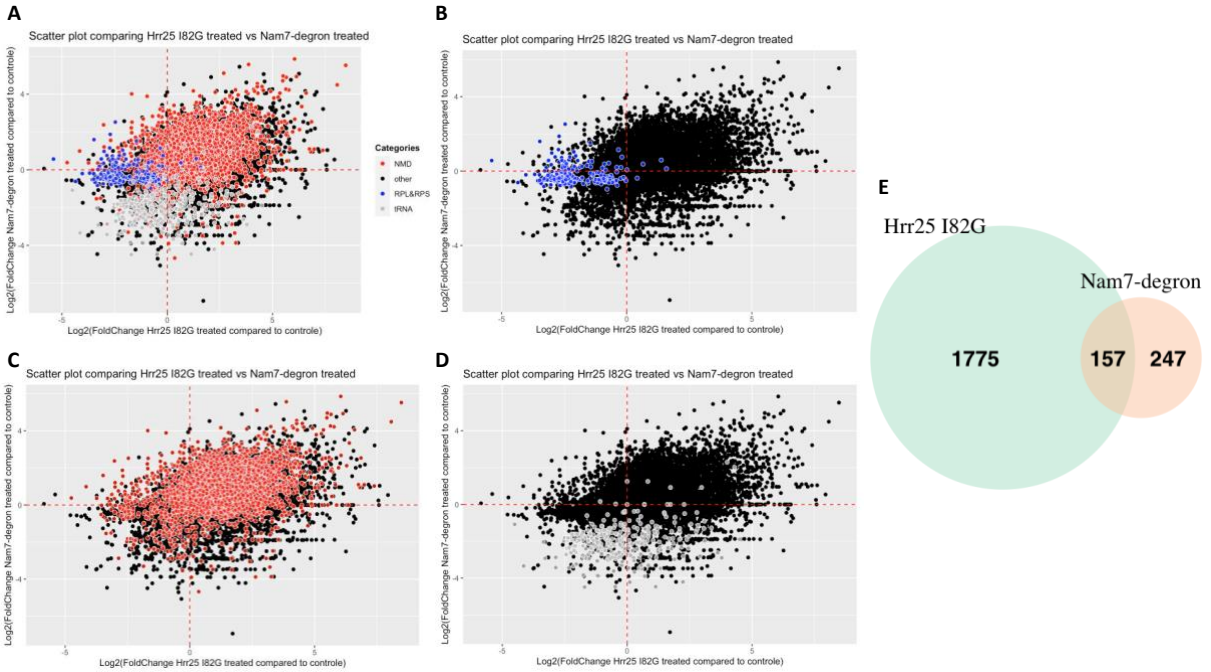

Figure 21: Similar NMD targets for Hrr25 kinase inhibition and Upf1 depletion. **A.** Scatter plot comparing Hrr25 I82G treated with Nam7-degron treated. The x-axis is the Log2 Fold change of the comparison Hrr25 I82G treated with the control. The y axis corresponds to the Log2 Fold change of the comparison Nam7-degron treated with the control. Black represents all points. Red represents the NMD substrates. Blue represents the ribosomal protein transcripts. Grey represents the transcripts for the tRNA. **B.** Same as A. Only the ribosomal protein transcripts are represented. **C.** Same as A. Only the NMD substrates are represented. **D.** Same as A. Only the transcripts for the tRNA are represented. **E.** Venn diagram comparing the transcripts upregulated in the comparison Hrr25 I82G treated with the control and the transcripts upregulated in the comparison Nam7-degron treated with the control. The intersection of both circles represents the transcripts in common in both conditions. For the transcripts upregulated in the comparison Hrr25 I82G treated with the control, only transcripts with a Log2 Fold change superior to 1 were taken.

To determine if what was observed using DESeq2 corresponds to the reality of the RNA sequencing, the data were visualised thanks to IGV (wig files). The order of the samples in those images is as follow: WT without drug, WT with drug, hrr25 I82G without drug, hrr25 I82G with drug, Nam7-degron without drug, Nam7-degron with drug. The samples hrr25 I82G with drug and Nam7-degron with drug are coloured in red to distinguish them from control samples. Multiple NMD substrates upregulated in both test conditions are shown in **Figure 22**

(A, B, C and D). In panel A, the NMD substrate DAL7 is represented. DAL7 contains uORFs in its 5'-UTR corresponding thus to a small ORF and a long 3' UTR. It is highly upregulated after degradation of Upf1, and it is mildly upregulated with inhibition of Hrr25 kinase activity. Panel B represents NMD substrate SUT828. In this case, upregulation is more important following inhibition of Hrr25 kinase activity. In panel C, multiple genes are represented. Two NMD substrates can be observed: SUT232 and XUT_11F-90. Both are upregulated in the test conditions. We can also see the gene tK(CUU)K. This gene is highly upregulated when Hrr25 kinase activity is inhibited while it is not the case with degradation of Nam7 corresponding to the observation made with the previous volcano plot (**Figure 22**D). We also looked at another group of genes: the mRNAs for the ribosomal proteins Rps and Rpl. We took an example of each category: RPS0A and RPL28 (**Figure 22**E and F respectively). In both cases, we can see that inhibition of Hrr25 led to a strong decrease in their RNS levels.

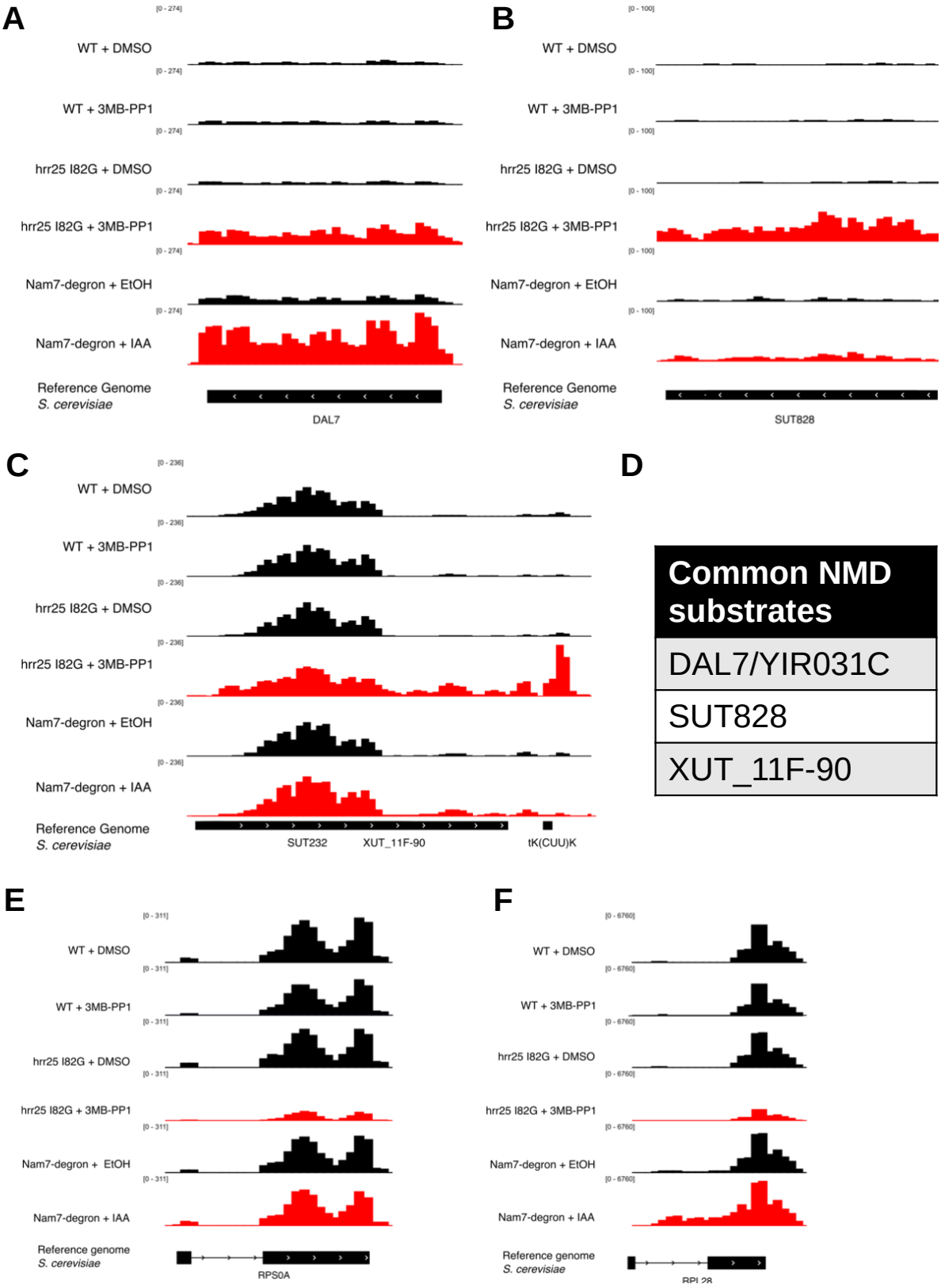

Figure 22: Shared substrates and divergence in RNA-seq reads with inhibition of Hrr25 kinase activity and specific degradation of Upf1. **A.** IGV image representing the reads of the different RNA-seq datasets for DAL7. **B.** IGV image representing the reads of the different RNA-seq datasets for SUT828. **C.** IGV image representing the reads of the different RNA-seq datasets

for SUT232, XUT_11F-90 and tK(CUU)K. **D.** List of shared NMD substrates between the two conditions inhibition of Hrr25 kinase activity and degradation of Nam7. **E.** IGV image representing the reads of the different RNA-seq datasets for RPS0A. **F.** IGV image representing the reads of the different RNA-seq datasets for RPL28.

Since those results showed that most RPL and RPS transcripts were downregulated in the specific context of inhibition of Hrr25 kinase activity, the mature mRNA for RPL28 can no longer be used as a reference for the previous RT-qPCR looking at 1490 as NMD substrate. RT-qPCR were reproduced for the NMD substrate 1490 using different house-keeping genes: ALA1, PGK1, SCR1 and ACT1 (**Figure 23**A, B, C and D respectively). Stabilisation of NMD substrate was visible in *upf1*Δ and treatment with CHX. However, only ALA1 showed a stabilisation of the NMD substrate in the context of treatment with 3MB-PP1 (**Figure 23**A), and it was not as high as with RPL28 (**Figure 18**D). Later analysis of RNA sequencing showed that all those house-keeping genes apart from SCR1 were downregulated in the specific context of inhibition of Hrr25 kinase activity.

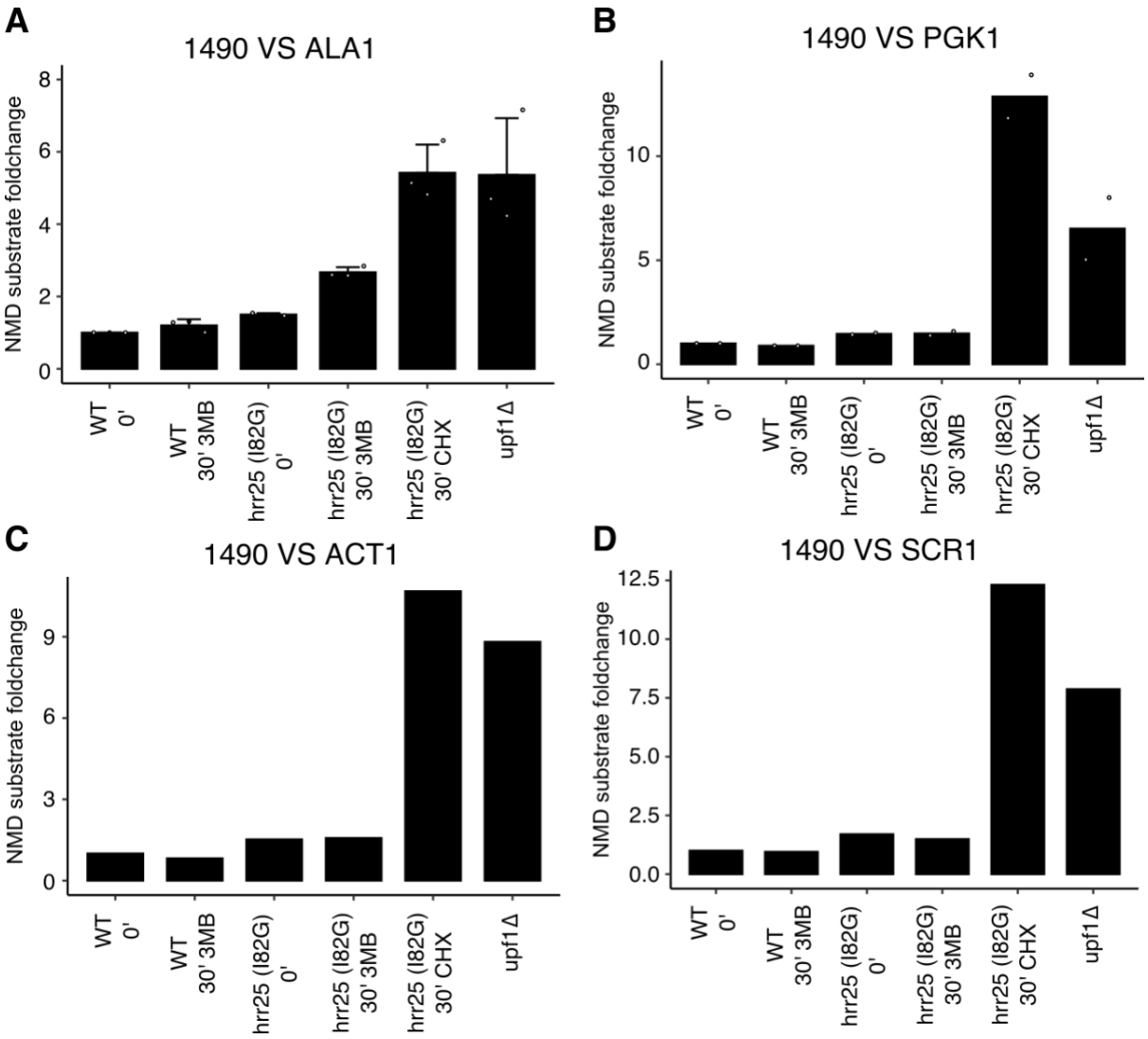

Figure 23: Stabilisation of NMD substrate 1490 in the context of inhibition of kinase activity depends on the housekeeping gene reference. **A.** Fold change comparing enrichment of NMD substrate transcript 1490 in the strain hrr25-I82G with enrichment in WT with 30 min treatment of 3MB-PP1 or of CHX. Here the positive controls are treatment with CHX and the *upf1*Δ strain. The housekeeping gene for the reference used here is endogenous ALA1 (n = 3). **B.** The same as A with the reference being PGK1 (n = 2). **C.** The same as A with the reference being ACT1 (n = 1). **D.** The same as A. with the reference being SCR1 (n = 1).

RNA sequencing showed thus that RT-qPCR is not enough to understand the whole picture of what happens in the cell when we inhibit Hrr25 kinase activity. This protein kinase seems to be very important not only for transcription termination as previously suggested (Nemec et al., 2019) but maybe also for other regulatory pathways of transcription.

2) The effect of Hrr25 inhibition on NMD substrates is independent of its function in transcription and translation

We discovered that Hrr25 kinase activity had an effect on NMD. However, as mentioned in the introduction, Hrr25 kinase is involved in multiple cellular processes such as mRNA translation – modification of tRNA or maturation of the 40S subunit (Abdel-Fattah et al., 2015; Ghalei et al., 2015) – or DNA transcription termination (Nemec et al., 2019). Hence, the effect of Hrr25 kinase activity on NMD could be an indirect effect of the impact on those processes. To discriminate a potential effect on NMD through transcription and translation, we used the plasmid 1490, carrying a sequence allowing transcription of a NMD substrate.

To discriminate Hrr25's function in transcription, we took advantage of the tetOFF system to inhibit transcription of the NMD substrate 1490 and did a kinetic test to measure its half-life. As described in the section Material and Method, inhibition of Hrr25 kinase activity was induced 15 minutes prior to the beginning of transcription arrest. Then, Doxycycline was introduced, and samples were taken at specific time points. The level of remaining NMD substrate was then determined thanks to RT-qPCR in comparison with a housekeeping gene (schematised in **Figure 24**). Two were tested at first, ALA1 and PGK1, and seeing no differences, only PGK1 was used for further tests.

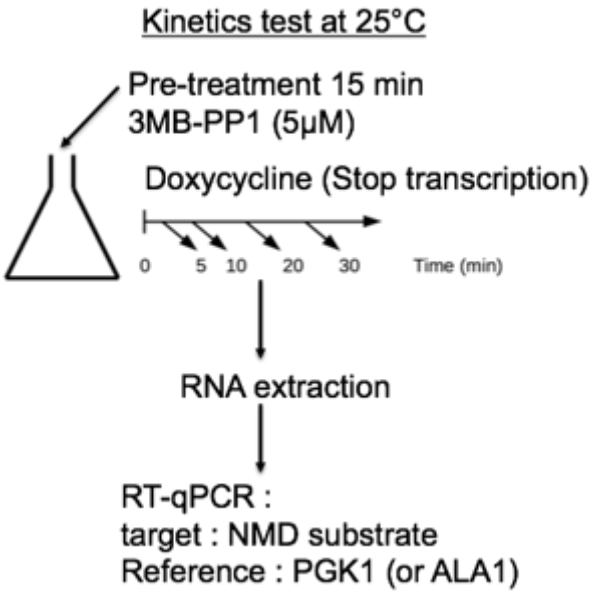

Figure 24: Principle of the kinetics test for the NMD substrate 1490.

In total, five replicates were made. Using R, from the time points, we extracted the degradation curve from each condition for each replicate. Then, we calculated the half-life from this curve and thus obtained for each condition, five half-lives. Next, we applicated on these data an ANOVA with two factors – the Strain and the Drug – and on these ANOVA, we performed a TukeyHSD test (**Figure 25**E). Comparing the effect of the treatment on our strains, control and test, the following can be observed:

- The solvent DMSO had no effect on the half-life of our substrate (**Figure 25**C).
- Inhibition of hrr25 I82G induced a slowing down in the degradation of the transcript 1490 (**Figure 25**D) going from a half-life of 7.3 min to a half-life of 10.3 min (**Figure 25**A and B). (pvalue = 0,0007)

Hence, this experiment showed that Hrr25 kinase activity might influence NMD that does not depend on its potential function in transcription termination (Nemec et al., 2019). However, these analysis needs to be supported by other results since the reference for those kinetic tests are not optimal. Indeed, as previously stated in the preliminary results of this study, the transcriptome is highly affected by the inhibition of Hrr25 kinase activity and so were the reference for the RT-qPCR.

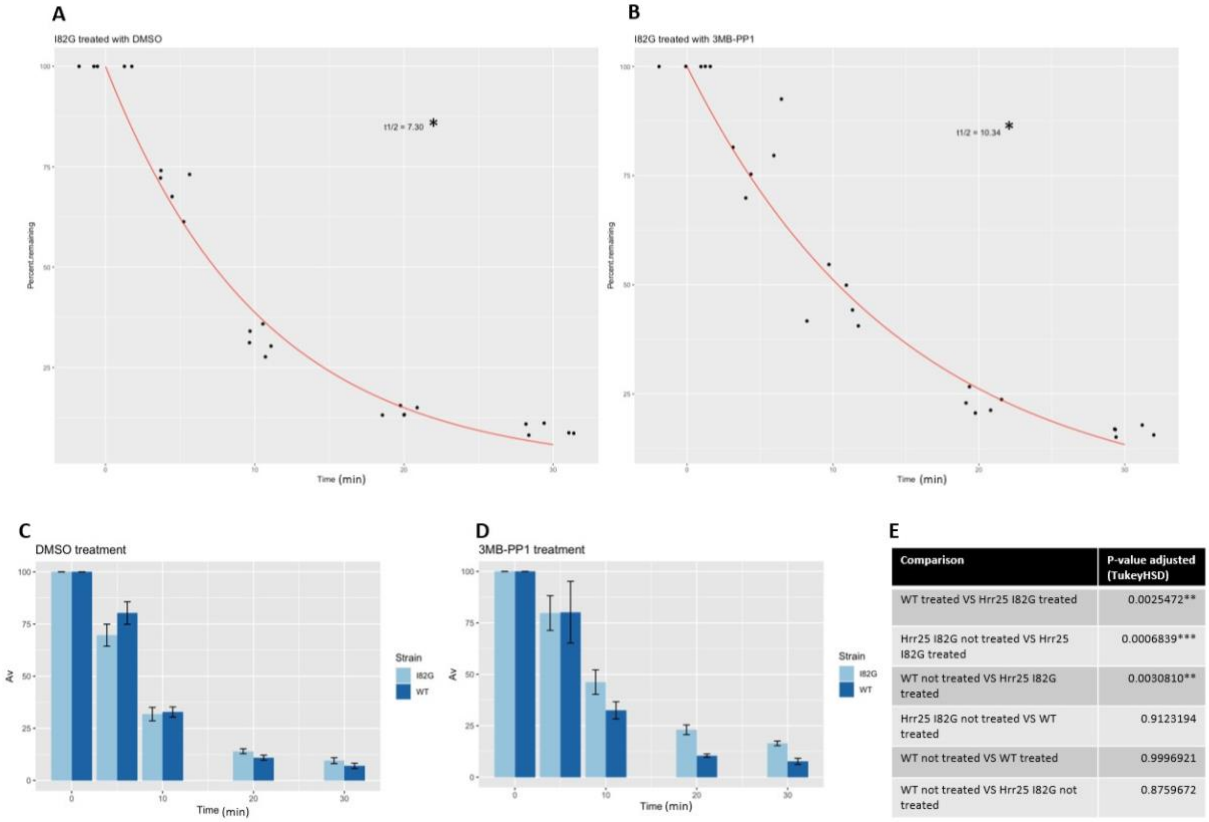

E

Comparison	P-value adjusted (TukeyHSD)
WT treated VS Hrr25 I82G treated	0.0025472**
Hrr25 I82G not treated VS Hrr25 I82G treated	0.0006839***
WT not treated VS Hrr25 I82G treated	0.0030810**
Hrr25 I82G not treated VS WT treated	0.9123194
WT not treated VS WT treated	0.9996921
WT not treated VS Hrr25 I82G not treated	0.8759672

Figure 25: Inhibition of Hrr25 kinase activity leads to an increase of half-life for the NMD substrate 1490 and this seems to be independent of Hrr25 function in DNA transcription. **A.** Degradation curve of the NMD substrate 1490 in the strain hrr25-I82G with DMSO. The half-life in this context is of approximately 7 min. **B.** Degradation curve of the NMD substrate 1490 in the strain hrr25-I82G treated with 3MB-PP1. The half-life in this context is approximately of 10 min. **C.** Barplot representing the average percentage of remaining NMD substrate in the cells according to time in WT condition (dark blue) and in I82G condition (light blue) with DMSO control. **D.** Barplot representing the average percentage of remaining NMD substrate in the cells according to time in WT condition (dark blue) and in I82G condition (light blue) with 3MB-PP1 treatment. **E.** The different comparison made by the TukeyHSD test with R and the p-value associated. * p-value <=0,01 ** p-value <=0,001 *** p-value <= 0,0001

The transcript used earlier has another advantage: the tag HA allow visualization of its protein through WB. We know now that in steady state both treatment with ATP analogue, i.e., Hrr25 kinase activity inhibition, and treatment with cycloheximide, ie translation inhibition, stabilize NMD substrates. The question is therefore: is translation still going on after 30 minutes of Hrr25 activity inhibition? For the treatment with CHX, we know that translation is inhibited.

Thus, even though RNA is stabilized, the level of the corresponding protein will be equivalent or lower than the no drug sample. With inhibition of Hrr25 kinase activity, we saw previously the RNA stabilisation is also observed for NMD substrate. However, for the protein, we do not know what the signal is going to be. If translation is affected after 30 minutes of inhibition, we can expect a similar response than for CHX treatment. If translation is still going on, we might expect a stronger signal as for the No drug sample since RNA is stabilised and translation will continue (schematized in **Figure 26**). As a control of gel loading, the protein G6PDH was used. Furthermore, to have a positive control for the NMD phenotype, the strain *upf1*Δ was transformed with the plasmid 1490.

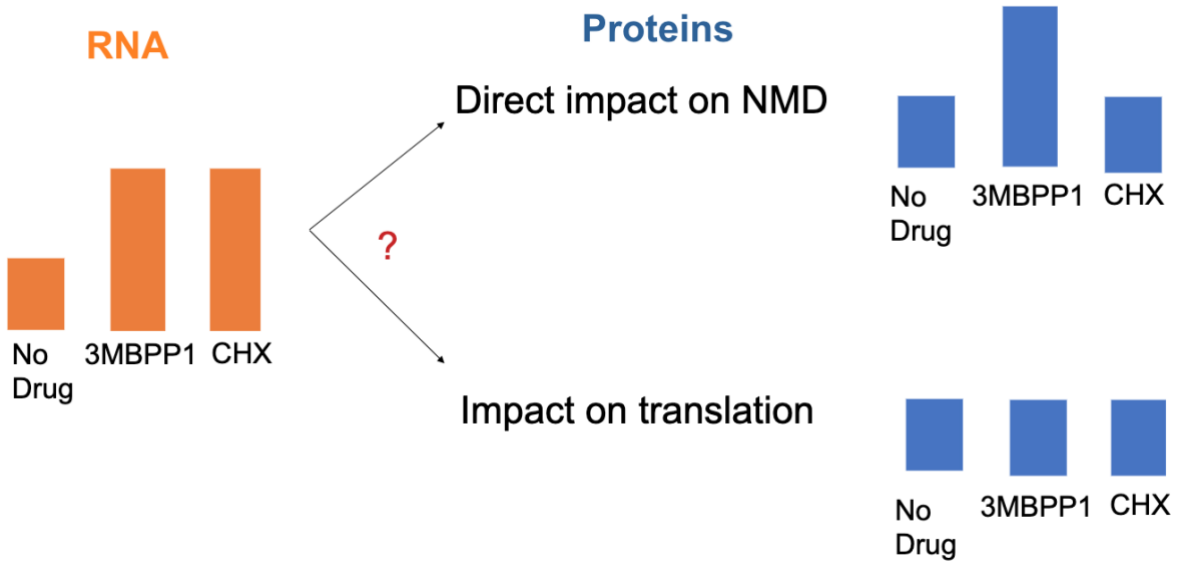

Figure 26: Diagram of the principle of the experiment to distinguish the effect on NMD of the kinase activity and the function in translation of Hrr25.

On this WB (**Figure 27**A), multiple observations were made:

- For the wild-type strain, BY4741, no protein for the transcript 1490 could be seen. The basal level for this protein was thus very low.
- For the positive control, *upf1*Δ, a very strong signal could be seen for the NMD substrate. With serial dilutions, we could see that this level was higher than 8 times the basal level.
- The signal for the strain of interest, hrr25 I82G, in no drug condition, was stronger than the wild-type conditions, showing that the mutation I82G was not without consequences on the cellular processes already.

- When the strain of interest was treated with CHX, a lower signal could be seen compared to the no drug sample. This was expected as CHX inhibits translation.
- After treatment with 3MB-PP1, a stronger signal compared to the no drug sample was observed. Thanks to dilution in series, we could see that this signal is more than two times the signal for the no drug control. This was the opposite reaction of treatment with CHX suggesting that translation was still going on after 30 minutes of inhibition of Hrr25 kinase activity.

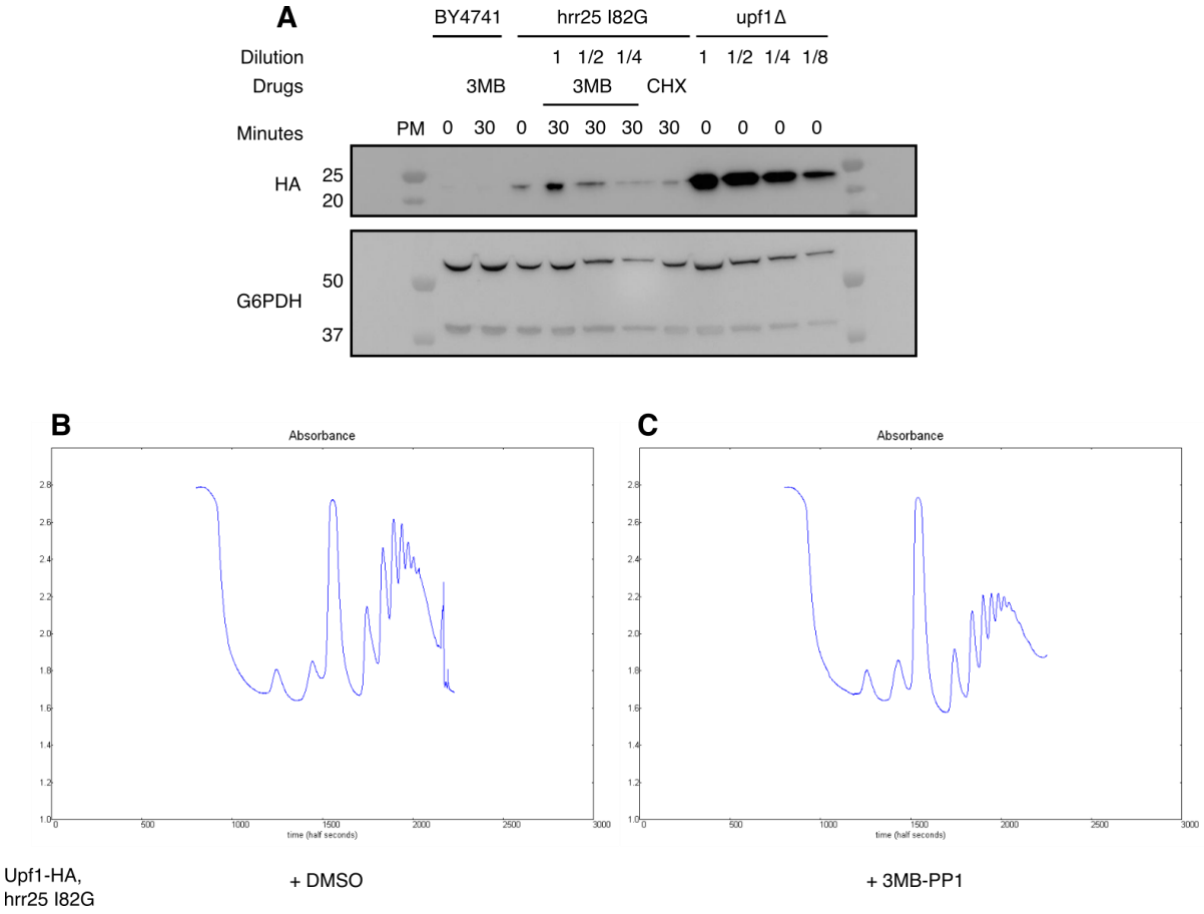

Figure 27: Impact of Hrr25 kinase activity on NMD is distinct from the function of Hrr25 in mRNA translation. **A.** Western Blot using anti-HA and anti-G6PDH antibodies on protein samples. Anti-HA antibody allows visualising the protein produced from the NMD substrate 1490. Anti-G6PDH antibody was used as a control of gel loading. **B.** Sucrose gradient fractionation profiles of the strain Upf1-HA, hrr25 I82G with DMSO. **C.** Gradient fractionation profiles of the strain Upf1-HA, hrr25 I82G treated with 3MB-PP1.

Two results showed nonetheless that translation was potentially affected even though it could not explain the effect of Hrr25 on NMD alone:

- Gradient fractionation profiles: reduction of the polysomes pic after inhibition of Hrr25 kinase activity (**Figure 27**B and C)
- Specific downregulation of the RPL and RPS proteins after inhibition of Hrr25 kinase activity.

One of Hrr25's target is Upf1 CTD

Having shown that Hrr25 has an effect on NMD rises multiple questions:

- **Does this effect involve phosphorylation of one or multiple proteins? If so, which proteins?**
- **Does Hrr25 affect the dynamics of the NMD complexes?**

To answer the first question, we have examined multiple proteins as possible phosphorylation target for Hrr25. Since Smg1 phosphorylates Upf1 in the SURF complex in complex organisms (Yamashita et al., 2001), we first explored the hypothesis that Hrr25 might be a functional homolog of Smg1 and thus would be the kinase phosphorylating Upf1 in yeast.

Protein levels for the NMD reporter 1490 were useful readout to look at target for Hrr25. Indeed, as seen previously, the effect of Hrr25 on NMD can be detected by looking at the protein from the transcript 1490 with the HA tag through WB. Stabilisation of the RNA and translation still going on leads to higher signal of the protein. However, by depleting the protein or removing the region of phosphorylation by Hrr25 from the NMD complexes, inhibition of Hrr25 kinase activity should no longer have any visible phenotype on NMD. Since in other organisms, Upf1 is the target of Smg1 kinase, we decided to see if this core NMD factor could be a target of Hrr25 phosphorylation. More particularly, we know that the C-terminal domain of Upf1 is a potential binding site for interaction with Ebs1 that contains a 14-3-3 like domain recognizing phosphorylated Serine residues. We thus decided to look at Upf1 C-terminal domain – 854-971. To do so, Upf1 was truncated with the introduction of an HA tag after codon for amino acid 853. Compared to the TAP tag, the HA tag has the advantage to be smaller and thus we could see Upf1 on a Western Blot with more resolution. To compare, we used a strain Upf1-HA. Hence, we look at the transcript 1490 in four strains: Upf1-HA and Upf1 (1-853) HA with Hrr25 WT in order to see the basal level of the protein 1490 in those conditions and Upf1-HA and Upf1 (1-853) HA with hrr25 I82G. Those strains were treated with either DMSO or 5µM 3MB-PP1 for 30 min. For the strain Upf1-HA hrr25 I82G, the same rising of the level

for transcript 1490 as with the hrr25 I82G strain could be seen (**Figure 28**A). For the Upf1 (1-853)-HA hrr25 I82G, the effect of inhibition of kinase activity could still be observed (**Figure 28**A).

Nevertheless, thanks to the small HA tag, different sizes could be seen for Upf1 (**Figure 28**A and B). However, the upper band – the heaviest version of Upf1 – disappeared after 30 minutes of inhibition of Hrr25 kinase activity suggesting that this band might be a phosphorylated version of Upf1 (**Figure 28**B). To confirm that, samples were treated with λ-phosphatase. This enzyme will allow elimination of all phosphorylation. After incubation with λ-phosphatase, the upper band of Upf1 disappeared (**Figure 28**C). However, if we add phosphatase inhibitors, the upper band of Upf1 persisted (**Figure 28**C). These results confirmed that the version of Upf1 that is heavier was due to a modification and that this modification is phosphorylation. Moreover, inhibition of Hrr25 kinase activity removed this phosphorylation. Thus, Hrr25 induces Upf1 phosphorylation either directly or indirectly through a kinase cascade.

In addition, removing the C-terminal domain of Upf1 (1-853) gave only one band for this protein in WB and the weight of this band did not depend on Hrr25 kinase activity anymore (**Figure 28**B). The phosphorylation event we are looking for, might probably happen in this region: 854 to 971.

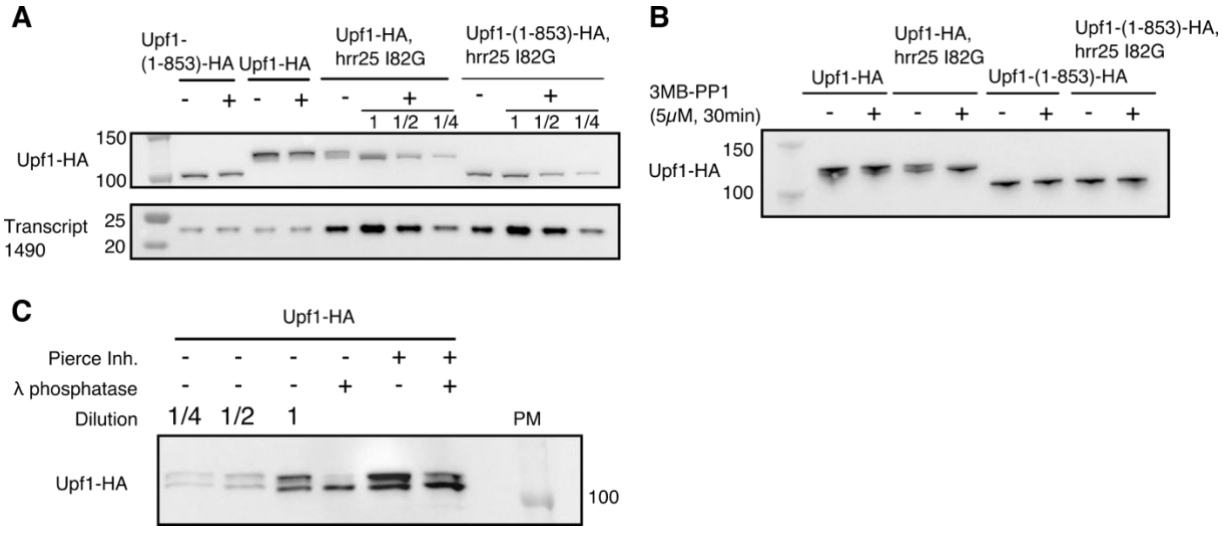

Figure 28: Upf1 C-terminal domain (854-971) might be a target of phosphorylation for Upf1. **A.** Western Blot using only anti-HA antibody. Here it allows to visualise not only the protein produced from the NMD substrate 1490 but also Upf1 truncated or not. **B.** Same as A. except

that migration of the proteins was longer to better visualise Upf1 truncated or not. Thus, the protein 1490 is not visible. **C.** Visualisation of λ-phosphatase treatment on Upf1-HA sample through Western Blot. As a control, λ-phosphatase treatment was also performed in presence of Pierce inhibitor (a phosphatase inhibitor cocktail).

A multiple alignment analysis (**Figure 29**A) provided by my supervisor showed two very highly conserved Serine residues in this region: S884 and S887 described as phosphorylated (Lanz et al., 2021). This sequence might correspond to a consensus sequence of phosphorylation by casein kinase I (Flotow et al., 1990; Meggio et al., 1992, 1991). In addition, in this region there is also another Serine residue that is not very conserved, but literature has described it as phosphorylated: S869 (Albuquerque et al., 2008). Those three residues were thus targeted for point mutations transforming them into Alanine that is non-phosphorylatable residue. Then looking by Western blot again at Upf1-HA, we could see that with these three mutations a single band is visible, suggesting that those residues can be phosphorylated. However, looking at NMD through WB with the plasmid 1490, no phenotype was visible (**Figure 29**B).

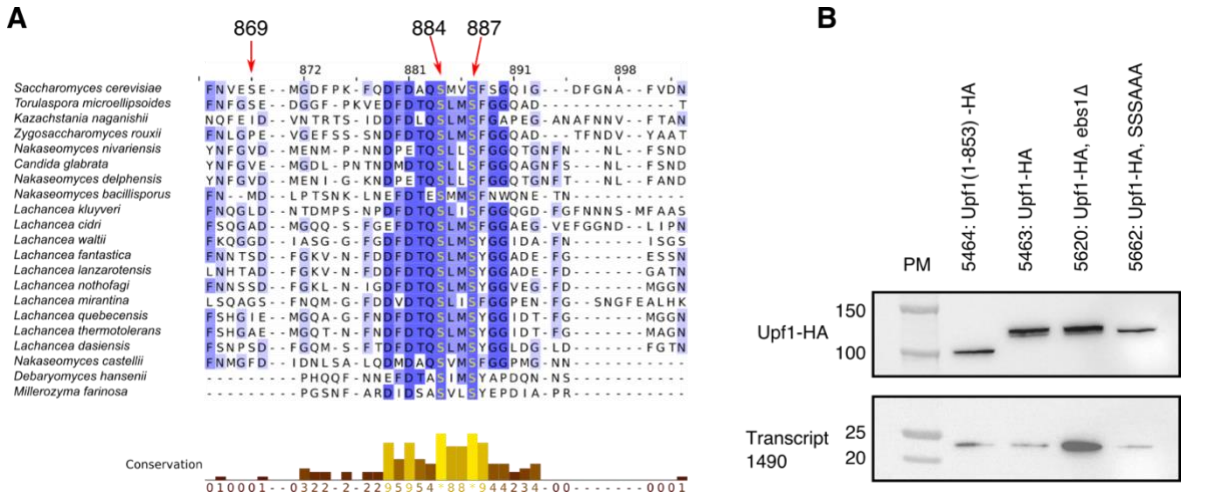

Figure 29: Potential phosphorylation sites in Upf1 C-terminal domain: S869, S884 and S887. **A.** Sequence alignment of Upf1 sequence from different fungi organisms using Jalview. **B.** Western Blot using only anti-HA antibody. We can thus visualise not only the protein produced from the NMD substrate 1490 but also different versions of Upf1-HA. SSSAAA corresponds to the triple mutation S869A, S884A and S887A.

Are there other sites of phosphorylation in Upf1 and in particular, in the C-terminal region? Maybe, phosphorylation is just a sign of Hrr25 presence in the complex and that its presence is more important than its kinase activity on Upf1.

Similarities between phosphor-Upf1 in yeast and in human cells.

Upf1 in yeast is thus like in other species, a phosphoprotein and this phosphorylation can appear during NMD thanks to the protein Hrr25. How is this mechanism regulated and when does this phosphorylation appear on Upf1? Using affinity purification followed by WB on different proteins from the NMD complexes can help distinguish stages of this mechanism. To do so, three proteins were used: Upf2 for the Detector complex, Nmd4 and Ebs1 for the Effector complex. While both versions of Upf1 can be seen when pulling on Nmd4 or Ebs1 (**Figure 30**B), we can see that Upf2 has specific affinity for Upf1 when is not phosphorylated (**Figure 30**C). Since Ebs1-TAP co-migrates with Upf1-HA, we decided to also look at Ebs1-(1-610)-TAP. Removing the C-terminal region of Ebs1 does not affect NMD and allowed us to differentiate Ebs1-TAP from Upf1-HA. Then, we can see that Ebs1-TAP binds to both versions of Upf1 but seems to prefer Upf1 in its phosphorylated state (**Figure 30**B). A similar behaviour can be seen in human cells for binding of the Smg5 and Smg7 proteins with Upf1 (Boehm et al., 2021; Jonas and Izaurralde, 2013).

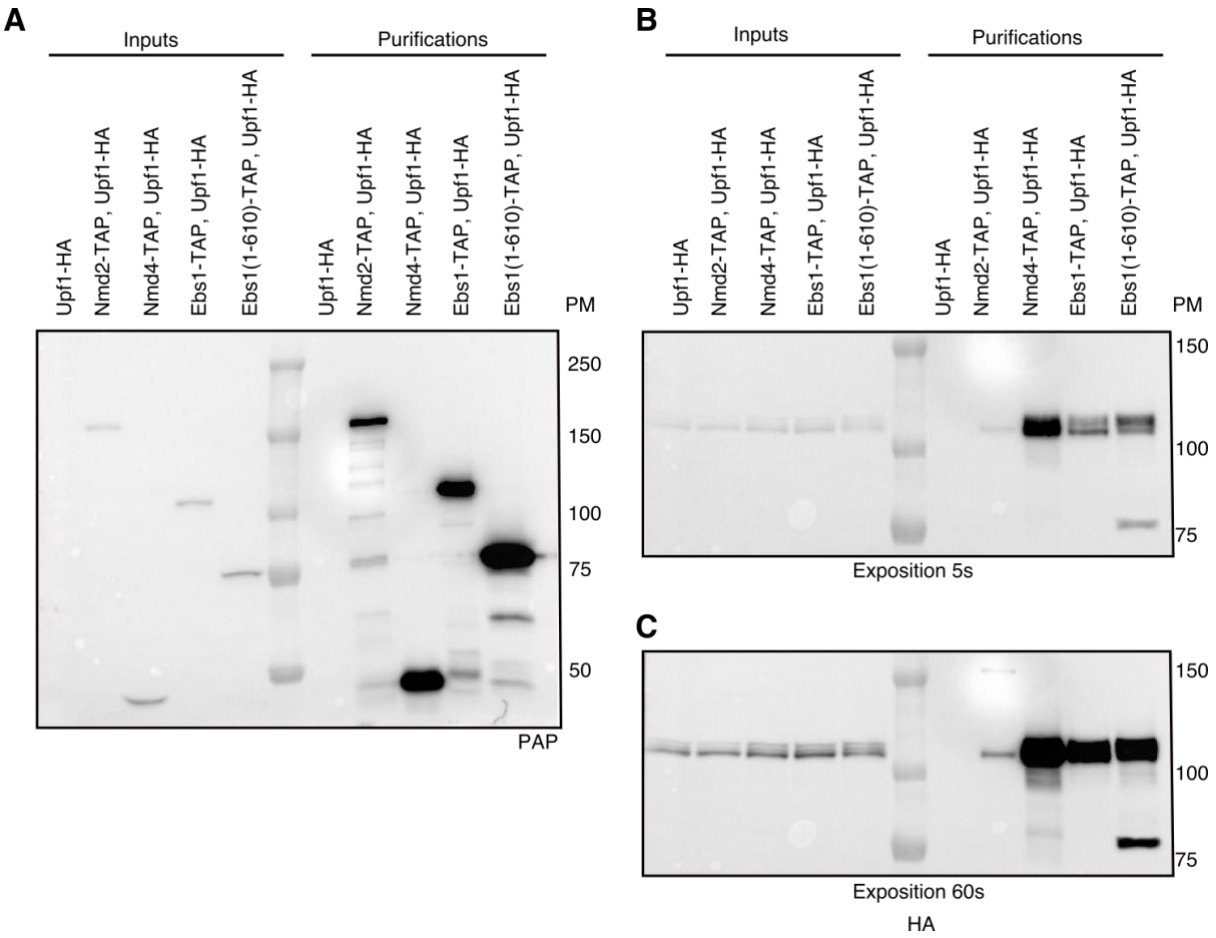

Figure 30: NMD factors bind to Upf1 in different states of phosphorylation. **A.** Western Blot using PAP antibody on input and purified proteins. PAP allows to detect the TAP tags. Hence Nmd2, Nmd4 and Ebs1 truncated or not could be seen on this membrane. **B.** Western Blot using anti-HA antibody on input and purified proteins. Anti-HA can also detect a little the TAP tag as we can see on the last lane – Ebs1(1-610)-TAP. **C.** The same as B. with a longer exposition time to better visualise Upf1 in the input samples.

Since NMD factors have different affinities with Upf1 according to its phosphorylation state, we wanted to see the effect of depletion of NMD factors on Upf1 phosphorylation. To do so, we either depleted Upf2 or Ebs1 in a Upf1-HA strain and then, through WB, we looked at the level of Upf1 phosphorylation. When Upf2 was depleted, Upf1 seemed hypophosphorylated whereas when Ebs1 was depleted, Upf1 seemed hyperphosphorylated (**Figure 31**B). This is coherent with what was observed in human cells further suggesting that Ebs1 is truly a functional homologue of Smg5/7 (Page et al., 1999).

We previously looked at polysomes through sucrose gradient sedimentation to visualise the impact of Hrr25 kinase activity inhibition on translation. This experiment can offer another piece of information that might help understanding the mechanism of phosphorylation regulation: where is Upf1 situated in those fractions and in which state is it? Thanks to HA-tag on Upf1, we can look through WB after collecting the fractions its position in the gradient (**Figure 31**A). Interestingly, in free fractions Upf1 is not phosphorylated at all. Phosphorylation of Upf1 starts to appear in fraction 8. Looking at NOG1 that associates with the subunit 60S of the ribosome, we can have an idea on the position of the different units of the ribosome and the polysomes. Nog1 signal corresponds to fraction 6 showing that all following fractions correspond to 80S and the polysomes. Hence, phosphorylation of Upf1 corresponds to fractions that sediment with the ribosome and polysomes. A similar result has been seen for human Upf1 (Pal et al., 2001).

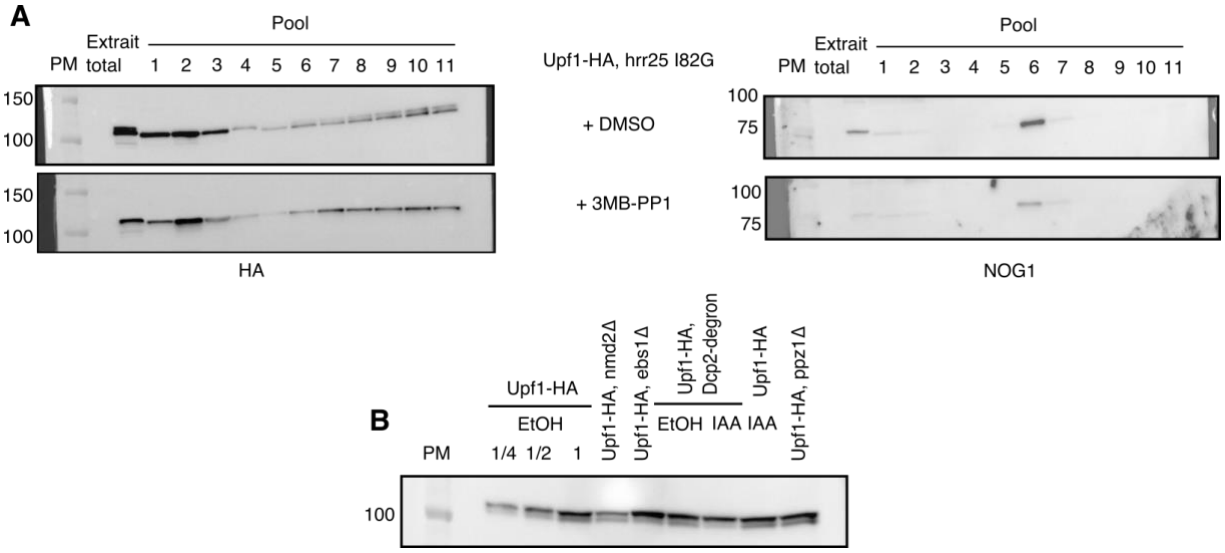

Figure 31: Position in the gradient fractions and the composition of NMD complexes influence the phosphorylation state of Upf1. **A.** Western Blots using anti-HA (on the left) and anti-NOG1 (on the right) antibodies on gradient fraction samples. The first lane corresponds to the membrane for the Upf1-HA hrr25 I82G strain with only DMSO while the second lane corresponds to the membrane for the Upf1-HA hrr25 I82G strain treated with 3MB-PP1. The anti-HA antibody allows to visualise Upf1 and its different states of phosphorylation. The anti-NOG1 antibody allows to see where NOG1 is situated in the gradient fractions. Since NOG1 associates with the subunit 60S of the ribosome, the lane where we can see NOG1 corresponds to the fraction 60S. Other fractions can then be deduced. **B.** Western Blots using anti-HA antibody to observe Upf1-HA and its state of phosphorylation in different conditions.

The state of phosphorylation of Upf1 in yeast is very similar to what happen in humans for its analogue. We can thus imagine that a similar mechanism of regulation is in action in both organisms. However, is the function for phosphorylation identical as well?

Hrr25 and its interactions with other NMD factors

While looking for the targets of Hrr25 in NMD, interesting results arose from a test performed on the NMD substrate carried by the plasmid 1490. We hypothesised that if we removed the target of Hrr25 in NMD, inhibition of Hrr25 would no longer have any impact on NMD substrate. We then constructed strains containing the mutant hrr25 I82G and depletion of putative targets.

We looked at two proteins or regions of protein:

- Ebs1
- Dcp2 C-terminal region: 301-970. This region is known as highly phosphorylated (data available on SGD[3]) and some phosphorylated serine residues were observed in MS experiments by Abdelkader Namane – S679, S682 and S751 (internal lab results).

Ebs1

As Ebs1 is not an essential gene, we can deplete this protein from the genome. Depletion of Ebs1 alone has a small efffect on NMD that is emphasised when Nmd4 is also depleted (Dehecq et al, 2018). Thanks to the transcript 1490, impact on NMD could be seen with each mutant separately – hrr25 I82G and *ebs1*Δ - and together. First, we can see that inhibition of Hrr25 kinase activity still led to an increase in proteins for our NMD substrate (**Figure 32**). Hence, inhibition still impacts NMD and Ebs1 might not be a target for phosphorylation. However, an interesting observation that we did not expect is that the impact on NMD with the two mutations is higher than the impact with only one mutation each. Could there be a synergistic effect between Hrr25 and Ebs1? If so, maybe we can see better the impact of Hrr25 inhibition on NMD in a context where Ebs1 is absent.

[3] Dcp2 protein details. Available on: https://www.yeastgenome.org/locus/S000005062/protein#sequence (last seen the 29/09/2022)

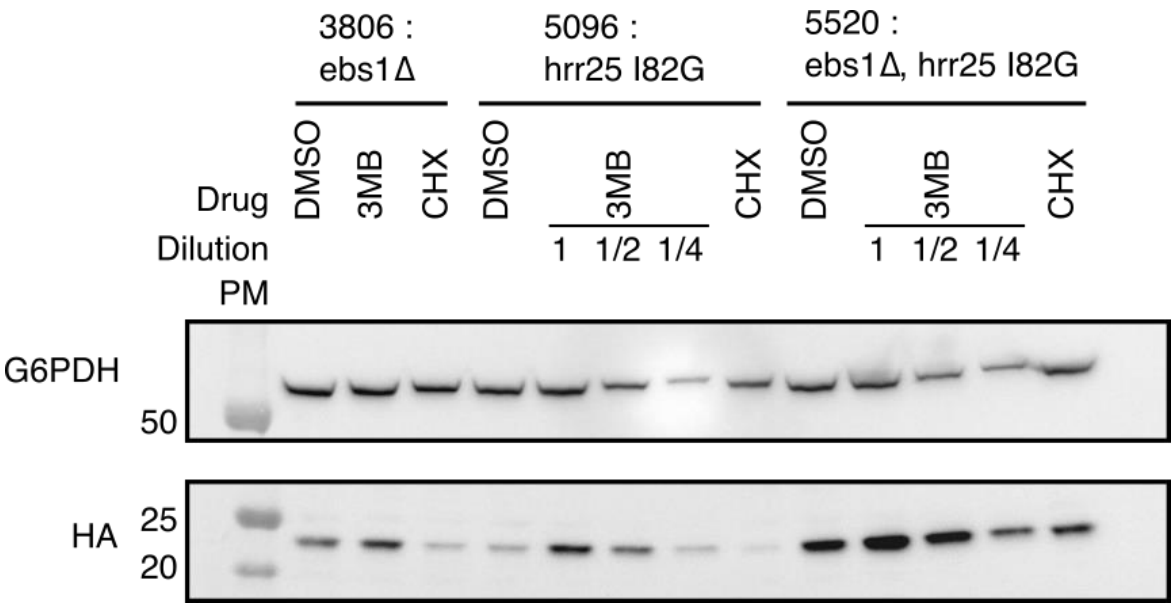

Figure 32: Depletion of Ebs1 and mutation of Hrr25 might have a synergistic effect on NMD. Western Blot using anti-HA and anti-G6PDH antibodies on protein samples. Anti-HA antibody allows visualising the protein produced from the NMD substrate 1490. Anti-G6PDH antibody was used as a control of gel loading.

Dcp2

Multiple factors designated Dcp2 as a putative target for Hrr25 phosphorylation. As stated previously, Dcp2 C-terminal region is highly phosphorylated and three of those phosphorylated residues have been seen in MS experiments in the Lab in the context of NMD. Two of them are similar to a consensus sequence of phosphorylation by kinases belonging to the family casein kinase I (Flotow et al., 1990; Meggio et al., 1992, 1991) such as Hrr25. Furthermore, an interaction between Hrr25 and Dcp2 has already been described in the context of P-bodies. Dcp2 C-terminal region is thus an ideal candidate for our study. However, even after removal of this domain, Hrr25 inhibition has still an impact on the NMD reporter 1490 in WB suggesting that Dcp2 terminal region might not be a target for Hrr25 phosphorylation (**Figure 33**). On the other hand, when looking at Dcp2-HA, hrr25 I82G strain, we can see that Dcp2 seems destabilised when Hrr25 kinase activity is inhibited.

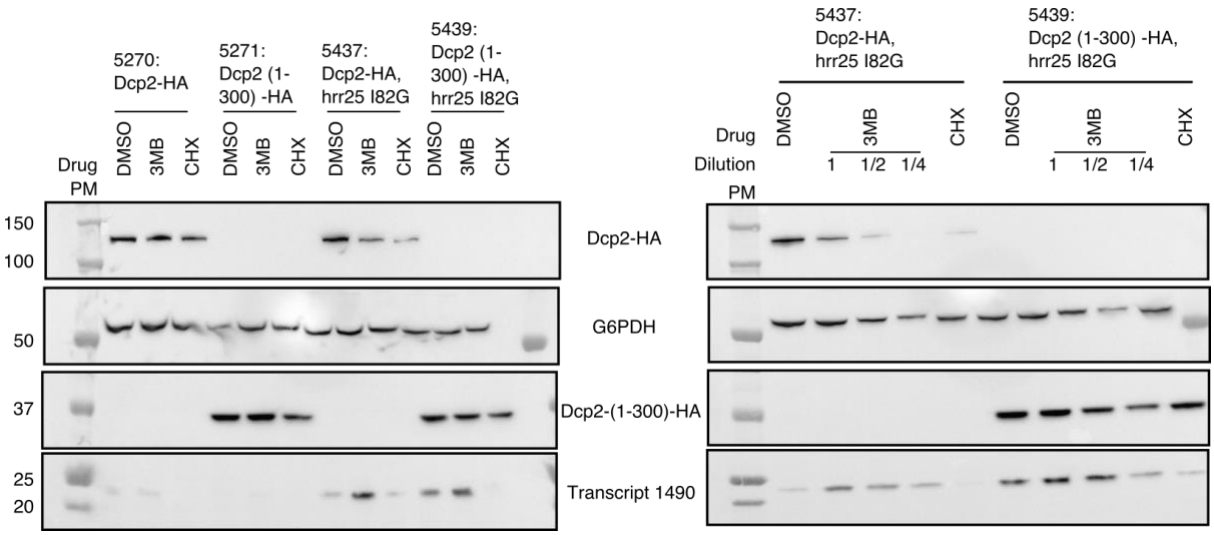

Figure 33: Inhibition of Hrr25 kinase activity might act on the stability of Dcp2 full-length. Western Blot using anti-HA and anti-G6PDH antibodies on protein samples. Anti-HA antibody allows visualising the protein produced from the NMD substrate 1490 and the different versions of Dcp2. Anti-G6PDH antibody is used as a control of gel loading. On the right side of the figure, we can see the membrane containing all samples controls and tests. On the left side of the figure, we can see only the tests samples but with serial dilutions to determine the NMD phenotype a little more precisely.

The synergic effect on NMD of Ebs1 and Hrr25 and the lack of a clear effect of the Dcp2 C-terminal domain led us to the question: "**Does Hrr25 affect the dynamic of the NMD complexes?".**

Recruitment of Hrr25 into NMD complexes

To answer the question of the impact of Hrr25 on the NMD complexes, the Tandem Affinity Purification and Mass spectrometry is used (see Material and Methods). First, we wanted to determine the impact of Hrr25 kinase activity on the dynamics of NMD complexes. For this, the bait protein used is Upf1 with the TAP tag. This modification was introduction in strains containing the mutation I82G for Hrr25 so that we could modulate kinase activity. Thus, after thirty minutes of incubation with 3MB-PP1, the complexes were purified using Affinity purification and by pulling on Upf1. Identification of Upf1 partners was performed through Mass Spectrometry. First thing observed with this analysis was that Hrr25 was lost after inhibition of kinase activity (**Figure 34**B). Hence, Hrr25 kinase activity is essential for recruitment of Hrr25 in NMD complexes. Moreover, during this inhibition no other proteins

were lost from the NMD complexes. Either kinase activity has no impact on NMD complexes dynamic, or those complexes are very stable, and 30 minutes is not enough to see changes in their composition.

The result that Hrr25 kinase activity is important for its recruitment in NMD complexes is consistent with the specific case of Hrr25 in P-bodies (Zhang et al., 2016). In this publication, they showed that Hrr25 is recruited in the P-bodies thanks to Dcp2 to avoid the kinase degradation. This recruitment is also dependent on its kinase activity. Hence, we asked ourselves if this recruitment in NMD complexes was not dependent as well on Dcp2.

To answer this, the same methodology was used with the same protein bait, Upf1. However, this time we used a strain with Dcp2 that was controlled by an AID system. Introduction of Auxin in the culture will induce specific degradation of Dcp2. Through mass spectrometry, we can observe a slight degradation of Dcp2 even in the absence of Auxin. Thus, comparison was made with the control Upf1-TAP (**Figure 34**C and D). We can see that after degradation of Dcp2, the core decapping complex – Dcp2, Dcp1 and Edc3– were lost from the NMD complexes. Moreover, Hrr25 also disappeared from the complexes, showing that interaction with the NMD complexes and more precisely its recruitment comes from the decapping complex and in particular, from Dcp2.

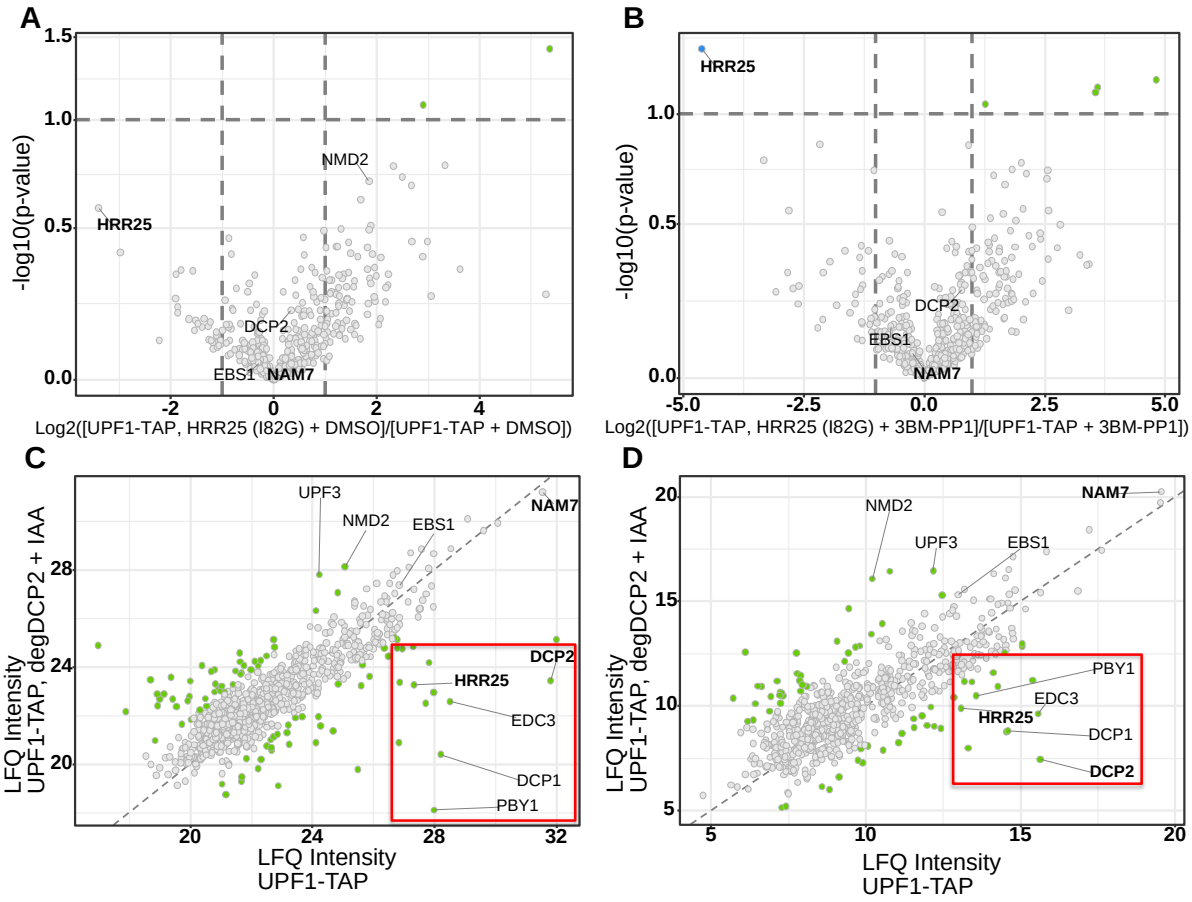

Figure 34: Hrr25's recruitment into yeast NMD complexes is dependent on its kinase activity and on Dcp2. **A.** Volcano plot comparing the Upf1-TAP, hrr25 I82G treated with the solvent DMSO sample to Upf1-TAP treated with DMSO sample. Three replicates were done for each condition. **B.** Volcano plot comparing the Upf1-TAP, hrr25 I82G treated with 3MB-PP1 sample to Upf1-TAP treated with 3MB-PP1 sample. Three replicates were done for each condition. **C.** Scatterplot representing on the y-axis the LFQ intensities of the sample Upf1-TAP, Dcp2-degron treated with Auxin and on the x-axis the LFQ intensities of the control Upf1-TAP. This plot corresponds to the first biological replicate of this experiment. **D.** Scatterplot representing on the y-axis the LFQ intensities of the sample Upf1-TAP, Dcp2-degron treated with Auxin and on the x-axis the LFQ intensities of the control Upf1-TAP. This plot corresponds to the second biological replicate of this experiment.

Discussion and Perspectives

NMD is a specific degradation pathway that not only helps taking care of faulty transcripts but also regulates around 10% of the products of DNA transcription. This function has a major impact in cellular processes such as neuronal differentiation. Defects in NMD can lead to a higher risk of cancer and apparition of PTC is an important source of genetic diseases. Understanding molecular mechanism of NMD could be the key to better the therapeutic approaches in certain cases.

First discovered and studied in *S. cerevisiae*, this model organism was put aside for NMD since several Smg proteins identified in complex eukaryotes were thought to have no equivalent in yeast. However, affinity purification, mass spectrometry and functional assays showed that equivalents could be found in *S. cerevisiae* as well (Clissold and Ponting, 2000; Dehecq et al., 2018; Luke et al., 2007; Wilmes et al., 2008). In this study, we found that Hrr25, a protein kinase, is involved in yeast NMD but also that this enzyme phosphorylates Upf1, showing that the regulation of NMD through phosphorylation might be conserved as well. These discoveries can help to understand NMD molecular mechanisms that do not depend on EJC.

Methods

Studying Hrr25, a very important casein kinase for yeast involved in so many cellular processes, was a very challenging work, technically speaking. Indeed, its functions in meiosis and maturation of the 40S subunit of the ribosome make this enzyme essential for yeast and new tools had to be developed when I initiated this project at my arrival in order to discover more about this yeast enzyme in NMD. Midway, we learnt that Hrr25 might have a function in DNA transcription and more particularly in snoRNA transcription termination (Nemec et al., 2019). In the RNA-sequencing that I performed, this effect could be confirmed. This information is problematic since it complicates the annotation processes. Indeed, then some transcripts might be noted as upregulated, but this upregulation might be due to defects of transcription termination for XUT, SUT and other transcripts (**Figure 35**).

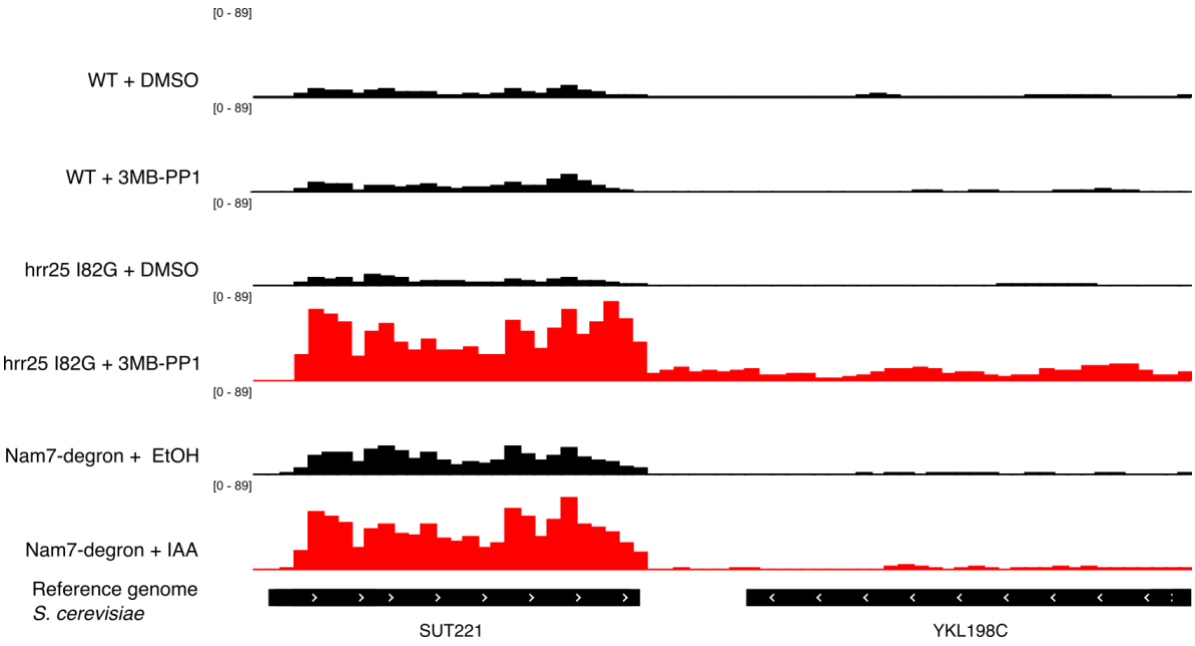

Figure 35: IGV image representing the reads of the different RNA-seq datasets for SUT221 and YKL178C.

Nevertheless, the whole transcriptome changes showed that Hrr25 intervenes in NMD an information that would have been incomplete if we only concentrated on RT-qPCR. In the latter experiment, the analysis relies on a housekeeping gene that is supposed to not vary over the conditions. However, using RT-qPCR with different housekeeping genes as reference, the impact on NMD was not the same according to those references leading to confusion. This could have made us suggest that the results were not reproducible and not robust. However, RNA-sequencing showed that the impact of Hrr25 on the transcriptome is broader than previously thought and that a bigger picture was needed to determine the role of Hrr25 in NMD.

With RT-qPCR, we saw that a dynamic experiment led to more robust results and helped understand better the importance of Hrr25 in NMD. Maybe, a more dynamic context could be of use for the proteomic study. Indeed, Mass Spectrometry allows to visualise the equilibrium of complexes at a certain point. However, every complex has different robustness. Therefore, a dynamic study on a longer period of time would lead to results giving a different point of view on those complexes and could help understand better the role of Hrr25 in NMD.

To help in the dissection of NMD complexes dynamics, degron systems for target proteins are ideal. However, adding the AID domain allows already a small depletion of the targeted protein even though IAA is not present. Thus, the strain itself does not correspond to a wild-type condition and slight effects could be seen. However, this system can be improved

thanks to a ß-estradiol inducible promoter for control of TIR1, in ubiquitination complex, production. A better system would thus be adding both a ß-estradiol inducible promoter and an AID domain (Mendoza-Ochoa et al., 2019). The ß-estradiol inducible promoter will be introduced in front of TIR1, part of the ubiquitination complex. The AID domain will still be added to the protein of interest, in this study either Upf1 or Dcp2. Hence to induce degradation, ß-estradiol should also be introduced in the culture to start production of TIR1 in addition to Auxin that will attached to the AID domain and target our protein for degradation. Frank Feuerback implemented this method in the laboratory very recently and thus could not be used in this study. Nevertheless, this method is now available and could be used for further experiments.

Last but not least, the next point we were struggling with is the difference in NMD phenotype between inhibition of Hrr25 kinase activity and Upf1 triple mutant. This difference might point out that not all phosphorylation sites have been identified. Indeed, in human cells, eight point mutations in Upf1 are necessary to obtain maximum phenotype for NMD (Durand et al., 2016). To determine if there are phosphorylation residues remaining in the C-terminal domain, we could perform 2D gel or use radioactivity. Radioactivity is sensitive but if not careful enough, this technic can be potentially dangerous for the person using it. Gel 2D can be fast but might not be as sensitive as radioactivity. Another obstacle might be the need of a particular context to see the full phenotype of phosphorylation on NMD such as depletion of another protein.

Regulation mechanism in eucaryotes: phosphorylation and state of phosphorylation are similar

Thanks to this work, we can see that both in yeast and in mammals Upf1 is phosphorylated by a kinase during NMD (this study; Kashima et al., 2006; Yamashita et al., 2001). Also in this study, we tried to characterise this phosphorylation of Upf1. As stated in the results, differences could be seen in phosphorylation state of Upf1 according to the complexes it belongs to. To achieve this, we used affinity purification with Upf2 and Ebs1 as target proteins. Upf2 purification allowed to retrieve the Upf complex while Ebs1 purification allowed to pull down the Upf-decapping complex. In this experiment, we observed that in Upf2 purification, Upf1 was not in phosphorylated state whereas in the Ebs1 purification, Ebs1 could bind to both versions of Upf1 with a preference for phosphorylated Upf1. To go further in characterisation of this regulation of phosphorylation, we looked at Upf1 phosphorylation state when NMD factors were depleted. We noticed that in *upf2*Δ cells Upf1 is in

hypophosphorylated state while in *ebs1*Δ cells Upf1 is in hyperphosphorylated state. Finally, we looked at the distribution of Upf1 in the polysomes thanks to gradient fractionation. This experiment revealed that Upf1 can be found throughout the gradient. Nevertheless, the phosphorylation form of Upf1 is only present in the polysome, the RNA bound fraction. These results were very similar to the ones obtained in human cells. Indeed, affinity purification of either Smg5 or Smg7 led to purification of Upf1 and preferentially pUpf1 (Boehm et al., 2021; Jonas et al., 2013). In addition, depletion of Smg5 or Smg7 also had as consequence hyperphosphorylation of Upf1 (Page et al., 1999). Moreover, thanks to 2D Gel analysis, the different phosphorylation states of Upf1 and pUpf1 were visible in the fraction containing the polysomes (pellet) but not in the free fraction (supernatant) (Pal et al., 2001).

These similarities suggest that the mechanism behind NMD might be better conserved throughout eukaryotes than previously thought; not only did we find a kinase in yeast that is involved in NMD independently of its other functions, but this kinase seems to phosphorylate the same target that is Upf1 and regulation of this phosphorylation shares common mechanisms. However, an important difference exists between complex organisms and yeast: Smg1 is essential for mammal NMD whereas Hrr25 is not. Furthermore, Smg1 is not always essential, such as in *C. elegans* (Chen et al., 2005).

An explanation to this difference might be the timing of recruitment of those two kinases. Indeed, while Smg1 is believed to be recruited at the beginning of the NMD process in SURF (Kashima et al., 2006), Hrr25 is recruited by Dcp2 in the Upf-decapping complex. The role of Hrr25 has not yet been determined in yeast NMD, but Smg1 function is related to the switch between SURF and DECID complexes and is critical for later recruitment of the degradation factors. Hrr25 on the other hand comes with the degradation factors either to help in the degradation activity or maybe later for the recycling process. Hence, we can assume that the function of Hrr25 in NMD might not be limitating for NMD.

Hrr25 a potential functional homolog of Smg1?

Discovery of involvement of Hrr25 in yeast NMD and seeing that it phosphorylates Upf1 can lead us to suggest that Hrr25 might be a functional homolog of Smg1. However, the timing of recruitment probably differs, and inhibition of kinase activity does not have the same effect on NMD.

Recently, another kinase has been involved with mammal NMD: AKT1 (Palma et al., 2021). This kinase has been identified thanks to a screening of NMD inhibitors. Palma and colleagues determined that AKT1 also phosphorylates Upf1, and its recruitment depends on

Upf3b. In another screening, the whole AKT signaling pathway was identified as involved in NMD (H. Cho et al., 2022). Further analysis showed that this pathway allowed phosphorylation of Upf1 in T151 (H. Cho et al., 2022). This phosphorylation event changes Upf1 conformation so that the CH domain does not inhibit helicase activity. Hence, AKT phosphorylation of Upf1 is a functional equivalent of Upf2 interaction with Upf1 (H. Cho et al., 2022). Moreover, it seems that depletion of either kinase led to inhibition of NMD and depletion of both does not have a cumulative effect. Does Upf1 need multiple phosphorylation events for efficient NMD?

Involvement of multiple kinases for regulation of NMD could also be suggested in yeast. Indeed, Hrr25 belongs to the CK1 family and as mentioned in the introduction, the main consensus sequence of phosphorylation is pS/pT-X-X-S*/T* with pS/pT being a Ser or a Thr residue phosphorylated and X representing any amino acid (Flotow et al., 1990; Meggio et al., 1992, 1991). Hence, CK1 members need a priming phosphorylation event in –3 position. For example, in translation termination, Hrr25 needs Pol II CTD to be hyperphosphorylated for interaction and downstream phosphorylation (Phatnani et al., 2004). Just as in transcription termination, Hrr25 kinase activity can allow fine tuning of NMD after a first phosphorylation event on Upf1.

Synergic action between Hrr25 and Ebs1

In this study, we highlighted three points showing that Hrr25 and Ebs1 might act in concert. First, we observed a stronger effect of Hrr25 inhibition on NMD when Ebs1 is depleted. Then, the serine residues that we identified as phosphorylated by Hrr25 on Upf1 C-terminal domain, are located in a domain which could be the domain of interaction between Upf1 and Ebs1. Finally, we noticed that in the mass spectrometry results Ebs1 seems to have a different behaviour than the rest of the proteins of the Effector complex.

Not only did we see that Hr25 possesses a function in NMD, but this effect seems stronger when we depleted Ebs1 (**Figure 32**). Ebs1 as we saw previously and more particularly in the introduction, might be the functional homologue of Smg5 and Smg7. This protein also contains a 14-3-3 domain that has been described in literature as a domain binding with more affinity to phosphorylated Serine residues (Fu et al., 2000; Muslin et al., 1996; Yaffe et al., 1997). What's more, the Serine residues saw potentially phosphorylated in Upf1 C-terminal domain in yeast corresponds to a domain that can participate to binding to Ebs1 (Dehecq et al., 2018). However, as seen in mammals, this specific binding between 14-3-3 domain and phosphorylated residues is questionable. Indeed, in recent studies it seems that there is a preference for phosphorylated Upf1 for Smg5/Smg7 proteins, but these proteins can also bind

to non-phosphorylated Upf1 (Durand et al., 2016). These data were also noticed in this study with affinity purification of Ebs1 (**Figure 30**). Phosphorylation is suggested now to enhance binding between Smg5/7 and Upf1 but is no longer considered as essential.

To better understand the role of phosphorylation in NMD and in particular in yeast NMD, we might take advantage of this synergistic effect for future experiments. NMD phenotype for inhibition of Hrr25 kinase activity might be better observed in a context where Ebs1 is depleted from the cells. We can thus repeat experiment with Upf1 triple mutated for the phosphorylated residues but also MS experiments to see the state of NMD complexes after inhibition of Hrr25 kinase activity in the absence of Ebs1.

Hrr25 might act on Dcp2 stability

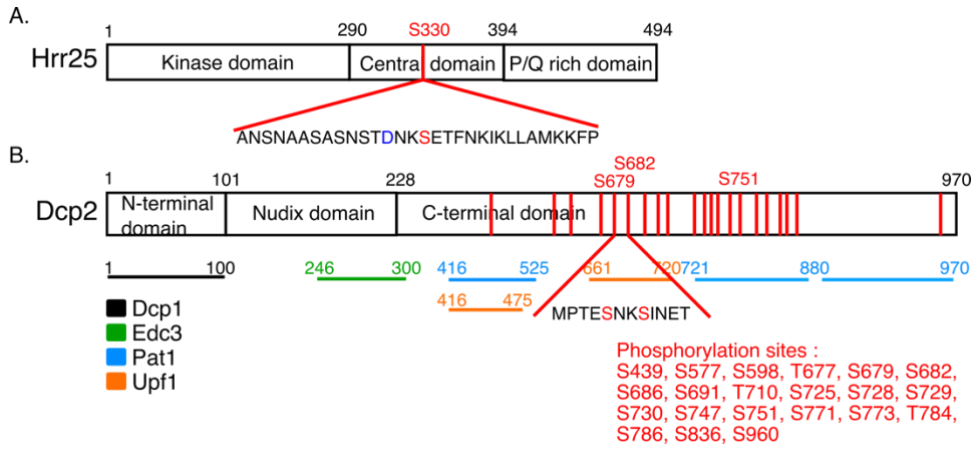

Figure 36: Hrr25 and Dcp2 are two phosphoproteins.

In NMD and in particular in Upf1-decapping complex, other proteins possess phosphorylation sites (see **Figure 36**). Thus, the remaining question is whether Upf1 is the only target in NMF for Hrr25 phosphorylation or not.

Dcp2 is an interacting partner for Hrr25 and may be a phosphorylation target in the context of NMD as an interaction between them was already described in literature but in a different context (Zhang et al., 2016). Indeed, it was shown that Hrr25 is recruited in P-bodies by interacting with Dcp2 and this interaction was also dependent on Hrr25 kinase activity. This recruitment was suggested to prevent Hrr25's own degradation in context of stress (Zhang et al., 2016) and seems important for Hrr25 function in meiosis (Zhang et al., 2018). Later on, the authors of this study discussed as Dcp2 being a possible target for Hrr25 (reviewed in Zhang and Herman, 2019). This hypothesis is supported by the presence of many phosphorylation sites in the C-terminal domain of Dcp2 (**Figure 36**B). In our MS experiment, three sites could be

seen as phosphorylated: S679, S682 and S751. Those are sites that might be protected by the different proteins for complexes to which belongs Dcp2. In our context of NMD, we could see that Hrr25 recruitment into yeast NMD complexes followed the same pattern as for the P-bodies.

No NMD phenotype could be seen when the C-terminal domain of Dcp2 was removed (He and Jacobson, 2015). However, removal of the Dcp2 C-terminal domain, led to a potential increase in protein stability. This domain contains auto-inhibition domains that allows regulation of decapping activity of Dcp2. Stability of Dcp2 full-length seemed to be impacted after inhibition of Hrr25 kinase activity. Signal seemed to decrease almost at the same level as with treatment with CHX while translation is not heavily affected after 30 min of incubation with ATP-analogue. Is it then possible that we dismissed Dcp2 as target of Hrr25 too quickly and that this phosphorylation might help stabilised Dcp2? Could it also affect Dcp2 decapping activity? Nevertheless, before further analysis, these results need to be repeated and other experiments should be done to confirm this potential effect.

Our project is part of a global collaboration in the context of ANR. Our collaborators are currently working on the development of a decapping *in vitro* assay using luminescence. This test would allow us to study the activity of Dcp2 with different factors and in different contexts. Therefore, we could take this to our advantage and try looking at the Dcp2 decapping activity with or without Hrr25 kinase activity.

In conclusion, our laboratory showed that the molecular mechanism for NMD might be better conserved than previously thought with the duo complexes revolving around Upf1 (Dehecq et al., 2018) and phosphorylation involved also in regulation of yeast NMD (this study). This work opens new questions for a future projects: (i) what is exactly the function of Hrr25 phosphorylation in yeast NMD? (ii) does this action need co-factors? (iii) is Upf1 the only target of Hrr25 in NMD? It would be interesting to determine if other kinases are involved in NMD since Hrr25 might need a priming phosphorylation event in order to act (Flotow et al., 1990; Meggio et al., 1992, 1991). Moreover, Upf1 is not the only Upf protein to be phosphorylated. Upf2 is also a phospho-protein (Wang et al., 2006). However, the role of its phosphorylation is unclear, and no kinase have been involved yet.

Bibliography

Abdel-Fattah, W., Jablonowski, D., Santo, R.D., Thüring, K.L., Scheidt, V., Hammermeister, A., Have, S. ten, Helm, M., Schaffrath, R., Stark, M.J.R., 2015. Phosphorylation of Elp1 by Hrr25 Is Required for Elongator-Dependent tRNA Modification in Yeast. PLOS Genetics 11, e1004931. https://doi.org/10.1371/journal.pgen.1004931

Agostinis, P., Pinna, L.A., Meggio, F., Marin, O., Goris, J., Vandenheede, J.R., Merlevede, W., 1989. A synthetic peptide substrate specific for casein kinase I. FEBS Lett 259, 75–78. https://doi.org/10.1016/0014-5793(89)81498-x

Akashi, M., Tsuchiya, Y., Yoshino, T., Nishida, E., 2002. Control of intracellular dynamics of mammalian period proteins by casein kinase I epsilon (CKIepsilon) and CKIdelta in cultured cells. Mol Cell Biol 22, 1693–1703. https://doi.org/10.1128/MCB.22.6.1693-1703.2002

Akhtar, Md.S., Heidemann, M., Tietjen, J.R., Zhang, D.W., Chapman, R.D., Eick, D., Ansari, A.Z., 2009. TFIIH Kinase Places Bivalent Marks on the Carboxy-Terminal Domain of RNA Polymerase II. Molecular Cell 34, 387–393. https://doi.org/10.1016/j.molcel.2009.04.016

Albuquerque, C.P., Smolka, M.B., Payne, S.H., Bafna, V., Eng, J., Zhou, H., 2008. A multidimensional chromatography technology for in-depth phosphoproteome analysis. Mol Cell Proteomics 7, 1389–1396. https://doi.org/10.1074/mcp.M700468-MCP200

Alhusaini, N., Coller, J., 2016. The deadenylase components Not2p, Not3p, and Not5p promote mRNA decapping. RNA 22, 709–721. https://doi.org/10.1261/rna.054742.115

Allmang, C., Petfalski, E., Podtelejnikov, A., Mann, M., Tollervey, D., Mitchell, P., 1999. The yeast exosome and human PM-Scl are related complexes of 3’ --> 5’ exonucleases. Genes Dev 13, 2148–2158. https://doi.org/10.1101/gad.13.16.2148

Amit, S., Hatzubai, A., Birman, Y., Andersen, J.S., Ben-Shushan, E., Mann, M., Ben-Neriah, Y., Alkalay, I., 2002. Axin-mediated CKI phosphorylation of beta-catenin at Ser 45: a molecular switch for the Wnt pathway. Genes Dev 16, 1066–1076. https://doi.org/10.1101/gad.230302

Amrani, N., Dong, S., He, F., Ganesan, R., Ghosh, S., Kervestin, S., Li, C., Mangus, D.A., Spatrick, P., Jacobson, A., 2006. Aberrant termination triggers nonsense-mediated mRNA decay. Biochem Soc Trans 34, 39–42. https://doi.org/10.1042/BST20060039

Amrani, N., Ganesan, R., Kervestin, S., Mangus, D.A., Ghosh, S., Jacobson, A., 2004. A faux 3’-UTR promotes aberrant termination and triggers nonsense-mediated mRNA decay. Nature 432, 112–118. https://doi.org/10.1038/nature03060

Andersen, C.B.F., Ballut, L., Johansen, J.S., Chamieh, H., Nielsen, K.H., Oliveira, C.L.P., Pedersen, J.S., Séraphin, B., Le Hir, H., Andersen, G.R., 2006. Structure of the exon junction core complex with a trapped DEAD-box ATPase bound to RNA. Science 313, 1968–1972. https://doi.org/10.1126/science.1131981

Applequist, S.E., Selg, M., Raman, C., Jäck, H.M., 1997. Cloning and characterization of

HUPF1, a human homolog of the Saccharomyces cerevisiae nonsense mRNA-reducing UPF1 protein. Nucleic Acids Res 25, 814–821. https://doi.org/10.1093/nar/25.4.814

Araki, Y., Takahashi, S., Kobayashi, T., Kajiho, H., Hoshino, S., Katada, T., 2001. Ski7p G protein interacts with the exosome and the Ski complex for 3'-to-5' mRNA decay in yeast. EMBO J 20, 4684–4693. https://doi.org/10.1093/emboj/20.17.4684

Argüello-Miranda, O., Zagoriy, I., Mengoli, V., Rojas, J., Jonak, K., Oz, T., Graf, P., Zachariae, W., 2017. Casein Kinase 1 Coordinates Cohesin Cleavage, Gametogenesis, and Exit from M Phase in Meiosis II. Developmental Cell 40, 37–52. https://doi.org/10.1016/j.devcel.2016.11.021

Aronoff, R., Baran, R., Hodgkin, J., 2001. Molecular identification of smg-4, required for mRNA surveillance in C. elegans. Gene 268, 153–164. https://doi.org/10.1016/s0378-1119(01)00414-0

Atkin, A.L., Schenkman, L.R., Eastham, M., Dahlseid, J.N., Lelivelt, M.J., Culbertson, M.R., 1997. Relationship between yeast polyribosomes and Upf proteins required for nonsense mRNA decay. J Biol Chem 272, 22163–22172. https://doi.org/10.1074/jbc.272.35.22163

Atkinson, G.C., Baldauf, S.L., Hauryliuk, V., 2008. Evolution of nonstop, no-go and nonsense-mediated mRNA decay and their termination factor-derived components. BMC Evolutionary Biology 8, 290. https://doi.org/10.1186/1471-2148-8-290

Aylon, Y., Kupiec, M., 2004. New insights into the mechanism of homologous recombination in yeast. Mutation Research/Reviews in Mutation Research 566, 231–248. https://doi.org/10.1016/j.mrrev.2003.10.001

Babu, P., Deschenes, R.J., Robinson, L.C., 2004. Akr1p-dependent palmitoylation of Yck2p yeast casein kinase 1 is necessary and sufficient for plasma membrane targeting. J Biol Chem 279, 27138–27147. https://doi.org/10.1074/jbc.M403071200

Badis, G., Saveanu, C., Fromont-Racine, M., Jacquier, A., 2004. Targeted mRNA degradation by deadenylation-independent decapping. Mol Cell 15, 5–15. https://doi.org/10.1016/j.molcel.2004.06.028

Bai, Y., Salvadore, C., Chiang, Y.C., Collart, M.A., Liu, H.Y., Denis, C.L., 1999. The CCR4 and CAF1 proteins of the CCR4-NOT complex are physically and functionally separated from NOT2, NOT4, and NOT5. Mol Cell Biol 19, 6642–6651. https://doi.org/10.1128/MCB.19.10.6642

Ballut, L., Marchadier, B., Baguet, A., Tomasetto, C., Séraphin, B., Le Hir, H., 2005. The exon junction core complex is locked onto RNA by inhibition of eIF4AIII ATPase activity. Nat Struct Mol Biol 12, 861–869. https://doi.org/10.1038/nsmb990

Basquin, J., Roudko, V.V., Rode, M., Basquin, C., Séraphin, B., Conti, E., 2012. Architecture of the nuclease module of the yeast Ccr4-not complex: the Not1-Caf1-Ccr4 interaction. Mol Cell 48, 207–218. https://doi.org/10.1016/j.molcel.2012.08.014

Becker, T., Armache, J.-P., Jarasch, A., Anger, A.M., Villa, E., Sieber, H., Motaal, B.A.,

Mielke, T., Berninghausen, O., Beckmann, R., 2011. Structure of the no-go mRNA decay complex Dom34–Hbs1 bound to a stalled 80S ribosome. Nat Struct Mol Biol 18, 715–720. https://doi.org/10.1038/nsmb.2057

Behm-Ansmant, I., Gatfield, D., Rehwinkel, J., Hilgers, V., Izaurralde, E., 2007a. A conserved role for cytoplasmic poly(A)-binding protein 1 (PABPC1) in nonsense-mediated mRNA decay. EMBO J 26, 1591–1601. https://doi.org/10.1038/sj.emboj.7601588

Behm-Ansmant, I., Kashima, I., Rehwinkel, J., Saulière, J., Wittkopp, N., Izaurralde, E., 2007b. mRNA quality control: an ancient machinery recognizes and degrades mRNAs with nonsense codons. FEBS Lett 581, 2845–2853. https://doi.org/10.1016/j.febslet.2007.05.027

Behrend, L., Milne, D.M., Stöter, M., Deppert, W., Campbell, L.E., Meek, D.W., Knippschild, U., 2000. IC261, a specific inhibitor of the protein kinases casein kinase 1-delta and -epsilon, triggers the mitotic checkpoint and induces p53-dependent postmitotic effects. Oncogene 19, 5303–5313. https://doi.org/10.1038/sj.onc.1203939

Belew, A.T., Advani, V.M., Dinman, J.D., 2011. Endogenous ribosomal frameshift signals operate as mRNA destabilizing elements through at least two molecular pathways in yeast. Nucleic Acids Res 39, 2799–2808. https://doi.org/10.1093/nar/gkq1220

Belgrader, P., Cheng, J., Maquat, L.E., 1993. Evidence to implicate translation by ribosomes in the mechanism by which nonsense codons reduce the nuclear level of human triosephosphate isomerase mRNA. Proc Natl Acad Sci U S A 90, 482–486. https://doi.org/10.1073/pnas.90.2.482

Bellí, G., Garí, E., Piedrafita, L., Aldea, M., Herrero, E., 1998. An activator/repressor dual system allows tight tetracycline-regulated gene expression in budding yeast. Nucleic Acids Res. 26, 942–947.

Bharati, A.P., Singh, N., Kumar, V., Kashif, M., Singh, A.K., Singh, P., Singh, S.K., Siddiqi, M.I., Tripathi, T., Akhtar, M.S., 2016. The mRNA capping enzyme of Saccharomyces cerevisiae has dual specificity to interact with CTD of RNA Polymerase II. Sci Rep 6, 31294. https://doi.org/10.1038/srep31294

Bianchin, C., Mauxion, F., Sentis, S., Séraphin, B., Corbo, L., 2005. Conservation of the deadenylase activity of proteins of the Caf1 family in human. RNA 11, 487–494. https://doi.org/10.1261/rna.7135305

Black, D.L., 2003. Mechanisms of alternative pre-messenger RNA splicing. Annu Rev Biochem 72, 291–336. https://doi.org/10.1146/annurev.biochem.72.121801.161720

Boeck, R., Tarun, S., Rieger, M., Deardorff, J.A., Müller-Auer, S., Sachs, A.B., 1996. The yeast Pan2 protein is required for poly(A)-binding protein-stimulated poly(A)-nuclease activity. J Biol Chem 271, 432–438. https://doi.org/10.1074/jbc.271.1.432

Boehm, V., Haberman, N., Ottens, F., Ule, J., Gehring, N.H., 2014. 3’ UTR length and messenger ribonucleoprotein composition determine endocleavage efficiencies at termination codons. Cell Rep 9, 555–568. https://doi.org/10.1016/j.celrep.2014.09.012

Boehm, V., Kueckelmann, S., Gerbracht, J.V., Kallabis, S., Britto-Borges, T., Altmüller, J., Krüger, M., Dieterich, C., Gehring, N.H., 2021. SMG5-SMG7 authorize nonsense-mediated mRNA decay by enabling SMG6 endonucleolytic activity. Nat Commun 12, 3965. https://doi.org/10.1038/s41467-021-24046-3

Bohnsack, M.T., Tollervey, D., Granneman, S., 2012. Identification of RNA helicase target sites by UV cross-linking and analysis of cDNA. Methods Enzymol 511, 275–288. https://doi.org/10.1016/B978-0-12-396546-2.00013-9

Bonneau, F., Basquin, J., Ebert, J., Lorentzen, E., Conti, E., 2009. The yeast exosome functions as a macromolecular cage to channel RNA substrates for degradation. Cell 139, 547–559. https://doi.org/10.1016/j.cell.2009.08.042

Bousquet-Antonelli, C., Presutti, C., Tollervey, D., 2000. Identification of a regulated pathway for nuclear pre-mRNA turnover. Cell 102, 765–775. https://doi.org/10.1016/s0092-8674(00)00065-9

Boutz, P.L., Stoilov, P., Li, Q., Lin, C.-H., Chawla, G., Ostrow, K., Shiue, L., Ares, M., Black, D.L., 2007. A post-transcriptional regulatory switch in polypyrimidine tract-binding proteins reprograms alternative splicing in developing neurons. Genes Dev 21, 1636–1652. https://doi.org/10.1101/gad.1558107

Brockman, J.L., Gross, S.D., Sussman, M.R., Anderson, R.A., 1992. Cell cycle-dependent localization of casein kinase I to mitotic spindles. Proc Natl Acad Sci U S A 89, 9454–9458. https://doi.org/10.1073/pnas.89.20.9454

Brockschmidt, C., Hirner, H., Huber, N., Eismann, T., Hillenbrand, A., Giamas, G., Radunsky, B., Ammerpohl, O., Bohm, B., Henne-Bruns, D., Kalthoff, H., Leithäuser, F., Trauzold, A., Knippschild, U., 2008. Anti-apoptotic and growth-stimulatory functions of CK1 delta and epsilon in ductal adenocarcinoma of the pancreas are inhibited by IC261 in vitro and in vivo. Gut 57, 799–806. https://doi.org/10.1136/gut.2007.123695

Brown, C.E., Sachs, A.B., 1998. Poly(A) tail length control in Saccharomyces cerevisiae occurs by message-specific deadenylation. Mol Cell Biol 18, 6548–6559. https://doi.org/10.1128/MCB.18.11.6548

Brown, C.E., Tarun, S.Z., Boeck, R., Sachs, A.B., 1996. PAN3 encodes a subunit of the Pab1p-dependent poly(A) nuclease in Saccharomyces cerevisiae. Mol Cell Biol 16, 5744–5753. https://doi.org/10.1128/MCB.16.10.5744

Brown, J.T., Bai, X., Johnson, A.W., 2000. The yeast antiviral proteins Ski2p, Ski3p, and Ski8p exist as a complex in vivo. RNA 6, 449–457. https://doi.org/10.1017/s1355838200991787

Bryja, V., Schulte, G., Rawal, N., Grahn, A., Arenas, E., 2007. Wnt-5a induces Dishevelled phosphorylation and dopaminergic differentiation via a CK1-dependent mechanism. J Cell Sci 120, 586–595. https://doi.org/10.1242/jcs.03368

Cali, B.M., Kuchma, S.L., Latham, J., Anderson, P., 1999. smg-7 is required for mRNA surveillance in Caenorhabditis elegans. Genetics 151, 605–616.

https://doi.org/10.1093/genetics/151.2.605

Carter, M.S., Doskow, J., Morris, P., Li, S., Nhim, R.P., Sandstedt, S., Wilkinson, M.F., 1995. A regulatory mechanism that detects premature nonsense codons in T-cell receptor transcripts in vivo is reversed by protein synthesis inhibitors in vitro. J Biol Chem 270, 28995–29003. https://doi.org/10.1074/jbc.270.48.28995

Chakrabarti, S., Jayachandran, U., Bonneau, F., Fiorini, F., Basquin, C., Domcke, S., Le Hir, H., Conti, E., 2011. Molecular mechanisms for the RNA-dependent ATPase activity of Upf1 and its regulation by Upf2. Mol Cell 41, 693–703. https://doi.org/10.1016/j.molcel.2011.02.010

Chambers, R.S., Dahmus, M.E., 1994. Purification and characterization of a phosphatase from HeLa cells which dephosphorylates the C-terminal domain of RNA polymerase II. Journal of Biological Chemistry 269, 26243–26248. https://doi.org/10.1016/S0021-9258(18)47186-4

Chambers, R.S., Kane, C.M., 1996. Purification and Characterization of an RNA Polymerase II Phosphatase from Yeast*. Journal of Biological Chemistry 271, 24498–24504. https://doi.org/10.1074/jbc.271.40.24498

Chamieh, H., Ballut, L., Bonneau, F., Le Hir, H., 2008. NMD factors UPF2 and UPF3 bridge UPF1 to the exon junction complex and stimulate its RNA helicase activity. Nat Struct Mol Biol 15, 85–93. https://doi.org/10.1038/nsmb1330

Chan, C.C., Dostie, J., Diem, M.D., Feng, W., Mann, M., Rappsilber, J., Dreyfuss, G., 2004. eIF4A3 is a novel component of the exon junction complex. RNA 10, 200–209. https://doi.org/10.1261/rna.5230104

Chan, W.-K., Bhalla, A.D., Le Hir, H., Nguyen, L.S., Huang, L., Gécz, J., Wilkinson, M.F., 2009. A UPF3-mediated regulatory switch that maintains RNA surveillance. Nat Struct Mol Biol 16, 747–753. https://doi.org/10.1038/nsmb.1612

Chan, W.-K., Huang, L., Gudikote, J.P., Chang, Y.-F., Imam, J.S., MacLean, J.A., Wilkinson, M.F., 2007. An alternative branch of the nonsense-mediated decay pathway. EMBO J 26, 1820–1830. https://doi.org/10.1038/sj.emboj.7601628

Chang, C.-T., Bercovich, N., Loh, B., Jonas, S., Izaurralde, E., 2014. The activation of the decapping enzyme DCP2 by DCP1 occurs on the EDC4 scaffold and involves a conserved loop in DCP1. Nucleic Acids Res 42, 5217–5233. https://doi.org/10.1093/nar/gku129

Chapin, A., Hu, H., Rynearson, S.G., Hollien, J., Yandell, M., Metzstein, M.M., 2014. In vivo determination of direct targets of the nonsense-mediated decay pathway in Drosophila. G3 (Bethesda) 4, 485–496. https://doi.org/10.1534/g3.113.009357

Charenton, C., Gaudon-Plesse, C., Fourati, Z., Taverniti, V., Back, R., Kolesnikova, O., Séraphin, B., Graille, M., 2017. A unique surface on Pat1 C-terminal domain directly interacts with Dcp2 decapping enzyme and Xrn1 5′–3′ mRNA exonuclease in yeast. Proc Natl Acad Sci U S A 114, E9493–E9501. https://doi.org/10.1073/pnas.1711680114

Charenton, C., Taverniti, V., Gaudon-Plesse, C., Back, R., Séraphin, B., Graille, M., 2016.

Structure of the active form of Dcp1–Dcp2 decapping enzyme bound to m^{7}GDP and its Edc3 activator. Nature Structural & Molecular Biology 23, 982–986. https://doi.org/10.1038/nsmb.3300

Chekanova, J.A., Gregory, B.D., Reverdatto, S.V., Chen, H., Kumar, R., Hooker, T., Yazaki, J., Li, P., Skiba, N., Peng, Q., Alonso, J., Brukhin, V., Grossniklaus, U., Ecker, J.R., Belostotsky, D.A., 2007. Genome-wide high-resolution mapping of exosome substrates reveals hidden features in the Arabidopsis transcriptome. Cell 131, 1340–1353. https://doi.org/10.1016/j.cell.2007.10.056

Chen, C., Tuck, S., Byström, A.S., 2009. Defects in tRNA Modification Associated with Neurological and Developmental Dysfunctions in Caenorhabditis elegans Elongator Mutants. PLOS Genetics 5, e1000561. https://doi.org/10.1371/journal.pgen.1000561

Chen, C.Y., Gherzi, R., Ong, S.E., Chan, E.L., Raijmakers, R., Pruijn, G.J., Stoecklin, G., Moroni, C., Mann, M., Karin, M., 2001. AU binding proteins recruit the exosome to degrade ARE-containing mRNAs. Cell 107, 451–464. https://doi.org/10.1016/s0092-8674(01)00578-5

Chen, Y., Sasai, N., Ma, G., Yue, T., Jia, J., Briscoe, J., Jiang, J., 2011. Sonic Hedgehog dependent phosphorylation by CK1α and GRK2 is required for ciliary accumulation and activation of smoothened. PLoS Biol 9, e1001083. https://doi.org/10.1371/journal.pbio.1001083

Chen, Y.-H., Su, L.-H., Sun, C.-H., 2008. Incomplete nonsense-mediated mRNA decay in Giardia lamblia. Int J Parasitol 38, 1305–1317. https://doi.org/10.1016/j.ijpara.2008.02.006

Chen, Z., Smith, K.R., Batterham, P., Robin, C., 2005. Smg1 Nonsense Mutations Do Not Abolish Nonsense-Mediated mRNA Decay in Drosophila melanogaster. Genetics 171, 403–406. https://doi.org/10.1534/genetics.105.045674

Cheng, J., Fogel-Petrovic, M., Maquat, L.E., 1990. Translation to near the distal end of the penultimate exon is required for normal levels of spliced triosephosphate isomerase mRNA. Mol Cell Biol 10, 5215–5225. https://doi.org/10.1128/mcb.10.10.5215-5225.1990

Chiu, S.-Y., Serin, G., Ohara, O., Maquat, L.E., 2003. Characterization of human Smg5/7a: a protein with similarities to Caenorhabditis elegans SMG5 and SMG7 that functions in the dephosphorylation of Upf1. RNA 9, 77–87. https://doi.org/10.1261/rna.2137903

Cho, E.-J., Kobor, M.S., Kim, M., Greenblatt, J., Buratowski, S., 2001. Opposing effects of Ctk1 kinase and Fcp1 phosphatase at Ser 2 of the RNA polymerase II C-terminal domain. Genes Dev. 15, 3319–3329. https://doi.org/10.1101/gad.935901

Cho, E.-J., Takagi, T., Moore, C.R., Buratowski, S., 1997. mRNA capping enzyme is recruited to the transcription complex by phosphorylation of the RNA polymerase II carboxy-terminal domain. Genes Dev. 11, 3319–3326. https://doi.org/10.1101/gad.11.24.3319

Cho, H., Abshire, E.T., Popp, M.W., Pröschel, C., Schwartz, J.L., Yeo, G.W., Maquat, L.E., 2022. AKT constitutes a signal-promoted alternative exon-junction complex that regulates nonsense-mediated mRNA decay. Molecular Cell. https://doi.org/10.1016/j.molcel.2022.05.013

Cho, N.H., Cheveralls, K.C., Brunner, A.-D., Kim, K., Michaelis, A.C., Raghavan, P., Kobayashi, H., Savy, L., Li, J.Y., Canaj, H., Kim, J.Y.S., Stewart, E.M., Gnann, C., McCarthy, F., Cabrera, J.P., Brunetti, R.M., Chhun, B.B., Dingle, G., Hein, M.Y., Huang, B., Mehta, S.B., Weissman, J.S., Gómez-Sjöberg, R., Itzhak, D.N., Royer, L.A., Mann, M., Leonetti, M.D., 2022. OpenCell: Endogenous tagging for the cartography of human cellular organization. Science 375, eabi6983. https://doi.org/10.1126/science.abi6983

Chowdhury, A., Mukhopadhyay, J., Tharun, S., 2007. The decapping activator Lsm1p-7p-Pat1p complex has the intrinsic ability to distinguish between oligoadenylated and polyadenylated RNAs. RNA 13, 998–1016. https://doi.org/10.1261/rna.502507

Clerici, M., Deniaud, A., Boehm, V., Gehring, N.H., Schaffitzel, C., Cusack, S., 2014. Structural and functional analysis of the three MIF4G domains of nonsense-mediated decay factor UPF2. Nucleic Acids Research 42, 2673–2686. https://doi.org/10.1093/nar/gkt1197

Clissold, P.M., Ponting, C.P., 2000. PIN domains in nonsense-mediated mRNA decay and RNAi. Curr Biol 10, R888-890. https://doi.org/10.1016/s0960-9822(00)00858-7

Coller, J.M., Tucker, M., Sheth, U., Valencia-Sanchez, M.A., Parker, R., 2001. The DEAD box helicase, Dhh1p, functions in mRNA decapping and interacts with both the decapping and deadenylase complexes. RNA 7, 1717–1727. https://doi.org/10.1017/s135583820101994x

Corden, J.L., 2013. RNA Polymerase II C-Terminal Domain: Tethering Transcription to Transcript and Template. Chem. Rev. 113, 8423–8455. https://doi.org/10.1021/cr400158h

Corden, J.L., Cadena, D.L., Ahearn, J.M., Dahmus, M.E., 1985. A unique structure at the carboxyl terminus of the largest subunit of eukaryotic RNA polymerase II. Proceedings of the National Academy of Sciences 82, 7934–7938. https://doi.org/10.1073/pnas.82.23.7934

Core, L.J., Waterfall, J.J., Lis, J.T., 2008. Nascent RNA sequencing reveals widespread pausing and divergent initiation at human promoters. Science 322, 1845–1848. https://doi.org/10.1126/science.1162228

Crawford, G.E., Faulkner, J.A., Crosbie, R.H., Campbell, K.P., Froehner, S.C., Chamberlain, J.S., 2000. Assembly of the Dystrophin-Associated Protein Complex Does Not Require the Dystrophin Cooh-Terminal Domain. Journal of Cell Biology 150, 1399–1410. https://doi.org/10.1083/jcb.150.6.1399

Creppe, C., Malinouskaya, L., Volvert, M.-L., Gillard, M., Close, P., Malaise, O., Laguesse, S., Cornez, I., Rahmouni, S., Ormenese, S., Belachew, S., Malgrange, B., Chapelle, J.-P., Siebenlist, U., Moonen, G., Chariot, A., Nguyen, L., 2009. Elongator Controls the Migration and Differentiation of Cortical Neurons through Acetylation of α-Tubulin. Cell 136, 551–564. https://doi.org/10.1016/j.cell.2008.11.043

Cruciat, C.-M., 2014. Casein kinase 1 and Wnt/β-catenin signaling. Curr Opin Cell Biol 31, 46–55. https://doi.org/10.1016/j.ceb.2014.08.003

Cruciat, C.-M., Dolde, C., Groot, R.E.A. de, Ohkawara, B., Reinhard, C., Korswagen, H.C.,

Niehrs, C., 2013. RNA Helicase DDX3 Is a Regulatory Subunit of Casein Kinase 1 in Wnt–β-Catenin Signaling. Science 339, 1436–1441. https://doi.org/10.1126/science.1231499

Cui, Y., Hagan, K.W., Zhang, S., Peltz, S.W., 1995. Identification and characterization of genes that are required for the accelerated degradation of mRNAs containing a premature translational termination codon. Genes Dev 9, 423–436. https://doi.org/10.1101/gad.9.4.423

Culbertson, M.R., Leeds, P.F., 2003. Looking at mRNA decay pathways through the window of molecular evolution. Curr Opin Genet Dev 13, 207–214. https://doi.org/10.1016/s0959-437x(03)00014-5

Culbertson, M.R., Underbrink, K.M., Fink, G.R., 1980. Frameshift suppression Saccharomyces cerevisiae. II. Genetic properties of group II suppressors. Genetics 95, 833–853. https://doi.org/10.1093/genetics/95.4.833

Czaplinski, K., Ruiz-Echevarria, M.J., Paushkin, S.V., Han, X., Weng, Y., Perlick, H.A., Dietz, H.C., Ter-Avanesyan, M.D., Peltz, S.W., 1998. The surveillance complex interacts with the translation release factors to enhance termination and degrade aberrant mRNAs. Genes Dev 12, 1665–1677. https://doi.org/10.1101/gad.12.11.1665

Daar, I.O., Maquat, L.E., 1988. Premature translation termination mediates triosephosphate isomerase mRNA degradation. Mol Cell Biol 8, 802–813. https://doi.org/10.1128/mcb.8.2.802-813.1988

Dahmus, M.E., 1996. Reversible Phosphorylation of the C-terminal Domain of RNA Polymerase II*. Journal of Biological Chemistry 271, 19009–19012. https://doi.org/10.1074/jbc.271.32.19009

Dahmus, M.E., 1995. Phosphorylation of the C-terminal domain of RNA polymerase II. Biochimica et Biophysica Acta (BBA) - Gene Structure and Expression 1261, 171–182. https://doi.org/10.1016/0167-4781(94)00233-S

Das, S., Sarkar, D., Das, B., 2017. The interplay between transcription and mRNA degradation in *Saccharomyces cerevisiae*. Microbial Cell 4, 212–228. https://doi.org/10.15698/mic2017.07.580

Daugeron, M.C., Mauxion, F., Séraphin, B., 2001. The yeast POP2 gene encodes a nuclease involved in mRNA deadenylation. Nucleic Acids Res 29, 2448–2455. https://doi.org/10.1093/nar/29.12.2448

David, L., Huber, W., Granovskaia, M., Toedling, J., Palm, C.J., Bofkin, L., Jones, T., Davis, R.W., Steinmetz, L.M., 2006. A high-resolution map of transcription in the yeast genome. Proc Natl Acad Sci U S A 103, 5320–5325. https://doi.org/10.1073/pnas.0601091103

Davis, C.A., Ares, M., 2006. Accumulation of unstable promoter-associated transcripts upon loss of the nuclear exosome subunit Rrp6p in Saccharomyces cerevisiae. Proc Natl Acad Sci U S A 103, 3262–3267. https://doi.org/10.1073/pnas.0507783103

Decker, C.J., Parker, R., 1993. A turnover pathway for both stable and unstable mRNAs in yeast: evidence for a requirement for deadenylation. Genes Dev 7, 1632–1643.

https://doi.org/10.1101/gad.7.8.1632

Decourty, L., Doyen, A., Malabat, C., Frachon, E., Rispal, D., Séraphin, B., Feuerbach, F., Jacquier, A., Saveanu, C., 2014. Long Open Reading Frame Transcripts Escape Nonsense-Mediated mRNA Decay in Yeast. Cell Reports 6, 593–598. https://doi.org/10.1016/j.celrep.2014.01.025

Dehecq, M., Decourty, L., Namane, A., Proux, C., Kanaan, J., Le Hir, H., Jacquier, A., Saveanu, C., 2018. Nonsense-mediated mRNA decay involves two distinct Upf1-bound complexes. EMBO J 37. https://doi.org/10.15252/embj.201899278

Del Valle-Pérez, B., Arqués, O., Vinyoles, M., de Herreros, A.G., Duñach, M., 2011. Coordinated action of CK1 isoforms in canonical Wnt signaling. Mol Cell Biol 31, 2877–2888. https://doi.org/10.1128/MCB.01466-10

Denning, G., Jamieson, L., Maquat, L.E., Thompson, E.A., Fields, A.P., 2001. Cloning of a novel phosphatidylinositol kinase-related kinase: characterization of the human SMG-1 RNA surveillance protein. J Biol Chem 276, 22709–22714. https://doi.org/10.1074/jbc.C100144200

Deshmukh, M.V., Jones, B.N., Quang-Dang, D.-U., Flinders, J., Floor, S.N., Kim, C., Jemielity, J., Kalek, M., Darzynkiewicz, E., Gross, J.D., 2008. mRNA Decapping Is Promoted by an RNA-Binding Channel in Dcp2. Molecular Cell 29, 324–336. https://doi.org/10.1016/j.molcel.2007.11.027

Doma, M.K., Parker, R., 2006. Endonucleolytic cleavage of eukaryotic mRNAs with stalls in translation elongation. Nature 440, 561–564. https://doi.org/10.1038/nature04530

D'Orazio, K.N., Wu, C.C.-C., Sinha, N., Loll-Krippleber, R., Brown, G.W., Green, R., 2019. The endonuclease Cue2 cleaves mRNAs at stalled ribosomes during No Go Decay. eLife 8, e49117. https://doi.org/10.7554/eLife.49117

Dumaz, N., Milne, D.M., Meek, D.W., 1999. Protein kinase CK1 is a p53-threonine 18 kinase which requires prior phosphorylation of serine 15. FEBS Lett 463, 312–316. https://doi.org/10.1016/s0014-5793(99)01647-6

Dunckley, T., Parker, R., 1999. The DCP2 protein is required for mRNA decapping in Saccharomyces cerevisiae and contains a functional MutT motif. EMBO J 18, 5411–5422. https://doi.org/10.1093/emboj/18.19.5411

Durand, S., Franks, T.M., Lykke-Andersen, J., 2016. Hyperphosphorylation amplifies UPF1 activity to resolve stalls in nonsense-mediated mRNA decay. Nat Commun 7, 12434. https://doi.org/10.1038/ncomms12434

Dziembowski, A., Lorentzen, E., Conti, E., Séraphin, B., 2007. A single subunit, Dis3, is essentially responsible for yeast exosome core activity. Nat Struct Mol Biol 14, 15–22. https://doi.org/10.1038/nsmb1184

Eick, D., Geyer, M., 2013. The RNA Polymerase II Carboxy-Terminal Domain (CTD) Code. Chem. Rev. 113, 8456–8490. https://doi.org/10.1021/cr400071f

Eide, E.J., Vielhaber, E.L., Hinz, W.A., Virshup, D.M., 2002. The circadian regulatory proteins BMAL1 and cryptochromes are substrates of casein kinase Iepsilon. J Biol Chem 277, 17248–17254. https://doi.org/10.1074/jbc.M111466200

Elyada, E., Pribluda, A., Goldstein, R.E., Morgenstern, Y., Brachya, G., Cojocaru, G., Snir-Alkalay, I., Burstain, I., Haffner-Krausz, R., Jung, S., Wiener, Z., Alitalo, K., Oren, M., Pikarsky, E., Ben-Neriah, Y., 2011. CKIα ablation highlights a critical role for p53 in invasiveness control. Nature 470, 409–413. https://doi.org/10.1038/nature09673

Erdeniz, N., Mortensen, U.H., Rothstein, R., 1997. Cloning-free PCR-based allele replacement methods. Genome Res 7, 1174–1183. https://doi.org/10.1101/gr.7.12.1174

Etchegaray, J.-P., Machida, K.K., Noton, E., Constance, C.M., Dallmann, R., Di Napoli, M.N., DeBruyne, J.P., Lambert, C.M., Yu, E.A., Reppert, S.M., Weaver, D.R., 2009. Casein kinase 1 delta regulates the pace of the mammalian circadian clock. Mol Cell Biol 29, 3853–3866. https://doi.org/10.1128/MCB.00338-09

Fan, S., Yuan, R., Ma, Y.X., Meng, Q., Goldberg, I.D., Rosen, E.M., 2001. Mutant BRCA1 genes antagonize phenotype of wild-type BRCA1. Oncogene 20, 8215–8235. https://doi.org/10.1038/sj.onc.1205033

Fatscher, T., Boehm, V., Weiche, B., Gehring, N.H., 2014. The interaction of cytoplasmic poly(A)-binding protein with eukaryotic initiation factor 4G suppresses nonsense-mediated mRNA decay. RNA 20, 1579–1592. https://doi.org/10.1261/rna.044933.114

Feaver, W.J., Svejstrup, J.Q., Henry, N.L., Kornberg, R.D., 1994. Relationship of CDK-activating kinase and RNA polymerase II CTD kinase TFIIH/TFIIK. Cell 79, 1103–1109. https://doi.org/10.1016/0092-8674(94)90040-X

Feigenbutz, M., Garland, W., Turner, M., Mitchell, P., 2013. The exosome cofactor Rrp47 is critical for the stability and normal expression of its associated exoribonuclease Rrp6 in Saccharomyces cerevisiae. PLoS One 8, e80752. https://doi.org/10.1371/journal.pone.0080752

Ferraiuolo, M.A., Lee, C.-S., Ler, L.W., Hsu, J.L., Costa-Mattioli, M., Luo, M.-J., Reed, R., Sonenberg, N., 2004. A nuclear translation-like factor eIF4AIII is recruited to the mRNA during splicing and functions in nonsense-mediated decay. Proc Natl Acad Sci U S A 101, 4118–4123. https://doi.org/10.1073/pnas.0400933101

Fichtner, L., Frohloff, F., Bürkner, K., Larsen, M., Breunig, K.D., Schaffrath, R., 2002. Molecular analysis of KTI12/TOT4, a Saccharomyces cerevisiae gene required for Kluyveromyces lactis zymocin action. Molecular Microbiology 43, 783–791. https://doi.org/10.1046/j.1365-2958.2002.02794.x

Fichtner, L., Jablonowski, D., Schierhorn, A., Kitamoto, H.K., Stark, M.J.R., Schaffrath, R., 2003. Elongator's toxin-target (TOT) function is nuclear localization sequence dependent and suppressed by post-translational modification. Molecular Microbiology 49, 1297–1307. https://doi.org/10.1046/j.1365-2958.2003.03632.x

Fichtner, L., Schaffrath, R., 2002. KTI11 and KTI13, Saccharomyces cerevisiae genes

controlling sensitivity to G1 arrest induced by Kluyveromyces lactis zymocin. Molecular Microbiology 44, 865–875. https://doi.org/10.1046/j.1365-2958.2002.02928.x

Fiorini, F., Bagchi, D., Le Hir, H., Croquette, V., 2015. Human Upf1 is a highly processive RNA helicase and translocase with RNP remodelling activities. Nat Commun 6, 7581. https://doi.org/10.1038/ncomms8581

Fiorini, F., Bonneau, F., Le Hir, H., 2012. Biochemical characterization of the RNA helicase UPF1 involved in nonsense-mediated mRNA decay. Methods Enzymol 511, 255–274. https://doi.org/10.1016/B978-0-12-396546-2.00012-7

Fiorini, F., Boudvillain, M., Le Hir, H., 2013. Tight intramolecular regulation of the human Upf1 helicase by its N- and C-terminal domains. Nucleic Acids Res 41, 2404–2415. https://doi.org/10.1093/nar/gks1320

Flotow, H., Graves, P.R., Wang, A.Q., Fiol, C.J., Roeske, R.W., Roach, P.J., 1990. Phosphate groups as substrate determinants for casein kinase I action. J Biol Chem 265, 14264–14269.

Flotow, H., Roach, P.J., 1991. Role of acidic residues as substrate determinants for casein kinase I. J Biol Chem 266, 3724–3727.

Ford, A.S., Guan, Q., Neeno-Eckwall, E., Culbertson, M.R., 2006. Ebs1p, a Negative Regulator of Gene Expression Controlled by the Upf Proteins in the Yeast Saccharomyces cerevisiae. Eukaryot Cell 5, 301–312. https://doi.org/10.1128/EC.5.2.301-312.2006

Fourati, Z., Roy, B., Millan, C., Coureux, P.-D., Kervestin, S., van Tilbeurgh, H., He, F., Usón, I., Jacobson, A., Graille, M., 2014. A highly conserved region essential for NMD in the Upf2 N-terminal domain. J Mol Biol 426, 3689–3702. https://doi.org/10.1016/j.jmb.2014.09.015

Franks, T.M., Singh, G., Lykke-Andersen, J., 2010. Upf1 ATPase-dependent mRNP disassembly is required for completion of nonsense- mediated mRNA decay. Cell 143, 938–950. https://doi.org/10.1016/j.cell.2010.11.043

Fribourg, S., Gatfield, D., Izaurralde, E., Conti, E., 2003. A novel mode of RBD-protein recognition in the Y14-Mago complex. Nat Struct Biol 10, 433–439. https://doi.org/10.1038/nsb926

Frischmeyer, P.A., Dietz, H.C., 1999. Nonsense-Mediated mRNA Decay in Health and Disease. Hum Mol Genet 8, 1893–1900. https://doi.org/10.1093/hmg/8.10.1893

Frischmeyer, P.A., van Hoof, A., O'Donnell, K., Guerrerio, A.L., Parker, R., Dietz, H.C., 2002. An mRNA surveillance mechanism that eliminates transcripts lacking termination codons. Science 295, 2258–2261. https://doi.org/10.1126/science.1067338

Frohloff, F., Fichtner, L., Jablonowski, D., Breunig, K.D., Schaffrath, R., 2001. Saccharomyces cerevisiae Elongator mutations confer resistance to the Kluyveromyces lactis zymocin. EMBO J 20, 1993–2003. https://doi.org/10.1093/emboj/20.8.1993

Fromont-Racine, M., Mayes, A.E., Brunet-Simon, A., Rain, J.C., Colley, A., Dix, I.,

Decourty, L., Joly, N., Ricard, F., Beggs, J.D., Legrain, P., 2000. Genome-wide protein interaction screens reveal functional networks involving Sm-like proteins. Yeast 17, 95–110. https://doi.org/10.1002/1097-0061(20000630)17:2<95::AID-YEA16>3.0.CO;2-H

Fu, C., Donovan, W.P., Shikapwashya-Hasser, O., Ye, X., Cole, R.H., 2014. Hot Fusion: An Efficient Method to Clone Multiple DNA Fragments as Well as Inverted Repeats without Ligase. PLoS One 9. https://doi.org/10.1371/journal.pone.0115318

Fu, H., Subramanian, R.R., Masters, S.C., 2000. 14-3-3 proteins: structure, function, and regulation. Annu Rev Pharmacol Toxicol 40, 617–647. https://doi.org/10.1146/annurev.pharmtox.40.1.617

Fulcher, L.J., Sapkota, G.P., 2020. Functions and regulation of the serine/threonine protein kinase CK1 family: moving beyond promiscuity. Biochemical Journal 477, 4603–4621. https://doi.org/10.1042/BCJ20200506

Gaba, A., Jacobson, A., Sachs, M.S., 2005. Ribosome occupancy of the yeast CPA1 upstream open reading frame termination codon modulates nonsense-mediated mRNA decay. Mol Cell 20, 449–460. https://doi.org/10.1016/j.molcel.2005.09.019

Gao, Z.-H., Seeling, J.M., Hill, V., Yochum, A., Virshup, D.M., 2002. Casein kinase I phosphorylates and destabilizes the beta-catenin degradation complex. Proc Natl Acad Sci U S A 99, 1182–1187. https://doi.org/10.1073/pnas.032468199

Garí, E., Piedrafita, L., Aldea, M., Herrero, E., 1997. A set of vectors with a tetracycline-regulatable promoter system for modulated gene expression in Saccharomyces cerevisiae. Yeast 13, 837–848. https://doi.org/10.1002/(SICI)1097-0061(199707)13:9<837::AID-YEA145>3.0.CO;2-T

Gatfield, D., Unterholzner, L., Ciccarelli, F.D., Bork, P., Izaurralde, E., 2003. Nonsense-mediated mRNA decay in Drosophila: at the intersection of the yeast and mammalian pathways. EMBO J 22, 3960–3970. https://doi.org/10.1093/emboj/cdg371

Gehring, N.H., Neu-Yilik, G., Schell, T., Hentze, M.W., Kulozik, A.E., 2003. Y14 and hUpf3b form an NMD-activating complex. Mol Cell 11, 939–949. https://doi.org/10.1016/s1097-2765(03)00142-4

Ghaemmaghami, S., Huh, W.-K., Bower, K., Howson, R.W., Belle, A., Dephoure, N., O'Shea, E.K., Weissman, J.S., 2003. Global analysis of protein expression in yeast. Nature 425, 737–741. https://doi.org/10.1038/nature02046

Ghalei, H., Schaub, F.X., Doherty, J.R., Noguchi, Y., Roush, W.R., Cleveland, J.L., Stroupe, M.E., Karbstein, K., 2015. Hrr25/CK1δ-directed release of Ltv1 from pre-40S ribosomes is necessary for ribosome assembly and cell growth. J Cell Biol 208, 745–759. https://doi.org/10.1083/jcb.201409056

Giaever, G., Chu, A.M., Ni, L., Connelly, C., Riles, L., Véronneau, S., Dow, S., Lucau-Danila, A., Anderson, K., André, B., Arkin, A.P., Astromoff, A., El-Bakkoury, M., Bangham, R., Benito, R., Brachat, S., Campanaro, S., Curtiss, M., Davis, K., Deutschbauer, A., Entian, K.-D., Flaherty, P., Foury, F., Garfinkel, D.J., Gerstein, M., Gotte, D., Güldener, U.,

Hegemann, J.H., Hempel, S., Herman, Z., Jaramillo, D.F., Kelly, D.E., Kelly, S.L., Kötter, P., LaBonte, D., Lamb, D.C., Lan, N., Liang, H., Liao, H., Liu, L., Luo, C., Lussier, M., Mao, R., Menard, P., Ooi, S.L., Revuelta, J.L., Roberts, C.J., Rose, M., Ross-Macdonald, P., Scherens, B., Schimmack, G., Shafer, B., Shoemaker, D.D., Sookhai-Mahadeo, S., Storms, R.K., Strathern, J.N., Valle, G., Voet, M., Volckaert, G., Wang, C., Ward, T.R., Wilhelmy, J., Winzeler, E.A., Yang, Y., Yen, G., Youngman, E., Yu, K., Bussey, H., Boeke, J.D., Snyder, M., Philippsen, P., Davis, R.W., Johnston, M., 2002. Functional profiling of the Saccharomyces cerevisiae genome. Nature 418, 387–391. https://doi.org/10.1038/nature00935

Glatt, S., Létoquart, J., Faux, C., Taylor, N.M.I., Séraphin, B., Müller, C.W., 2012a. The Elongator subcomplex Elp456 is a hexameric RecA-like ATPase. Nat Struct Mol Biol 19, 314–320. https://doi.org/10.1038/nsmb.2234

Glatt, S., Müller, C.W., 2013. Structural insights into Elongator function. Current Opinion in Structural Biology, Theory and simulation / Macromolecular assemblies 23, 235–242. https://doi.org/10.1016/j.sbi.2013.02.009

Glatt, S., Séraphin, B., Müller, C.W., 2012b. Elongator. Transcription 3, 273–276. https://doi.org/10.4161/trns.21525

Glatt, S., Zabel, R., Kolaj-Robin, O., Onuma, O.F., Baudin, F., Graziadei, A., Taverniti, V., Lin, T.-Y., Baymann, F., Séraphin, B., Breunig, K.D., Müller, C.W., 2016. Structural basis for tRNA modification by Elp3 from Dehalococcoides mccartyi. Nat Struct Mol Biol 23, 794–802. https://doi.org/10.1038/nsmb.3265

Glover, M.L., Burroughs, A.Max., Monem, P.C., Egelhofer, T.A., Pule, M.N., Aravind, L., Arribere, J.A., 2020. NONU-1 Encodes a Conserved Endonuclease Required for mRNA Translation Surveillance. Cell Reports 30, 4321-4331.e4. https://doi.org/10.1016/j.celrep.2020.03.023

González, C.I., Ruiz-Echevarría, M.J., Vasudevan, S., Henry, M.F., Peltz, S.W., 2000. The yeast hnRNP-like protein Hrp1/Nab4 marks a transcript for nonsense-mediated mRNA decay. Mol Cell 5, 489–499. https://doi.org/10.1016/s1097-2765(00)80443-8

Gout, J.-F., Li, W., Fritsch, C., Li, A., Haroon, S., Singh, L., Hua, D., Fazelinia, H., Smith, Z., Seeholzer, S., Thomas, K., Lynch, M., Vermulst, M., 2017. The landscape of transcription errors in eukaryotic cells. Sci Adv 3, e1701484. https://doi.org/10.1126/sciadv.1701484

Graille, M., Séraphin, B., 2012. Surveillance pathways rescuing eukaryotic ribosomes lost in translation. Nat Rev Mol Cell Biol 13, 727–735. https://doi.org/10.1038/nrm3457

Grange, T., de Sa, C.M., Oddos, J., Pictet, R., 1987. Human mRNA polyadenylate binding protein: evolutionary conservation of a nucleic acid binding motif. Nucleic Acids Res 15, 4771–4787. https://doi.org/10.1093/nar/15.12.4771

Graves, P.R., Haas, D.W., Hagedorn, C.H., DePaoli-Roach, A.A., Roach, P.J., 1993. Molecular cloning, expression, and characterization of a 49-kilodalton casein kinase I isoform from rat testis. J Biol Chem 268, 6394–6401.

Gross, S.D., Anderson, R.A., 1998. Casein kinase I: spatial organization and positioning of a multifunctional protein kinase family. Cell Signal 10, 699–711. https://doi.org/10.1016/s0898-6568(98)00042-4

Grousl, T., Ivanov, P., Frýdlová, I., Vasicová, P., Janda, F., Vojtová, J., Malínská, K., Malcová, I., Nováková, L., Janosková, D., Valásek, L., Hasek, J., 2009. Robust heat shock induces eIF2alpha-phosphorylation-independent assembly of stress granules containing eIF3 and 40S ribosomal subunits in budding yeast, Saccharomyces cerevisiae. J Cell Sci 122, 2078–2088. https://doi.org/10.1242/jcs.045104

Grudzien-Nogalska, E., Kiledjian, M., 2017. New Insights into Decapping Enzymes and Selective mRNA Decay. Wiley Interdiscip Rev RNA 8. https://doi.org/10.1002/wrna.1379

Guan, Q., Zheng, W., Tang, S., Liu, X., Zinkel, R.A., Tsui, K.-W., Yandell, B.S., Culbertson, M.R., 2006. Impact of nonsense-mediated mRNA decay on the global expression profile of budding yeast. PLoS Genet 2, e203. https://doi.org/10.1371/journal.pgen.0020203

Gudipati, R.K., Xu, Z., Lebreton, A., Séraphin, B., Steinmetz, L.M., Jacquier, A., Libri, D., 2012. Extensive degradation of RNA precursors by the exosome in wild-type cells. Mol Cell 48, 409–421. https://doi.org/10.1016/j.molcel.2012.08.018

Hagan, K.W., Ruiz-Echevarria, M.J., Quan, Y., Peltz, S.W., 1995. Characterization of cis-acting sequences and decay intermediates involved in nonsense-mediated mRNA turnover. Mol Cell Biol 15, 809–823. https://doi.org/10.1128/MCB.15.2.809

Halbach, F., Reichelt, P., Rode, M., Conti, E., 2013. The yeast ski complex: crystal structure and RNA channeling to the exosome complex. Cell 154, 814–826. https://doi.org/10.1016/j.cell.2013.07.017

Hall, G.W., Thein, S., 1994. Nonsense codon mutations in the terminal exon of the beta-globin gene are not associated with a reduction in beta-mRNA accumulation: a mechanism for the phenotype of dominant beta-thalassemia. Blood 83, 2031–2037.

Hanna-Addams, S., Liu, S., Liu, H., Chen, S., Wang, Z., 2020. CK1α, CK1δ, and CK1ε are necrosome components which phosphorylate serine 227 of human RIPK3 to activate necroptosis. Proc Natl Acad Sci U S A 117, 1962–1970. https://doi.org/10.1073/pnas.1917112117

Harigaya, Y., Jones, B.N., Muhlrad, D., Gross, J.D., Parker, R., 2010. Identification and Analysis of the Interaction between Edc3 and Dcp2 in Saccharomyces cerevisiae. Mol Cell Biol 30, 1446–1456. https://doi.org/10.1128/MCB.01305-09

Harlen, K.M., Trotta, K.L., Smith, E.E., Mosaheb, M.M., Fuchs, S.M., Churchman, L.S., 2016. Comprehensive RNA Polymerase II Interactomes Reveal Distinct and Varied Roles for Each Phospho-CTD Residue. Cell Reports 15, 2147–2158. https://doi.org/10.1016/j.celrep.2016.05.010

He, F., Brown, A.H., Jacobson, A., 1997. Upf1p, Nmd2p, and Upf3p are interacting components of the yeast nonsense-mediated mRNA decay pathway. Mol Cell Biol 17, 1580–1594. https://doi.org/10.1128/MCB.17.3.1580

He, F., Brown, A.H., Jacobson, A., 1996. Interaction between Nmd2p and Upf1p is required for activity but not for dominant-negative inhibition of the nonsense-mediated mRNA decay pathway in yeast. RNA 2, 153–170.

He, F., Jacobson, A., 2015. Control of mRNA decapping by positive and negative regulatory elements in the Dcp2 C-terminal domain. RNA 21, 1633–1647. https://doi.org/10.1261/rna.052449.115

He, F., Jacobson, A., 1995. Identification of a novel component of the nonsense-mediated mRNA decay pathway by use of an interacting protein screen. Genes & Development 9, 437–454. https://doi.org/10.1101/gad.9.4.437

He, F., Li, C., Roy, B., Jacobson, A., 2014. Yeast Edc3 targets RPS28B mRNA for decapping by binding to a 3' untranslated region decay-inducing regulatory element. Mol Cell Biol 34, 1438–1451. https://doi.org/10.1128/MCB.01584-13

He, F., Peltz, S.W., Donahue, J.L., Rosbash, M., Jacobson, A., 1993. Stabilization and ribosome association of unspliced pre-mRNAs in a yeast upf1- mutant. Proc Natl Acad Sci U S A 90, 7034–7038. https://doi.org/10.1073/pnas.90.15.7034

Hengartner, C.J., Myer, V.E., Liao, S.-M., Wilson, C.J., Koh, S.S., Young, R.A., 1998. Temporal Regulation of RNA Polymerase II by Srb10 and Kin28 Cyclin-Dependent Kinases. Molecular Cell 2, 43–53. https://doi.org/10.1016/S1097-2765(00)80112-4

Hennigan, A.N., Jacobson, A., 1996. Functional mapping of the translation-dependent instability element of yeast MATalpha1 mRNA. Mol Cell Biol 16, 3833–3843. https://doi.org/10.1128/MCB.16.7.3833

Hintermair, C., Heidemann, M., Koch, F., Descostes, N., Gut, M., Gut, I., Fenouil, R., Ferrier, P., Flatley, A., Kremmer, E., Chapman, R.D., Andrau, J.-C., Eick, D., 2012. Threonine-4 of mammalian RNA polymerase II CTD is targeted by Polo-like kinase 3 and required for transcriptional elongation. EMBO J 31, 2784–2797. https://doi.org/10.1038/emboj.2012.123

Hintermair, C., Voß, K., Forné, I., Heidemann, M., Flatley, A., Kremmer, E., Imhof, A., Eick, D., 2016. Specific threonine-4 phosphorylation and function of RNA polymerase II CTD during M phase progression. Sci Rep 6, 27401. https://doi.org/10.1038/srep27401

Ho, Y., Gruhler, A., Heilbut, A., Bader, G.D., Moore, L., Adams, S.-L., Millar, A., Taylor, P., Bennett, K., Boutilier, K., Yang, L., Wolting, C., Donaldson, I., Schandorff, S., Shewnarane, J., Vo, M., Taggart, J., Goudreault, M., Muskat, B., Alfarano, C., Dewar, D., Lin, Z., Michalickova, K., Willems, A.R., Sassi, H., Nielsen, P.A., Rasmussen, K.J., Andersen, J.R., Johansen, L.E., Hansen, L.H., Jespersen, H., Podtelejnikov, A., Nielsen, E., Crawford, J., Poulsen, V., Sørensen, B.D., Matthiesen, J., Hendrickson, R.C., Gleeson, F., Pawson, T., Moran, M.F., Durocher, D., Mann, M., Hogue, C.W.V., Figeys, D., Tyers, M., 2002. Systematic identification of protein complexes in Saccharomyces cerevisiae by mass spectrometry. Nature 415, 180–183. https://doi.org/10.1038/415180a

Ho, Y., Mason, S., Kobayashi, R., Hoekstra, M., Andrews, B., 1997. Role of the casein kinase I isoform, Hrr25, and the cell cycle-regulatory transcription factor, SBF, in the transcriptional

response to DNA damage in Saccharomyces cerevisiae. PNAS 94, 581–586. https://doi.org/10.1073/pnas.94.2.581

Hocine, S., Singer, R.H., Grünwald, D., 2010. RNA Processing and Export. Cold Spring Harb Perspect Biol 2, a000752. https://doi.org/10.1101/cshperspect.a000752

Hodgkin, J., Papp, A., Pulak, R., Ambros, V., Anderson, P., 1989. A new kind of informational suppression in the nematode Caenorhabditis elegans. Genetics 123, 301–313. https://doi.org/10.1093/genetics/123.2.301

Hoekstra, M.F., Dhillon, N., Carmel, G., DeMaggio, A.J., Lindberg, R.A., Hunter, T., Kuret, J., 1994. Budding and fission yeast casein kinase I isoforms have dual-specificity protein kinase activity. Mol Biol Cell 5, 877–886. https://doi.org/10.1091/mbc.5.8.877

Hoekstra, M.F., Liskay, R.M., Ou, A.C., DeMaggio, A.J., Burbee, D.G., Heffron, F., 1991. HRR25, a putative protein kinase from budding yeast: association with repair of damaged DNA. Science 253, 1031–1034.

Hogg, J.R., Goff, S.P., 2010. Upf1 senses 3'UTR length to potentiate mRNA decay. Cell 143, 379–389. https://doi.org/10.1016/j.cell.2010.10.005

Holbrook, J.A., Neu-Yilik, G., Hentze, M.W., Kulozik, A.E., 2004. Nonsense-mediated decay approaches the clinic. Nat Genet 36, 801–808. https://doi.org/10.1038/ng1403

Hoshino, S., Imai, M., Kobayashi, T., Uchida, N., Katada, T., 1999. The eukaryotic polypeptide chain releasing factor (eRF3/GSPT) carrying the translation termination signal to the 3'-Poly(A) tail of mRNA. Direct association of erf3/GSPT with polyadenylate-binding protein. J Biol Chem 274, 16677–16680. https://doi.org/10.1074/jbc.274.24.16677

Houalla, R., Devaux, F., Fatica, A., Kufel, J., Barrass, D., Torchet, C., Tollervey, D., 2006. Microarray detection of novel nuclear RNA substrates for the exosome. Yeast 23, 439–454. https://doi.org/10.1002/yea.1369

Hsin, J.-P., Sheth, A., Manley, J.L., 2011. RNAP II CTD Phosphorylated on Threonine-4 Is Required for Histone mRNA 3′ End Processing. Science 334, 683–686. https://doi.org/10.1126/science.1206034

Hu, W., Sweet, T.J., Chamnongpol, S., Baker, K.E., Coller, J., 2009. Co-translational mRNA decay in Saccharomyces cerevisiae. Nature 461, 225–229. https://doi.org/10.1038/nature08265

Huang, B., Johansson, M.J.O., Byström, A.S., 2005. An early step in wobble uridine tRNA modification requires the Elongator complex. RNA 11, 424–436. https://doi.org/10.1261/rna.7247705

Huang, B., Lu, J., Byström, A.S., 2008. A genome-wide screen identifies genes required for formation of the wobble nucleoside 5-methoxycarbonylmethyl-2-thiouridine in Saccharomyces cerevisiae. RNA 14, 2183–2194. https://doi.org/10.1261/rna.1184108

Huart, A.-S., MacLaine, N.J., Meek, D.W., Hupp, T.R., 2009. CK1alpha plays a central role

in mediating MDM2 control of p53 and E2F-1 protein stability. J Biol Chem 284, 32384–32394. https://doi.org/10.1074/jbc.M109.052647

Hwang, J., Sato, H., Tang, Y., Matsuda, D., Maquat, L.E., 2010. UPF1 association with the cap-binding protein, CBP80, promotes nonsense-mediated mRNA decay at two distinct steps. Mol Cell 39, 396–409. https://doi.org/10.1016/j.molcel.2010.07.004

Ivanov, P.V., Gehring, N.H., Kunz, J.B., Hentze, M.W., Kulozik, A.E., 2008. Interactions between UPF1, eRFs, PABP and the exon junction complex suggest an integrated model for mammalian NMD pathways. EMBO J 27, 736–747. https://doi.org/10.1038/emboj.2008.17

Izeradjene, K., Douglas, L., Delaney, A.B., Houghton, J.A., 2004. Casein kinase I attenuates tumor necrosis factor-related apoptosis-inducing ligand-induced apoptosis by regulating the recruitment of fas-associated death domain and procaspase-8 to the death-inducing signaling complex. Cancer Res 64, 8036–8044. https://doi.org/10.1158/0008-5472.CAN-04-0762

Jablonowski, D., Butler, A.R., Fichtner, L., Gardiner, D., Schaffrath, R., Stark, M.J.R., 2001a. Sit4p Protein Phosphatase Is Required for Sensitivity of Saccharomyces cerevisiae to Kluyveromyces lactis Zymocin. Genetics 159, 1479–1489. https://doi.org/10.1093/genetics/159.4.1479

Jablonowski, D., Fichtner, L., Stark, M.J.R., Schaffrath, R., 2004. The Yeast Elongator Histone Acetylase Requires Sit4-dependent Dephosphorylation for Toxin-Target Capacity. MBoC 15, 1459–1469. https://doi.org/10.1091/mbc.e03-10-0750

Jablonowski, D., Frohloff, F., Fichtner, L., Stark, M.J.R., Schaffrath, R., 2001b. Kluyveromyces lactis zymocin mode of action is linked to RNA polymerase II function via Elongator. Molecular Microbiology 42, 1095–1105. https://doi.org/10.1046/j.1365-2958.2001.02705.x

Jablonowski, D., Schaffrath, R., 2002. Saccharomyces cerevisiae RNA Polymerase II Is Affected by Kluyveromyces lactis Zymocin*. Journal of Biological Chemistry 277, 26276–26280. https://doi.org/10.1074/jbc.M203354200

Järås, M., Miller, P.G., Chu, L.P., Puram, R.V., Fink, E.C., Schneider, R.K., Al-Shahrour, F., Peña, P., Breyfogle, L.J., Hartwell, K.A., McConkey, M.E., Cowley, G.S., Root, D.E., Kharas, M.G., Mullally, A., Ebert, B.L., 2014. Csnk1a1 inhibition has p53-dependent therapeutic efficacy in acute myeloid leukemia. J Exp Med 211, 605–612. https://doi.org/10.1084/jem.20131033

Jensen, T.H., Jacquier, A., Libri, D., 2013. Dealing with Pervasive Transcription. Molecular Cell 52, 473–484. https://doi.org/10.1016/j.molcel.2013.10.032

Jin, Y., Eser, U., Struhl, K., Churchman, L.S., 2017. The Ground State and Evolution of Promoter Region Directionality. Cell 170, 889-898.e10. https://doi.org/10.1016/j.cell.2017.07.006

Joerger, A.C., Fersht, A.R., 2007. Structure-function-rescue: the diverse nature of common p53 cancer mutants. Oncogene 26, 2226–2242. https://doi.org/10.1038/sj.onc.1210291

Jonas, S., Izaurralde, E., 2013. The role of disordered protein regions in the assembly of decapping complexes and RNP granules. Genes Dev. 27, 2628–2641. https://doi.org/10.1101/gad.227843.113

Jonas, S., Weichenrieder, O., Izaurralde, E., 2013. An unusual arrangement of two 14-3-3-like domains in the SMG5–SMG7 heterodimer is required for efficient nonsense-mediated mRNA decay. Genes Dev 27, 211–225. https://doi.org/10.1101/gad.206672.112

Joncourt, R., Eberle, A.B., Rufener, S.C., Mühlemann, O., 2014. Eukaryotic initiation factor 4G suppresses nonsense-mediated mRNA decay by two genetically separable mechanisms. PLoS One 9, e104391. https://doi.org/10.1371/journal.pone.0104391

Jones, J.C., Phatnani, H.P., Haystead, T.A., MacDonald, J.A., Alam, S.M., Greenleaf, A.L., 2004. C-terminal Repeat Domain Kinase I Phosphorylates Ser2 and Ser5 of RNA Polymerase II C-terminal Domain Repeats*. Journal of Biological Chemistry 279, 24957–24964. https://doi.org/10.1074/jbc.M402218200

Jung, D., Giallourakis, C., Mostoslavsky, R., Alt, F.W., 2006. Mechanism and control of V(D)J recombination at the immunoglobulin heavy chain locus. Annu Rev Immunol 24, 541–570. https://doi.org/10.1146/annurev.immunol.23.021704.115830

Jungfleisch, J., Blasco-Moreno, B., Díez, J., 2016. Use of Cellular Decapping Activators by Positive-Strand RNA Viruses. Viruses 8. https://doi.org/10.3390/v8120340

Kadlec, J., Guilligay, D., Ravelli, R.B., Cusack, S., 2006. Crystal structure of the UPF2-interacting domain of nonsense-mediated mRNA decay factor UPF1. RNA 12, 1817–1824. https://doi.org/10.1261/rna.177606

Kadlec, J., Izaurralde, E., Cusack, S., 2004. The structural basis for the interaction between nonsense-mediated mRNA decay factors UPF2 and UPF3. Nat Struct Mol Biol 11, 330–337. https://doi.org/10.1038/nsmb741

Karamyshev, A.L., Karamysheva, Z.N., 2018. Lost in Translation: Ribosome-Associated mRNA and Protein Quality Controls. Front Genet 9, 431. https://doi.org/10.3389/fgene.2018.00431

Kashima, I., Yamashita, A., Izumi, N., Kataoka, N., Morishita, R., Hoshino, S., Ohno, M., Dreyfuss, G., Ohno, S., 2006. Binding of a novel SMG-1-Upf1-eRF1-eRF3 complex (SURF) to the exon junction complex triggers Upf1 phosphorylation and nonsense-mediated mRNA decay. Genes Dev 20, 355–367. https://doi.org/10.1101/gad.1389006

Kataoka, N., Diem, M.D., Kim, V.N., Yong, J., Dreyfuss, G., 2001. Magoh, a human homolog of Drosophila mago nashi protein, is a component of the splicing-dependent exon-exon junction complex. EMBO J 20, 6424–6433. https://doi.org/10.1093/emboj/20.22.6424

Kataoka, N., Yong, J., Kim, V.N., Velazquez, F., Perkinson, R.A., Wang, F., Dreyfuss, G., 2000. Pre-mRNA splicing imprints mRNA in the nucleus with a novel RNA-binding protein that persists in the cytoplasm. Mol Cell 6, 673–682. https://doi.org/10.1016/s1097-2765(00)00065-4

Katis, V.L., Lipp, J.J., Imre, R., Bogdanova, A., Okaz, E., Habermann, B., Mechtler, K., Nasmyth, K., Zachariae, W., 2010. Rec8 Phosphorylation by Casein Kinase 1 and Cdc7-Dbf4 Kinase Regulates Cohesin Cleavage by Separase during Meiosis. Developmental Cell 18, 397–409. https://doi.org/10.1016/j.devcel.2010.01.014

Kawakami, F., Suzuki, K., Ohtsuki, K., 2008. A novel consensus phosphorylation motif in sulfatide- and cholesterol-3-sulfate-binding protein substrates for CK1 in vitro. Biol Pharm Bull 31, 193–200. https://doi.org/10.1248/bpb.31.193

Keogh, M.-C., Podolny, V., Buratowski, S., 2003. Bur1 Kinase Is Required for Efficient Transcription Elongation by RNA Polymerase II. Molecular and Cellular Biology 23, 7005–7018. https://doi.org/10.1128/MCB.23.19.7005-7018.2003

Keppetipola, N., Sharma, S., Li, Q., Black, D.L., 2012. Neuronal regulation of pre-mRNA splicing by polypyrimidine tract binding proteins, PTBP1 and PTBP2. Crit Rev Biochem Mol Biol 47, 360–378. https://doi.org/10.3109/10409238.2012.691456

Kim, V.N., Kataoka, N., Dreyfuss, G., 2001. Role of the nonsense-mediated decay factor hUpf3 in the splicing-dependent exon-exon junction complex. Science 293, 1832–1836. https://doi.org/10.1126/science.1062829

King, D.P., Takahashi, J.S., 2000. Molecular genetics of circadian rhythms in mammals. Annu Rev Neurosci 23, 713–742. https://doi.org/10.1146/annurev.neuro.23.1.713

Kitamoto, H., Jablonowski, D., Nagase, J., Schaffrath, R., 2002. Defects in yeast RNA polymerase II transcription elicit hypersensitivity to G1 arrest induced by Kluyveromyces lactis zymocin. Mol Gen Genomics 268, 49–55. https://doi.org/10.1007/s00438-002-0720-3

Klauer, A.A., van Hoof, A., 2012. Degradation of mRNAs that lack a stop codon: A decade of nonstop progress. Wiley Interdiscip Rev RNA 3, 649–660. https://doi.org/10.1002/wrna.1124

Knippschild, U., Gocht, A., Wolff, S., Huber, N., Löhler, J., Stöter, M., 2005. The casein kinase 1 family: participation in multiple cellular processes in eukaryotes. Cellular Signalling 17, 675–689. https://doi.org/10.1016/j.cellsig.2004.12.011

Knippschild, U., Milne, D.M., Campbell, L.E., DeMaggio, A.J., Christenson, E., Hoekstra, M.F., Meek, D.W., 1997. p53 is phosphorylated in vitro and in vivo by the delta and epsilon isoforms of casein kinase 1 and enhances the level of casein kinase 1 delta in response to topoisomerase-directed drugs. Oncogene 15, 1727–1736. https://doi.org/10.1038/sj.onc.1201541

Kobor, M.S., Archambault, J., Lester, W., Holstege, F.C.P., Gileadi, O., Jansma, D.B., Jennings, E.G., Kouyoumdjian, F., Davidson, A.R., Young, R.A., Greenblatt, J., 1999. An Unusual Eukaryotic Protein Phosphatase Required for Transcription by RNA Polymerase II and CTD Dephosphorylation in S. cerevisiae. Molecular Cell 4, 55–62. https://doi.org/10.1016/S1097-2765(00)80187-2

Kononenko, A.V., Mitkevich, V.A., Atkinson, G.C., Tenson, T., Dubovaya, V.I., Frolova, L.Y., Makarov, A.A., Hauryliuk, V., 2010. GTP-dependent structural rearrangement of the eRF1:eRF3 complex and eRF3 sequence motifs essential for PABP binding. Nucleic Acids

Res 38, 548–558. https://doi.org/10.1093/nar/gkp908

Kramer, S., McLennan, A.G., 2019. The complex enzymology of mRNA decapping: Enzymes of four classes cleave pyrophosphate bonds. Wiley Interdisciplinary Reviews: RNA 10, e1511. https://doi.org/10.1002/wrna.1511

Krishnamurthy, S., He, X., Reyes-Reyes, M., Moore, C., Hampsey, M., 2004. Ssu72 Is an RNA Polymerase II CTD Phosphatase. Molecular Cell 14, 387–394. https://doi.org/10.1016/S1097-2765(04)00235-7

Krogan, N.J., Cagney, G., Yu, H., Zhong, G., Guo, X., Ignatchenko, A., Li, J., Pu, S., Datta, N., Tikuisis, A.P., Punna, T., Peregrín-Alvarez, J.M., Shales, M., Zhang, X., Davey, M., Robinson, M.D., Paccanaro, A., Bray, J.E., Sheung, A., Beattie, B., Richards, D.P., Canadien, V., Lalev, A., Mena, F., Wong, P., Starostine, A., Canete, M.M., Vlasblom, J., Wu, S., Orsi, C., Collins, S.R., Chandran, S., Haw, R., Rilstone, J.J., Gandi, K., Thompson, N.J., Musso, G., St Onge, P., Ghanny, S., Lam, M.H.Y., Butland, G., Altaf-Ul, A.M., Kanaya, S., Shilatifard, A., O'Shea, E., Weissman, J.S., Ingles, C.J., Hughes, T.R., Parkinson, J., Gerstein, M., Wodak, S.J., Emili, A., Greenblatt, J.F., 2006. Global landscape of protein complexes in the yeast Saccharomyces cerevisiae. Nature 440, 637–643. https://doi.org/10.1038/nature04670

Kumar, R., Tao, M., 1975. Multiple forms of casein kinase from rabbit erythrocytes. Biochim Biophys Acta 410, 87–98. https://doi.org/10.1016/0005-2744(75)90209-0

Kunz, J.B., Neu-Yilik, G., Hentze, M.W., Kulozik, A.E., Gehring, N.H., 2006. Functions of hUpf3a and hUpf3b in nonsense-mediated mRNA decay and translation. RNA 12, 1015–1022. https://doi.org/10.1261/rna.12506

Kuroha, K., Akamatsu, M., Dimitrova, L., Ito, T., Kato, Y., Shirahige, K., Inada, T., 2010. Receptor for activated C kinase 1 stimulates nascent polypeptide-dependent translation arrest. EMBO Rep 11, 956–961. https://doi.org/10.1038/embor.2010.169

Kurosaki, T., Imamachi, N., Pröschel, C., Mitsutomi, S., Nagao, R., Akimitsu, N., Maquat, L.E., 2021. Loss of the fragile X syndrome protein FMRP results in misregulation of nonsense-mediated mRNA decay. Nat Cell Biol 23, 40–48. https://doi.org/10.1038/s41556-020-00618-1

Kurosaki, T., Maquat, L.E., 2013. Rules that govern UPF1 binding to mRNA 3' UTRs. Proc Natl Acad Sci U S A 110, 3357–3362. https://doi.org/10.1073/pnas.1219908110

Kurosaki, T., Popp, M.W., Maquat, L.E., 2019. Quality and quantity control of gene expression by nonsense-mediated mRNA decay. Nature Reviews Molecular Cell Biology 1. https://doi.org/10.1038/s41580-019-0126-2

LaCava, J., Houseley, J., Saveanu, C., Petfalski, E., Thompson, E., Jacquier, A., Tollervey, D., 2005. RNA degradation by the exosome is promoted by a nuclear polyadenylation complex. Cell 121, 713–724. https://doi.org/10.1016/j.cell.2005.04.029

LaGrandeur, T.E., Parker, R., 1998. Isolation and characterization of Dcp1p, the yeast mRNA decapping enzyme. EMBO J 17, 1487–1496. https://doi.org/10.1093/emboj/17.5.1487

Lanz, M.C., Yugandhar, K., Gupta, S., Sanford, E.J., Faça, V.M., Vega, S., Joiner, A.M.N., Fromme, J.C., Yu, H., Smolka, M.B., 2021. In-depth and 3-dimensional exploration of the budding yeast phosphoproteome. EMBO Rep 22, e51121. https://doi.org/10.15252/embr.202051121

Laurent, J.M., Garge, R.K., Teufel, A.I., Wilke, C.O., Kachroo, A.H., Marcotte, E.M., 2019. Humanization of yeast genes with multiple human orthologs reveals principles of functional divergence between paralogs. bioRxiv 668335. https://doi.org/10.1101/668335

Le Hir, H., Gatfield, D., Braun, I.C., Forler, D., Izaurralde, E., 2001a. The protein Mago provides a link between splicing and mRNA localization. EMBO Rep 2, 1119–1124. https://doi.org/10.1093/embo-reports/kve245

Le Hir, H., Gatfield, D., Izaurralde, E., Moore, M.J., 2001b. The exon-exon junction complex provides a binding platform for factors involved in mRNA export and nonsense-mediated mRNA decay. EMBO J 20, 4987–4997. https://doi.org/10.1093/emboj/20.17.4987

Le Hir, H., Izaurralde, E., Maquat, L.E., Moore, M.J., 2000a. The spliceosome deposits multiple proteins 20-24 nucleotides upstream of mRNA exon-exon junctions. EMBO J 19, 6860–6869. https://doi.org/10.1093/emboj/19.24.6860

Le Hir, H., Moore, M.J., Maquat, L.E., 2000b. Pre-mRNA splicing alters mRNP composition: evidence for stable association of proteins at exon-exon junctions. Genes Dev 14, 1098–1108.

Lebreton, A., Tomecki, R., Dziembowski, A., Séraphin, B., 2008. Endonucleolytic RNA cleavage by a eukaryotic exosome. Nature 456, 993–996. https://doi.org/10.1038/nature07480

Lee, J.M., Greenleaf, A.L., 1997. Modulation of RNA Polymerase II Elongation Efficiency by C-terminal Heptapeptide Repeat Domain Kinase I*. Journal of Biological Chemistry 272, 10990–10993. https://doi.org/10.1074/jbc.272.17.10990

Lee, S.R., Pratt, G.A., Martinez, F.J., Yeo, G.W., Lykke-Andersen, J., 2015. Target Discrimination in Nonsense-Mediated mRNA Decay Requires Upf1 ATPase Activity. Mol Cell 59, 413–425. https://doi.org/10.1016/j.molcel.2015.06.036

Lee, S.-Y., Kim, H., Li, C.M., Kang, J., Najafov, A., Jung, M., Kang, S., Wang, S., Yuan, J., Jung, Y.-K., 2019. Casein kinase-1γ1 and 3 stimulate tumor necrosis factor-induced necroptosis through RIPK3. Cell Death Dis 10, 923. https://doi.org/10.1038/s41419-019-2146-4

Leeds, P., Peltz, S.W., Jacobson, A., Culbertson, M.R., 1991. The product of the yeast UPF1 gene is required for rapid turnover of mRNAs containing a premature translational termination codon. Genes Dev 5, 2303–2314. https://doi.org/10.1101/gad.5.12a.2303

Leeds, P., Wood, J.M., Lee, B.S., Culbertson, M.R., 1992. Gene products that promote mRNA turnover in Saccharomyces cerevisiae. Mol Cell Biol 12, 2165–2177. https://doi.org/10.1128/mcb.12.5.2165-2177.1992

Li, D., Ai, Y., Guo, J., Dong, B., Li, L., Cai, G., Chen, S., Xu, D., Wang, F., Wang, X., 2020.

Casein kinase 1G2 suppresses necroptosis-promoted testis aging by inhibiting receptor-interacting kinase 3. Elife 9, e61564. https://doi.org/10.7554/eLife.61564

Li, Q., Fazly, A.M., Zhou, H., Huang, S., Zhang, Z., Stillman, B., 2009. The Elongator Complex Interacts with PCNA and Modulates Transcriptional Silencing and Sensitivity to DNA Damage Agents. PLOS Genetics 5, e1000684. https://doi.org/10.1371/journal.pgen.1000684

Li, S., Prasanna, X., Salo, V.T., Vattulainen, I., Ikonen, E., 2019. An efficient auxin-inducible degron system with low basal degradation in human cells. Nat Methods 16, 866–869. https://doi.org/10.1038/s41592-019-0512-x

Li, S., Wilkinson, M.F., 1998. Nonsense surveillance in lymphocytes? Immunity 8, 135–141. https://doi.org/10.1016/s1074-7613(00)80466-5

Liao, S.-M., Zhang, J., Jeffery, D.A., Koleske, A.J., Thompson, C.M., Chao, D.M., Viljoen, M., van Vuuren, H.J.J., Young, R.A., 1995. A kinase–cyclin pair in the RNA polymerase II holoenzyme. Nature 374, 193–196. https://doi.org/10.1038/374193a0

Licatalosi, D.D., Geiger, G., Minet, M., Schroeder, S., Cilli, K., McNeil, J.B., Bentley, D.L., 2002. Functional Interaction of Yeast Pre-mRNA 3′ End Processing Factors with RNA Polymerase II. Molecular Cell 9, 1101–1111. https://doi.org/10.1016/S1097-2765(02)00518-X

Lin, F.-J., Shen, L., Jang, C.-W., Falnes, P.Ø., Zhang, Y., 2013. Ikbkap/Elp1 Deficiency Causes Male Infertility by Disrupting Meiotic Progression. PLOS Genetics 9, e1003516. https://doi.org/10.1371/journal.pgen.1003516

Liu, C., Karam, R., Zhou, Y., Su, F., Ji, Y., Li, G., Xu, G., Lu, L., Wang, C., Song, M., Zhu, J., Wang, Y., Zhao, Y., Foo, W.C., Zuo, M., Valasek, M.A., Javle, M., Wilkinson, M.F., Lu, Y., 2014. The UPF1 RNA surveillance gene is commonly mutated in pancreatic adenosquamous carcinoma. Nat Med 20, 596–598. https://doi.org/10.1038/nm.3548

Liu, C., Li, Y., Semenov, M., Han, C., Baeg, G.H., Tan, Y., Zhang, Z., Lin, X., He, X., 2002. Control of beta-catenin phosphorylation/degradation by a dual-kinase mechanism. Cell 108, 837–847. https://doi.org/10.1016/s0092-8674(02)00685-2

Liu, C.-Y., Zha, Z.-Y., Zhou, X., Zhang, H., Huang, W., Zhao, D., Li, T., Chan, S.W., Lim, C.J., Hong, W., Zhao, S., Xiong, Y., Lei, Q.-Y., Guan, K.-L., 2010. The hippo tumor pathway promotes TAZ degradation by phosphorylating a phosphodegron and recruiting the SCF{beta}-TrCP E3 ligase. J Biol Chem 285, 37159–37169. https://doi.org/10.1074/jbc.M110.152942

Liu, Q., Greimann, J.C., Lima, C.D., 2006. Reconstitution, activities, and structure of the eukaryotic RNA exosome. Cell 127, 1223–1237. https://doi.org/10.1016/j.cell.2006.10.037

Liu, Y., Kung, C., Fishburn, J., Ansari, A.Z., Shokat, K.M., Hahn, S., 2004. Two Cyclin-Dependent Kinases Promote RNA Polymerase II Transcription and Formation of the Scaffold Complex. Molecular and Cellular Biology 24, 1721–1735. https://doi.org/10.1128/MCB.24.4.1721-1735.2004

Longman, D., Plasterk, R.H.A., Johnstone, I.L., Cáceres, J.F., 2007. Mechanistic insights and identification of two novel factors in the C. elegans NMD pathway. Genes Dev 21, 1075–1085. https://doi.org/10.1101/gad.417707

Longtine, M.S., McKenzie, A., Demarini, D.J., Shah, N.G., Wach, A., Brachat, A., Philippsen, P., Pringle, J.R., 1998. Additional modules for versatile and economical PCR-based gene deletion and modification in Saccharomyces cerevisiae. Yeast 14, 953–961. https://doi.org/10.1002/(SICI)1097-0061(199807)14:10<953::AID-YEA293>3.0.CO;2-U

Lord, C., Bhandari, D., Menon, S., Ghassemian, M., Nycz, D., Hay, J., Ghosh, P., Ferro-Novick, S., 2011. Sequential interactions with Sec23 control the direction of vesicle traffic. Nature 473, 181–186. https://doi.org/10.1038/nature09969

Losson, R., Lacroute, F., 1979. Interference of nonsense mutations with eukaryotic messenger RNA stability. Proc Natl Acad Sci U S A 76, 5134–5137. https://doi.org/10.1073/pnas.76.10.5134

Love, M.I., Huber, W., Anders, S., 2014. Moderated estimation of fold change and dispersion for RNA-seq data with DESeq2. Genome Biol 15, 550. https://doi.org/10.1186/s13059-014-0550-8

Lu, J., Plank, T.-D., Su, F., Shi, X., Liu, C., Ji, Y., Li, S., Huynh, A., Shi, C., Zhu, B., Yang, G., Wu, Y., Wilkinson, M.F., Lu, Y., 2016. The nonsense-mediated RNA decay pathway is disrupted in inflammatory myofibroblastic tumors. J Clin Invest 126, 3058–3062. https://doi.org/10.1172/JCI86508

Luke, B., Azzalin, C.M., Hug, N., Deplazes, A., Peter, M., Lingner, J., 2007. Saccharomyces cerevisiae Ebs1p is a putative ortholog of human Smg7 and promotes nonsense-mediated mRNA decay. Nucleic Acids Res 35, 7688–7697. https://doi.org/10.1093/nar/gkm912

Lykke-Andersen, J., Shu, M.-D., Steitz, J.A., 2000. Human Upf Proteins Target an mRNA for Nonsense-Mediated Decay When Bound Downstream of a Termination Codon. Cell 103, 1121–1131. https://doi.org/10.1016/S0092-8674(00)00214-2

Lykke-Andersen, S., Chen, Y., Ardal, B.R., Lilje, B., Waage, J., Sandelin, A., Jensen, T.H., 2014. Human nonsense-mediated RNA decay initiates widely by endonucleolysis and targets snoRNA host genes. Genes Dev 28, 2498–2517. https://doi.org/10.1101/gad.246538.114

Lynch, M., Ackerman, M.S., Gout, J.-F., Long, H., Sung, W., Thomas, W.K., Foster, P.L., 2016. Genetic drift, selection and the evolution of the mutation rate. Nat Rev Genet 17, 704–714. https://doi.org/10.1038/nrg.2016.104

Makeyev, E.V., Zhang, J., Carrasco, M.A., Maniatis, T., 2007. The MicroRNA miR-124 promotes neuronal differentiation by triggering brain-specific alternative pre-mRNA splicing. Mol Cell 27, 435–448. https://doi.org/10.1016/j.molcel.2007.07.015

Malabat, C., Feuerbach, F., Ma, L., Saveanu, C., Jacquier, A., 2015. Quality control of transcription start site selection by nonsense-mediated-mRNA decay. eLife 4, e06722. https://doi.org/10.7554/eLife.06722

Marin, O., Bustos, V.H., Cesaro, L., Meggio, F., Pagano, M.A., Antonelli, M., Allende, C.C., Pinna, L.A., Allende, J.E., 2003. A noncanonical sequence phosphorylated by casein kinase 1 in beta-catenin may play a role in casein kinase 1 targeting of important signaling proteins. Proc Natl Acad Sci U S A 100, 10193–10200. https://doi.org/10.1073/pnas.1733909100

Marin, O., Meggio, F., Sarno, S., Andretta, M., Pinna, L.A., 1994. Phosphorylation of synthetic fragments of inhibitor-2 of protein phosphatase-1 by casein kinase-1 and -2. Evidence that phosphorylated residues are not strictly required for efficient targeting by casein kinase-1. Eur J Biochem 223, 647–653. https://doi.org/10.1111/j.1432-1033.1994.tb19037.x

Medghalchi, S.M., Frischmeyer, P.A., Mendell, J.T., Kelly, A.G., Lawler, A.M., Dietz, H.C., 2001. Rent1, a trans-effector of nonsense-mediated mRNA decay, is essential for mammalian embryonic viability. Human Molecular Genetics 10, 99–105. https://doi.org/10.1093/hmg/10.2.99

Meggio, F., Perich, J.W., Marin, O., Pinna, L.A., 1992. The comparative efficiencies of the Ser(P)-, Thr(P)- and Tyr(P)-residues as specificity determinants for casein kinase-1. Biochem Biophys Res Commun 182, 1460–1465. https://doi.org/10.1016/0006-291x(92)91898-z

Meggio, F., Perich, J.W., Reynolds, E.C., Pinna, L.A., 1991. A synthetic beta-casein phosphopeptide and analogues as model substrates for casein kinase-1, a ubiquitous, phosphate directed protein kinase. FEBS Lett 283, 303–306. https://doi.org/10.1016/0014-5793(91)80614-9

Mehlgarten, C., Jablonowski, D., Breunig, K.D., Stark, M.J.R., Schaffrath, R., 2009. Elongator function depends on antagonistic regulation by casein kinase Hrr25 and protein phosphatase Sit4. Mol. Microbiol. 73, 869–881. https://doi.org/10.1111/j.1365-2958.2009.06811.x

Mehlgarten, C., Jablonowski, D., Wrackmeyer, U., Tschitschmann, S., Sondermann, D., Jäger, G., Gong, Z., Byström, A.S., Schaffrath, R., Breunig, K.D., 2010. Elongator function in tRNA wobble uridine modification is conserved between yeast and plants. Molecular Microbiology 76, 1082–1094. https://doi.org/10.1111/j.1365-2958.2010.07163.x

Mehlgarten, C., Schaffrath, R., 2003. Mutant casein kinase I (Hrr25p/Kti14p) abrogates the G1 cell cycle arrest induced by Kluyveromyces lactiszymocin in budding yeast. Mol. Genet. Genomics 269, 188–196. https://doi.org/10.1007/s00438-003-0807-5

Melero, R., Uchiyama, A., Castaño, R., Kataoka, N., Kurosawa, H., Ohno, S., Yamashita, A., Llorca, O., 2014. Structures of SMG1-UPFs complexes: SMG1 contributes to regulate UPF2-dependent activation of UPF1 in NMD. Structure 22, 1105–1119. https://doi.org/10.1016/j.str.2014.05.015

Mendell, J.T., Medghalchi, S.M., Lake, R.G., Noensie, E.N., Dietz, H.C., 2000. Novel Upf2p orthologues suggest a functional link between translation initiation and nonsense surveillance complexes. Mol Cell Biol 20, 8944–8957. https://doi.org/10.1128/MCB.20.23.8944-8957.2000

Mendell, J.T., Sharifi, N.A., Meyers, J.L., Martinez-Murillo, F., Dietz, H.C., 2004. Nonsense surveillance regulates expression of diverse classes of mammalian transcripts and mutes genomic noise. Nat Genet 36, 1073–1078. https://doi.org/10.1038/ng1429

Mendoza-Ochoa, G.I., Barrass, J.D., Terlouw, B.R., Maudlin, I.E., de Lucas, S., Sani, E., Aslanzadeh, V., Reid, J.A.E., Beggs, J.D., 2019. A fast and tuneable auxin-inducible degron for depletion of target proteins in budding yeast. Yeast 36, 75–81. https://doi.org/10.1002/yea.3362

Meng, Q.-J., Logunova, L., Maywood, E.S., Gallego, M., Lebiecki, J., Brown, T.M., Sládek, M., Semikhodskii, A.S., Glossop, N.R.J., Piggins, H.D., Chesham, J.E., Bechtold, D.A., Yoo, S.-H., Takahashi, J.S., Virshup, D.M., Boot-Handford, R.P., Hastings, M.H., Loudon, A.S.I., 2008. Setting clock speed in mammals: the CK1 epsilon tau mutation in mice accelerates circadian pacemakers by selectively destabilizing PERIOD proteins. Neuron 58, 78–88. https://doi.org/10.1016/j.neuron.2008.01.019

Miller, J.N., Pearce, D.A., 2014. Nonsense-mediated decay in genetic disease: friend or foe? Mutat Res Rev Mutat Res 762, 52–64. https://doi.org/10.1016/j.mrrev.2014.05.001

Milne, D.M., Palmer, R.H., Campbell, D.G., Meek, D.W., 1992. Phosphorylation of the p53 tumour-suppressor protein at three N-terminal sites by a novel casein kinase I-like enzyme. Oncogene 7, 1361–1369.

Miśkiewicz, K., Jose, L.E., Bento-Abreu, A., Fislage, M., Taes, I., Kasprowicz, J., Swerts, J., Sigrist, S., Versées, W., Robberecht, W., Verstreken, P., 2011. ELP3 Controls Active Zone Morphology by Acetylating the ELKS Family Member Bruchpilot. Neuron 72, 776–788. https://doi.org/10.1016/j.neuron.2011.10.010

Mitchell, P., Petfalski, E., Shevchenko, A., Mann, M., Tollervey, D., 1997. The exosome: a conserved eukaryotic RNA processing complex containing multiple 3'-->5' exoribonucleases. Cell 91, 457–466. https://doi.org/10.1016/s0092-8674(00)80432-8

Mitchell, P., Tollervey, D., 2003. An NMD Pathway in Yeast Involving Accelerated Deadenylation and Exosome-Mediated 3′→5′ Degradation. Molecular Cell 11, 1405–1413. https://doi.org/10.1016/S1097-2765(03)00190-4

Mitterer, V., Murat, G., Réty, S., Blaud, M., Delbos, L., Stanborough, T., Bergler, H., Leulliot, N., Kressler, D., Pertschy, B., 2016. Sequential domain assembly of ribosomal protein S3 drives 40S subunit maturation. Nat Commun 7, 10336. https://doi.org/10.1038/ncomms10336

Mitterer, V., Shayan, R., Ferreira-Cerca, S., Murat, G., Enne, T., Rinaldi, D., Weigl, S., Omanic, H., Gleizes, P.-E., Kressler, D., Plisson-Chastang, C., Pertschy, B., 2019. Conformational proofreading of distant 40S ribosomal subunit maturation events by a long-range communication mechanism. Nat Commun 10, 1–15. https://doi.org/10.1038/s41467-019-10678-z

Mort, M., Ivanov, D., Cooper, D.N., Chuzhanova, N.A., 2008. A meta-analysis of nonsense mutations causing human genetic disease. Human Mutation 29, 1037–1047. https://doi.org/10.1002/humu.20763

Muhlrad, D., Parker, R., 1999. Aberrant mRNAs with extended 3' UTRs are substrates for rapid degradation by mRNA surveillance. RNA 5, 1299–1307. https://doi.org/10.1017/s1355838299990829

Murray, S., Udupa, R., Yao, S., Hartzog, G., Prelich, G., 2001. Phosphorylation of the RNA Polymerase II Carboxy-Terminal Domain by the Bur1 Cyclin-Dependent Kinase. Molecular and Cellular Biology 21, 4089–4096. https://doi.org/10.1128/MCB.21.13.4089-4096.2001

Muslin, A.J., Tanner, J.W., Allen, P.M., Shaw, A.S., 1996. Interaction of 14-3-3 with Signaling Proteins Is Mediated by the Recognition of Phosphoserine. Cell 84, 889–897. https://doi.org/10.1016/S0092-8674(00)81067-3

Nagy, E., Maquat, L.E., 1998. A rule for termination-codon position within intron-containing genes: when nonsense affects RNA abundance. Trends Biochem Sci 23, 198–199. https://doi.org/10.1016/s0968-0004(98)01208-0

Nakatogawa, H., 2015. Hrr25: an emerging major player in selective autophagy regulation in Saccharomyces cerevisiae. Autophagy 11, 432–433. https://doi.org/10.1080/15548627.2015.1017195

Namane, A., Saveanu, C., 2022. Composition and Dynamics of Protein Complexes Measured by Quantitative Mass Spectrometry of Affinity-Purified Samples. Methods Mol Biol 2477, 225–236. https://doi.org/10.1007/978-1-0716-2257-5_13

Neil, H., Malabat, C., d'Aubenton-Carafa, Y., Xu, Z., Steinmetz, L.M., Jacquier, A., 2009. Widespread bidirectional promoters are the major source of cryptic transcripts in yeast. Nature 457, 1038–1042. https://doi.org/10.1038/nature07747

Nelson, J.O., Moore, K.A., Chapin, A., Hollien, J., Metzstein, M.M., 2016. Degradation of Gadd45 mRNA by nonsense-mediated decay is essential for viability [WWW Document]. eLife. https://doi.org/10.7554/eLife.12876

Nemec, C.M., Singh, A.K., Ali, A., Tseng, S.C., Syal, K., Ringelberg, K.J., Ho, Y.-H., Hintermair, C., Ahmad, M.F., Kar, R.K., Gasch, A.P., Akhtar, M.S., Eick, D., Ansari, A.Z., 2019. Noncanonical CTD kinases regulate RNA polymerase II in a gene-class-specific manner. Nature Chemical Biology 15, 123. https://doi.org/10.1038/s41589-018-0194-1

Nemec, C.M., Yang, F., Gilmore, J.M., Hintermair, C., Ho, Y.-H., Tseng, S.C., Heidemann, M., Zhang, Y., Florens, L., Gasch, A.P., Eick, D., Washburn, M.P., Varani, G., Ansari, A.Z., 2017. Different phosphoisoforms of RNA polymerase II engage the Rtt103 termination factor in a structurally analogous manner. Proc Natl Acad Sci U S A 114, E3944–E3953. https://doi.org/10.1073/pnas.1700128114

Neu-Yilik, G., Raimondeau, E., Eliseev, B., Yeramala, L., Amthor, B., Deniaud, A., Huard, K., Kerschgens, K., Hentze, M.W., Schaffitzel, C., Kulozik, A.E., 2017. Dual function of UPF3B in early and late translation termination. EMBO J 36, 2968–2986. https://doi.org/10.15252/embj.201797079

Nicholson-Shaw, T., Ajaj, Y., Perelis, M., Fulzele, A., Yeo, G.W., Bennett, E.J., Lykke-

Andersen, J., 2022. The 2',3' cyclic phosphatase Angel1 facilitates mRNA degradation during human ribosome-associated quality control. https://doi.org/10.1101/2022.04.28.489582

Nissan, T., Rajyaguru, P., She, M., Song, H., Parker, R., 2010. Decapping Activators in Saccharomyces cerevisiae Act by Multiple Mechanisms. Molecular Cell 39, 773–783. https://doi.org/10.1016/j.molcel.2010.08.025

Olivas, W., Parker, R., 2000. The Puf3 protein is a transcript-specific regulator of mRNA degradation in yeast. EMBO J 19, 6602–6611. https://doi.org/10.1093/emboj/19.23.6602

Oliveira, C.C., McCarthy, J.E., 1995. The relationship between eukaryotic translation and mRNA stability. A short upstream open reading frame strongly inhibits translational initiation and greatly accelerates mRNA degradation in the yeast Saccharomyces cerevisiae. J Biol Chem 270, 8936–8943. https://doi.org/10.1074/jbc.270.15.8936

Ostapenko, D., Solomon, M.J., 2003. Budding Yeast CTDK-I Is Required for DNA Damage-Induced Transcription. Eukaryotic Cell 2, 274–283. https://doi.org/10.1128/EC.2.2.274-283.2003

Otero, G., Fellows, J., Li, Y., de Bizemont, T., Dirac, A.M.G., Gustafsson, C.M., Erdjument-Bromage, H., Tempst, P., Svejstrup, J.Q., 1999. Elongator, a Multisubunit Component of a Novel RNA Polymerase II Holoenzyme for Transcriptional Elongation. Molecular Cell 3, 109–118. https://doi.org/10.1016/S1097-2765(00)80179-3

Ozsolak, F., Kapranov, P., Foissac, S., Kim, S.W., Fishilevich, E., Monaghan, A.P., John, B., Milos, P.M., 2010. Comprehensive Polyadenylation Site Maps in Yeast and Human Reveal Pervasive Alternative Polyadenylation. Cell 143, 1018–1029. https://doi.org/10.1016/j.cell.2010.11.020

Page, M.F., Carr, B., Anders, K.R., Grimson, A., Anderson, P., 1999. SMG-2 is a phosphorylated protein required for mRNA surveillance in Caenorhabditis elegans and related to Upf1p of yeast. Mol Cell Biol 19, 5943–5951. https://doi.org/10.1128/MCB.19.9.5943

Pal, M., Ishigaki, Y., Nagy, E., Maquat, L.E., 2001. Evidence that phosphorylation of human Upfl protein varies with intracellular location and is mediated by a wortmannin-sensitive and rapamycin-sensitive PI 3-kinase-related kinase signaling pathway. RNA 7, 5–15.

Palma, M., Leroy, C., Salomé-Desnoulez, S., Werkmeister, E., Kong, R., Mongy, M., Le Hir, H., Lejeune, F., 2021. A role for AKT1 in nonsense-mediated mRNA decay. Nucleic Acids Research. https://doi.org/10.1093/nar/gkab882

Pefanis, E., Wang, J., Rothschild, G., Lim, J., Chao, J., Rabadan, R., Economides, A.N., Basu, U., 2014. Noncoding RNA transcription targets AID to divergently transcribed loci in B cells. Nature 514, 389–393. https://doi.org/10.1038/nature13580

Pelechano, V., Wei, W., Steinmetz, L.M., 2015. Widespread Co-translational RNA Decay Reveals Ribosome Dynamics. Cell 161, 1400–1412. https://doi.org/10.1016/j.cell.2015.05.008

Pelechano, V., Wei, W., Steinmetz, L.M., 2013. Extensive transcriptional heterogeneity

revealed by isoform profiling. Nature 497, 127–131. https://doi.org/10.1038/nature12121

Peltz, S.W., Brown, A.H., Jacobson, A., 1993. mRNA destabilization triggered by premature translational termination depends on at least three cis-acting sequence elements and one trans-acting factor. Genes Dev 7, 1737–1754. https://doi.org/10.1101/gad.7.9.1737

Perlick, H.A., Medghalchi, S.M., Spencer, F.A., Kendzior, R.J., Dietz, H.C., 1996. Mammalian orthologues of a yeast regulator of nonsense transcript stability. Proc Natl Acad Sci U S A 93, 10928–10932. https://doi.org/10.1073/pnas.93.20.10928

Petitjean, A., Mathe, E., Kato, S., Ishioka, C., Tavtigian, S.V., Hainaut, P., Olivier, M., 2007. Impact of mutant p53 functional properties on TP53 mutation patterns and tumor phenotype: lessons from recent developments in the IARC TP53 database. Hum Mutat 28, 622–629. https://doi.org/10.1002/humu.20495

Pfaffenwimmer, T., Reiter, W., Brach, T., Nogellova, V., Papinski, D., Schuschnig, M., Abert, C., Ammerer, G., Martens, S., Kraft, C., 2014. Hrr25 kinase promotes selective autophagy by phosphorylating the cargo receptor Atg19. EMBO Rep 15, 862–870. https://doi.org/10.15252/embr.201438932

Phatnani, H.P., Greenleaf, A.L., 2006. Phosphorylation and functions of the RNA polymerase II CTD. Genes Dev. 20, 2922–2936. https://doi.org/10.1101/gad.1477006

Phatnani, H.P., Jones, J.C., Greenleaf, A.L., 2004. Expanding the Functional Repertoire of CTD Kinase I and RNA Polymerase II: Novel PhosphoCTD-Associating Proteins in the Yeast Proteome. Biochemistry 43, 15702–15719. https://doi.org/10.1021/bi048364h

Pisareva, V.P., Skabkin, M.A., Hellen, C.U.T., Pestova, T.V., Pisarev, A.V., 2011. Dissociation by Pelota, Hbs1 and ABCE1 of mammalian vacant 80S ribosomes and stalled elongation complexes. EMBO J 30, 1804–1817. https://doi.org/10.1038/emboj.2011.93

Popp, M.W., Maquat, L.E., 2018. Nonsense-mediated mRNA Decay and Cancer. Current Opinion in Genetics & Development, Cancer genomics 48, 44–50. https://doi.org/10.1016/j.gde.2017.10.007

Powers, K.T., Szeto, J.-Y.A., Schaffitzel, C., 2020. New insights into no-go, non-stop and nonsense-mediated mRNA decay complexes. Current Opinion in Structural Biology, Catalysis and Regulation ● Protein Nucleic Acid Interaction 65, 110–118. https://doi.org/10.1016/j.sbi.2020.06.011

Prelich, G., 2002. RNA polymerase II carboxy-terminal domain kinases: emerging clues to their function. Eukaryot Cell 1, 153–162. https://doi.org/10.1128/EC.1.2.153-162.2002

Pulak, R., Anderson, P., 1993. mRNA surveillance by the Caenorhabditis elegans smg genes. Genes Dev 7, 1885–1897. https://doi.org/10.1101/gad.7.10.1885

Pulgar, V., Marin, O., Meggio, F., Allende, C.C., Allende, J.E., Pinna, L.A., 1999. Optimal sequences for non-phosphate-directed phosphorylation by protein kinase CK1 (casein kinase-1)--a re-evaluation. Eur J Biochem 260, 520–526. https://doi.org/10.1046/j.1432-1327.1999.00195.x

Qiu, H., Hu, C., Hinnebusch, A.G., 2009. Phosphorylation of the Pol II CTD by KIN28 Enhances BUR1/BUR2 Recruitment and Ser2 CTD Phosphorylation Near Promoters. Molecular Cell 33, 752–762. https://doi.org/10.1016/j.molcel.2009.02.018

Rahl, P.B., Chen, C.Z., Collins, R.N., 2005. Elp1p, the Yeast Homolog of the FD Disease Syndrome Protein, Negatively Regulates Exocytosis Independently of Transcriptional Elongation. Molecular Cell 17, 841–853. https://doi.org/10.1016/j.molcel.2005.02.018

Ramanathan, A., Robb, G.B., Chan, S.-H., 2016. mRNA capping: biological functions and applications. Nucleic Acids Research 44, 7511–7526. https://doi.org/10.1093/nar/gkw551

Reppert, S.M., Weaver, D.R., 2002. Coordination of circadian timing in mammals. Nature 418, 935–941. https://doi.org/10.1038/nature00965

Ridley, S.P., Sommer, S.S., Wickner, R.B., 1984. Superkiller mutations in Saccharomyces cerevisiae suppress exclusion of M2 double-stranded RNA by L-A-HN and confer cold sensitivity in the presence of M and L-A-HN. Mol Cell Biol 4, 761–770. https://doi.org/10.1128/mcb.4.4.761-770.1984

Rigaut, G., Shevchenko, A., Rutz, B., Wilm, M., Mann, M., Séraphin, B., 1999. A generic protein purification method for protein complex characterization and proteome exploration. Nature Biotechnology 17, 1030. https://doi.org/10.1038/13732

Robinson, L.C., Menold, M.M., Garrett, S., Culbertson, M.R., 1993. Casein kinase I-like protein kinases encoded by YCK1 and YCK2 are required for yeast morphogenesis. Mol Cell Biol 13, 2870–2881. https://doi.org/10.1128/mcb.13.5.2870-2881.1993

Rodriguez, C.R., Cho, E.-J., Keogh, M.-C., Moore, C.L., Greenleaf, A.L., Buratowski, S., 2000. Kin28, the TFIIH-Associated Carboxy-Terminal Domain Kinase, Facilitates the Recruitment of mRNA Processing Machinery to RNA Polymerase II. Molecular and Cellular Biology 20, 104–112. https://doi.org/10.1128/MCB.20.1.104-112.2000

Ruiz-Echevarría, M.J., Peltz, S.W., 2000. The RNA binding protein Pub1 modulates the stability of transcripts containing upstream open reading frames. Cell 101, 741–751. https://doi.org/10.1016/s0092-8674(00)80886-7

Sachs, A.B., Bond, M.W., Kornberg, R.D., 1986. A single gene from yeast for both nuclear and cytoplasmic polyadenylate-binding proteins: domain structure and expression. Cell 45, 827–835. https://doi.org/10.1016/0092-8674(86)90557-x

Saito, S., Hosoda, N., Hoshino, S., 2013. The Hbs1-Dom34 Protein Complex Functions in Non-stop mRNA Decay in Mammalian Cells*. Journal of Biological Chemistry 288, 17832–17843. https://doi.org/10.1074/jbc.M112.448977

Sayani, S., Janis, M., Lee, C.Y., Toesca, I., Chanfreau, G.F., 2008. Widespread impact of nonsense-mediated mRNA decay on the yeast intronome. Mol Cell 31, 360–370. https://doi.org/10.1016/j.molcel.2008.07.005

Schaeffer, D., Tsanova, B., Barbas, A., Reis, F.P., Dastidar, E.G., Sanchez-Rotunno, M.,

Arraiano, C.M., van Hoof, A., 2009. The exosome contains domains with specific endoribonuclease, exoribonuclease and cytoplasmic mRNA decay activities. Nat Struct Mol Biol 16, 56–62. https://doi.org/10.1038/nsmb.1528

Schäfer, T., Maco, B., Petfalski, E., Tollervey, D., Böttcher, B., Aebi, U., Hurt, E., 2006. Hrr25-dependent phosphorylation state regulates organization of the pre-40S subunit. Nature 441, 651–655. https://doi.org/10.1038/nature04840

Schäfer, T., Strauss, D., Petfalski, E., Tollervey, D., Hurt, E., 2003. The path from nucleolar 90S to cytoplasmic 40S pre-ribosomes. EMBO J. 22, 1370–1380. https://doi.org/10.1093/emboj/cdg121

Schiestl, R.H., Gietz, R.D., 1989. High efficiency transformation of intact yeast cells using single stranded nucleic acids as a carrier. Curr Genet 16, 339–346. https://doi.org/10.1007/BF00340712

Schneider, C., Kudla, G., Wlotzka, W., Tuck, A., Tollervey, D., 2012. Transcriptome-wide analysis of exosome targets. Mol Cell 48, 422–433. https://doi.org/10.1016/j.molcel.2012.08.013

Schneider, C., Leung, E., Brown, J., Tollervey, D., 2009. The N-terminal PIN domain of the exosome subunit Rrp44 harbors endonuclease activity and tethers Rrp44 to the yeast core exosome. Nucleic Acids Res 37, 1127–1140. https://doi.org/10.1093/nar/gkn1020

Schroeder, S.C., Schwer, B., Shuman, S., Bentley, D., 2000. Dynamic association of capping enzymes with transcribing RNA polymerase II. Genes Dev. 14, 2435–2440. https://doi.org/10.1101/gad.836300

Schweingruber, C., Rufener, S.C., Zünd, D., Yamashita, A., Mühlemann, O., 2013. Nonsense-mediated mRNA decay — Mechanisms of substrate mRNA recognition and degradation in mammalian cells. Biochimica et Biophysica Acta (BBA) - Gene Regulatory Mechanisms, RNA Decay Mechanisms 1829, 612–623. https://doi.org/10.1016/j.bbagrm.2013.02.005

Seila, A.C., Calabrese, J.M., Levine, S.S., Yeo, G.W., Rahl, P.B., Flynn, R.A., Young, R.A., Sharp, P.A., 2008. Divergent transcription from active promoters. Science 322, 1849–1851. https://doi.org/10.1126/science.1162253

Serin, G., Gersappe, A., Black, J.D., Aronoff, R., Maquat, L.E., 2001. Identification and characterization of human orthologues to Saccharomyces cerevisiae Upf2 protein and Upf3 protein (Caenorhabditis elegans SMG-4). Mol Cell Biol 21, 209–223. https://doi.org/10.1128/MCB.21.1.209-223.2001

Shalem, O., Groisman, B., Choder, M., Dahan, O., Pilpel, Y., 2011. Transcriptome kinetics is governed by a genome-wide coupling of mRNA production and degradation: a role for RNA Pol II. PLoS Genet 7, e1002273. https://doi.org/10.1371/journal.pgen.1002273

Shatkin, A.J., Manley, J.L., 2000. The ends of the affair: capping and polyadenylation. Nat Struct Biol 7, 838–842. https://doi.org/10.1038/79583

She, M., Decker, C.J., Chen, N., Tumati, S., Parker, R., Song, H., 2006. Crystal structure and

functional analysis of Dcp2p from Schizosaccharomyces pombe. Nat Struct Mol Biol 13, 63–70. https://doi.org/10.1038/nsmb1033

Sheppard, D.N., Carson, M.R., Ostedgaard, L.S., Denning, G.M., Welsh, M.J., 1994. Expression of cystic fibrosis transmembrane conductance regulator in a model epithelium. American Journal of Physiology-Lung Cellular and Molecular Physiology 266, L405–L413. https://doi.org/10.1152/ajplung.1994.266.4.L405

Shetty, A., Reim, N.I., Winston, F., 2019. Auxin-Inducible Degron System for Depletion of Proteins in Saccharomyces cerevisiae. Curr Protoc Mol Biol 128, e104. https://doi.org/10.1002/cpmb.104

Shibuya, T., Tange, T.Ø., Sonenberg, N., Moore, M.J., 2004. eIF4AIII binds spliced mRNA in the exon junction complex and is essential for nonsense-mediated decay. Nat Struct Mol Biol 11, 346–351. https://doi.org/10.1038/nsmb750

Shigeoka, T., Kato, S., Kawaichi, M., Ishida, Y., 2012. Evidence that the Upf1-related molecular motor scans the 3'-UTR to ensure mRNA integrity. Nucleic Acids Res 40, 6887–6897. https://doi.org/10.1093/nar/gks344

Shoemaker, C.J., Eyler, D.E., Green, R., 2010. Dom34:Hbs1 promotes subunit dissociation and peptidyl-tRNA drop-off to initiate no-go decay. Science 330, 369–372. https://doi.org/10.1126/science.1192430

Shum, E.Y., Jones, S.H., Shao, A., Dumdie, J., Krause, M.D., Chan, W.-K., Lou, C.-H., Espinoza, J.L., Song, H.-W., Phan, M.H., Ramaiah, M., Huang, L., McCarrey, J.R., Peterson, K.J., De Rooij, D.G., Cook-Andersen, H., Wilkinson, M.F., 2016. The Antagonistic Gene Paralogs Upf3a and Upf3b Govern Nonsense-Mediated RNA Decay. Cell 165, 382–395. https://doi.org/10.1016/j.cell.2016.02.046

Siddiqui, N., Mangus, D.A., Chang, T.-C., Palermino, J.-M., Shyu, A.-B., Gehring, K., 2007. Poly(A) nuclease interacts with the C-terminal domain of polyadenylate-binding protein domain from poly(A)-binding protein. J Biol Chem 282, 25067–25075. https://doi.org/10.1074/jbc.M701256200

Singh, G., Rebbapragada, I., Lykke-Andersen, J., 2008. A competition between stimulators and antagonists of Upf complex recruitment governs human nonsense-mediated mRNA decay. PLoS Biol 6, e111. https://doi.org/10.1371/journal.pbio.0060111

Solinger, J.A., Paolinelli, R., Klöß, H., Scorza, F.B., Marchesi, S., Sauder, U., Mitsushima, D., Capuani, F., Stürzenbaum, S.R., Cassata, G., 2010. The Caenorhabditis elegans Elongator Complex Regulates Neuronal α-tubulin Acetylation. PLOS Genetics 6, e1000820. https://doi.org/10.1371/journal.pgen.1000820

Spellman, R., Rideau, A., Matlin, A., Gooding, C., Robinson, F., McGlincy, N., Grellscheid, S.N., Southby, J., Wollerton, M., Smith, C.W.J., 2005. Regulation of alternative splicing by PTB and associated factors. Biochem Soc Trans 33, 457–460. https://doi.org/10.1042/BST0330457

Stevens, A., 1980. An mRNA decapping enzyme from ribosomes of Saccharomyces

cerevisiae. Biochem Biophys Res Commun 96, 1150–1155. https://doi.org/10.1016/0006-291x(80)90072-8

Stevens, A., 1978. An exoribonuclease from Saccharomyces cerevisiae: effect of modifications of 5’ end groups on the hydrolysis of substrates to 5’ mononucleotides. Biochem Biophys Res Commun 81, 656–661. https://doi.org/10.1016/0006-291x(78)91586-3

Stöter, M., Bamberger, A.-M., Aslan, B., Kurth, M., Speidel, D., Löning, T., Frank, H.-G., Kaufmann, P., Löhler, J., Henne-Bruns, D., Deppert, W., Knippschild, U., 2005. Inhibition of casein kinase I delta alters mitotic spindle formation and induces apoptosis in trophoblast cells. Oncogene 24, 7964–7975. https://doi.org/10.1038/sj.onc.1208941

Sun, X., Perlick, H.A., Dietz, H.C., Maquat, L.E., 1998. A mutated human homologue to yeast Upf1 protein has a dominant-negative effect on the decay of nonsense-containing mRNAs in mammalian cells. Proc Natl Acad Sci U S A 95, 10009–10014. https://doi.org/10.1073/pnas.95.17.10009

Supek, F., Lehner, B., Lindeboom, R.G.H., 2021. To NMD or Not To NMD: Nonsense-Mediated mRNA Decay in Cancer and Other Genetic Diseases. Trends in Genetics 37, 657–668. https://doi.org/10.1016/j.tig.2020.11.002

Takahashi, S., Araki, Y., Sakuno, T., Katada, T., 2003. Interaction between Ski7p and Upf1p is required for nonsense-mediated 3’-to-5’ mRNA decay in yeast. EMBO J 22, 3951–3959. https://doi.org/10.1093/emboj/cdg374

Takano, A., Uchiyama, M., Kajimura, N., Mishima, K., Inoue, Y., Kamei, Y., Kitajima, T., Shibui, K., Katoh, M., Watanabe, T., Hashimotodani, Y., Nakajima, T., Ozeki, Y., Hori, T., Yamada, N., Toyoshima, R., Ozaki, N., Okawa, M., Nagai, K., Takahashi, K., Isojima, Y., Yamauchi, T., Ebisawa, T., 2004. A missense variation in human casein kinase I epsilon gene that induces functional alteration and shows an inverse association with circadian rhythm sleep disorders. Neuropsychopharmacology 29, 1901–1909. https://doi.org/10.1038/sj.npp.1300503

Tange, T.Ø., Shibuya, T., Jurica, M.S., Moore, M.J., 2005. Biochemical analysis of the EJC reveals two new factors and a stable tetrameric protein core. RNA 11, 1869–1883. https://doi.org/10.1261/rna.2155905

Tani, H., Mizutani, R., Salam, K.A., Tano, K., Ijiri, K., Wakamatsu, A., Isogai, T., Suzuki, Y., Akimitsu, N., 2012. Genome-wide determination of RNA stability reveals hundreds of short-lived noncoding transcripts in mammals. Genome Res 22, 947–956. https://doi.org/10.1101/gr.130559.111

Tarassov, K., Messier, V., Landry, C.R., Radinovic, S., Molina, M.M.S., Shames, I., Malitskaya, Y., Vogel, J., Bussey, H., Michnick, S.W., 2008. An in Vivo Map of the Yeast Protein Interactome. Science 320, 1465–1470. https://doi.org/10.1126/science.1153878

Tharun, S., Parker, R., 2001. Targeting an mRNA for decapping: displacement of translation factors and association of the Lsm1p-7p complex on deadenylated yeast mRNAs. Mol Cell 8, 1075–1083. https://doi.org/10.1016/s1097-2765(01)00395-1

Thore, S., Mauxion, F., Séraphin, B., Suck, D., 2003. X-ray structure and activity of the yeast Pop2 protein: a nuclease subunit of the mRNA deadenylase complex. EMBO Rep 4, 1150–1155. https://doi.org/10.1038/sj.embor.7400020

Toh-E, A., Guerry, P., Wickner, R.B., 1978. Chromosomal superkiller mutants of Saccharomyces cerevisiae. J Bacteriol 136, 1002–1007. https://doi.org/10.1128/jb.136.3.1002-1007.1978

Tong, A.H.Y., Lesage, G., Bader, G.D., Ding, H., Xu, H., Xin, X., Young, J., Berriz, G.F., Brost, R.L., Chang, M., Chen, Y., Cheng, X., Chua, G., Friesen, H., Goldberg, D.S., Haynes, J., Humphries, C., He, G., Hussein, S., Ke, L., Krogan, N., Li, Z., Levinson, J.N., Lu, H., Ménard, P., Munyana, C., Parsons, A.B., Ryan, O., Tonikian, R., Roberts, T., Sdicu, A.-M., Shapiro, J., Sheikh, B., Suter, B., Wong, S.L., Zhang, L.V., Zhu, H., Burd, C.G., Munro, S., Sander, C., Rine, J., Greenblatt, J., Peter, M., Bretscher, A., Bell, G., Roth, F.P., Brown, G.W., Andrews, B., Bussey, H., Boone, C., 2004. Global mapping of the yeast genetic interaction network. Science 303, 808–813. https://doi.org/10.1126/science.1091317

Tsuboi, T., Kuroha, K., Kudo, K., Makino, S., Inoue, E., Kashima, I., Inada, T., 2012. Dom34:Hbs1 Plays a General Role in Quality-Control Systems by Dissociation of a Stalled Ribosome at the 3′ End of Aberrant mRNA. Molecular Cell 46, 518–529. https://doi.org/10.1016/j.molcel.2012.03.013

Tuazon, P.T., Traugh, J.A., 1991. Casein kinase I and II--multipotential serine protein kinases: structure, function, and regulation. Adv Second Messenger Phosphoprotein Res 23, 123–164.

Tucker, M., Staples, R.R., Valencia-Sanchez, M.A., Muhlrad, D., Parker, R., 2002. Ccr4p is the catalytic subunit of a Ccr4p/Pop2p/Notp mRNA deadenylase complex in Saccharomyces cerevisiae. EMBO J 21, 1427–1436. https://doi.org/10.1093/emboj/21.6.1427

Tucker, M., Valencia-Sanchez, M.A., Staples, R.R., Chen, J., Denis, C.L., Parker, R., 2001. The Transcription Factor Associated Ccr4 and Caf1 Proteins Are Components of the Major Cytoplasmic mRNA Deadenylase in Saccharomyces cerevisiae. Cell 104, 377–386. https://doi.org/10.1016/S0092-8674(01)00225-2

Valadkhan, S., Jaladat, Y., 2010. The spliceosomal proteome: at the heart of the largest cellular ribonucleoprotein machine. Proteomics 10, 4128–4141. https://doi.org/10.1002/pmic.201000354

Valkov, E., Jonas, S., Weichenrieder, O., 2017. Mille viae in eukaryotic mRNA decapping. Curr. Opin. Struct. Biol. 47, 40–51. https://doi.org/10.1016/j.sbi.2017.05.009

van Dijk, E., Cougot, N., Meyer, S., Babajko, S., Wahle, E., Séraphin, B., 2002. Human Dcp2: a catalytically active mRNA decapping enzyme located in specific cytoplasmic structures. EMBO J 21, 6915–6924. https://doi.org/10.1093/emboj/cdf678

van Dijk, E.L., Chen, C.L., d'Aubenton-Carafa, Y., Gourvennec, S., Kwapisz, M., Roche, V., Bertrand, C., Silvain, M., Legoix-Né, P., Loeillet, S., Nicolas, A., Thermes, C., Morillon, A., 2011. XUTs are a class of Xrn1-sensitive antisense regulatory non-coding RNA in yeast. Nature 475, 114–117. https://doi.org/10.1038/nature10118

van Hoof, A., Frischmeyer, P.A., Dietz, H.C., Parker, R., 2002. Exosome-mediated recognition and degradation of mRNAs lacking a termination codon. Science 295, 2262–2264. https://doi.org/10.1126/science.1067272

van Leeuwen, F.W., de Kleijn, D.P., van den Hurk, H.H., Neubauer, A., Sonnemans, M.A., Sluijs, J.A., Köycü, S., Ramdjielal, R.D., Salehi, A., Martens, G.J., Grosveld, F.G., Peter, J., Burbach, H., Hol, E.M., 1998. Frameshift mutants of beta amyloid precursor protein and ubiquitin-B in Alzheimer's and Down patients. Science 279, 242–247. https://doi.org/10.1126/science.279.5348.242

Varjosalo, M., Taipale, J., 2008. Hedgehog: functions and mechanisms. Genes Dev 22, 2454–2472. https://doi.org/10.1101/gad.1693608

Vielhaber, E., Eide, E., Rivers, A., Gao, Z.H., Virshup, D.M., 2000. Nuclear entry of the circadian regulator mPER1 is controlled by mammalian casein kinase I epsilon. Mol Cell Biol 20, 4888–4899. https://doi.org/10.1128/MCB.20.13.4888-4899.2000

Wallmeroth, D., Lackmann, J.-W., Kueckelmann, S., Altmüller, J., Dieterich, C., Boehm, V., Gehring, N.H., 2022. Human UPF3A and UPF3B enable fault-tolerant activation of nonsense-mediated mRNA decay. EMBO J 41, e109191. https://doi.org/10.15252/embj.2021109191

Wang, L., Lewis, M.S., Johnson, A.W., 2005. Domain interactions within the Ski2/3/8 complex and between the Ski complex and Ski7p. RNA 11, 1291–1302. https://doi.org/10.1261/rna.2060405

Wang, L., Lu, A., Zhou, H.-X., Sun, R., Zhao, J., Zhou, C.-J., Shen, J.-P., Wu, S.-N., Liang, C.-G., 2013. Casein kinase 1 alpha regulates chromosome congression and separation during mouse oocyte meiotic maturation and early embryo development. PLoS One 8, e63173. https://doi.org/10.1371/journal.pone.0063173

Wang, W., Cajigas, I.J., Peltz, S.W., Wilkinson, M.F., González, C.I., 2006. Role for Upf2p Phosphorylation in Saccharomyces cerevisiae Nonsense-Mediated mRNA Decay. Mol Cell Biol 26, 3390–3400. https://doi.org/10.1128/MCB.26.9.3390-3400.2006

Wang, W., Czaplinski, K., Rao, Y., Peltz, S.W., 2001. The role of Upf proteins in modulating the translation read-through of nonsense-containing transcripts. EMBO J. 20, 880–890. https://doi.org/10.1093/emboj/20.4.880

Webster, M.W., Chen, Y.-H., Stowell, J.A.W., Alhusaini, N., Sweet, T., Graveley, B.R., Coller, J., Passmore, L.A., 2018. mRNA Deadenylation Is Coupled to Translation Rates by the Differential Activities of Ccr4-Not Nucleases. Mol Cell 70, 1089-1100.e8. https://doi.org/10.1016/j.molcel.2018.05.033

Welch, E.M., Jacobson, A., 1999. An internal open reading frame triggers nonsense-mediated decay of the yeast SPT10 mRNA. EMBO J 18, 6134–6145. https://doi.org/10.1093/emboj/18.21.6134

Wen, J., Brogna, S., 2010. Splicing-dependent NMD does not require the EJC in Schizosaccharomyces pombe. EMBO J 29, 1537–1551.

https://doi.org/10.1038/emboj.2010.48

Weng, Y., Czaplinski, K., Peltz, S.W., 1996. Genetic and biochemical characterization of mutations in the ATPase and helicase regions of the Upf1 protein. Mol Cell Biol 16, 5477–5490. https://doi.org/10.1128/MCB.16.10.5477

Wessel, D., Flügge, U.I., 1984. A method for the quantitative recovery of protein in dilute solution in the presence of detergents and lipids. Anal Biochem 138, 141–143. https://doi.org/10.1016/0003-2697(84)90782-6

Wilmes, G.M., Bergkessel, M., Bandyopadhyay, S., Shales, M., Braberg, H., Cagney, G., Collins, S.R., Whitworth, G.B., Kress, T.L., Weissman, J.S., Ideker, T., Guthrie, C., Krogan, N.J., 2008. A genetic interaction map of RNA-processing factors reveals links between Sem1/Dss1-containing complexes and mRNA export and splicing. Mol Cell 32, 735–746. https://doi.org/10.1016/j.molcel.2008.11.012

Winkler, G.S., Kristjuhan, A., Erdjument-Bromage, H., Tempst, P., Svejstrup, J.Q., 2002. Elongator is a histone H3 and H4 acetyltransferase important for normal histone acetylation levels in vivo. Proc Natl Acad Sci U S A 99, 3517–3522. https://doi.org/10.1073/pnas.022042899

Winkler, G.S., Petrakis, T.G., Ethelberg, S., Tokunaga, M., Erdjument-Bromage, H., Tempst, P., Svejstrup, J.Q., 2001. RNA Polymerase II Elongator Holoenzyme Is Composed of Two Discrete Subcomplexes*. Journal of Biological Chemistry 276, 32743–32749. https://doi.org/10.1074/jbc.M105303200

Winter, M., Milne, D., Dias, S., Kulikov, R., Knippschild, U., Blattner, C., Meek, D., 2004. Protein kinase CK1delta phosphorylates key sites in the acidic domain of murine double-minute clone 2 protein (MDM2) that regulate p53 turnover. Biochemistry 43, 16356–16364. https://doi.org/10.1021/bi0489255

Wittkopp, N., Huntzinger, E., Weiler, C., Saulière, J., Schmidt, S., Sonawane, M., Izaurralde, E., 2009. Nonsense-mediated mRNA decay effectors are essential for zebrafish embryonic development and survival. Mol Cell Biol 29, 3517–3528. https://doi.org/10.1128/MCB.00177-09

Wittmann, J., Hol, E.M., Jäck, H.-M., 2006. hUPF2 silencing identifies physiologic substrates of mammalian nonsense-mediated mRNA decay. Mol Cell Biol 26, 1272–1287. https://doi.org/10.1128/MCB.26.4.1272-1287.2006

Wittschieben, B.Ø., Otero, G., de Bizemont, T., Fellows, J., Erdjument-Bromage, H., Ohba, R., Li, Y., Allis, C.D., Tempst, P., Svejstrup, J.Q., 1999. A Novel Histone Acetyltransferase Is an Integral Subunit of Elongating RNA Polymerase II Holoenzyme. Molecular Cell 4, 123–128. https://doi.org/10.1016/S1097-2765(00)80194-X

Wollerton, M.C., Gooding, C., Wagner, E.J., Garcia-Blanco, M.A., Smith, C.W.J., 2004. Autoregulation of polypyrimidine tract binding protein by alternative splicing leading to nonsense-mediated decay. Mol Cell 13, 91–100. https://doi.org/10.1016/s1097-2765(03)00502-1

Wu, S., Chen, L., Becker, A., Schonbrunn, E., Chen, J., 2012. Casein kinase 1α regulates an MDMX intramolecular interaction to stimulate p53 binding. Mol Cell Biol 32, 4821–4832. https://doi.org/10.1128/MCB.00851-12

Wyers, F., Rougemaille, M., Badis, G., Rousselle, J.-C., Dufour, M.-E., Boulay, J., Régnault, B., Devaux, F., Namane, A., Séraphin, B., Libri, D., Jacquier, A., 2005. Cryptic pol II transcripts are degraded by a nuclear quality control pathway involving a new poly(A) polymerase. Cell 121, 725–737. https://doi.org/10.1016/j.cell.2005.04.030

Xu, F., Wang, Y.-L., Chang, J.-J., Du, S.-C., Diao, L., Jiang, N., Wang, H.-J., Ma, D., Zhang, J., 2014. Mammalian sterile 20-like kinase 1/2 inhibits the Wnt/β-catenin signalling pathway by directly binding casein kinase 1ε. Biochem J 458, 159–169. https://doi.org/10.1042/BJ20130986

Xu, Z., Wei, W., Gagneur, J., Perocchi, F., Clauder-Münster, S., Camblong, J., Guffanti, E., Stutz, F., Huber, W., Steinmetz, L.M., 2009. Bidirectional promoters generate pervasive transcription in yeast. Nature 457, 1033–1037. https://doi.org/10.1038/nature07728

Yaffe, M.B., Rittinger, K., Volinia, S., Caron, P.R., Aitken, A., Leffers, H., Gamblin, S.J., Smerdon, S.J., Cantley, L.C., 1997. The Structural Basis for 14-3-3:Phosphopeptide Binding Specificity. Cell 91, 961–971. https://doi.org/10.1016/S0092-8674(00)80487-0

Yamashita, A., Ohnishi, T., Kashima, I., Taya, Y., Ohno, S., 2001. Human SMG-1, a novel phosphatidylinositol 3-kinase-related protein kinase, associates with components of the mRNA surveillance complex and is involved in the regulation of nonsense-mediated mRNA decay. Genes Dev. 15, 2215–2228. https://doi.org/10.1101/gad.913001

Yang, H., Rudge, D.G., Koos, J.D., Vaidialingam, B., Yang, H.J., Pavletich, N.P., 2013. mTOR kinase structure, mechanism and regulation. Nature 497, 217–223. https://doi.org/10.1038/nature12122

Ye, Q., Ur, S.N., Su, T.Y., Corbett, K.D., 2016. Structure of the Saccharomyces cerevisiae Hrr25:Mam1 monopolin subcomplex reveals a novel kinase regulator. The EMBO Journal 35, 2139–2151. https://doi.org/10.15252/embj.201694082

Yi, H., Park, J., Ha, M., Lim, J., Chang, H., Kim, V.N., 2018. PABP Cooperates with the CCR4-NOT Complex to Promote mRNA Deadenylation and Block Precocious Decay. Mol Cell 70, 1081-1088.e5. https://doi.org/10.1016/j.molcel.2018.05.009

Zhang, B., Butler, A.M., Shi, Q., Xing, S., Herman, P.K., 2018. P-Body Localization of the Hrr25/Casein Kinase 1 Protein Kinase Is Required for the Completion of Meiosis. Molecular and Cellular Biology 38, e00678-17. https://doi.org/10.1128/MCB.00678-17

Zhang, B., Herman, P.K., 2019. It is all about the process(ing): P-body granules and the regulation of signal transduction. Curr Genet. https://doi.org/10.1007/s00294-019-01016-3

Zhang, B., Shi, Q., Varia, S.N., Xing, S., Klett, B.M., Cook, L.A., Herman, P.K., 2016. The Activity-Dependent Regulation of Protein Kinase Stability by the Localization to P-Bodies. Genetics 203, 1191–1202. https://doi.org/10.1534/genetics.116.187419

Zhang, C., Lopez, M.S., Dar, A.C., LaDow, E., Finkbeiner, S., Yun, C.-H., Eck, M.J., Shokat, K.M., 2013. Structure-guided Inhibitor Design Expands the Scope of Analog-Sensitive Kinase Technology. ACS Chem Biol 8, 1931–1938. https://doi.org/10.1021/cb400376p

Zhang, D.W., Rodríguez-Molina, J.B., Tietjen, J.R., Nemec, C.M., Ansari, A.Z., 2012. Emerging Views on the CTD Code. Genet Res Int 2012. https://doi.org/10.1155/2012/347214

Zhang, J., Sun, X., Qian, Y., LaDuca, J.P., Maquat, L.E., 1998a. At least one intron is required for the nonsense-mediated decay of triosephosphate isomerase mRNA: a possible link between nuclear splicing and cytoplasmic translation. Mol Cell Biol 18, 5272–5283. https://doi.org/10.1128/MCB.18.9.5272

Zhang, J., Sun, X., Qian, Y., Maquat, L.E., 1998b. Intron function in the nonsense-mediated decay of beta-globin mRNA: indications that pre-mRNA splicing in the nucleus can influence mRNA translation in the cytoplasm. RNA 4, 801–815. https://doi.org/10.1017/s1355838298971849

Zhang, S., Ruiz-Echevarria, M.J., Quan, Y., Peltz, S.W., 1995. Identification and characterization of a sequence motif involved in nonsense-mediated mRNA decay. Mol Cell Biol 15, 2231–2244. https://doi.org/10.1128/MCB.15.4.2231

Zhang, Z., Dietrich, F.S., 2005. Identification and characterization of upstream open reading frames (uORF) in the 5' untranslated regions (UTR) of genes in Saccharomyces cerevisiae. Curr Genet 48, 77–87. https://doi.org/10.1007/s00294-005-0001-x

Zhao, B., Li, L., Tumaneng, K., Wang, C.-Y., Guan, K.-L., 2010. A coordinated phosphorylation by Lats and CK1 regulates YAP stability through SCF(beta-TRCP). Genes Dev 24, 72–85. https://doi.org/10.1101/gad.1843810

Zhou, J., Hidaka, K., Futcher, B., 2000. The Est1 Subunit of Yeast Telomerase Binds the Tlc1 Telomerase RNA. Mol Cell Biol 20, 1947–1955.

Zientara-Rytter, K., Ozeki, K., Nazarko, T.Y., Subramani, S., 2018. Pex3 and Atg37 compete to regulate the interaction between the pexophagy receptor, Atg30, and the Hrr25 kinase. Autophagy 14, 368–384. https://doi.org/10.1080/15548627.2017.1413521

Zinder, J.C., Lima, C.D., 2017. Targeting RNA for processing or destruction by the eukaryotic RNA exosome and its cofactors. Genes Dev 31, 88–100. https://doi.org/10.1101/gad.294769.116

Zünd, D., Gruber, A.R., Zavolan, M., Mühlemann, O., 2013. Translation-dependent displacement of UPF1 from coding sequences causes its enrichment in 3' UTRs. Nat Struct Mol Biol 20, 936–943. https://doi.org/10.1038/nsmb.2635

Strains

Name	Genetic background	Description
	BY4741	Mat a
	BY4742	Mat α
LMA1667	*upf1*Δ	*upf1*Δ ::kanMX6
LMA3806	*ebs1*Δ	*ebs1*Δ ::kanMX6
LMA5096	Hrr25 I82G	Introduction of mutation I82G in HRR25
LMA5097	Nmd4-CRAP	Nmd4-CRAP::URA3
LMA5098	Nmd4-CRAP/Hrr25 I82G	Nmd4-CRAP::URA3, with mutation I82G in HRR25
LMA5128	Dcp1-TAP	Dcp1-TAP::HIS3
LMA5129	Dcp1-TAP/Hrr25 I82G	Dcp1-TAP::HIS3, with mutation I82G in HRR25
LMA5209	GAL-Hrr25	promoter GAL1 in front of Hrr25
LMA5520	Hrr25 I82G, *ebs1*Δ	Introduction of *ebs1*Δ ::kanMX6 in the original strain LMA5096
LMA5334	Upf1-degron	NAM7-polyG-3FLAG-AID::kanMX6/ura::TIR1 derived from LMA 5215
LMA5463	Upf1-HA	Introduction of the 3HA tag in C-ter of Upf1 in WT strain (BY4741)
LMA5464	Upf1-(1-853)-HA	Truncation of C-ter domain of Upf1 with the 3HA tag in the WT strain (BY4741)
LMA5465	Upf1-HA, hrr25 I82G	Introduction of the 3HA tag in C-ter of Upf1 in LMA5096
LMA5466	Upf1-(1-853)-HA, hrr25 I82G	Truncation of C-ter domain of Upf1 with the 3HA tag in LMA5096
LMA5270	Dcp2-HA	Introduction of the 3HA tag in C-ter of Dcp2 in WT strain (BY4741)
LMA5271	Dpc2-(1-300)-HA	Truncation of C-ter domain of Dcp2 with the 3HA tag in the WT strain (BY4741)
LMA5437	Hrr25 I82G, Dcp2-HA	Introduction of the 3HA tag in C-ter of Dcp2 in LMA5096

LMA5439	Hrr25 I82G, Dcp2-(1-300)-HA	Truncation of C-ter domain of Dcp2 with the 3HA tag in LMA5096
LMA5618	Upf1-HA, *nmd2*Δ	Introduction of 3HA tag at C-ter of Upf1 in the original strain *nmd2*Δ::KAN
LMA5620	Upf1-HA, *ebs1*Δ	Introduction of 3HA tag at C-ter of Upf1 in the original strain LMA3806
LMA5626	Upf1-HA, dcp2-degron	Introduction of 3HA tag at C-ter of Upf1 in the original strain LMA4423
LMA5648	Upf1-HA, Nmd2-TAP	Introduction of 3HA tag at C-ter of Upf1 in the original strain Nmd2-TAP
LMA5650	Upf1-HA, Nmd4-TAP	Introduction of 3HA tag at C-ter of Upf1 in the original strain Nmd4-TAP
LMA5652	Upf1-HA, Ebs1-TAP	Introduction of 3HA tag at C-ter of Upf1 in the original strain Ebs1-TAP
LMA5673	Upf1-HA, Ebs1-(1-610)-TAP	Truncation of the C-ter domain of Ebs1 with TAP tag in LMA5463
LMA5662	Upf1-HA, S869A, S884A, S887A	Introduction of point mutations S869A, S884A and S887A in original strain LMA5463
LMA2194	Upf1-TAP	Upf1-TAP-HISMX
LMA5416	Upf1-TAP, hrr25 I82G	Introduction of TAP tag in C-ter of Upf1 in LMA5096
LMA4965	Upf1-TAP, *ebs1*Δ	*ebs1*Δ ::KanMX6/Upf1-TAP-HIS
LMA4458	Upf1-TAP, dcp2-degron	Introduction of TAP tag in C-ter of Upf1 in LMA3668
LMA5215	Ura3::TIR1	
LMA3668	Dcp2-degron	Dcp2-Flag-IAA17-kanMX6-TIR1 derivated from BY4742
LMA4423	Dcp2-degron	Dcp2-3Flag-AID-kanMX6-TIR1 derivated from BY4741

Table 9: Strains used in this study.

Plasmids

Plasmid ID	Description	*Sc* Marker	*Ecoli* Marker
1328	PBS1539-HTP	URA3	Ampi
1443	pCM189NTAP-CH (Upf1) 1-208	URA3	Ampi
1451	PFA6a-polyG-3FLAG-miniAID_opt-kanMX6	kanMX6	Ampi/KAN
1490	pTG189-HA-frALA1-KANMX4-TEF'TER	URA3/Kan	Ampi
1615	pCM189-Hrr25	URA3	Ampi
1616	pCM189-Hrr25 I82G	URA3	Ampi
1617	pCM189-Hrr25 K38A	URA3	Ampi
1715	pCM189 NTAP-Nam7 S884A S887A	URA3	Ampi

Table 10: Plasmids used in this study.

Oligonucleotides

Oligonucleotides used for construction of yeast strain and plasmids

Name	Sequence	Target	Use
AG1	AAAAACCAAAAAGAAAAGATATATTTATAGAAAGGATACATTAAAAAGAGgaattcgagctcgtttaaac	HRR25	Construction pGAL1 longtine in front of HRR25 (fw)
AG2	CTCCCAATCTTCCTGCCAATACGAAATTTCCTTCCTACTCTTAAGTCcattttgagatccgggtttt	HRR25	Construction pGAL1 longtine in front of HRR25 (rv)
AG6	GTTCCTGAAACGCAGATGTG	pGAL1	Control for insertion of pGAL1 in front of HRR25
AG7	GCCGTGGTAAATGTCACCAAAG	HRR25	Control for insertion of pGAL1 in front of HRR25
AG22	GCATTTGGTGGTGAAAACAC	HRR25	To retrieve pGAL1-KanMX from DNA
AG23	GGATGTCTGGACCTGATCG	HRR25	To retrieve pGAL1-KanMX from DNA
AG24	CGAGGAAAAGGAGACGAAG	HRR25	Control for insertion of pGAL1
AG25	CTCTCTGCCAAACCATCTG	HRR25	Control for insertion of pGAL1
AG8	gatgcggccctcctgcagggccctaAGCATAATCTGGAACATCATATGGATACAACCAAATTGACTGGCCAG	HRR25	Introduction of HRR25 in the plasmid pCM189 (rv)
AG9	cacactaaattaccggatcaattcgggggatccAAAGAGATGGACTTAAGAGTAGGAAGGAAATTTC	HRR25	Introduction of HRR25 in the plasmid pCM189 (fw)
AG10	GAATATAATGCTATGGTCGGTGATCTTCTAGGCCC	HRR25	Introduction of the mutation I82G in HRR25 (fw)

AG11	GGGCCTAGAAGATCACCGACCATA GCATTATATTC	HRR25	Introduction of the mutation I82G in HRR25 (rv)
AG12	GAAGAAGTAGCCATCGCTCTGGAA TCGATCAG	HRR25	Introduction of the mutation K38A in HRR25 (fw)
AG13	CTGATCGATTCCAGAGCGATGGCT ACTTCTTC	HRR25	Introduction of the mutation K38A in HRR25 (rv)

Table 11: Construction of yeast strain and associated plasmids.

Oligonucleotides used for qPCR experiments

Name	Sequence	Target	Use
CS887	CCATCTCACTGTTGAGACGG	Pre-mRNA L28	Forward Primer for SYBR RT-qPCR
CS888	CTCAGTTTGCGATGGAAGAG	Pre-mRNA L28	Reverse Primer for SYBR RT-qPCR
CS889	ATGTTGACCACCGGCCATAC	L28	Forward Primer for SYBR RT-qPCR
CS946	TCACGTCTCAGCCGGTAAAG	L28	Reverse Primer for SYBR RT-qPCR
AG45	GGATCCAGCGATGTCGTATC	Transcript 1490	Forward Primer for SYBR RT-qPCR
AG46	GGACATTAGTAGCGGTCCATTT	Transcript 1490	Reverse Primer for SYBR RT-qPCR
CS1020	AGGCTTTGGAGAACCCAACCAG	PGK1	Forward Primer for SYBR RT-qPCR
CS1021	TTGTCAGCAACCTTGGCACCAC	PGK1	Reverse Primer for SYBR RT-qPCR
CS1038	AAGGTCGTGTTGCTCACGGTTG	ALA1	Forward Primer for SYBR RT-qPCR
CS1039	GGCAAGCGCAGAACCATCAATAC	ALA1	Reverse Primer for SYBR RT-qPCR
GB987	CAATTATCCGACTGATATGTGC	SCR1	Forward Primer for SYBR RT-qPCR
GB998	GGTAGTTCTGGGTCCTTAG	SCR1	Reverse Primer for SYBR RT-qPCR
LA124	CAAGGTATCATGGTCGGTATGG	ACT1	Forward Primer for SYBR RT-qPCR
LA126	CGTGTTCAATTGGGTAACGTAAAG	ACT1	Reverse Primer for SYBR RT-qPCR

Table 12: Oligonucleotides used for qPCR experiments.

Oligonucleotides used for the triple mutant strain

Name	Sequence	Target
AG67	aattccagctgaccaccatgGCTGAAATGGGTGACTTTCCGAAG	NAM7
AG68	gatccccgggaattgccatgTATTCCCAAATTGCTGAAGTC	NAM7
CS1199	CATGGCAATTCCCGGGGATCGTGATTCTGGGTAGAAGATCG	URA3KL
CS1200	GAGCAATGAACCCAATAACGAAATC	URA3KL
CS1201	CTTGACGTTCGTTCGACTGATGAGC	URA3KL
CS1202	CATGGTGGTCAGCTGGAATTCGATGATGTAGTTTCTGGTT	URA3KL
CS1213	gcaaatgtatggacccaacg	URA3KL
CS1217	TGTGGTATCATTTTCTACAGCC	NAM7
CS1218	GGTAATCCTAGATCTTTGGC	NAM7

Table 13: Construction of Upf1 triple mutant strain.

List of Abbreviations

A

AID: Auxin-inducible Degradation

Ampi: Ampicillin

ATP: Adenosine triphosphate

C

C-ter: C-terminal domain

CBP: Calmodulin Binding Peptide

cDNA: complementary DNA

CHX: Cycloheximide

CK1: Casein Kinase 1

CTD: C-Terminal repeat Domain

CUT: Cryptic Unstable Transcripts

D

DECID: Decay Inducing complex

DMSO: Dimethyl sulfoxide

DNA: DeoxyriboNucleic Acid

dNTP: deoxyNucleoside triphosphate

DOX: Doxycycline

DSE: Downstream Sequence Element

DTT: Dithiothreitol

E

EBM: EJC Binding Motif

EDTA: Ethylenediaminetetraacetic acid

EJC: Exon-Junction Complex

eRF: eukaryotic Release Factor

F

FRMP: Fragile X Mental Retardation Protein

FSB: First Strand Buffer

fw: Forward

G

G418: Geneticin

H

HA: Human influenza virus Hemagglutinin epitope

HD: Helicase Domain

Hrr25: HO and radiation repair 25

HU: Hydroxyurea

I

IAA: Auxin

IgG: Immunoglobulins G

IGV: Integrative Genomics Viewer

K

KAT: Lysine Acetyl Transferase

Kti: Killer toxin insensitive

M

mcm^5: 5-methoxycarbonylmethyl

mcm^5s^2: 5-methoxycarbonylmethyl-2-thio

MIF4G: Middle domain of eukaryotic initiation factor 4G

MS: Mass Spectrometry

N

N-ter: N terminal domain

ncm^5: 5-carbamoylmethyl

NEB: NewEnglands Biolabs

NGD: No-Go Decay

NMD: Nonsense-mediated mRNA decay

NSD: No-Stop Decay

nt: nucleotides

Nudix: Nucleoside Diphosphate linked to a variable moeity X

O

OD: Optical Density

ORF: Open Reading Frame

P

P-bodies: Processing bodies

PABP: Poly-A Binding Protein

PAP: Peroxidase anti-Peroxidase complex

PCR: Polymerase Chain Reaction

Pol II: RNA polymerase II

poly-A: polyadenylate

Ptbp: Polypyrimidine-Tract-Binding Protein

PTC: Premature Termination Codon

Q

qPCR: quantitative Polymerase Chain Reaction

R

RNA: RiboNucleic Acid

ssRNA: single stranded RNA

rRNA: ribosomal RiboNucleic Acid

tRNA: transfer RiboNucleic Acid

mRNA: messenger RNA

RNR: Ribonucleotide Reductase

RRM: RNA Recognition Motif

RT: Reverse Transcription

RT-qPCR: Reverse Transcription followed by quantitative Polymerase Chain Reaction

rv: Reverse

S

SAM: S-Adenosyl Methionine

SDS: Sodium Dodecyl Sulfate

Ser: Serine

SGD: *Saccharomyces* Genome Database

SKI: SuperKIller

smg: suppressors with morphogenic effect on genitalia

SURF: Smg1-Upf1-eRF

SUT: Stable Unannotated Transcripts

T

TAP: Tandem Affinity Purification

TCA: Trichloroacetic acid

TCR: T-cell Receptors

TE: TrisHCl and EDTA

TEV: Tobacco Etch Virus protease

TES: TrisHCl EDTA and SDS

tetO: Tetracycline Operator

Thr: Threonine

Tyr: Tyrosine

U

uORF: upstream Open Reading Frame

upf: up-frameshift

UTR: Untranslated Region

W

WB: Western Blot

WT: wild type

X

XUT: Xrn1-sensitive Unstable Transcripts

Y

YPD: Yeast extract Peptone Dextrose

List of Figures

Figure 1: mRNA degradation pathways in eukaryotes (simplified from Kramer and McLennan, 2019)..... 9

Figure 2: Cleavage sites of different hydrolase enzymes in eukaryotes (simplified from Kramer and McLennan, 2019). The names of the enzymes correspond to *S. cerevisiae* (Dcs1 and Dcp2) 11

Figure 3: The Upf proteins. Domains and interactions of Upf1 (A), Upf2 (B) and Upf3 (C).17

Figure 4: Domains and interactions of Nmd4 (A) and Ebs1 (B). 22

Figure 5: Yeast NMD complexes revolving around Upf1 (Dehecq et al., 2018) and their possible equivalent in mammals. 38

Figure 6: Hrr25 is a multi-functions protein (adapted from BioGRID)..... 42

Figure 7: Strategy for the insertion of the GAL1 promoter with a selection marker upstream genomic HRR25 in yeast using homologous recombination. 49

Figure 8: Construction of a pCM189-Hrr25 plasmid using Gibson assembly..... 52

Figure 9: Affinity purification using TAP and IgG magnetic beads..... 56

Figure 10: Structure of ATP-analogues, 1NA-PP1 and 3MB-PP1, compared to the structure of ATP (inspired from Zhang et al., 2013). In red is the common structure binding to the ATP pocket. In blue is the different structures constructed for going into the widening induced by the mutation I82G..... 67

Figure 11: Complementation test principle for the pGAL1-HRR25 strain using plasmids with variants of Hrr25. 68

Figure 12: Complementation of the lack of HRR25 with plasmid-borne Hrr25 variants. **A.** Representation of which HRR25 is expressed in each condition (chromosomal, from plasmid, or from both). **B.** Isolation of clones for transformation of plasmid containing HRR25 wild type in BY4741 on top and pGAL1-HRR25 strain on bottom. Clones were streaked on three different media. **C.** Same as B, but with the plasmid bearing *hrr25*-I82G. **D.** Same as B, with *hrr25*-K38A. 69

Figure 13: Absorbance at 600 nm after 24 hours of growth in liquid media. **A.** Absorbance at 600 nm for cultures of different constructions in medium containing galactose and doxycycline. Endogenous HRR25 in pGAL1-HRR25 strain is expressed but not HRR25 from plasmid. **B.** Absorbance at 600 nm for cultures of different constructions in medium containing galactose only. Endogenous HRR25 in pGAL1-HRR25 strain is expressed, together with HRR25 from the plasmid. **C.** Absorbance at 600 nm for cultures of different constructions in glucose containing medium containing doxycycline. Endogenous HRR25 in pGAL1-HRR25 strain is not expressed neither is HRR25 from plasmid. **D.** Absorbance at 600 nm for cultures of different constructions in medium containing no galactose and no doxycycline. HRR25 from plasmid

strain is expressed but not endogenous HRR25 in pGAL1-HRR25. Error bars represent standard deviation of technical replicate values. 71

Figure 14: 3MB-PP1 blocks growth of the hrr25-I82G mutant strain. A. Absorbance at 600 nm of the pGAL1-HRR25 strain with plasmid containing hrr25-I82G after 29 hours of growth in medium lacking uracil in presence of ATP-analogue, inhibitor of mutant I82G, or in presence of the same amount of DMSO. B. Absorbance at 600 nm of strain pGAL1-HRR25 with plasmid containing hrr25-I82G after 30 hours of growth in medium lacking uracil in presence of different concentrations of 3MB-PP1. Error bars represent standard deviation of technical replicate values. 72

Figure 15: Representation of two targets of qPCR for NMD measurement. For pre-L28, NMD substrate, the two primers used were CS887 and CS888. Both are located in the intron. For L28 mature, the two primers used were CS889 and CS946. CS946 overlaps the two exons so that only mature mRNA is amplified. 73

Figure 16: Representation of the transcript produced by the plasmid 1490. 74

Figure 17: The ATP analogue 3MB-PP1 can specifically inhibit the kinase activity of the mutant hrr25 I82G. Growth test of strains containing hrr25-I82G mutant and controls. Serial dilutions were performed on YPD plates with or without 3MB-PP1. Plates were observed after 27h of incubation at 30°C. 75

Figure 18: Inhibition of Hrr25 activity leads to stabilisation of an NMD substrate in yeast. **A.** In the pGAL1-HRR25 system, Fold change comparing changes of NMD substrate pre mRNA of L28 in the pGAL1-HRR25 strain with plasmid containing HRR25 WT or hrr25-I82G with changes of NMD substrate in WT strain with or without introduction of inhibitor 3MB-PP1. The strain *upf1*Δ does not have the core NMD factor Upf1 and hence, NMD is inhibited. This is the positive control. **B.** In the system where hrr25 I82G is endogenous, fold change levels comparing changes of NMD substrate transcript 1490 in the strain hrr25-I82G with changes in WT with 30 min treatment of 3MB-PP1 or of CHX. Here the positive controls are treatment with CHX and the *upf1*Δ strain. The housekeeping gene for the reference used here is RPL28. 76

Figure 19: Representation of the AID system (simplified from Shetty et al., 2019). 77

Figure 20: Inhibition of Hrr25 kinase activity highly affects transcriptome and most particularly the NMD substrates. **A.** Volcano plot of the comparison of Hrr25 I82G treated with 3MB-PP1 vs Hrr25 I82G not treated. On the x-axis is the Log2 Fold Change of the comparison and on the y-axis is the –Log2 of the adjusted p-value. Black represents all points. Red represents the NMD substrates. Blue represents the ribosomal protein transcripts. Grey represents the transcripts for the tRNA. **B.** The same as A but for the comparison of Hrr25 I82G not treated vs the control (BY4741 with DMSO). **C.** Venn diagram comparing the transcripts upregulated in the comparison Hrr25 I82G treated vs the control and the transcripts upregulated in the comparison Nam7-degron treated vs the control. The intersection of both circles represents the transcripts in common in both conditions. **D.** The same as A but for the comparison of Nam7-degron treated with IAA vs Nam7-degron not treated. **E.** The same as A but for the comparison of Nam7-degron treated vs the control. F. The same as A but for the comparison of Wild-Type strain (BY4741) treated with 3MB-PP1 vs the control. 78

Figure 21: Similar NMD targets for Hrr25 kinase inhibition and Upf1 depletion. **A.** Scatter plot comparing Hrr25 I82G treated with Nam7-degron treated. The x-axis is the Log2 Fold change of the comparison Hrr25 I82G treated with the control. The y axis corresponds to the Log2 Fold change of the comparison Nam7-degron treated with the control. Black represents all points. Red represents the NMD substrates. Blue represents the ribosomal protein transcripts. Grey represents the transcripts for the tRNA. **B.** Same as A. Only the ribosomal protein transcripts are represented. **C.** Same as A. Only the NMD substrates are represented. **D.** Same as A. Only the transcripts for the tRNA are represented. **E.** Venn diagram comparing the transcripts upregulated in the comparison Hrr25 I82G treated with the control and the transcripts upregulated in the comparison Nam7-degron treated with the control. The intersection of both circles represents the transcripts in common in both conditions. For the transcripts upregulated in the comparison Hrr25 I82G treated with the control, only transcripts with a Log2 Fold change superior to 1 were taken. 80

Figure 22: Shared substrates and divergence in RNA-seq reads with inhibition of Hrr25 kinase activity and specific degradation of Upf1. **A.** IGV image representing the reads of the different RNA-seq datasets for DAL7. **B.** IGV image representing the reads of the different RNA-seq datasets for SUT828. **C.** IGV image representing the reads of the different RNA-seq datasets for SUT232, XUT_11F-90 and tK(CUU)K. **D.** List of shared NMD substrates between the two conditions inhibition of Hrr25 kinase activity and degradation of Nam7. **E.** IGV image representing the reads of the different RNA-seq datasets for RPS0A. **F.** IGV image representing the reads of the different RNA-seq datasets for RPL28. 82

Figure 23: Stabilisation of NMD substrate 1490 in the context of inhibition of kinase activity depends on the housekeeping gene reference. **A.** Fold change comparing enrichment of NMD substrate transcript 1490 in the strain hrr25-I82G with enrichment in WT with 30 min treatment of 3MB-PP1 or of CHX. Here the positive controls are treatment with CHX and the *upf1*Δ strain. The housekeeping gene for the reference used here is endogenous ALA1 (n = 3). **B.** The same as A with the reference being PGK1 (n = 2). **C.** The same as A with the reference being ACT1 (n = 1). **D.** The same as A. with the reference being SCR1 (n = 1). 84

Figure 24: Principle of the kinetics test for the NMD substrate 1490. 85

Figure 25: Inhibition of Hrr25 kinase activity leads to an increase of half-life for the NMD substrate 1490 and this seems to be independent of Hrr25 function in DNA transcription. **A.** Degradation curve of the NMD substrate 1490 in the strain hrr25-I82G with DMSO. The half-life in this context is of approximately 7 min. **B.** Degradation curve of the NMD substrate 1490 in the strain hrr25-I82G treated with 3MB-PP1. The half-life in this context is approximately of 10 min. **C.** Barplot representing the average percentage of remaining NMD substrate in the cells according to time in WT condition (dark blue) and in I82G condition (light blue) with DMSO control. **D.** Barplot representing the average percentage of remaining NMD substrate in the cells according to time in WT condition (dark blue) and in I82G condition (light blue) with 3MB-PP1 treatment. **E.** The different comparison made by the TukeyHSD test with R and the p-value associated. * p-value <=0,01 ** p-value <=0,001 *** p-value <= 0,0001 87

Figure 26: Diagram of the principle of the experiment to distinguish the effect on NMD of the kinase activity and the function in translation of Hrr25. 88

Figure 27: Impact of Hrr25 kinase activity on NMD is distinct from the function of Hrr25 in mRNA translation. **A.** Western Blot using anti-HA and anti-G6PDH antibodies on protein samples. Anti-HA antibody allows visualising the protein produced from the NMD substrate 1490. Anti-G6PDH antibody was used as a control of gel loading. **B.** Sucrose gradient fractionation profiles of the strain Upf1-HA, hrr25 I82G with DMSO. **C.** Gradient fractionation profiles of the strain Upf1-HA, hrr25 I82G treated with 3MB-PP1. 89

Figure 28: Upf1 C-terminal domain (854-971) might be a target of phosphorylation for Upf1. **A.** Western Blot using only anti-HA antibody. Here it allows to visualise not only the protein produced from the NMD substrate 1490 but also Upf1 truncated or not. **B.** Same as A. except that migration of the proteins was longer to better visualise Upf1 truncated or not. Thus, the protein 1490 is not visible. **C.** Visualisation of λ-phosphatase treatment on Upf1-HA sample through Western Blot. As a control, λ-phosphatase treatment was also performed in presence of Pierce inhibitor (a phosphatase inhibitor cocktail). 91

Figure 29: Potential phosphorylation sites in Upf1 C-terminal domain: S869, S884 and S887. **A.** Sequence alignment of Upf1 sequence from different fungi organisms using Jalview. **B.** Western Blot using only anti-HA antibody. We can thus visualise not only the protein produced from the NMD substrate 1490 but also different versions of Upf1-HA. SSSAAA corresponds to the triple mutation S869A, S884A and S887A. 92

Figure 30: NMD factors bind to Upf1 in different states of phosphorylation. **A.** Western Blot using PAP antibody on input and purified proteins. PAP allows to detect the TAP tags. Hence Nmd2, Nmd4 and Ebs1 truncated or not could be seen on this membrane. **B.** Western Blot using anti-HA antibody on input and purified proteins. Anti-HA can also detect a little the TAP tag as we can see on the last lane – Ebs1(1-610)-TAP. **C.** The same as B. with a longer exposition time to better visualise Upf1 in the input samples. 94

Figure 31: Position in the gradient fractions and the composition of NMD complexes influence the phosphorylation state of Upf1. **A.** Western Blots using anti-HA (on the left) and anti-NOG1 (on the right) antibodies on gradient fraction samples. The first lane corresponds to the membrane for the Upf1-HA hrr25 I82G strain with only DMSO while the second lane corresponds to the membrane for the Upf1-HA hrr25 I82G strain treated with 3MB-PP1. The anti-HA antibody allows to visualise Upf1 and its different states of phosphorylation. The anti-NOG1 antibody allows to see where NOG1 is situated in the gradient fractions. Since NOG1 associates with the subunit 60S of the ribosome, the lane where we can see NOG1 corresponds to the fraction 60S. Other fractions can then be deduced. **B.** Western Blots using anti-HA antibody to observe Upf1-HA and its state of phosphorylation in different conditions. 95

Figure 32: Depletion of Ebs1 and mutation of Hrr25 might have a synergistic effect on NMD. Western Blot using anti-HA and anti-G6PDH antibodies on protein samples. Anti-HA antibody allows visualising the protein produced from the NMD substrate 1490. Anti-G6PDH antibody was used as a control of gel loading. 97

Figure 33: Inhibition of Hrr25 kinase activity might act on the stability of Dcp2 full-length. Western Blot using anti-HA and anti-G6PDH antibodies on protein samples. Anti-HA antibody allows visualising the protein produced from the NMD substrate 1490 and the different versions of Dcp2. Anti-G6PDH antibody is used as a control of gel loading. On the right side of the figure, we can see the membrane containing all samples controls and tests. On the left side of

the figure, we can see only the tests samples but with serial dilutions to determine the NMD phenotype a little more precisely. 98

Figure 34: Hrr25's recruitment into yeast NMD complexes is dependent on its kinase activity and on Dcp2. **A.** Volcano plot comparing the Upf1-TAP, hrr25 I82G treated with the solvent DMSO sample to Upf1-TAP treated with DMSO sample. Three replicates were done for each condition. **B.** Volcano plot comparing the Upf1-TAP, hrr25 I82G treated with 3MB-PP1 sample to Upf1-TAP treated with 3MB-PP1 sample. Three replicates were done for each condition. **C.** Scatterplot representing on the y-axis the LFQ intensities of the sample Upf1-TAP, Dcp2-degron treated with Auxin and on the x-axis the LFQ intensities of the control Upf1-TAP. This plot corresponds to the first biological replicate of this experiment. **D.** Scatterplot representing on the y-axis the LFQ intensities of the sample Upf1-TAP, Dcp2-degron treated with Auxin and on the x-axis the LFQ intensities of the control Upf1-TAP. This plot corresponds to the second biological replicate of this experiment. 100

Figure 35: IGV image representing the reads of the different RNA-seq datasets for SUT221 and YKL178C. 102

Figure 36: Hrr25 and Dcp2 are two phosphoproteins. 106

List of Tables

Table 1: Core proteins involved in the NMD mechanisms. 16

Table 2: Core proteins involved in the NMD mechanisms with new possible functional homologues of Smg5, Smg6 and Smg7 in yeast. 21

Table 3: Core proteins involved in the NMD mechanisms with new possible functional homologues of Smg5, Smg6, Smg7 and Smg1 in yeast. 40

Table 4: Sequence of CK1 phosphorylation sites (reviewed in Fulcher and Sapkota, 2020). 41

Table 5: PCR program used for the Reverse transcription using SuperSript III enzyme. 55

Table 6: qPCR program used. 55

Table 7: Composition of the gel 6% (on the left) and of the stacking gel (on the right). 59

Table 8: Dilution and incubation time used in this study according to the antibody used. 60

Table 9: Strains used in this study. 146

Table 10: Plasmids used in this study. 147

Table 11: Construction of yeast strain and associated plasmids. 149

Table 12: Oligonucleotides used for qPCR experiments. 150

Table 13: Construction of Upf1 triple mutant strain. 151

Importance des interactions protéine-protéine et de la phosphorylation dans le nonsense-mediated mRNA decay (NMD)

Résumé :

Chez *Saccharomyces cerevisiae*, la voie de dégradation majoritaire des ARN messagers passe par le clivage de la liaison pyrophosphate entre l'ARNm et la structure de la coiffe à l'extrémité 5'. Cette étape, importante pour la dégradation de l'ensemble des ARNm, est particulièrement clé dans la dégradation d'une classe d'ARN instables, cibles de la voie de dégradation nommée nonsense-mediated mRNA decay (NMD). Cette-dernière permet la dégradation de transcrits contenant un codon STOP prématuré et donc dépend de la traduction. D'abord considérée comme une voie de dégradation présente à travers les eucaryotes à cause de la grande conservation de ses facteurs principaux – les protéines Upf -, la découverte des protéines Smg dans *C. elegans* (Page et al., 1999) et la description du mécanisme SURF/DECID dépendant de la phosphorylation d'Upf1 (Kashima et al., 2006) semblaient indiquer des différences majeures entre les organismes.

Récemment, notre laboratoire a décrit l'architecture des complexes NMD chez la levure. Ces-derniers sont centrés autour d'Upf1 et ont été nommés Détecteur et Effecteur. Dans le second, nous avons pu identifier la protéine kinase Hrr25 comme un membre du complexe Upf1 avec les protéines du decapping, Dcp2, Dcp1 et Edc3 (Dehecq et al., 2018). Cette protéine conservée est l'analogue des caséines kinases 1 chez l'humain - CK1δ and CK1ε - et elle est impliquée dans de nombreux processus majeurs de la cellule, comme la modification des ARNt, la biogénèse des ribosomes, l'élongation de la transcription et la méiose (Abdel-Fattah et al., 2015 ; Ghalei et al., 2015 ; Ye et al., 2016 ; Nemec et al., 2019). J'ai montré que l'activité kinase de Hrr25 a un rôle dans le NMD qui est indépendant de ses fonctions dans la traduction de l'ARNm mais aussi dans la transcription de l'ADN. Nous avons aussi montré que l'association de Hrr25 avec Upf1 s'appuie sur l'activité kinase de Hrr25 et sur la présence de la protéine portant l'activité decapping, Dcp2. Nous avons pu identifier des résidus Sérine très conservées dans la région C-terminal d'Upf1 levure dont la phosphorylation dépend de Hrr25 et dont la régulation, à l'image de celle impliquée dans d'autres organismes, dépend de la présence d'autres facteurs NMD comme Upf2 et Ebs1 (l'équivalent de Smg5/7). Ces résultats indiquent que les protéines kinase peuvent moduler le NMD par des interactions directes avec les enzymes impliquées dans la dégradation des ARN. Ils suggèrent également que, contrairement à ce que l'on pouvait croire, des protéines kinase sont requises de manière universelle pour le NMD.

Mots clés : Phosphorylation, Protéine, NMD

Impact of protein-protein interactions and phosphorylation on RNA decapping for nonsense mediated mRNA decay (NMD)

Abstract :

In yeast, mRNA degradation is mainly initiated through the cleavage of the pyrophosphate bond between the mRNA and the cap structure at its 5'-end. While this step is important for the decay of most mRNAs, it is particularly critical to initiate the degradation of unstable RNA, targets of the NMD machinery. This pathway allows degradation of transcripts that contain a premature termination codon and thus is entirely dependent on translation. First considered as conserved throughout eucaryotes due to high sequence similarity of its core factors – the Upf proteins -, the discovery of the Smg proteins in *C. elegans* (Page et al., 1999) and the description of the SURF/DECID mechanism depending on phosphorylation of Upf1 (Kashima et al., 2006) indicated a divergence of NMD mechanisms between organisms.

However, recently our laboratory described two NMD complexes revolving around Upf1 – named Detector and Effector - and identified the protein kinase Hrr25 as a member of a Upf1-decapping complex (Dehecq et al., 2018). The conserved protein kinase Hrr25 is the yeast equivalent of mammalian casein kinase 1 (CK1δ and CK1ε) and is involved in major cellular processes, including tRNA modification, ribosome biogenesis, transcription elongation and meiosis (Abdel-Fattah et al., 2015; Ghalei et al., 2015; Ye et al., 2016; Nemec et al., 2019). I demonstrated that the Hrr25 kinase activity has a role in NMD that is independent of its function in mRNA translation and DNA transcription. The association of Hrr25 to Upf1 was dependent on the kinase activity of the protein and on the presence of the decapping enzyme Dcp2. We identified conserved serine residues located in the C-terminal region of yeast Upf1 whose phosphorylation was dependent on Hrr25 and was modulated, like the phosphorylation of Upf1 in other organisms, by the presence of other NMD factors, such as Upf2 and Ebs1 (SMG5/7 equivalent). These results indicate that protein kinases can modulate NMD by direct interactions with the enzymes involved in RNA degradation and suggest that, contrary to previous beliefs, protein kinases are universally required for NMD.

Keywords : Phosphorylation, Protein, NMD